BERICHTE
aus dem Fachbereich Geowissenschaften
der Universität Bremen

No. 264

Kopf, A., E.C.C. Alexandrakis, J. Blees, K. Bogus, B. Dennielou, A. Förster, F.E. Girault, T. Haarmann, H. Hanff, M. Hentscher, N.E. Kaul, S. Klar, S. Krastel, M. Lange, M.-A. Meier, J.F. Metzen, V. Spiess, S. Stegmann, F. Strozyk, T. Volen Krumova

REPORT AND PRELIMINARY RESULTS OF METEOR CRUISE M73/1: LIMA-LAMO (*Ligurian Margin Landslide Measurements & Observatory*), Cadiz, 22.07.2007 - Genoa, 11.08.2007

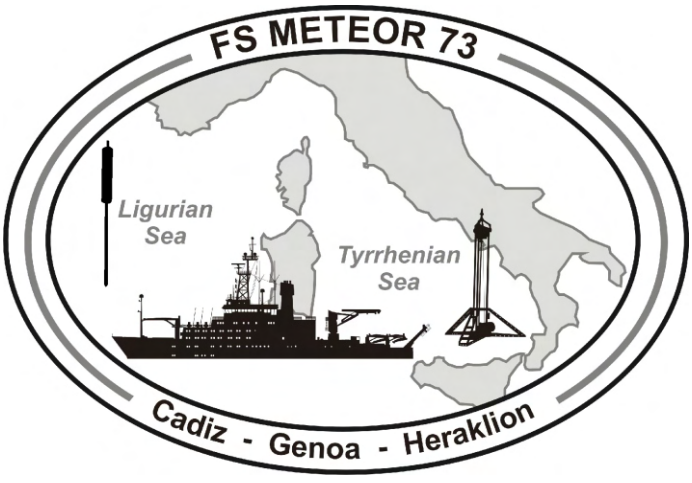

Berichte, Fachbereich Geowissenschaften, Universität Bremen, No. 264, 163 pages, Bremen 2008

ISSN 0931-0800

The "Berichte aus dem Fachbereich Geowissenschaften" are produced at irregular intervals by the Department of Geosciences, Bremen University.

They serve for the publication of experimental works, Ph.D.-theses and scientific contributions made by members of the department.

Reports can be ordered from:

Monika Bachur

Forschungszentrum Ozeanränder, RCOM

Universität Bremen

Postfach 330 440

D 28334 BREMEN

Phone: (49) 421 218-65516

Fax: (49) 421 218-65515

e-mail: MBachur@uni-bremen.de

http://elib3.suub.uni-bremen.de/publications/diss/html

Citation:
Kopf, A., and cruise participants
Report and preliminary results of METEOR Cruise M73/1, Cadiz 22.07.2007 – Genoa 11.08.2007.
Berichte, Fachbereich Geowissenschaften, Universität Bremen, No. 264, 163 pages. Bremen, 2008.

ISSN 0931-0800

Table of Contents

Preface 4

Participants *RV Meteor* 5

Participating institutions 5

1. Abstract 6

2. Introduction 8

3. Geological background 10

4. Scientific rationale and State-of-the-art 13

5. Methods 17

5.1. Multibeam Swathmapping 17
5.2. Water Sound Velocity (CTD) 18
5.3. Parasound profiling 18
5.4. Seismic reflection profiling 19
5.5. Heat flow measurements 25
5.6. CPT testing 28
5.7. Gravity coring and sediment description 31
5.8. Physical properties 35
5.9. Pore water geochemistry 39
5.10. Remotely operated vehicle (ROV) 40

6. Preliminary Results 41

6.1. Multibeam Swathmapping 41
6.2. Water Sound Velocity (CTD) 43
6.3. Parasound profiling 43
6.4. Seismic reflection profiling 48
6.5. Heat flow measurements 55
6.6. CPT testing 66
6.7. Gravity coring and sediment description 72
6.8. Physical properties 89
6.9. Pore water geochemistry 90
6.10. Remotely operated vehicle (ROV) 95

7. References 97

8. Acknowledgements 101

9. Appendices 102

9.1. Station list 103
9.2. List of seismic profiles 118
9.3. Lithologs and core photographs 121
9.4. MSCL results 167
9.5. Group photo 168
9.6. Press coverage 169

Preface

The expedition M73/1, *LIMA-LAMO* (Ligurian Margin Landslide Measurements & Observatory), aims to shed light on submarine landslide processes at the Ligurian Margin by using geophysical methods, *in situ* measurements and seafloor sampling. The regional goals are the small area south of Nice, the Baye des Anges, and the Var estuary, canyon, and ridge. At various levels of the continental margin, mass wasting has been observed. While some of the processes can be related to anthropogenic influence (e.g. the Nice airport landslide and tsunami in 1979), others are related to seismic activity, submarine groundwater outflow, and riverine input. Furthermore, the area hosts anticipated IODP boreholes, which in the long run will be incorporated into cabled observatories in the frame of the EU real-time network of excellence *ESONET* (European Seafloor Observatory Network). For this endeavor, *Meteor* Leg M73/1 carried out critical site survey and pilot work on the potentially unstable slope where offshore construction is planned in the foreseeable future. The research serves to test key hypotheses concerning the trigger mechanisms (ground water charging of slope sediments, high excess pore pressures, sensitive clay horizons). Methods utilised included free-fall CPT- and heat flow measurements, pore fluid and bottom water sampling, CTD measurement using a shallow-water ROV, detailed geophysical characterisation, and sediment sampling for geotechnical experiments.

The study area has water depths between 15 and ca. 2500 m at the failed shallow slope and along the path the landslide and debris flows took. In addition, the moderately deep and deep slope also sports landslide scars some of which have been studied in some detail. Hence, we were essentially aiming to focus on four different areas:

- The Nice airport slide and adjacent stable slope in 15-300 m water depth;
- The mid-slope with both ridges and gullies where the landslide mass was traveling, including some unaffected stable slope regions, all in 500-1000 m water depth;
- The deeper slope (1500-2000 m water depth) west of the Var Canyon with several landslide scars and talus; and
- The Var Canyon region with its flanks, terraces, and channels in down to approximately 2500 m water depth.

Personnel aboard RV *Meteor*

1. Prof. Dr. Achim Kopf	M73/1-A, B, C	RCOM Univ. HB
2. Prof. Dr. Volkhard Spiess	M73/1-B	Univ. HB
3. Dr. Sebastian Krastel	M73/1-B	Univ. HB
4. Dr. Norbert Kaul	M73/1-A	Univ. HB
5. Frank Strozyk	M73/1-A, C	RCOM Univ. HB
6. Jan F. Metzen	M73/1-A, B, C	Univ. HB
7. Steffen Klar	M73/1-A	RCOM Univ. HB
8. Eleni C.C. Alexandrakis	M73/1-A, B, C	Univ. HB
9. Dr. Bernard Dennielou	M73/1-A, B, C	IFREMER
10. Annika Förster	M73/1-A, B, C	RCOM Univ. HB
11. Kara Bogus	M73/1-B, C	Univ. HB
12. Tim Haarmann	M73/1-A, B, C	Univ. HB
13. Jan Blees	M73/1-A, B, C	Univ. HB
14. Michael Hentscher	M73/1-A, B, C	Univ. HB
15. France E. Girault	M73/1-A, B, C	ETH Zürich
16. Men-Andrin Meier	M73/1-A, B, C	ETH Zürich
17. Hendrik Hanff	M73/1-A, B, C	RCOM Univ. HB
18. Matthias Lange	M73/1-A, B, C	RCOM Univ. HB
19. Tsveta Volen Krumova	M73/1-A, B, C	RCOM Univ. HB
20. Sylvie Stegmann	M73/1-A	RCOM Univ. HB
21. Winnie Abraham	M73/1-A	Univ. HB
22. Simone Ulmer	M73/1-C	ETH Zürich
23. Thorsten Truscheit	M73/1-A, B, C	DWD

Participating institutions

DFG-Research Centre Ocean Margins (RCOM)
University Bremen
Leobener Strasse
28359 Bremen --- GERMANY

University of Bremen
Klagenfurter Strasse
28359 Bremen --- GERMANY

IFREMER
B.P. 70
29280 Plouzané --- FRANCE

Geological Institute
Eidgenössisch-Technische Hochschule Zürich
Universitaetsstrasse 16, CHN H71
CH-8092 Zürich --- SWITZERLAND

1. Abstract

Cruise M73/1 “LIMA-LAMO” with R/V *Meteor* studied the western Ligurian Margin off Southern France. This area in the northeastern part of the western Mediterranean Sea represents a tectonically active margin with a lot of microseismicity and mass wasting. Landslide processes, turbidites, and other consequences of slope instability were the aim of this RCOM expedition into the area of Var Canyon and turbiditic system and the Baie des Anges, both located south of Nice at the French Riviera. The study area can be divided into five regions:

i. The Nice airport slide and adjacent stable slope in 15-300 m water depth;
ii. The mid-slope with both ridges and gullies where the landslide mass was traveling, including some unaffected stable slope regions, all in 500-1000 m water depth;
iii. The deeper slope (1500-2000 m water depth) adjacent to the Var Canyon with landslide scars and talus (“western slide”);
iv. An even larger slide complex further away from the canyon system (“eastern slide”); and
v. The Var Canyon region with its flanks, terraces, and channels in down to approximately 2500 m water depth.

Initial tentative results gain many new insights in the various study regions. At the northernmost area (i) adjacent to the Nice airport, weak clay layers in conjunction with the construction work south of the airport as well as fresh water flux in coarse-grained sediments at the margin seem to be the most likely landslide triggers. Pore water salinity was found to be <20% of normal seawater in those layers right at the headwall of the landslide scar. In gravity cores immediately east or west along strike, normal salinity was measured. Charging of sediments with ground water originating further north was confirmed by excess pore pressure signals during CPTU deployments. The entire area was mapped using the high resolution SIMRAD EM710 system, which reveals small-scale steps and scars in the landslide scar. ROV surveys along these small scars show steep walls and talus immediate down-slope of them, both being indicative of very recent seafloor sediment deformation.

In area (ii), we visited four channels which are proposed pathways of the 1979 wasted mass. Coring, which was characterised by either low or no recovery in those locations, provided indirect evidence for high transport rates and no deposition in the recent past.

Sediment gets accumulated on the flanks and crests of the ridges where undisturbed successions of hemipelagics were recovered. CPT and HF deployments were hindered by low penetration and did not allow us to favour one of the channels over the others.

In areas (iii) and (iv), two extensive landslide scars were studied somewhat east of the main channel of the Var Canyon system. Either feature was imaged by a series of seismic reflection profiles. The distinct bodies of redeposited material (i.e. debrites) were then sampled together with reference sediments outside the features. Materials are mainly silty clays with some coarser sections. Pore water showed regular seawater composition, and more detailed post-cruise analyses are required to illuminate mass wasting dynamics and timing.

In area (v), there is evidence for turbidites and mass wasting deposits all over the Var Canyon system, often with sharp erosive surfaces at the base. The comprehensive coring program recovered push cores from a variety of sites, which were visited with the same device 2 years ago. Results from cruise M73-1 confirm the earlier findings by providing excellent agreement (and hence very little recent deposition) in the majority of the cases.

In addition to the regional work in areas (i) through (v), we carried out a several-day MCS surveyto acquire cross-lines over each of the proposed drilling locations within IODP proposal 685-full. The lines serve as a prerequisite for instrumented boreholes in the near future.

2. Introduction

Humans settling along ocean margins are blessed with repeated earthquakes, landslides, and other threats for human life, ecosystems and infrastructure. Given that 60% of the Earth's population lives within the frontal 50 km of the coast, enormous scientific and economic efforts are hence undertaken to shed light on the processes responsible for such ocean margin geohazards as well as their precursors. Given the highly dynamic setting and complexity of collision zones in the Mediterranean Sea, many processes are still poorly understood. Among the shortcomings in understanding collision zones, the temporal variation of deep-seated processes as well as their manifestations at shallower levels is the emerging key question. As a consequence, both marine and continental geosciences, including scientific drilling, accommodated accordingly and have started long-term observation. Boreholes (e.g. in Greece [Corinth], Germany [KTB], California [SAFOD]), and even wider areas on the ocean floor (e.g. in the Monterey Bay [MARS], the Sagami Bay in Japan, or the Juan de Fuca plate [NEPTUNE]) are implemented with *state-of-the-art* technology to measure and monitor parameters *in situ* in space and time. In Europe, ESONET has identified a total of 203 data end-users in 11 countries with a wide-spread need for data monitoring of the solid earth beneath the sea, the interface between the solid earth and sea, and the water column. Two of the strongest partners, the University of Bremen (Germany) and IFREMER Brest (France) have now joined forces on a multi-disciplinary level to work at the Ligurian Margin within ESONET and the Integrated Ocean Drilling Program (IODP) (see below).

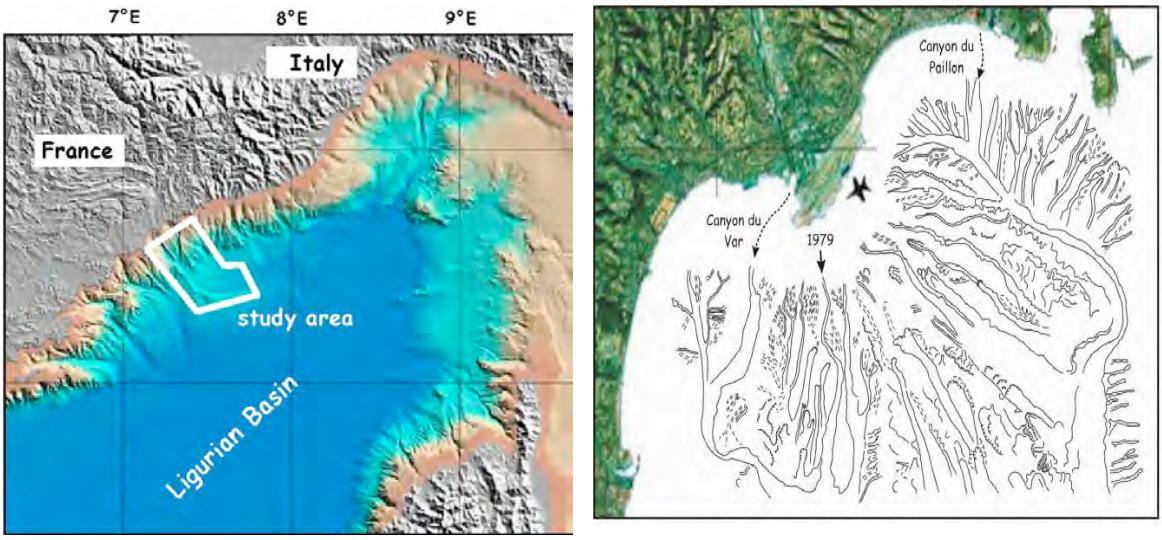

Fig. 1: (a) Bathymetric map of the Ligurian Sea and surrounding land masses; (b) Structural/geomorphic map of the study area at the Var estuary and canyon.

In general, *in situ* monitoring is essential for many geoscientific research disciplines, and the possibility to use fiber-optic cables for real-time data transmission and for improved control on long-term experiments has triggered major projects in Europe, the USA, Canada, or Japan. Especially early warning networks for EQs and tsunamis have further become a major societal interest. The Ligurian margin is well suited for such a project because of its proximity, well known morphological and tectonic setting (Figs. 1-2), and regional seismicity and landsliding (Figs. 3-4). It may also serve as demonstration and test for the Earth Science community. A fiber optic cable was deployed for the ANTARES Neutrino telescope to 2400 m water depth, and a junction is available for other scientific uses. A broadband ocean bottom seismometer (OBS) is already in operation at the ANTARES node, and *in situ* pore pressure monitoring is one of the major targets for future installation, probably within the framework of the IODP (see proposal 685-full by Henry et al., 2005).

3. Geological background

The geological setting in the Ligurian Basin is that of a tectonically active and unstable margin. Much of the morphology on- and offshore as well as the main tectonic lineaments, their direction of movement and seismicity is illustrated in map view (Figs. 1-3) and SW-NE cross section (Fig. 4).

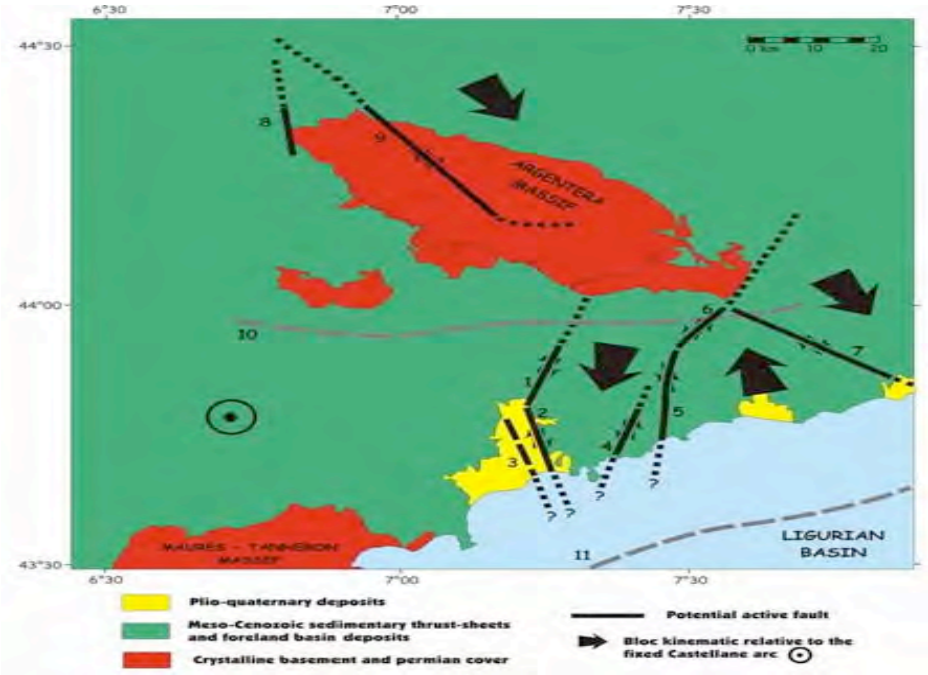

Fig. 2: Tectonic map of the area showing major faults and direction of movement. See text and cross section in Figure 4.

Most of the sediment is received from the erosion of the Alps in the north (Fig. 1; see Mulder et al., 1998). Tectonic deformation rates are small, however, a background seismic activity is present, with the largest earthquakes occurring offshore (M~6 in 1887, and M 6.3 in 1963; see Fig. 3). This activity may be explained by compression on the rim of the Alpine belt, which is now collapsing at least in the French-Italian part (Fig. 4). However, the active offshore fault network, consisting of both compressional and extensional structures, is incompletely understood.

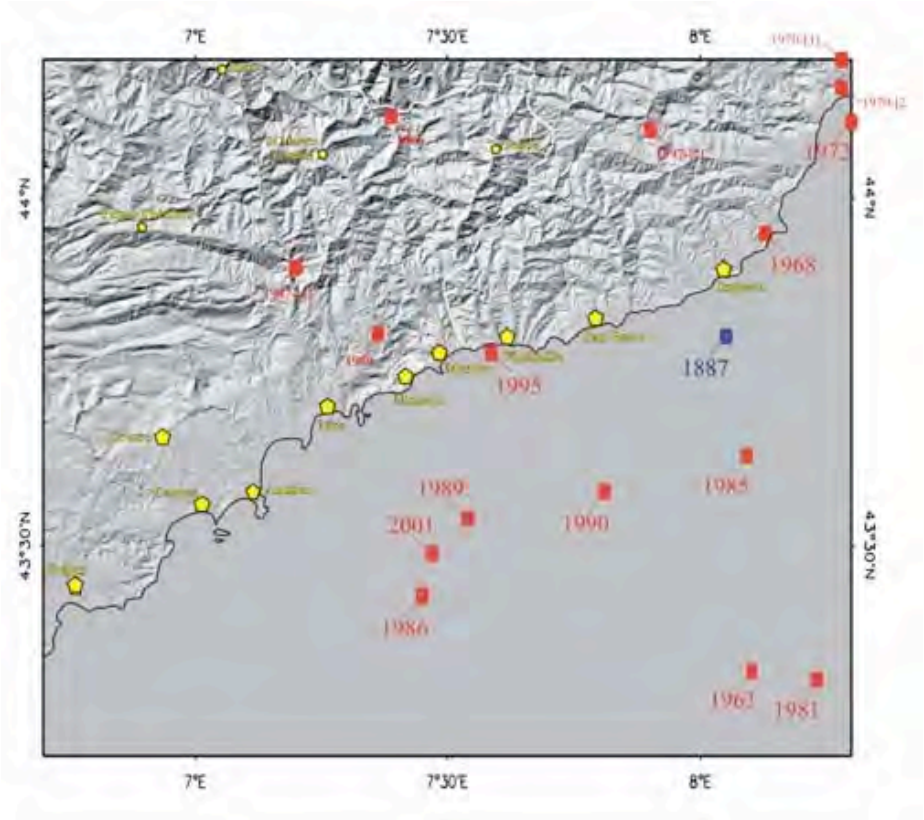

Fig. 3: Regional seismicity in the study area. Shown are events larger M 3.5 between 1960-2001.

In 1979, a large underwater landslide (accompanied by a tsunami) destroyed parts of the International Airport of Nice, France (Savoye et al., 2005). The estimated initial volume of the slide amounts to $8.7 \times 10^6 m^3$ (Assier-Rzadkiewicz et al. 2000), which quickly transformed into a debris flow and then a turbidity current, this way amalgamating more material and a lot of water (Mulder et al. 1997). During the emplacement, two submarine cables were broken, and a small 2-3 m high tsunami affected the Gulf of Antibes (Gennesseaux et al. 1980). Since then, frequent geophysical surveys added pieces to the geomorphological puzzle of the complex tectonics and sediment dynamics in the area (Fig. 1b). Deep-water SAR and SeaMARC sidescan sonar studies documented the distinctive landslide and debris flow gravel deposits on top of the Var canyon sediments. Still, finer-grained material has also been attributed to the debris flow (Dubar & Anthony 1995). Its acoustic signature suggests chaotic sedimentary fabrics and overpressure, which makes those deposits a prime target for *in situ* pore pressure testing.

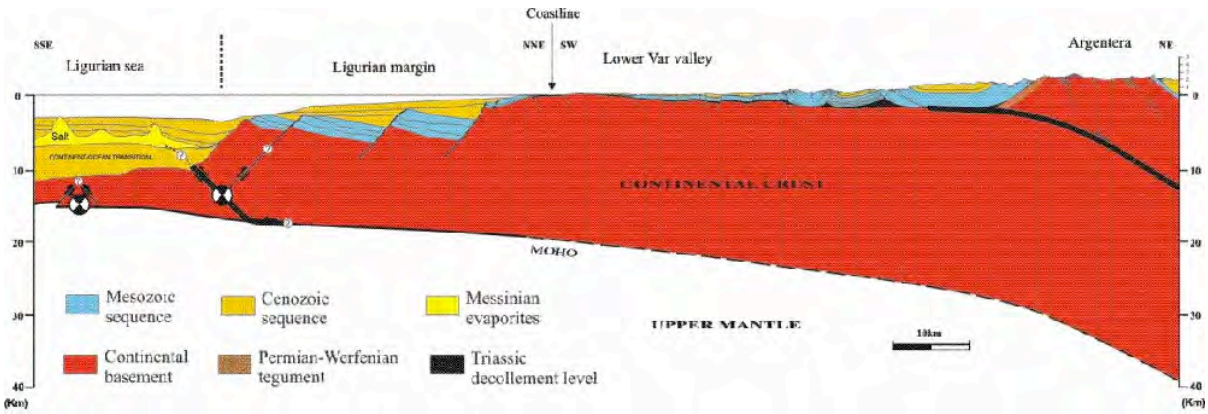

Fig. 4: Schematic cross section through the study area in SW-NE direction. Earthquakes are most abundant on the deep-seated crustal faults in the SW.

The geophysical information collected so far has helped to constrain numerical simulations of the landslide initiation and emplacement. The model runs attest that the initial slide quickly turned into a rapid turbidity current with a minimum thickness of 30 m (Upper Var valley) to 120 m (Lower Var valley). Even at the Lower Var valley, it spilled over the eastern Var Sedimentary Ridge with velocities of 2.5 cm/s (Savoye et al., 2005). Regardless of these simulations, critical information is missing about the current risk of slope failure, especially in these redeposited sediments with assumed elevated pore pressure. Given the amount of expensive infrastructure on the seafloor (Fig. 5) and the potential loss in case of another EQ, landslide and/or tsunami along the densely populated French and Italian Riviera, a need for additional *in situ* measurements and long-term observations exists.

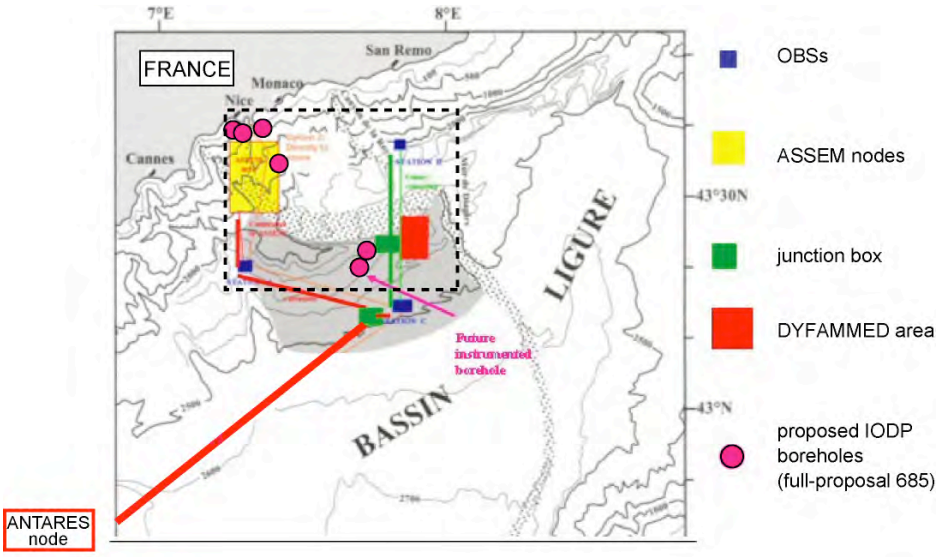

Fig. 5: Preliminary design of the Ligurian Margin seafloor observatory and locations for planned IODP drilling in the area (pink dots). The main focus of cruiseM73/1 with RV *METEOR* was on the acoustic and sediment physical investigation within the dashed box.

4. Scientific rationale and State-of-the-art

The scientific motivation for the proposed work is best outlined with respect to the understanding of parameters controlling sediment physics, and ultimately geohazards such as earthquakes and landslides (Sultan et al., 2004). The two main players in weakening a sediment as to where it may fail and slip are weak mineral phases and excess fluid pressures. While the first are mainly restricted to the clay mineral group (with the weakening being enhanced by their preferred fabric alignment), the latter may originate from various processes in nature which cause net water release or water influx into a system. These include basically all geological settings onshore and offshore, and are as diverse as mineral transformation reactions (clay minerals, opal-quartz reactions, etc.), diagenesis, hydrothermal alteration, lateral flow, mud volcanism, tectonic/tidal/sedimentary/glacial loading, weathering processes, or metamorphism. Other factors causing high excess fluid pressures are restricted to marine settings, and include gas hydrate dissociation or rapid sediment accumulation.

When returning to tectonically active, hazard-prone zones like the Ligurian Margin, the key issue remains whether brittle failure in a formation or slip on an existing fault is triggered by fluid pressure transients, or solely by the mineralogy of the fault gouge (see competing hypotheses by e.g., Byerlee, 1978, 1990 vs. Rice, 1992). A considerable amount of work has been done in recent years to solve this problem (Logan & Rauenzahn, 1987; Saffer et al., 2001; Kopf & Brown, 2003), attesting that the pore pressure may be of similar importance as the friction coefficient of the gouge material itself. As a consequence, one of the central research goals into the behaviour and evolution of sediment failure is to separate the effects of intrinsic frictional properties and fluid pressure variations. For research expedition M73/1, the main aim is to clearly distinguish between those effects by

a) **C**one **P**enetrating **T**esting (CPT) where pore pressure and sediment strength are obtained,
b) Measuring mid-term fluid pressure background and transients related to seismic events (in collaboration with IFREMER Brest, France, on a complementary cruise with RV *L'Atalante* using the Penfeld seafloor penetrometer and piezoprobes), and
c) Doing selected laboratory tests on sediment gravity cores to determine mechanical behaviour.

A) Cone Penetration Tests are a widely used method for *in situ* sediment characterisation in onshore and offshore settings, both in science and industry (e.g., Lunne et al., 1997). With the autonomous, modular free-fall probes (hereafter as FF-CPT) developed in Bremen, a

straightforward cost- and time-effective way was found to measure sediment resistance and pore pressure response to insertion into soft sediments. Measurements are carried out pogo-style, and after retrieval of the data disk, pore pressure evolution and sediment stiffness (measured as frictional resistance of the tip and a mantle sleeve; see Fig. 6a) as well as temperature are immediately available. In addition to the direct observations, other parameters can be rapidly estimated from the CPT data.

The maximum insertion pressure produced at the probe tip can be used to estimate the undrained shear strength of the sediment (C_u). For typical deep sea sediments, Esrig et al. (1977) suggest the relation: $C_u = U_{imax}/6$, where U_{imax} is the maximum insertion pressure. The decay of excess pore pressure produced by the insertion is governed by the consolidation process around the probe and can be modeled as radial consolidation. Bennett et al. (1985) predict the coefficient of horizontal consolidation (C_h) from the time taken for 50% of U_{imax} to dissipate, and C_h can then be used to determine the permeability k. In places where coring and Penfeld deployments are too time-consuming, pogo-style CPT measurements will not only provide first-hand *in situ* results, but with secondary parameters to estimate slope stability and hazard potential.

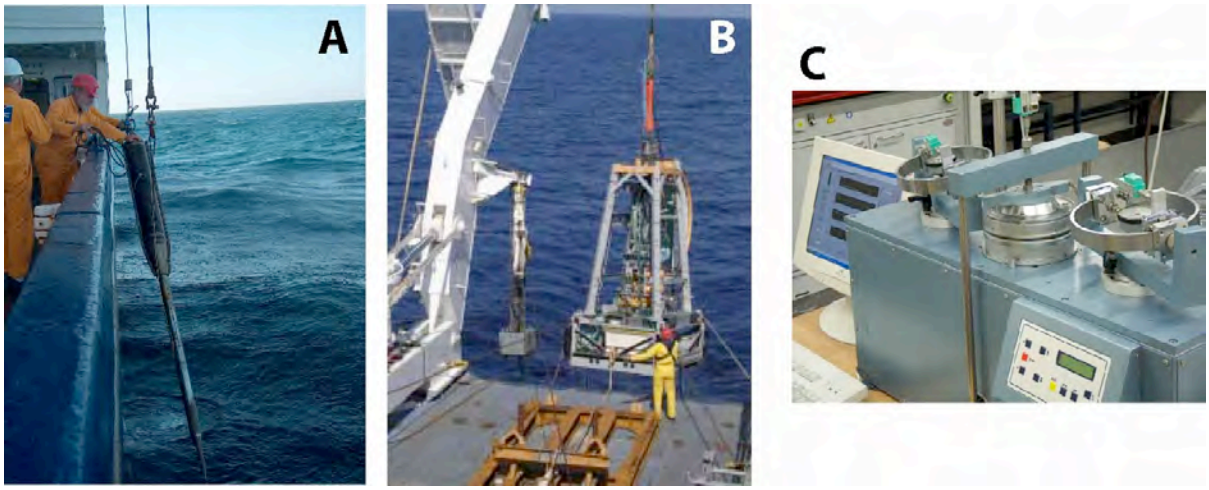

Fig. 6: (a) RCOM CPT lance; (b) Penfeld seabed penetrometer IFREMER (for details see Meunier et al., 2004) ; (c) Ring shear device at RCOM.

B) In order to make use of the above *in situ* data in hazard mitigation, longer-term observations become a necessity. Temporal records of pore pressure changes have been demonstrated to correlate with regional tectonic stresses and seismic activity in a number of places, e.g. the Juan de Fuca Ridge (Becker & Davis, 2003) or the Caucasian orogenic wedge (Kopf et al., 2005). Cruise M73/1 was set up in close cooperation with IFREMER Brest, France, partners of which conducted cruise PRISME in Oct./Nov. 2007 (see above,

and Fig. 6b). Immediately below the Nice Airport slide scar, IFREMER has set up a long-term piezoprobe to study pore pressure in conjunction with regional seismicity, rainfall, etc..

In the highly populated, industrially developed, wealthy region of the French Riviera, there is a strong societal demand to investigate the risks that earthquakes, tsunami and slope instability processes represent. In particular, the need for real-time monitoring within an Eastern Mediterranean alert network justifies projects to extend the underwater cable network within the framework of ESONET. The current layout of the Ligurian Margin Observatory project (as proposed to IODP; see Fig. 5, and Henry et al., 2005) includes to develop technologies for monitoring zones of submarine instability, for instance strain and pore pressure measurement. Beyond applications for safety, those developments are important for general understanding of deformation processes in sediments (stress vs. strain) and fluid-mechanical coupling.

C) A growing body of geotechnical laboratory work attests that frictional stability may be more important than the absolute shear strength of a material in controlling failure and sliding/faulting (see review by Scholz, 1998). Frictional stability is a function of the change in friction coefficient (μ) at a given effective stress, which is primarily rate dependent. While high-porosity rocks show velocity strengthening (i.e. μ increases with increasing shear rate, e.g. during slip), low-porosity rocks weaken. In general, EQs are believed to nucleate in unstable materials, so that the replacement of clays in "weak" shear zones by precipitation (carbonate, zeolites, quartz) or mineral transformation processes would result in either unstable stick slip or conditionally stable behaviour (Moore and Saffer, 2001). Similarly, mechanically weak constituents such as sensitive clay minerals are believed to provide the failure plane for landslides and other hazardous mass wasting processes.

To ground-truth both our *in situ* data (see previous two paragraphs, A and B) and the geophysical information of the seafloor and shallow subbottom, designated soil mechanical laboratory experiments are part of the overall study M73/1 (see Ch. 5, *Methods* below). These include standard soil mechanical procedures to obtain the sediments index properties (wet and dry density, porosity), grain size distribution, liquid and plastic limits, and permeability and shear strength at various confining stresses and rates. Simple tests are conducted on board (vane shear apparatus, falling cone penetrometer) while more sophisticated ones will be carried out shore-based (e.g. ring shear tests; Fig. 6c, or dynamic triaxial tests). Especially the latter suite of parameters provides a profound measure on slope

stability on the seafloor, on how stable a given sediment may deform under certain conditions (namely at depth), and whether permeability allows for the build-up of significant pore pressures.

In addition, a number of locations from an earlier expedition (as well as all the proposed IODP drill sites; Fig. 5) were proposed to be revisited during M73/1 (Fig. 7). The main objective of this endeavour, which originated from a joint research with IFREMER Brest, France, was to shed light on the most recent sedimentary dynamics in the Var canyon and turbidite system over a length of several 100 kilometers.

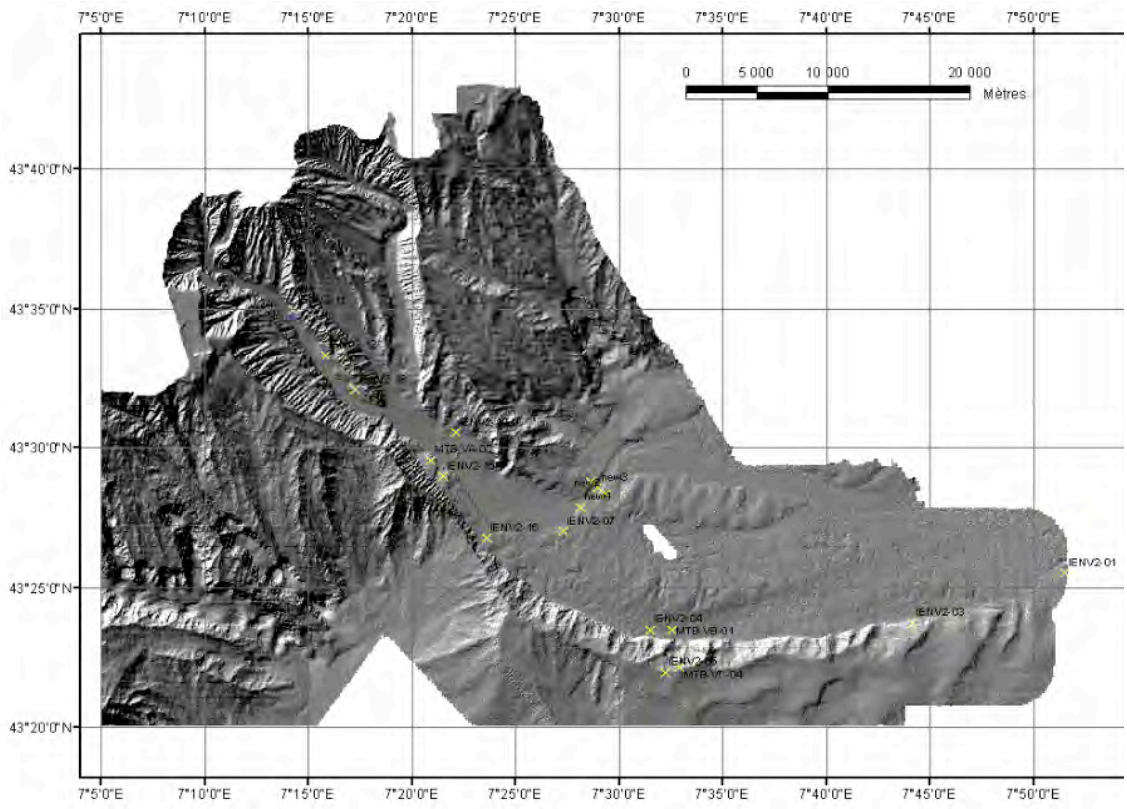

Fig. 7: Locations of gravity and push coring proposed by IFREMER Brest, France for sedimentological reconnaissance work. Light grey crosses represent earlier sampling.

5. Methods

5.1. Multibeam Swathmapping

(F. Strozyk, S. Krastel, A. Kopf)

KONGSBERG Multibeam Bathymetry Systems

During cruise M73/1, the recently upgraded multibeam systems from KONGSBERG MARITIME (formerly SIMRAD) was used. To allow for efficient and economic bathymetric mapping in shallow and in deep water, two systems, a shallow-water EM710 as well as a deep-water EM120 system are installed. The complete layout of both systems as installed on R/V *Meteor* allows both the bridge and the scientists full control (e.g. upload of way point lists, track charts, etc.). In addition, the construction of the hull below waterline which holds the transducers was completely modified to achieve a more stable performance of the systems and to reduce the influence of air bubbles on sound transmission, which had been a great problem with the former installation of the HYDROSWEEP transducers that prevented the successful operation of the system even in moderate weather.

The EM710 installed is a new 1-by-1-degree broadband multibeam echosounder operating in the 70-kHz to 100-kHz band. It uses CW (continuous wave) pulses in shallow modes and FM (chirp) pulses in deep modes. The maximum water depth for this system is up to 1500 m to 2000 m, however, the most efficient depth range for the EM710 is less than 500 m. In this depth it has a better resolution and a slightly wider swath than the EM120. For greater depths, the EM120 is the system of choice. Several features of the EM710 had not been tested in much detail before cruise M73/1 and several problems have still to be settled by KONGSBERG. For example, a synchronised operation of both multibeam systems is not yet possible which led to interference with the EM120.

As the main area of investigation of cruise M73/1 had water depths between 15 m and >2000 m, both the EM120 and the EM710 were operated. However, since shallow water was mapped only in working areas (i) and (ii), the EM710 data were disregarded for the majority of our operations, and only EM120 data were used.

For a more comprehensive description of the two systems, please refer to Weinrebe et al. (2006).

5.2. Water Sound Velocity (CTD)

(H. Hanff, M. Lange)

An ANDERAA Seaguard CTD was used to collect information on temperature, salinity, current velocity and pressure in the Ligurian Basin (Fig. 8). Since the Seaguard system was limited to 300 m water depth, pre-existing profiles of these parameters for greater water depth were obtained from a data basis for the Mediterranean Sea. The main purpose of this procedure was to calibrate the geophysical acquisition systems to determine the influence of saline, warm Mediterranean waters on the echosounder and geophysical acquisition systems (e.g., for the conversion of the recorded SIMRAD travel times into depth values).

Fig. 8: CTD on board R/V *Meteor* prior to deployment.

5.3. Parasound profiling

(F. Strozyk, J. Metzen, S. Krastel, V. Spiess)

The permanently installed *Meteor* sediment echosounder ATLAS ParaSound was used during M73/1 for imaging the uppermost portion (10s of metres) of the sedimentary section. According to the research program of the M73/1 expedition, the PARASOUND along-track survey was mainly aimed to study distribution of sediments along ship track, their facial and

structural appearance, as well as revealing appropriate locations for sediment sampling by gravity corers and for the heat flow and CPT measurements. The PARASOUND was set into operational mode during seismic profiling and transitions within the work area. The operating system generated pulses of PHF (primary high frequency, 18/33 kHz, 2.2x2.5 and 4.0x4.5°), SHF (secondary high frequency, 36.5-40 kHz, 2.0x2.3°), SLF (secondary low frequency, 0.5-6 kHz, 4.5x5.0°) and PLF (primary low frequency, 3/12 kHz, 6.0x7.0° and 24.0x28.0°), while the pulse periods could be changed from single pulse in shallower waters to pulse trains in deeper water depths. Recorded data formats contained PHF, SHF and PLF/SLF as raw data and segy-format. Cruise tracks were recorded with the ship-intern GPS navigation. The main tasks of the operators were system and quality control and the adjustment of the reception window using 10-100 m delays and online-filtering and clipping to 25 mV. Because of the limited penetration of the parasounder signal into sediments, only a short window close to the seafloor was recorded. Additionally, variable water depths, sediment thicknesses and a partially high relief made a recording-window of 200-400 m necessary. Sediment penetration depth ranges from 20 to >200 m depending on water depths, relief and sediment physical properties.

Parasound data were generally collected along all the seismic lines as well as during most of the other operations except point measurements such as cone penetrometer tests (CPT), heat flow (HF) deployments, or when core was taken.

5.4. Seismic reflection profiling

(S. Krastel, V. Spiess, F. Strozyk)

Introduction

With the high-resolution multichannel seismic equipment of Bremen University, small scale sedimentary structures and closely spaced layers can be imaged on a meter scale, which can usually not be resolved by means of conventional seismic systems (Hübscher & Spieß, 1997). During R/V Meteor Cruise M73/1, a Generator-Injector (GI) airgun with a chamber volume of 2 x 1.7 L (~20-300 Hz), a Mini-GI-Gun with a volume of 2*0.25 l (~30-400Hz) and a Micro-GI-Gun with a volume of 2*0.1 L (~50-600Hz) were used as seismic sources. Data were recorded with two streamer systems: a 500m-long 80 channel streamer with up to 13 hydrophones per group and a 50m-long 48 channel shallow water streamer

with single hydrophones. Figure 9 gives an outline of the system setup as it was used during R/V *Meteor* cruise M73/1. Table 1 lists the individual setting for each profile.

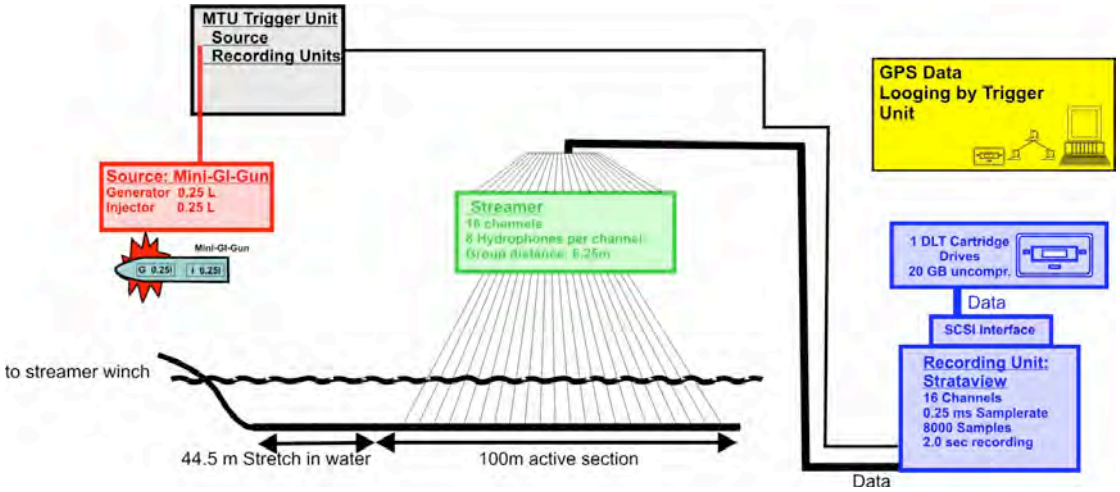

Fig. 9: Seismic system setup during cruise M73/1.

Table 1: Source and receiver settings for individual profiles during cruise M73/1.

Profiles	Source	Streamer
GeoB07-224 - GeoB07-259	2*1.7l GI-Gun, 30ms Delay	500m Deep Water
GeoB07-260 – GeoB07-268	2*0.1L Micro-GI, 20ms Delay	50m Shallow Water
GeoB07-269 - GeoB07-273	2*0.1L Micro-GI, 25ms Delay	50m Shallow Water
GeoB07-274 – GeoB07-304	2*0.1L Micro-GI, 25ms Delay	500m Deep Water
GeoB07-305 – GeoB07-306	2*0.25L Mini-GI, 25ms Delay	500m Deep Water
GeoB07-307	2*1.7l GI-Gun, 50ms Delay	500m Deep Water
GeoB07-308 – GeoB07-315	2*0.1L Micro-GI, 25ms Delay	500m Deep Water
GeoB07-316 - GeoB07-326	2*0.1L Micro-GI, 25ms Delay	50m Shallow Water

Seismic Sources

During seismic surveying, a GI-Gun with normal chamber volume (2 x 1.7 L), a Mini-GI Gun (2*0.25l), and a Micro-GI-Gun (2*0.1l) were shot. Table 1 lists the selected source type for each profile. The 2*1.7l GI-Gun was towed from the starboard side crane approximately 17 m behind the ship's stern (Fig. 10). The gun was connected to a bow with the GI-Gun hanging on two chains 40 cm beneath. An elongated buoy, which stabilized the guns in a horizontal position at a water depth of ~1.2 m, was connected to the bow by two rope loops. The Injector was triggered with a delay of 30 ms or 50ms (see Tab. 1) with respect to the Generator signal, which basically eliminated the bubble signal.

The Mini- and the Micro-GI-Gun were towed from the port side crane appx. 10m behind the ship's stern. The same casing was used for both guns but the volume was reduced for the Micro-GI-Gun by applying especially designed shuttles and reducers. The shuttles and reducers are a proto-type developed provided free of charge by Sercel Marine Sources Division. The Micro-GI-Gun was the main source used during the cruise. While the frequency spectra of a Mini-GI-Gun is similar to that of a GI-Gun with reduced chamber volume (2*0.4l, ~30-400Hz, main frequency ~200Hz), the frequency spectra of the Micro-GI-Gun shows significantly higher frequencies (up to 600Hz) and also a higher main frequency (~300Hz). Both Mini- and Micro-GI-Gun were towed in a similar way as the 1.7l GI-Gun but in a depth of only ~70cm. The Injector of Mini- and Micro-GI-Gun was shot with a delay of 25ms for most profiles, which turned to be the best value for bubble suppression (see Tab. 1). The shooting interval was selected based on water depth. Maximum shooting interval in deep water was 5s, resulting in a shot point spacing of ~8m at 4 knots cruising speed. The Micro-GI-Gun was shot as quickly as 1s in shallow water resulting in a shot point distance of only ~1.5m. All guns were shot a 140bar. Air was provided by the *Meteor* compressor container. All guns worked very reliable without any problems. The geometry of source and receiver systems during the measurements is shown in Figure 10.

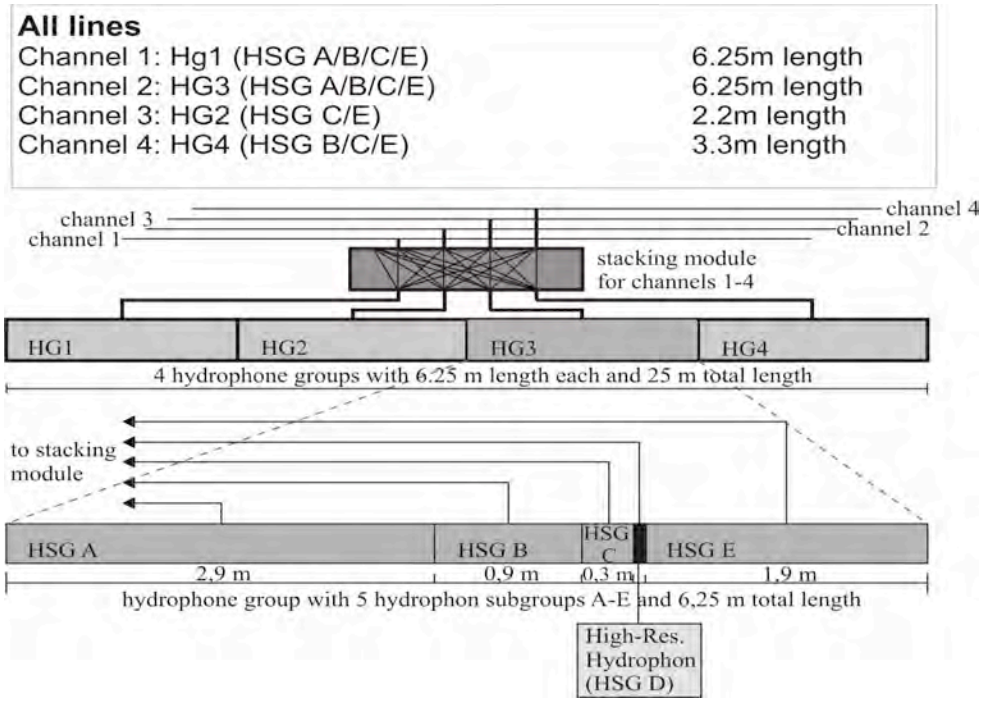

Fig. 10: Deck and seismic gun setting during cruise M73/1.

Streamer

Two different streamers were used during Cruise M73/1. A 50m-long 48 channel shallow water streamer was used in shallow water depths (<400m), while a 500m-long 80-channel streamer was used for greater water depth. The selected streamer for individual profiles is listed in Table 1.

The 500m-long 80-channel streamer (SYNTRON) included a lead-in (54m in water) and 10 active sections of 50 m length. A 20 m long Meteor rope with a buoy at the end was connected to the tail swivel. A 30 m long deck cable connected the streamer to the recording system.

Active 50-m-sections are subdivided in 8 hydrophone groups (Fig. 11). Each of the 6.25m long hydrophone groups is again subdivided into 5 subgroups of different length. A programming module distributes the subgroups of 4 hydrophone groups, i.e. a total of 20 groups, to 4 channels. For all profiles every second 6.25 m hydrophone subgroup was completely used with all 13 hydrophones, whereas the two additional channels were reduced in length to 2.2 m and 3.3 m, respectively (Fig. 11). Locations of individual hydrophone groups are given in Table 2. For the entire cruise output channels 1 to 80 were directly connected to the MaMuCS recording system, independent of the hydrophone group length (see below). Depth control of the streamer was achieved by four DigiBird Remote Units. The designated streamer depth was 3m (see below).

Table 2: Channel assignment and midpoint distances of hydrophone groups of the deep-water streamer during cruise M73/1.

Segment of 25 m length	Hydrophone Group No.	Channel No. In Section	Midpoint Distance
A (0-25 m)	1	1	3.1 m
A	2	3	11.3 m
A	3	2	15.6 m
A	4	4	23.3 m
B (25-50 m)	1	5	28.1 m
B	2	7	36.3 m
B	3	6	40.6 m
B	4	8	48.3 m

A 50m-long 48-channel streamer, which was especially designed for shallow water applications was used in water depths <400m. Each group is made out of a single hydrophone; the distance between hydrophones is 1m. The distance to the first hydrophone is 1m. The data were also recorded with the MaMuCS-System (see below). The streamer was connected to the acquisition system through a combined tow-lead/deck cable. 21 m of

the combined tow-lead/deck cable were in water (see Fig. 10). Depth control for the shallow water streamer was achieved by small buoys, which were attached to the streamer by a 1.5m long elastic rope resulting in a towing depth of the streamers of ~1m. Both streamers were deployed close to the ship's axis (Fig. 10).

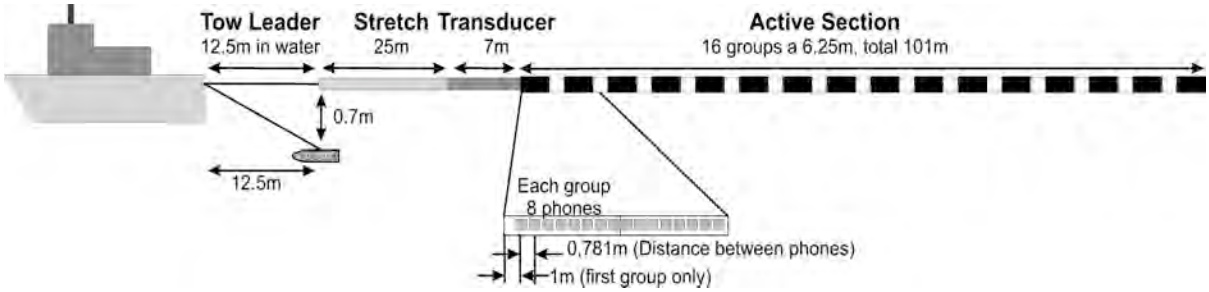

Fig. 11: Schematic sketch of the seismic acquisition configuration

Bird Controller

Four DigiBird Remote Units (RUs 11, 12, 13, 14) were available and could be configured using the bird controlling unit. The standard positions of all RUs are given in Figure **12**. Each RU includes a depth and a heading sensor as well as adjustable wings. The RUs are controlled by a bird controller in the seismic lab. Controller and RUs communicate via communication coils nested within the streamer. A twisted pair wire within the deck cable connects controller and coils.

Each shot trigger started the bird scan of water depth, wing angle and heading data. The current location of the streamer can be displayed as a depth profile on a monitor and stored on the controller PC starting.

Before the streamer was deployed, each RU was programmed in the seismic lab to keep an operating depth of 3 m. The RUs thus forced the streamer to the chosen depth by adjusting the wing angles accordingly. Possible depth variations of the streamer could be checked later during preliminary data processing and depth control appeared to be successful.

Data acquisition systems

All data were recorded with a MaMuCS-System (Marine Multi Channel Seismic Acquisition System) which was developed at Bremen University. This system allows digitizing up to 96 channels, demultiplexing and storage in SEG-Y format on a hard disc. Data were recorded at a sampling frequency of 8 kHz. Brute stacks are prepared from the

system and displayed on monitor. Recoding length was between 0.8s and 4.5s depending on shooting rate, source and water depth. The delay was adjusted to the water depth. The MaMuCS-PC was also used for logging the ship's GPS data and also for distribution the GPS data to other PCs via the network.

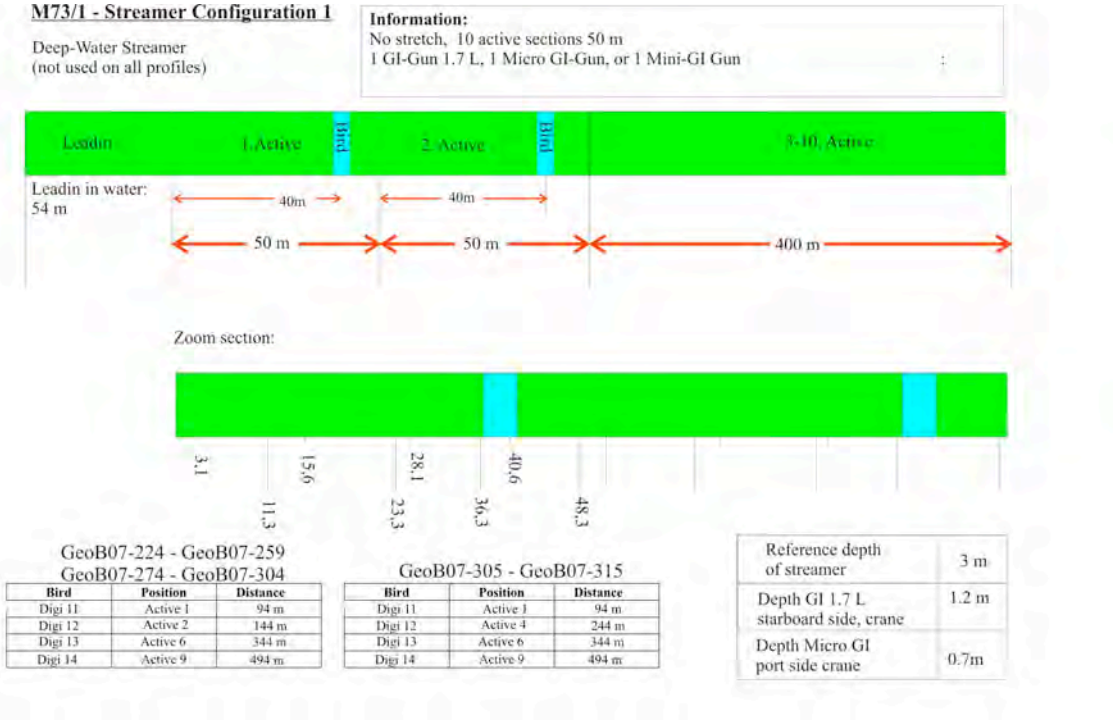

Fig. 12: Deep water streamer setting during R/V *Meteor* cruise M73/1.

Trigger unit

The custom trigger unit used during R/V *Meteor* cruise M73/1 controls seismic sources acquisitions systems, and bird controller (Fig. 10). The unit is set up on an IBM compatible PC with a Windows NT 4.0 operating system and includes a real-time controller interface card (SORCUS) with 16 I/O channels, synchronized by an internal clock. The unit is connected to combined amplifier unit and a gun amplifier unit. The PC runs a custom software, which allows to define arbitrary combinations of trigger signals. The trigger scheme was adjusted to the water depth during the survey.

5.5. Heat flow measurements

(N. Kaul, J. F. Metzen)

On cruise M73/1 a temperature gradient probe (Fig. 13) from the University of Bremen, *Meerestechnik und Sensorik* was used to obtain temperature gradients with miniaturised autonomous temperature data loggers (MTL, Fig. 14; Pfender & Villinger, 2002). Five MTLs were attached at 0.72 m intervals to the strength member of the probe plus an additional sensor to monitor the water temperature above the weight stand. At latter position, a tilt sensor was installed as well.

Parameters of autonomous temperature data loggers:

Instruments serial no.:	sediment and water temp. logger: 1854- 200C, -158C (damaged), -194C (probably mailfunctioning), -122B, -121B, -201C, -115B (damaged, probably mailfunctioning), -203 (damaged)
tilt logger:	1856- 002
Sample rate:	1 sec
Recording length:	18 hours potential maximum
Spacing:	0.72 m at 0.77, 1.49, 2.21, 2.93, 3.65 m below the weight; One water temperature sensor at weight head with sensor tip looking up and one tilt sensor.

Above mentioned ‘damaged’ loggers hit hard material, e.g. pebbles or a boulder, while penetrating into the sediment, hence the senor-tip was bend. Nor occurred any data loss neither was the measurement function limited afterwards. Only the listed ‘probably malfunctioning’ logger tips looked that damaged that these loggers where replaced.
Measurements (seafloor penetration) were carried in two different ways:

(i) Lowering the probe some tens of meters above the sea floor from the water level, allowing the temperature sensors to equilibrate for 2 to 5 minutes, then dropping the probe into the sediment with a constant winch speed. Once the probe stuck in the bottom, it was left undisturbed for 7 minutes to gain ‘equilibrium’ sediment temperature. Then, the probe was slowly pulled out of the sediment and heaved to deck level.

(ii) ‘Pogo-Style’ penetration: After pulling the probe out of the sediments, it was just heaved to a save depth, approximately 100 to 200m above the seafloor, and the ship was moved to the next penetration site where the instrument has about 2 to 5 minutes to come to a stable position before next penetration. The advantages of this method are: i) no further equilibration time in the water column is required, and ii) a great amount of heaving

becomes obsolete, so that veering time is saved. All other measurement procedure is as described above.

For the HF probe measurement spacing used in this survey, transit between penetration points lasted about 10 to 15 minutes, a recording cycle in the sea floor is 7 minutes, yielding a rate of about 0.5 – 1 hour per penetration.

Fig. 13: Heat flow gradient probe on the deck during M73-1 probe.

Winch speed during deployment and retrieval of cable is 1.2 m/s. The initial penetration velocity is 1.0 or 0.8 m/s, depending on expected sediment strength - the lower velocity applied for very soft sediments. Total weight of the instrument is approximately 600 kg. Deployment of the HF probe is amid ship on the starboard side, utilising a small A-frame with the cable winch and one assistant crane for deck operation. This procedure ensures safe operation even during medium sea state and minimum interference due to the ships vertical movement during station work. On R/V *Meteor* two to three deckhands are necessary during deployment and three during operation since the heavy-duty winch employs one operator and one or two deckhands for deployment and recovery of the probe. Control of bottom contact is solely by load plotter. The load signal is clearly identifiable as paid out cable is less than 1000 m and cable weight is moderate.

Fig. 14: Miniature temperature logger (MTL) and its housing with supporting fin along the HF probe.

Heat flow data reduction

Processing temperature data includes calibration of thermistor sensors, calculation of sediment temperatures and temperature gradients and calculation of thermal conductivities when applicable. While the 7-minute wait is not long enough for the sediment temperatures to return to equilibrium after the frictional disturbance of penetration, it is long enough to extrapolate to an equilibrium temperature with a high degree of precision. Each temperature time series, from each thermistor, is extrapolated to an equilibrium temperature by the program 'T2C' (Hartmann & Villinger, 2002). Because the calibration of each thermistor by the manufacturer is only good to 0.1°C, a secondary calibration is applied. In this case it was performed in advance with reference to a high precision thermometer (Brancker) to an accuracy of better than 5 mK. Sediment conductivities were not measured during this survey, but recovered material from gravity and piston cores allow determination of thermal conductivities at the geo labs of University Bremen.

Fourier's law of heat conduction in one-dimension shows that heat flow (Q) is the product of the thermal gradient (dT/dz) and thermal conductivity (k). If these terms are constant over the depth of the measurements then the calculation of heat flow is trivial. However if these values are changing proportionately to each other, as is the case for a constant basal heat flux, then heat flow can be derived from Bullard's (1939) relation given by,

$$\Delta T = Q \; S \; \Delta z_i / k_i \; ,$$

where Δz_i is the thickness and k_i is the thermal conductivity over the i^{th} interval. In this case heat flow can easily be calculated as the slope of the line given by the summation. To

properly calculate the temperature gradient a correction for the penetration tilt angle is applied. In most cases the tilt angle is less than 10° and the tilt correction is modest. Thermal conductivities are sensitive to the sediment porosity over the depth range of the measurements. Thermal conductivities are summarised as harmonic means.

5.6. CPT Testing

(S. Stegmann, A. Kopf, M. Lange)

On R/V *Meteor* cruise M73/1, we used two RCOM free-fall CPTU probes. Cone Penetration Testing (CPT) is an effective method for *in situ* measurements of these geotechnical parameters with one instrument (Lunne et al., 1997). Two different marine CPT probes measure sedimentary strength (tip resistance, sleeve friction), pore pressure, tilt and acceleration. Both CPT systems rely on an industry 15 cm^2 piezo-cone with the sensors at the tip and a pressure housing containing a microprocessor at the top. In addition, deceleration and tilt are monitored for vertical profiling of the penetrated sediment column. The lightweight (40-170 kg), shallow water (200 m depth) lance works completely autonomous with a volatile memory and battery package. The sturdier, deeper water (currently 2500 m depth, anticipated 4000 m depth) system uses both power and telemetry for real-time data transmission from *Meteor*, although spare batteries accommodate for limited use in autonomous mode. In detail, please refer to the two chapters below.

Instruments

The lightweight free-fall CPT (FF-CPT) instrument for shallow marine use consists of an industrial 15 cm^2 piezocone and a water-proof housing containing a microprocessor, volatile memory, battery, and accelerometer (Fig. 15; see also Stegmann et al., 2006). Strain gauges inside the probe measure the cone resistance and sleeve friction by subtraction. A single pore pressure port (u_2) is equipped with an absolute 10 MPa pressure sensor. An inclinometer is used installed to monitor the penetration angle at +/-20° relative to vertical. An accelerometer provides information about the descent velocities and deceleration behaviour of the instrument upon penetration. It enables to calculate penetration depth during multiple deployments by integration. The aluminium pressure housing tolerates 2 MPa confining pressure (ca. 200 m water depth) and hosts the power supply and microprocessor. Frequency

of data acquisition is variable, and is has usually been set to 40 Hz during our tests. Binary data are temporarily stored on a Micro Flash Card and then downloaded to a PC. The two non-volatile battery packs available provide performance times of about six and twelve hours, respectively. The length of the lance may be varied from 0.5 m to a max. 6.5 m depending on what type of sediment is anticipated. The extension is accomplished by adding 1m-long metal rods and internal extension data/power cables within them. The weight of the instrument thus ranges from ca. 45 kg to max. 110 kg. If deep penetration is desired, modular weight pieces (15 kg each) can be mounted to the pressure housing at the top of the instrument, then reaching a max. 170 kg. The instrument is deployed pogo-style and remains in the seafloor for about 20 minutes for individual measurements.

The deep-water CPT probe (short DW-CPT) is a sturdier version of the shallow water FF-CPT. It has a length of 580 cm with a standard 15 cm^2 piezocone with strain gauges inside the probe measure the cone resistance and sleeve friction by subtraction (Fig. 15; see Stegmann & Kopf, 2007). Like the SW-CPT, it contains an accelerometer, tilt meter, and a microcontroller. Pore pressure ports at the cone (u_1) and ca. 80 cm above the cone (u_3) are connected to Validyne DP215 differential pressure transducers via stainless steel tubing. Pore pressure changes can be monitored over a range of 100 kPa with a resolution of ca. 10 Pa; the sensors are protected with valves if high excess pore pressures are met. They are further used to bleed the tubing in case of gas is trapped inside, especially during the initial phase of deployment when the instrument is lowered through the water column.

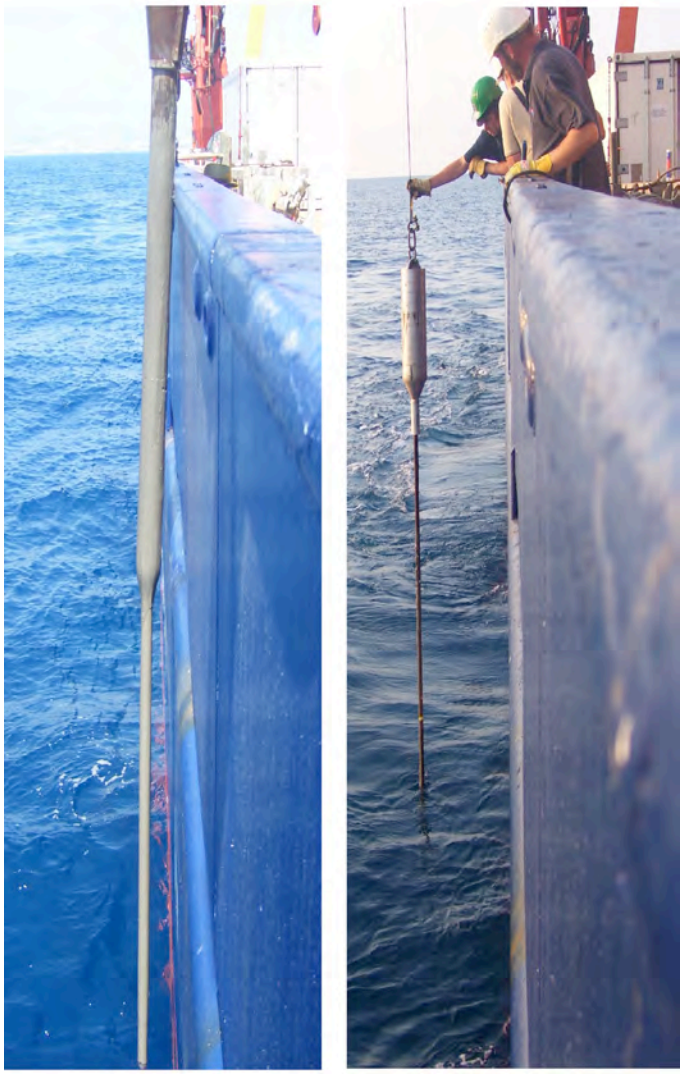

Fig. 15: Deep-water (left) and shallow-water FF-CPTU (right) instruments during M73-1.

The DW-CPT may be used in autonomous mode, where two batteries power a microcontroller, the sensors, and valves. In addition, it can be run with a Seabird Electronics (SBE36) telemetric system so that depth, tilt of the probe, and information from all sensors can be monitored on board the vessel. The SBE36 system with PDIM deck unit is schematically shown in Figure 16. It provides power and real-time data acquisition as well as control of the instrument via a attached PC with custom-programmed LabView control software. During cruise M73-1, we used the DW-CPT with the telemetric control during all the deployments.

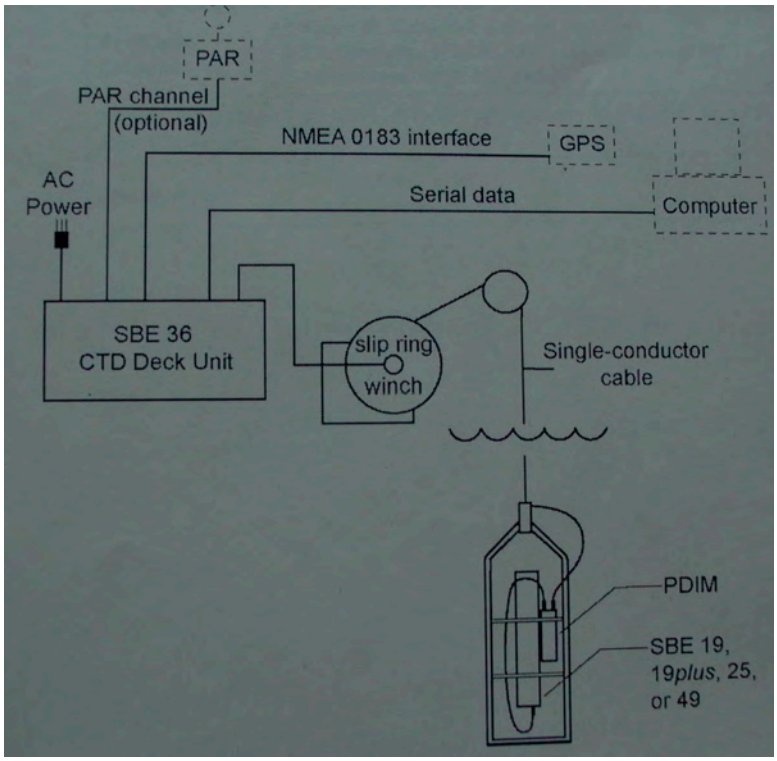

Fig. 16: Schematic of SBE36 and PDIM telemetric unit.

5.7. Gravity coring and sediment description

(B. Dennielou, T. Krumova, A. Förster, F. Girault, M.-A. Meier)

In order to recover sediment cores, a push corer of a total length of 1 m (Fig. 17) as well as a gravity corer with tube lengths of alternatively 2 to 10 m and a weight of approximately 1.6 tons were used during M73/1 (Fig. 18). For lengths exceeding 5 m, a cradle installed at the starboard-side of the vessel was used to get the instrument from the deck into vertical position aside the ship, and vice versa. Before using the coring tools, the plastic liners inside the steel tubes have been marked lengthwise with a straight line in order to retain the orientation of the core for potential paleomagnetic analyses.

Fig. 17: Push corer by IFREMER Brest.

Fig. 18: Gravity corer deployed during cruise M73/1.

Once on board, the sediment cores were cut into sections of 1 m length, closed with caps on both ends and labelled according to a standard scheme (Fig. 19). By definition, the half core with the marked line was stored as archive half (after having passed the MSCL – see Ch. 5.8.3), while description, sampling, etc. were carried out on the remaining half. For the detailed procedures each working half core underwent, see below.

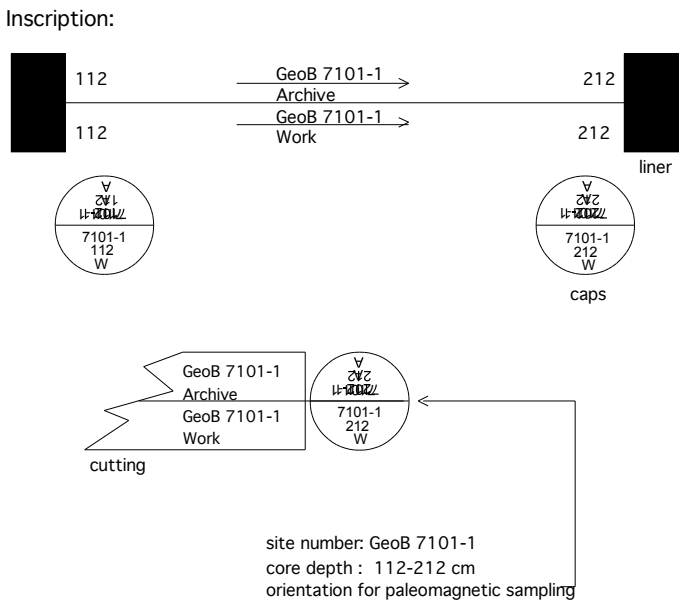

Fig. 19: Scheme of the inscription of gravity core segments used during M73/1.

Sediment description

Split gravity cores were photographed and described from a largely sedimentological standpoint. Grain size and composition of sediments were determined mainly visually using a simple hand-lens, HCl-testing and analyzing smear slides of dominant lithologies under a cross-polarizing microscope in accordance with Rothwell (1989). The size of grains was assessed based on Wenthworth's (1922) classification. The colour of the material was determined visually on board using Munsell's colour chart nomenclature, and also has been studied spectrophotometrically after the cruise on the Multi-Sensor Core Logger (MSCL). For each core, a composite one-page core log sheet was compiled. It shows core photographs next to a graphical core log and gives information on redeposition-/event layers (i.e., sand layers, volcanic ash layers or clear evidence for mass movement deposits, such as mud clasts in muddy or sandy matrix, tilted beds and repetition of strata), bioturbation and the assigned lithological units in three different columns. The core log is combined with results from the fall cone penetration test (see below). A wide variety of features, such as sediment lithology, primary sedimentary structures, bioturbation, soft-sediment deformation, and coring disturbance is indicated by patterns and symbols in the graphic logs. A key to the full set of patterns and symbols used on the barrel sheets is shown in Figure 20**.** The symbols are schematic, but they are placed as close as possible to their proper stratigraphic position. All core descriptions are provided in Appendix 9.3 (see below).

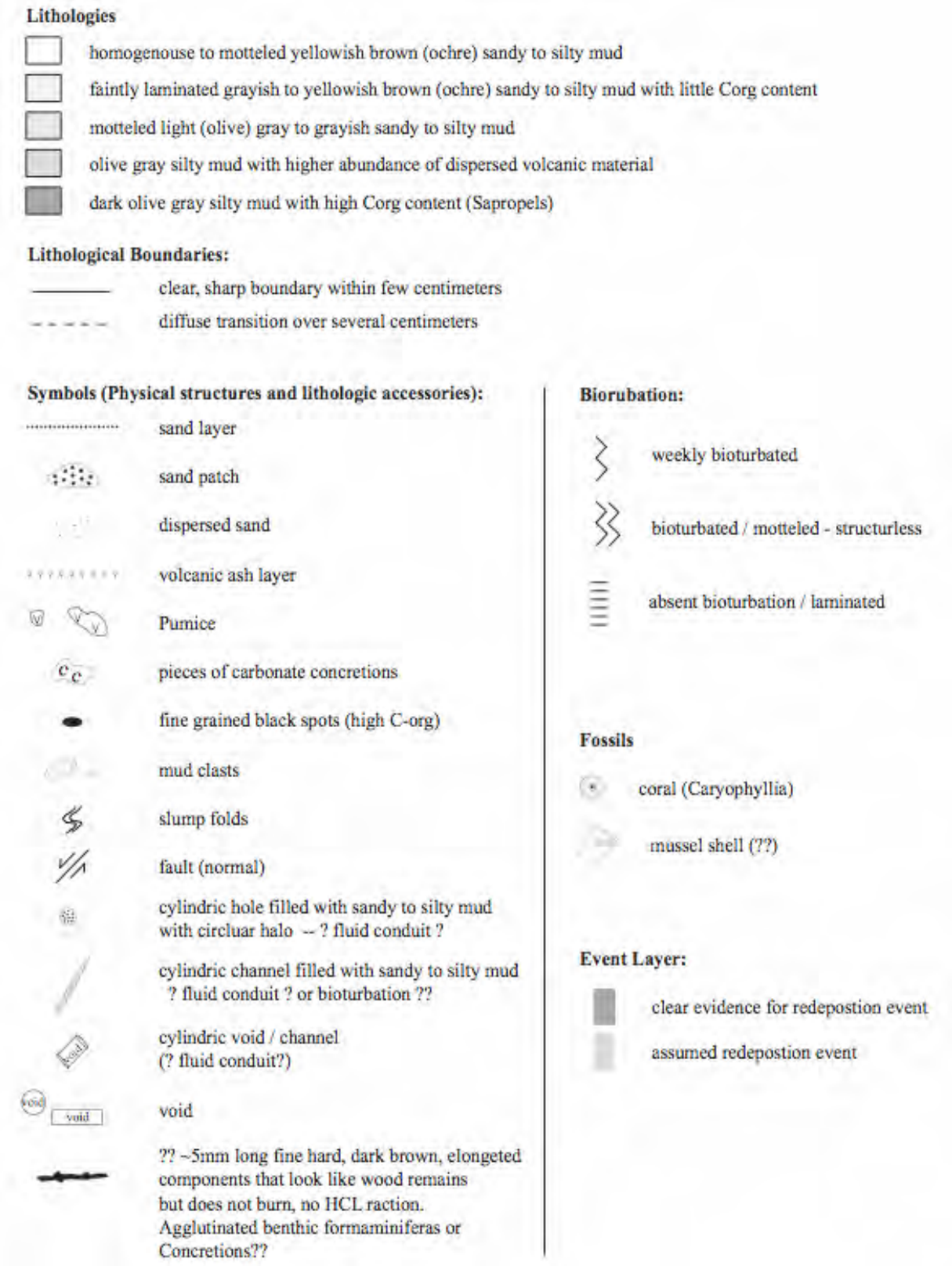

Fig. 20: Key of symbols for barrel sheets of gravity core description.

5.8. Physical properties

(A. Förster, E. Alexandrakis, S. Stegmann, A. Kopf)

During cruise M73/1, shipboard physical properties measurements were restricted to falling cone penetration tests and vane shear tests on the working half of the core. Since no container with a Multi-Sensor Core Logger (MSCL) could be placed on board RV *Meteor*, these measurements on the undisturbed archive half of the cores were carried out immediately after the cruise at RCOM Bremen. A description of the instrument is given below (Ch. 5.8.3.).

5.8.1. Cone penetrometer

The geotechnical properties along the sediment cores were determined according to British Standards Institutions (BS1377, 1975). A Wykeham-Farrance cone penetrometer WF 21600 (Fig. 21a) was used for a first-order estimate of the sediment's stiffness. For the measurement, the metal cone was brought to a point exactly on the split core face. A manual displacement transducer was then used to measure the distance prior to and after release of the cone (i.e. penetration after free fall of the cone). Precision is 0.1 mm of displacement. The distances measured can then be translated into sediment strength (see Hansbo, 1957).

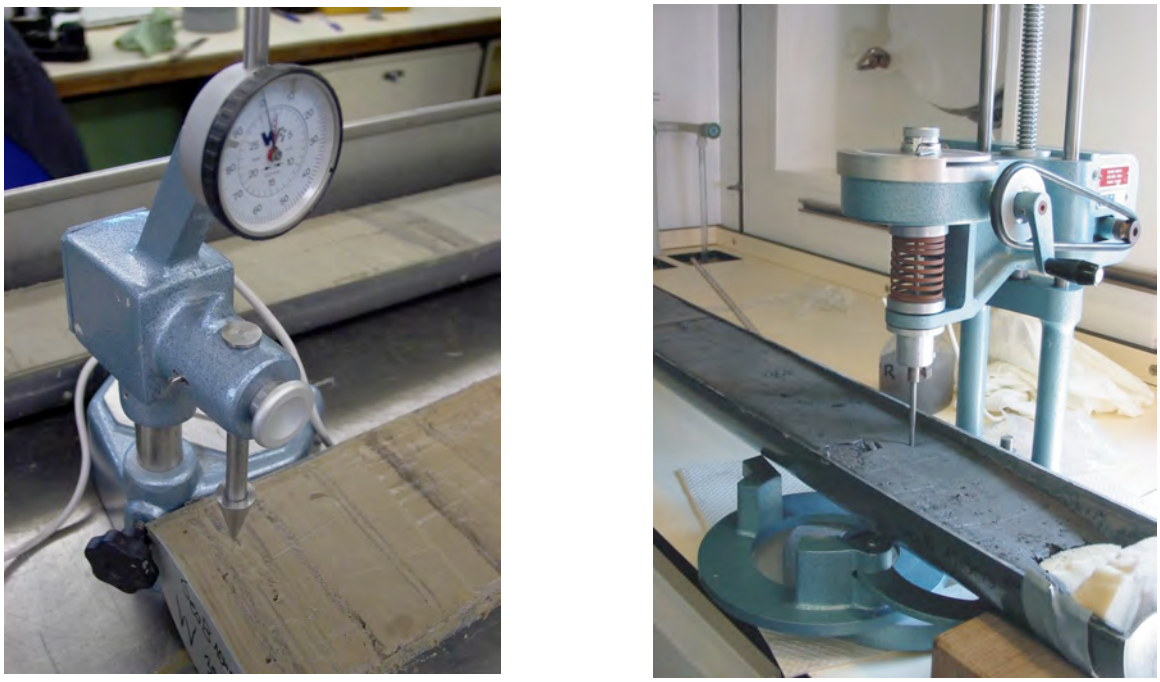

Figure 21. (a) Falling cone penetrometer and (b) Vane shear device used on the split core surface.

A falling cone penetrometer with a defined weight (80.51 g) and geometry (30° cone) was used by Hansbo (1957) during a detailed study of the relationship between the cone penetration and soil strength. The undrained shear strength s_u can be calculated from the variables mass and tip angle of the falling cone, gravity *g*, penetration depth *d* and the cone factor *k* via the "cone factor". Wood (1985) calculated from fall-cone and miniature vane tests average values of cone factors (in our case k=0,85 for a 30° cone). The undrained shear strength can then be calculated using the equation $s_u = (k*m*g)/d^2$.

Shore-based laboratory testing will include ring shear experiments as well as dynamic triaxial shear tests to obtain residual strength and rate-dependent frictional properties as well as the liquefaction potential of the materials recovered.

5.8.2. Vane shear testing

In addition to the Cone Penetrometer a Mennerich Geotechnik (Hannover) vane shear apparatus was used for more information about sediment stiffness and residual shear strength (Fig. 21b). For the measurements, a four-bladed vane (L = 12.5 mm, h = 6.25 mm, d = 12.5 mm) was inserted into the split undisturbed core faces and rotated at a constant rate of 90°/min.

A spring transmits the rotation at the vane. The torque required shearing the sediment along the vertical and horizontal edges of the vane. The undrained shear strength, s_U depends on the torque T, the vane constant K, the maximum torque angle at failure σ and the spring constant B that relates the deflection angle to the torque (Blum, 1997). The vane constant, K is a function of the vane size and geometry and was used during the measurements with $K=\pi*d^2*(h/2)+\pi*(d^2/6)$ for full dipping vanes. The undrained shear strength can then be calculated using the equation $s_U= T/K$. Shore-based laboratory testing will include ring shear tests to obtain residual strength and rate-dependent frictional properties of the materials recovered.

5.8.3. Multi-sensor core logger

The *GEOTEK* MSCL device at RCOM Bremen combines three sensors on an automated track (see schematic diagram in Fig. 22). The P-wave velocity, gamma ray attenuation (bulk density), and the magnetic susceptibility were recorded, and from this data the fractional porosity and impedance were calculated. RGB images were also produced with a full color

digital line scan imaging system. Magnetic susceptibility, bulk density, and line scan photography were generally measured on all cores.

Magnetic Susceptibility

Magnetic susceptibility was measured with a Bartington point sensor MS2 using an 80-mm internal diameter sensor loop (88-mm coil diameter) operating at a frequency of 565 Hz and an alternating field of 80 A/m (0.1 mT). The sensitivity range was set to the low sensitivity setting (1.0 Hz). The sample period and interval were set to 2 s and 4 cm, respectively, unless noted otherwise. The mean raw value of the measurements was calculated and stored automatically. The quality of these results degrades in XCB and RCB cores, where the core may be undersized
and/or disturbed. Nevertheless, general downhole trends are useful for stratigraphic correlations. The MS2 meter measures relative susceptibilities, which have not been corrected for the differences between core and coil diameters.

Gamma-Ray Attenuation

Bulk density was estimated for split core sections as they passed through the GRA bulk densiometer using sampling periods and intervals of 2 s and 4 cm, respectively, unless noted otherwise. A thin gamma beam from a Caesium-137 source with energies around 0.662 MeV is passed through the core and the relative intensity of this beam can be used to measure the gamma density. These photons are scattered by electrons in the core and loose some of their energy. To determine the gamma density the number of unscattered electrons is measured by counting photons with the same principle energy as the photon source. The gamma density of an aluminum billet of stepped thickness is used to obtain calibration equations to convert gamma density into actual density values.

P-Wave Velocity

The P-wave velocity is measured at 4-cm intervals and 2-s periods using two PWL transducers. The PWL measured P-wave velocity across the unsplit core sections. In order to determine the P-wave velocity, the PWL transmits 500-kHz P-wave pulses through the core at a frequency of 1 kHz. The transmitting and receiving transducers are aligned perpendicular to the core axis while a pair of displacement transducers monitors the separation between the P-wave transducers. Variations in the outer diameter of the liner do not degrade the accuracy of the velocities, but the unconsolidated sediment or rock core must completely fill the liner for the PWL to provide accurate results. During this

measurement good acoustic coupling between the core liner and transducer is achieved by adding water to the contact points.

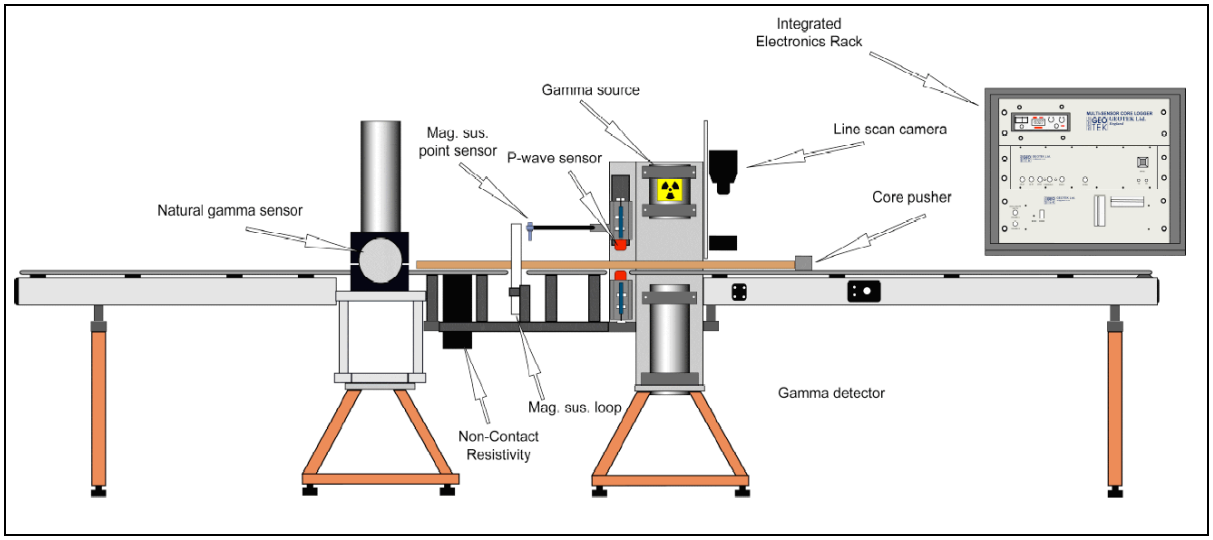

Fig. 22: Schematic of the Geotek Multi Sensor Core Logger (MSCL).

5.9. Pore water chemistry

(J. Blees, K. Bogus, T. Haarmann, M. Hentscher)

Pore water sampling

All gravity cores were taken by plastic liners and cut into 1 m segments on deck. To prevent a warming of the sediments on board, the sediment cores were immediately transferred into the cooling room after recovery and maintained at a temperature of about 4°C. The wet sediment was exposed by means of cutting a small ‘window’ in the plastic liner at an interval of 25 cm. Eh and pH were measured directly in the sediment using punch-in electrodes before the pore water was extracted. From most of the cut segments of the cores 5 ml syringe samples of wet sediment were taken for methane analysis. The pore water was then extracted by means of rhizons (pore size 0.1 µm) (see Fig. 23a). The gravity cores were each processed in this way within a few hours after recovery. Depending on the porosity of the sediments, the amount of pore water recovered ranged between 4 and 20 ml. Solid phase samples of the majority of cores were taken for total digestions, sequential extractions and mineralogical analyses at 25 cm intervals, kept in gas-tight glass- and heavy plastic bottles under an argon atmosphere and stored at 4°C.

Pore water analyses of the following parameters were carried out during this cruise: Eh, pH, ammonium, alkalinity, iron (Fe^{2+}). Salinity was also measured for selected cores where fluid freshening was suspected (see Ch. 6.9.). Eh and pH, as mentioned earlier, were determined with punch-in electrodes before pore water was extracted. Ammonium was measured using a conductivity method. Alkalinity was calculated from a volumetric analysis by titration of either 0.5 or 1 ml of the pore water samples with 0.01 M HCl, respectively. For the analyses of dissolved iron (Fe^{2+}), subsamples of 1 ml were taken from pore water extracted by rhizons, immediately complexed with 50 µl of "Ferrospectral" and determined photometrically. Salinity was measured using a conductivity probe placed directly into the pore water samples.

For further analyses at the University of Bremen and the Alfred Wegener Institute for Polar and Marine Research (AWI) in Bremerhaven, aliquots of the remaining pore water samples were diluted 1:10 and acidified with $HNO_{3\ (suprapure)}$ for determination of cations (Ca, Mg, Sr, K, Ba, S, Mn, Si, B, Li) by ICP-OES and AAS. Additionally, 1.5 ml subsamples of the pore water were added to a ZnAc solution (600 µl) in order to fix all hydrogen sulfide present as ZnS for later analysis. Finally, all remaining pore water was stored at 4°C for any additional analyses at the University of Bremen and the AWI Bremerhaven. A complete overview of sampling procedures and analytical techniques used on board and in the laboratories at the University of Bremen is available on http://www.geochemie.uni-bremen.de/koelling/MGCmain.html.

5.10. Remotely operated vehicle (ROV)

(A. Kopf, H. Hanff, S. Klar, M. Lange)

The remotely-operated vehicle (ROV) "Spy" is a shallow-water device (operable down to 250 m water depth). Its depth range is largely limited by the total length of the cable, which is supplied on a separate winch. The ROV is powered by either 230 DC or 350 DC and is controlled by a console unit with VHS TV screen and a keyboard for the operations. The ROV is equipped with two underwater cameras. One is looking towards the ground while the other one is looking forward. For operation at night or in areas with poor visibility, it is equipped with a pair of headlights. Two turbines at the back control forward/backward movement, while another pair of subvertically mounted turbines control submersion or ascent (Fig. 23b). Its total weight of 60 kg (in air) has to be balanced depending on water

density and payload. During cruise M73/1, it was largely used for surveying for low salinity fluid (with a CTD; see ch. 5.2) and seafloor anomalies (using the cameras).

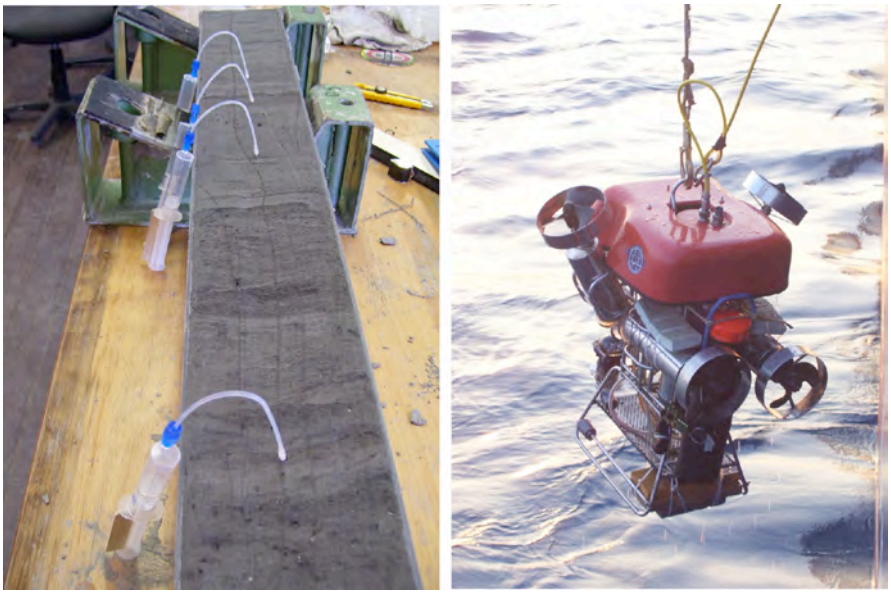

Fig. 23: (a) Rhizon sampling on the split core; (b) ROV with high-resolution CTD system (between the turbines at the back of the device) for surveying bottom waters with regards to salinity anomalies from fresh water discharge. See “Results” below.

6. Preliminary Results

The preliminary results from cruise M73/1 can be divided in a number of topics related to five distinct areas. They are

- Nice Airport slide
- Shallow to Mid-slope area
- Eastern Landslide Complex
- Western Landslide Complex
- Var Canyon turbiditic system,

and are schematically shown in Figure 24. In Chapter 6, many of the sub-chapters follow the distinction into these five areas, which are generally highlighted by sub-headers.

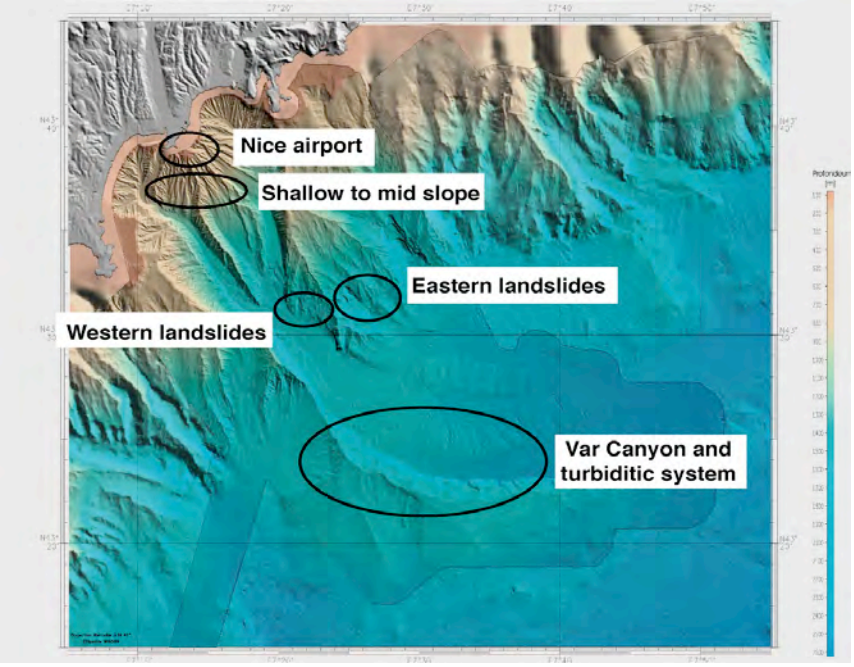

Fig. 24: The five study areas visited during cruise M73/1.

6.1. Multibeam Swathmapping

(F. Strozyk, J. Metzen, S. Krastel, V. Spiess)

Raw data of both operating systems (SIMRAD EM120 and EM710) was gridded using MB-System and/or the ship-internal SIMRAD software. Grid spacing is 25 m for the EM120 and 10 m for the EM710. Depth-plots of both datasets are presented in Figures 25a and 25b. Depth in the covered area of ~2000 km^2 ranges from 10 m – 2500 m below sea level for the EM120 system, which recorded data during the whole cruise.

and 25b. Depth in the covered area of ~2000 km^2 ranges from 10 m – 2500 m below sea level for the EM120 system, which recorded data during the whole cruise.

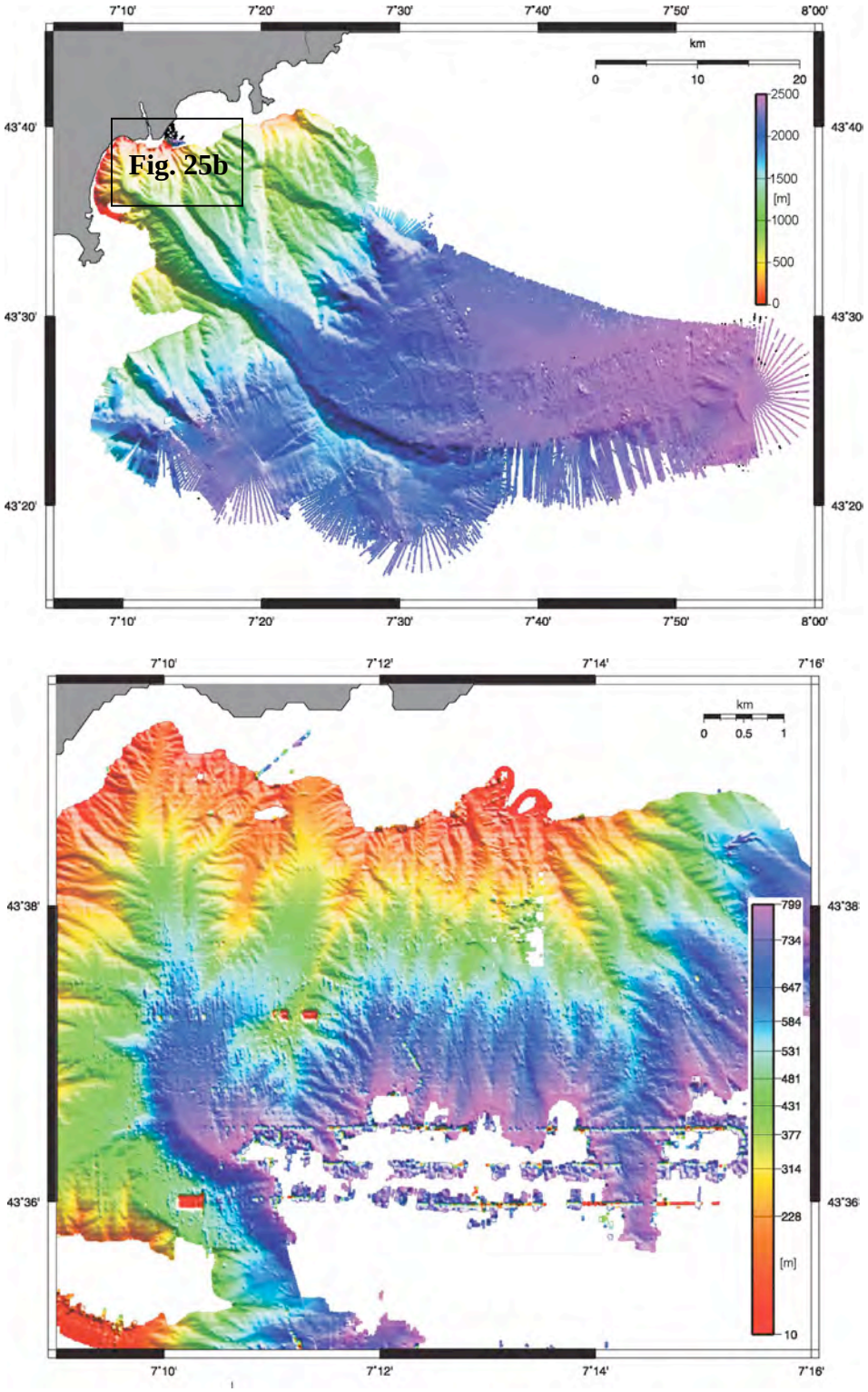

Fig. 25: (a) Depth plot of the EM120 multibeam system. The high amount of gaps within data of deeper waters indicates an unbalanced data acquisition due to ship speed. (b) Depth plot of the EM710 multibeam data. E-W-tracks in the southern area indicate the increase of errors with increasing depth and the limited range of this system.

EM710 provides data of the Nice Airport, the shallow- and mid-slope and the upper Var Canyon. It was primarily used as an addition for the EM120 in the shallower coastal area. Data reaches 10m – 800 m water depth within ~100 km^2, whereof data below 500 m shows a strong increase of errors and data gaps: with increasing water depth, coverage of bathymetric data got more and more fragmented due to an inaccurate interaction of ship speed and duration of the multibeam signal.

Data of both operating systems deliver the typical dendritic canyon-structures in combination with "fingering" ridges of the slope south of Nice in shallower waters up to 800 m depth. The Var canyon, leading from the NW coast to south, then south-east, is clearly observable on both data sets. Its continuation and expiring to the abyssal plain in greater water depth is only provided by the EM120 data.

Bathymetry data revealed two headwall structures in between 7°20'E to 7°30'E and 43°30'N to 43°33'N. Both appear as horseshoe-like escarpments in 1200 m to 1800 m water depth. A dense grid of seismic and Parasound profiles were shot in the areas of both slides events for further and detailed information.

6.2. Water Sound Velocity (CTD)

(M. Lange, A. Kopf)

Only one CTD profile was run at the beginning of the cruise (see station list, Appendix). Data served to calibrate the geophysical acquisition systems, but are otherwise not meaningful with respect to the objectives of cruise *LIMA-LAMO*, and are hence not presented here. As explained in Chapter 5.2, the CTD was also mounted on the ROV in order to get possible salinity variations in the ground water-prone coarse sediments at the Nice airport landslide scar. Since the CTD was limited to 300 m water depth, the deeper portion of the CTD profile was compiled from published data for the Mediterranean Sea.

6.3. Parasound profiling

(F. Strozyk, J. Metzen, S. Krastel, V. Spiess)

With the exception for some trouble-shooting using the ATLAS Parasound system at the beginning of M73/1, most tracks along seismic profiles and cruise transits could be recorded without technical or any other problems. Due to their inconsistent quality and problems when steep slopes are crossed, Parasound profiles were used in addition to multi-channel

seismic to locate slide sediments and potential headwalls. In the following paragraphs, we present typical Parasound recordings for each of the M73/1 study areas. For information on the location, refer to Figure 26 where the tracks are shown.

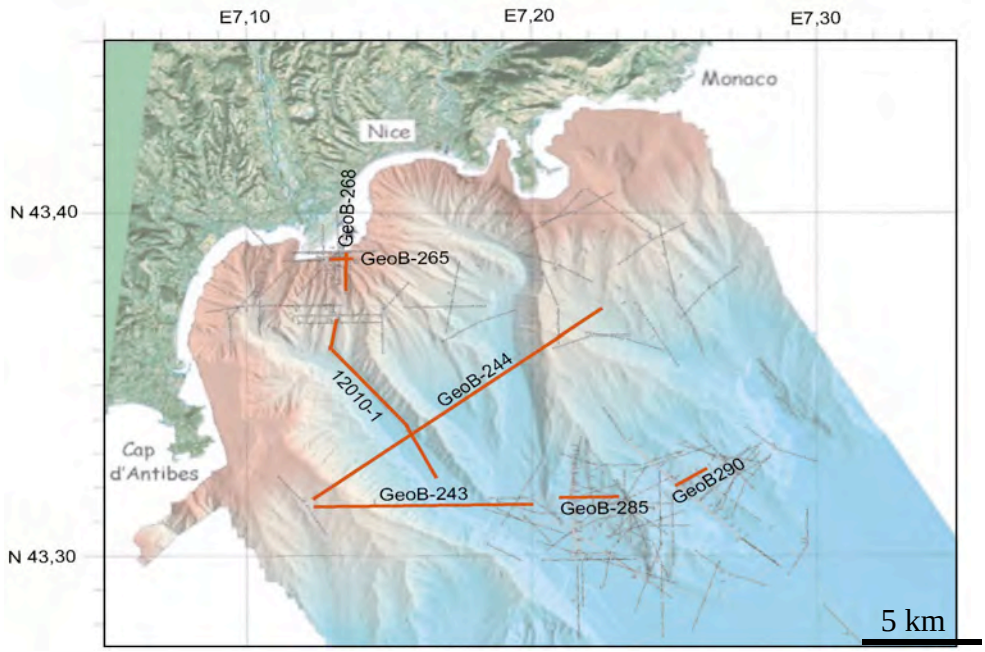

Fig. 26: Profile plan of parasound/MUCS profiles during M73-1.

Nice Airport

Parasound profile GeoB-265 (Fig. 27) shows a typical example of shallow-water profiling. Ground-penetration is 40-70 m in average. This cross-profile through the alternating system of ridges and canyons shows multiple smaller, lens-shaped slide-bodies on slopes at decreasing gradients.

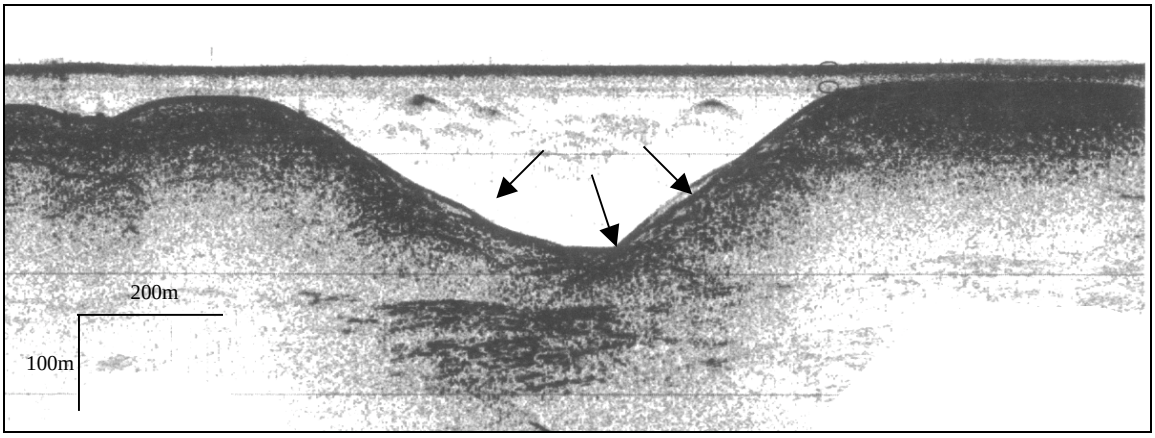

Fig. 27: Parasound E-W-profile GeoB-265 in 40 m to 160 m water depth. Arrows indicate the assumed appearance of slide sediments. See Figure 26 for location.

Shallow- and Mid-Slope

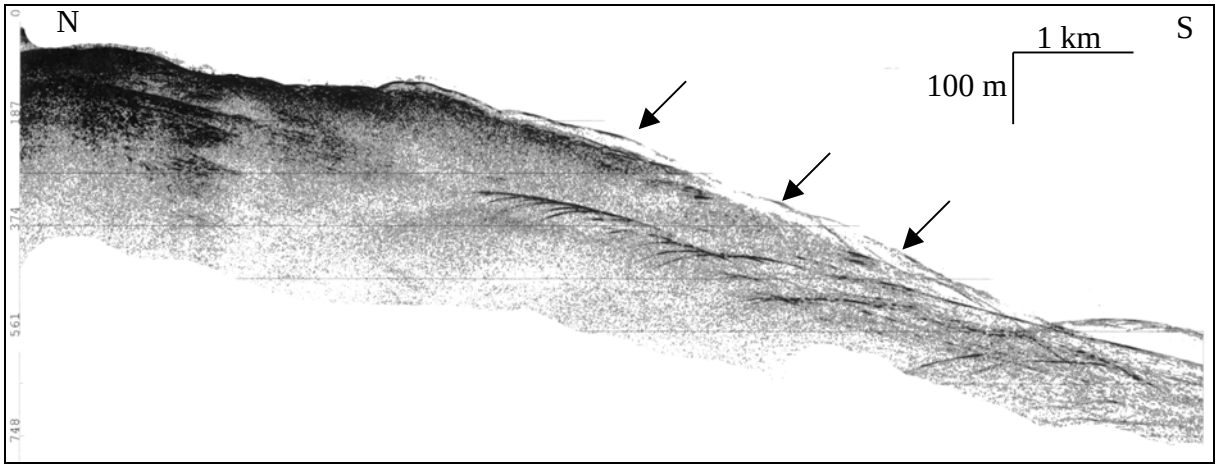

Fig. 28: Parasound N-S-profile GeoB-268 in <30 to >500 m water depth throughout down-slope slide sedimentation. See Figure 26 for location.

Profile GeoB-268 ranges from shallower waters (<30 m) near the Nice Airport (Area 1) to deeper waters of the shallow- and mid-slope (Area 2). It is located within one of the south-leading canyons, which are highly suspected as transport paths for slid sediments. Among others, this profile shows up a nearly continuous appearance of slide sediments, which could be recognized as transparent units on top of more or less intact slope sediments.

Eastern and western Landslides

The eastern and western landslide complexes appear to be multiple events with an elongated scar in downslope direction. Within the area of the eastern landslide, a headwall structure striking SE was identified on bathymetric data. Parasound profile GeoB-290 shows the eastern sidewall of this escarpment (Fig. 29a). The assumed quantities of slid sediment could not definitely be interpreted on available data. In general, no wide-ranging plane-bedded sediments are identifiable.

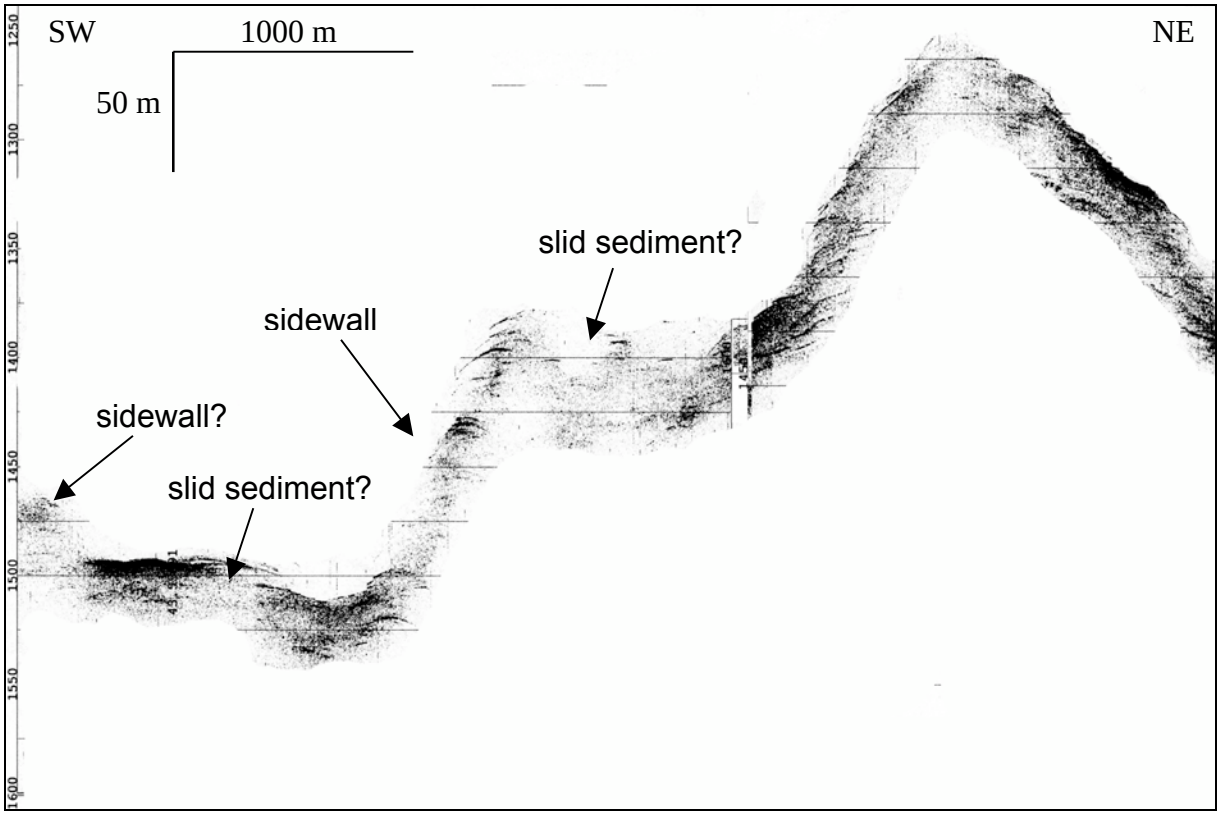

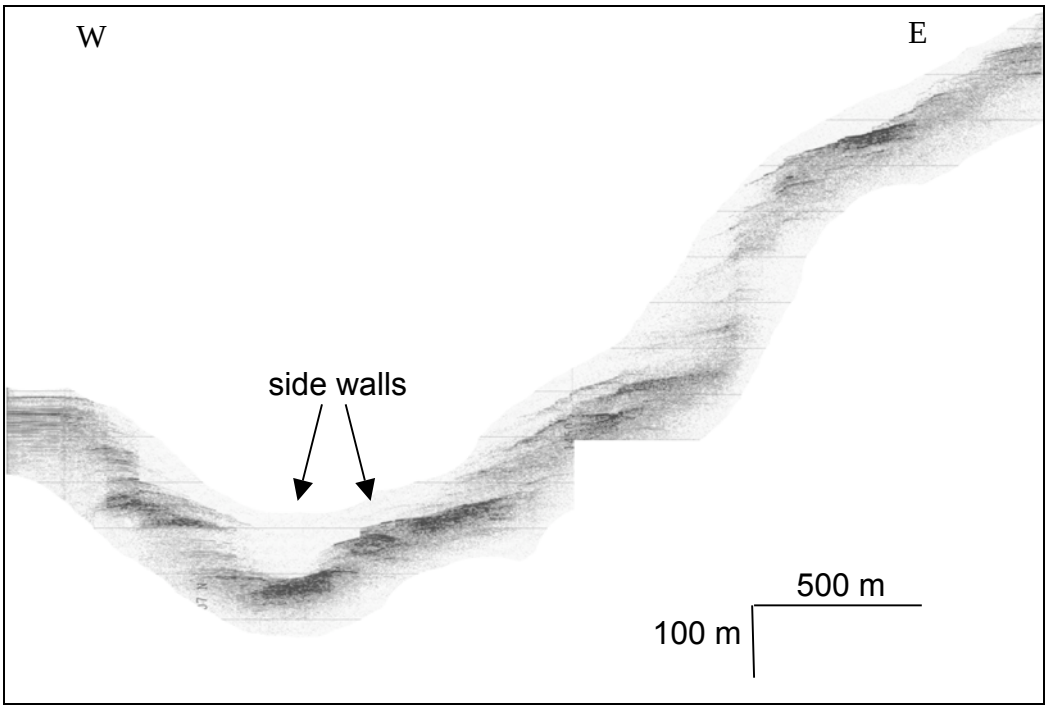

Fig. 29: (a) Parasound NE-SW-profile GeoB-290 in 1250-1520 m water depth across the Eastern Landslide. Sediment penetration is up to 40 m. (b) Parasound E-W-profile GeoB-285 in 1450 m to 1720 m water depth, showing sidewalls of the escarpment. Sediment penetration is 10-25 m. See Figure 26 for location.

The western landslide (Fig. 29b) was primarily recognized by its elongated headwall, which is found in >1600 m water depth heading south. Slid sediments are assumed within the southern extension of the Var Canyon in front of this escarpment.

Var Canyon and turbiditic system

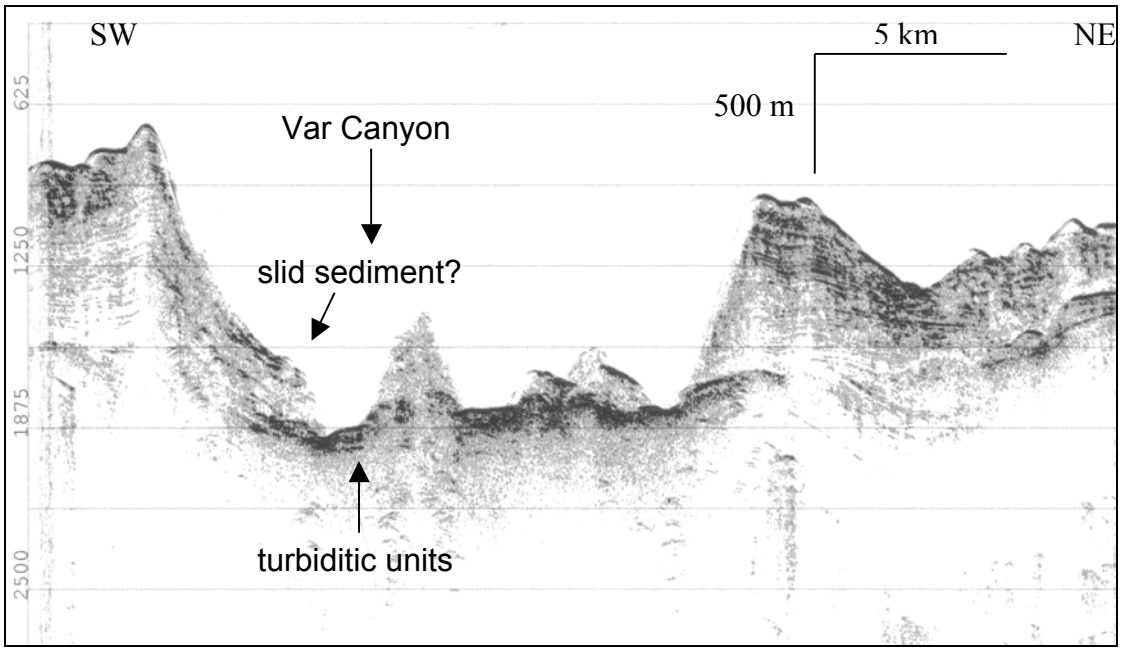

Fig. 30: Parasound NE-SW-profile GeoB-244, crossing the entire canyon-system in 700 m to 1900 m water depth. This profile pronounces the identification of three NW-SE-canyons and their separation with ridges. See Figure 26 for location.

Parasound profile GeoB-244 reveals the separation of three canyons and an accumulation of slid sediments at the bottom-most parts of slopes in this area (Fig. 30). Within the canyons, coring and bathymetry data indicate massive turbiditic units, which are also found in shallower and deeper waters up and down the Var canyon.

In addition, profile GeoB12010-1 shows a section down-slope from the mid-slope region (area 2) along the Var Canyon (area 5) and reveals an irregular surface (Fig. 31). Most of these structures refer to relief irregularities like extensions of the slope, but some of them may represent thick accumulations of turbiditic sediments and slide bodies.

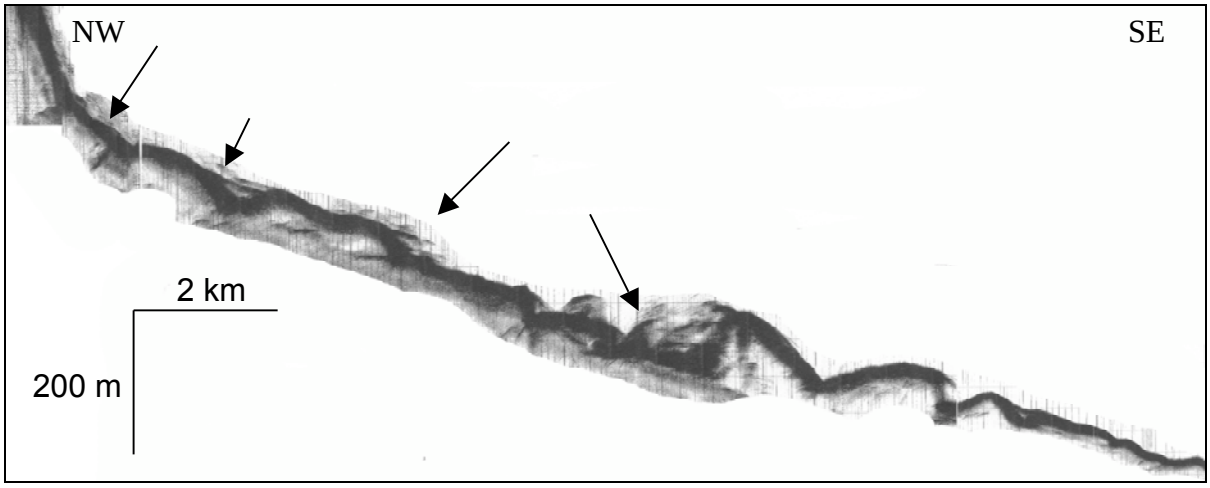

Fig. 31: Down-slope profile 12010-1 along the mid-slope and Var Canyon. Water depths are 1250 m to ~1900 m. Sediment penetration ranges from 80 m (shallower part) to 20 m (deepest parts). Arrows indicate assumed appearance of slid sediments and/or turbiditic units. See Figure 26 for location.

6.4. Seismic reflection profiling

(S. Krastel, V. Spiess, F. Strozyk)

Preliminary data processing was carried out for all profiles onboard. Several channels of each shot were filtered and stacked. These brute stacked were loaded to a seismic interpretation system (Kingdom Suite) and used for preliminary interpretation. The seismic survey was split in several parts (Fig. 32). The full list of lines is shown in Appendix 9.3. (see below).

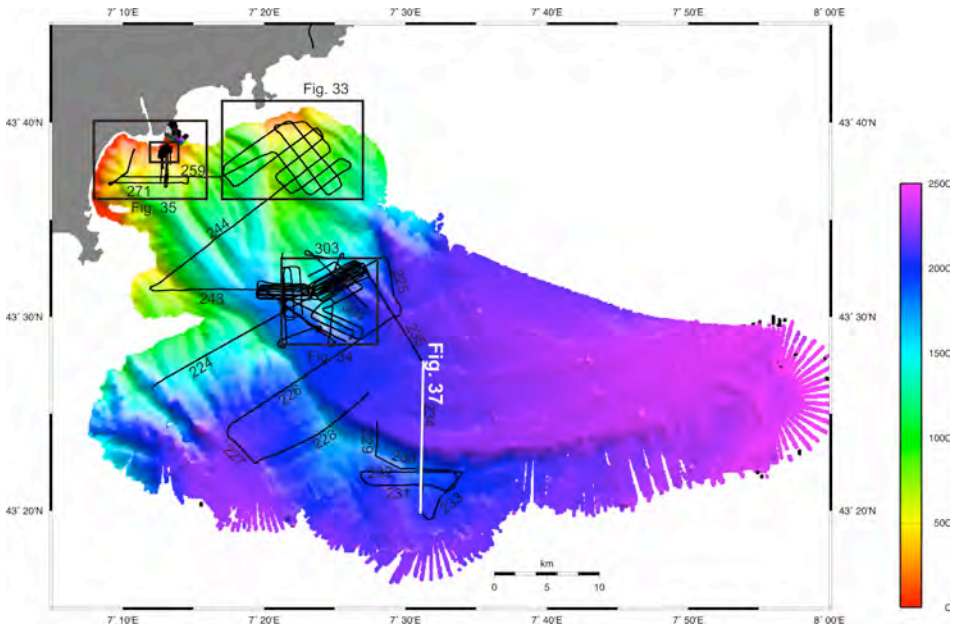

Fig. 32: Overview map of seismic reflection profiles.

More detailed track charts of the various M73/1 target areas are given in Figures 33-36, covering the mid-slope gullies, the eastern and western landslide complexes, and the Nice Airport landslide area (including a close up because of the narrowly spaced lines).

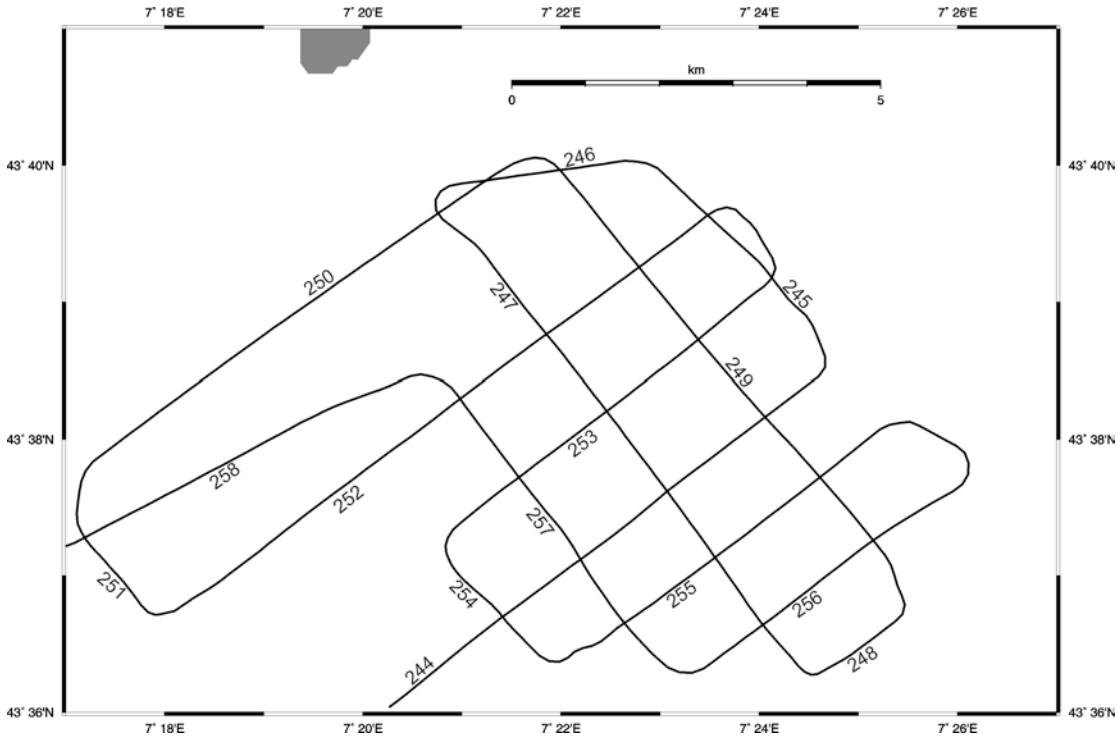

Fig. 33: Close up of track chart in a mid slope location.

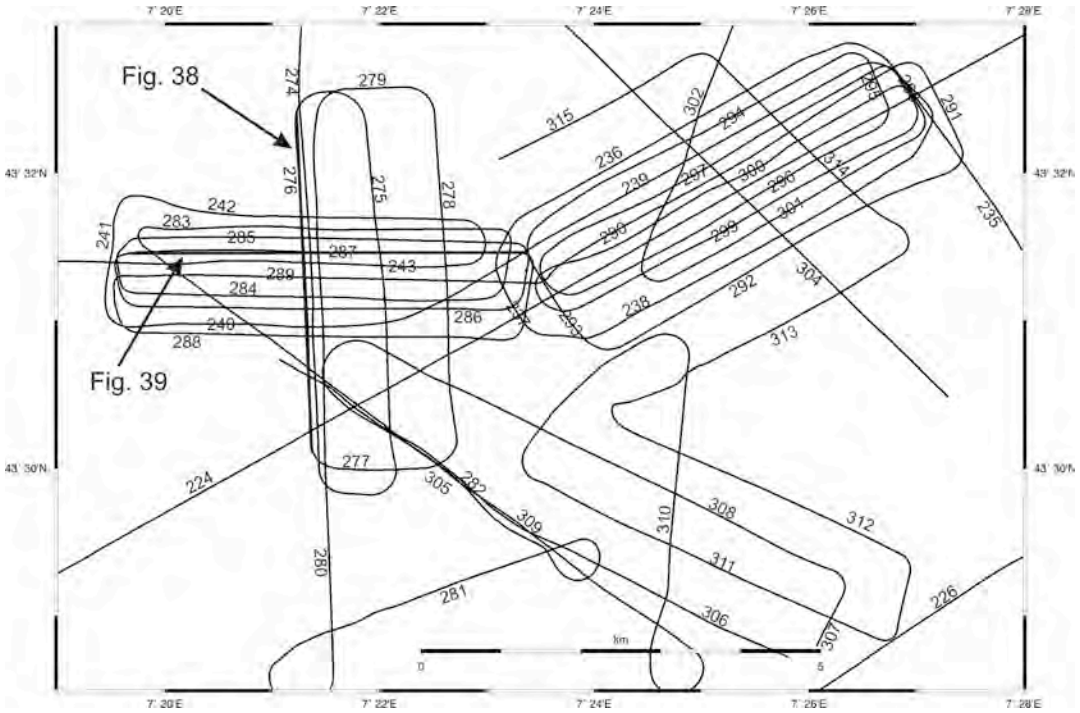

Fig. 34: Close up of track chart of the two landslide areas (eastern and western slide complex; see Fig. 24).

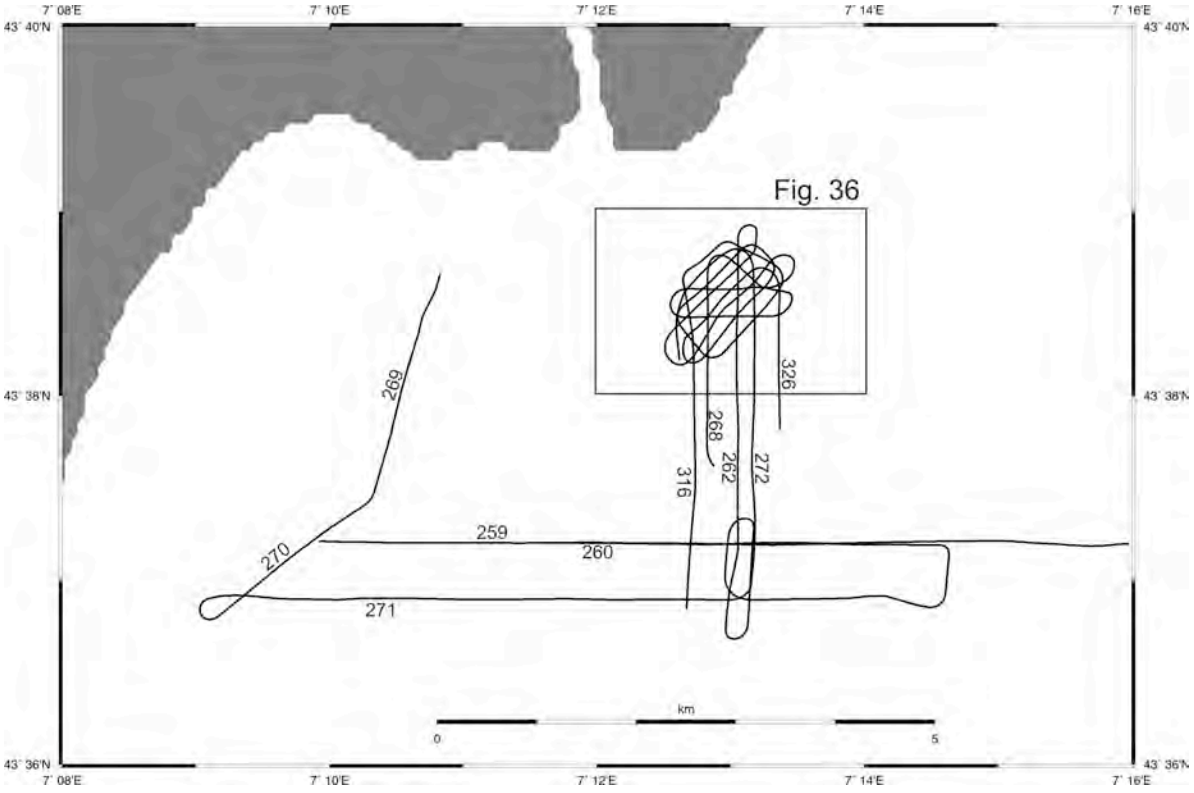

Fig. 35: Close up of track chart in the vicinity of Nice Airport.

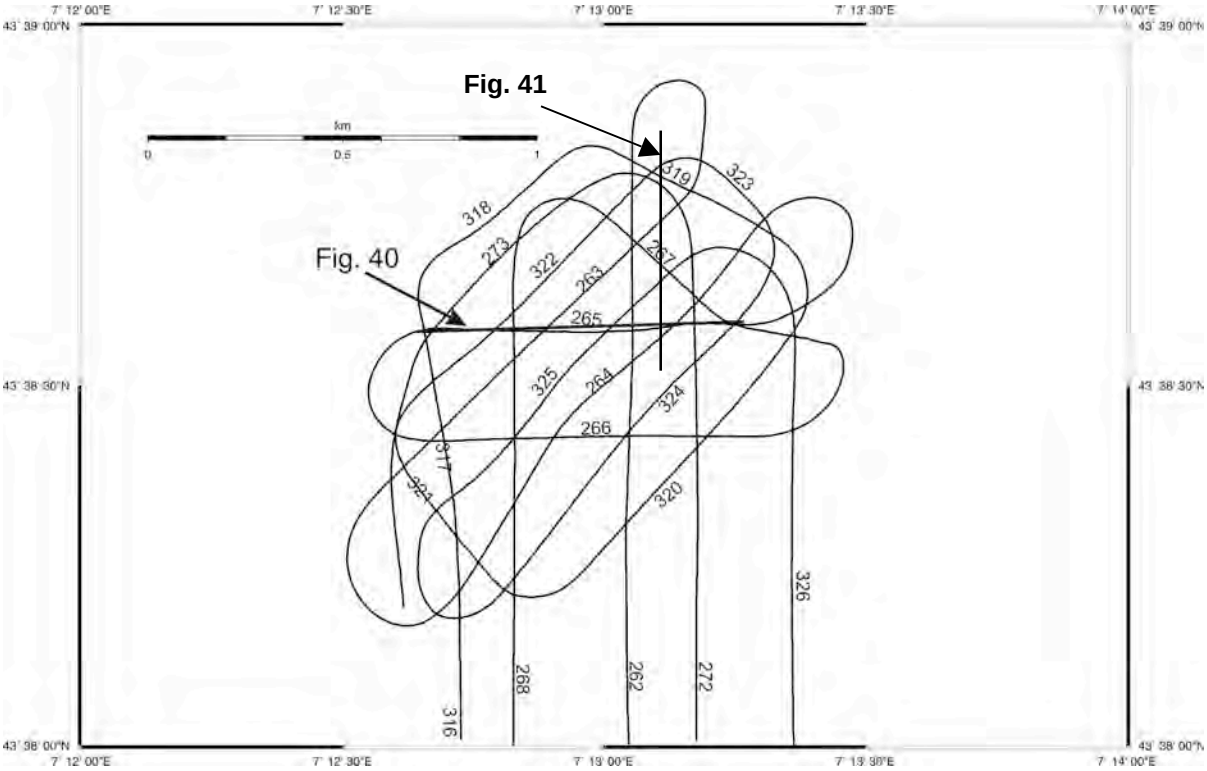

Fig. 36: Close up of track chart in the headwall area of the Nice Airport Slide.

The Var Fan System consists of a long fan valley and a high levee on the south side of the fan valley, the so called Var Sedimentary Ridge. Both features can be seen on Figure 37. The Var Sedimentary Ridge is characterized be well-stratified reflectors with a good continuity. The slightly divergent reflection pattern is typical for turbiditic levees. Two proposed IODP sites (LIMO-2a and LIMO-6b; see Henry et al., 2005) are located on the levee. The levee reflectors show medium amplitudes except for a narrow vertical zone between shot points 300 and 400, which is characterized by acoustic transparency. The zone of acoustic transparency is rooted at an anticline and might represent a small diapir. The seismic pattern of the fan valley is typical for silty to sandy sediments, which are imaged as high amplitudes reflectors with varying continuity. Turbidity currents spread through the entire fan valley and no distinct thalweg is visible. A V-shaped area with high amplitude reflectors is found slightly south of the present fan valley in a subsurface depth of ~150m. The high amplitude reflectors indicate a sandy infill of an older thalweg, hence suggesting a lateral migration of the fan valley.

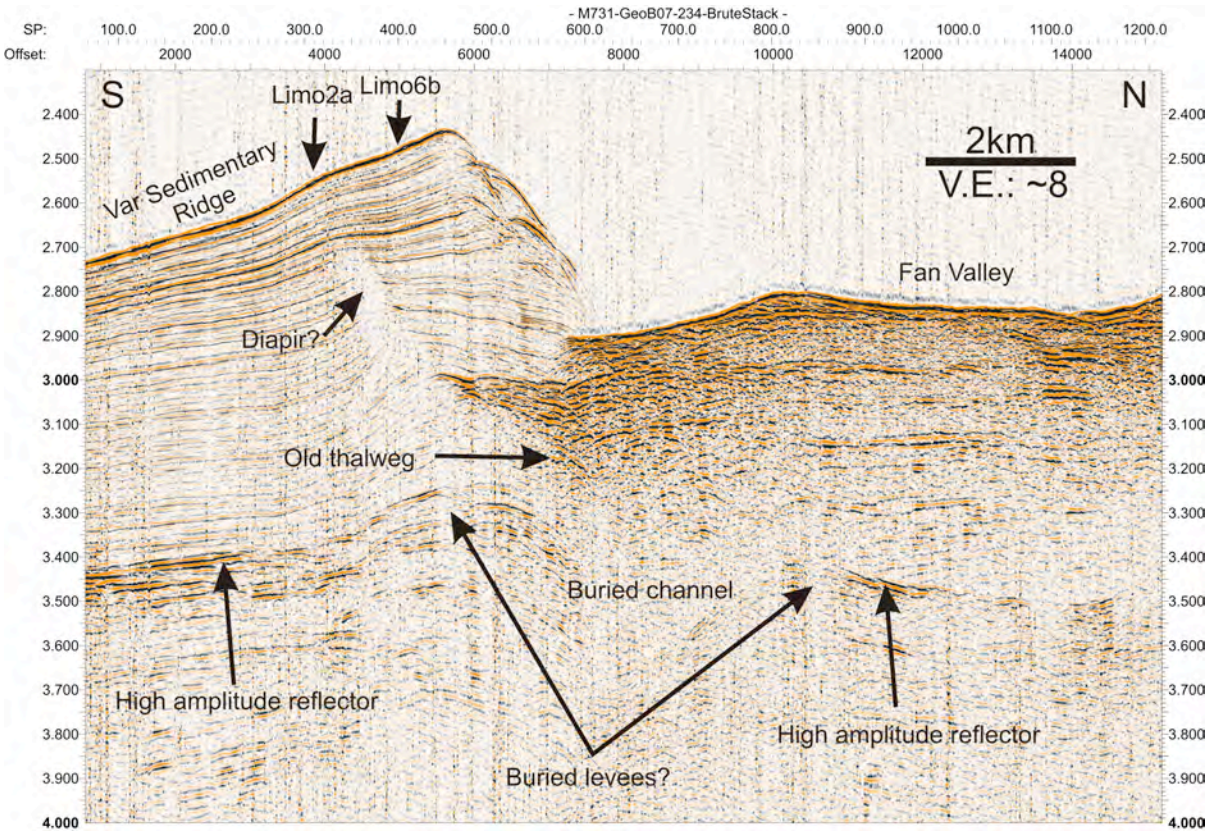

Fig. 37: Brute stack of seismic line GeoB07-234. See Fig. 32 for location.

An high amplitude reflector is imaged at a depth between 3.2s and 3.5s (Fig. 37). This reflector seems to mark a major sequence boundary with some onlap features though the exact relationship between sediments above and beneath this reflector is difficult to determine in the brute stack. A major depression of the sequence boundary is found between shot points 500 and 800. It is filled with flat lying reflectors, which represent the infill of an old channel. Buried levees might exist on both sides of the buried channel.

Several headwalls in a mid slope location were identified based on the bathymetric data. Two of these slides were survey by a dense net of seismic profiles, which will allow us to study the geometry and dynamics of these slides in great detail post-cruise. Figures 38 and 39 show seismic lines crossing the western slide.

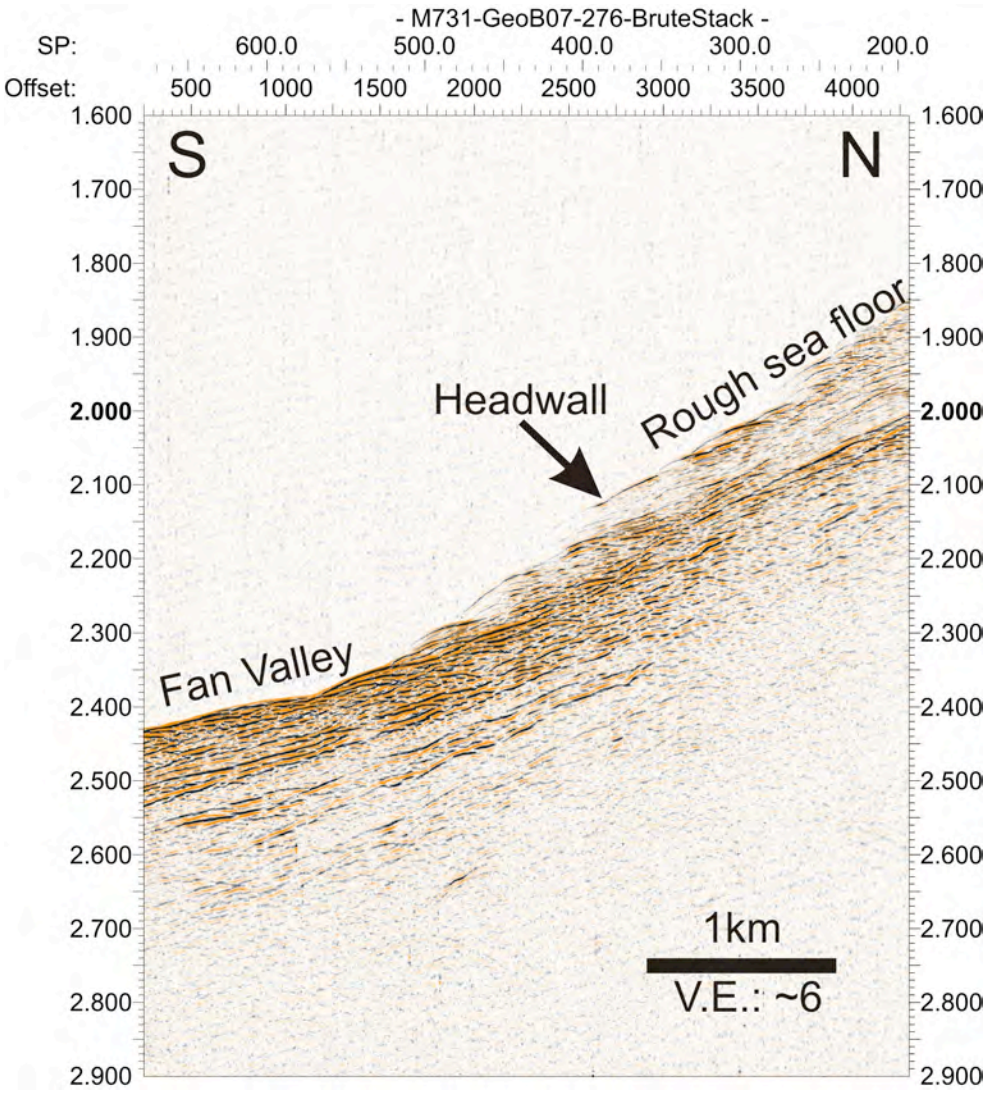

Fig. 38: Brute stack of Profile GeoB07-276. See Fig. 34 for location of profile.

Figure 38 follows the main slope gradient and crosses the headwall of the slide. Fig. 39 crosses the upper mainly erosive slide area perpendicular to the main slope angle. Both profiles demonstrate the complexity of this area with a number of slides and some indications for creeping. The headwall as imaged on Fig. 38 is not very clear due to side echoes but approximate headwall height is ~40m. The slide evacuated an elongated valley like depression with a width of ~300m and a length of 1.5km. No clear glide plain is visible on the seismic data. The area above and beneath the headwall shows a rough sea floor, which is most likely the result of older sliding or sea floor creeping. A buried slide with a thickness ~60m is clearly imaged on Profile GeoB07-287 (Fig. 39). The entire mid slope area seems to be unstable at this location.

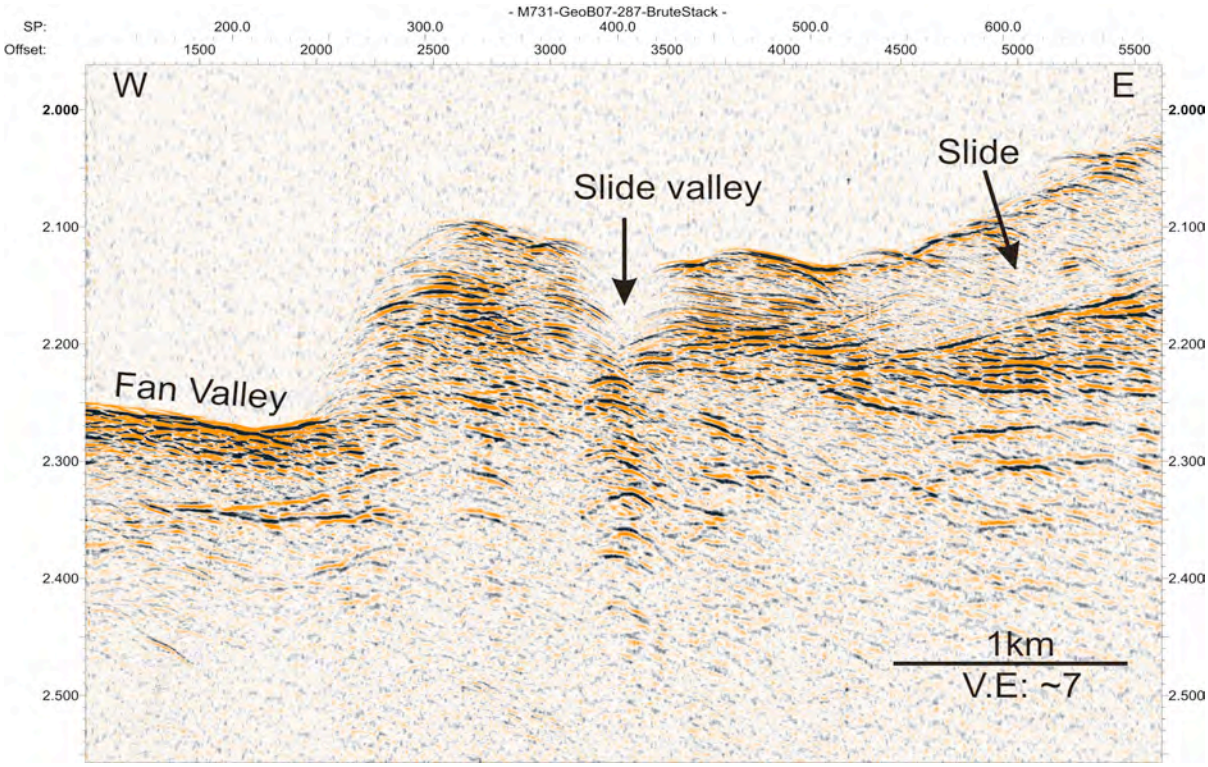

Fig. 39: Brute stack of Profile GeoB07-287. See Fig. 34 for location of profile.

A number of profiles were collected in the headwall area of the Nice Airport Slide. Unfortunately the main headwall was that close to the coast, that not straight profile crosses the headwall. Figure 40 shows a profile running almost parallel to the headwall. A 90 m-deep canyon is visualised at the western part of the profile. The high amplitude reflectors marking the thalweg suggest a sandy canyon floor. The uppermost 15m of sediment east of

the canyon are characterised by a transparent to chaotic seismic facies, which might represent slide deposits.

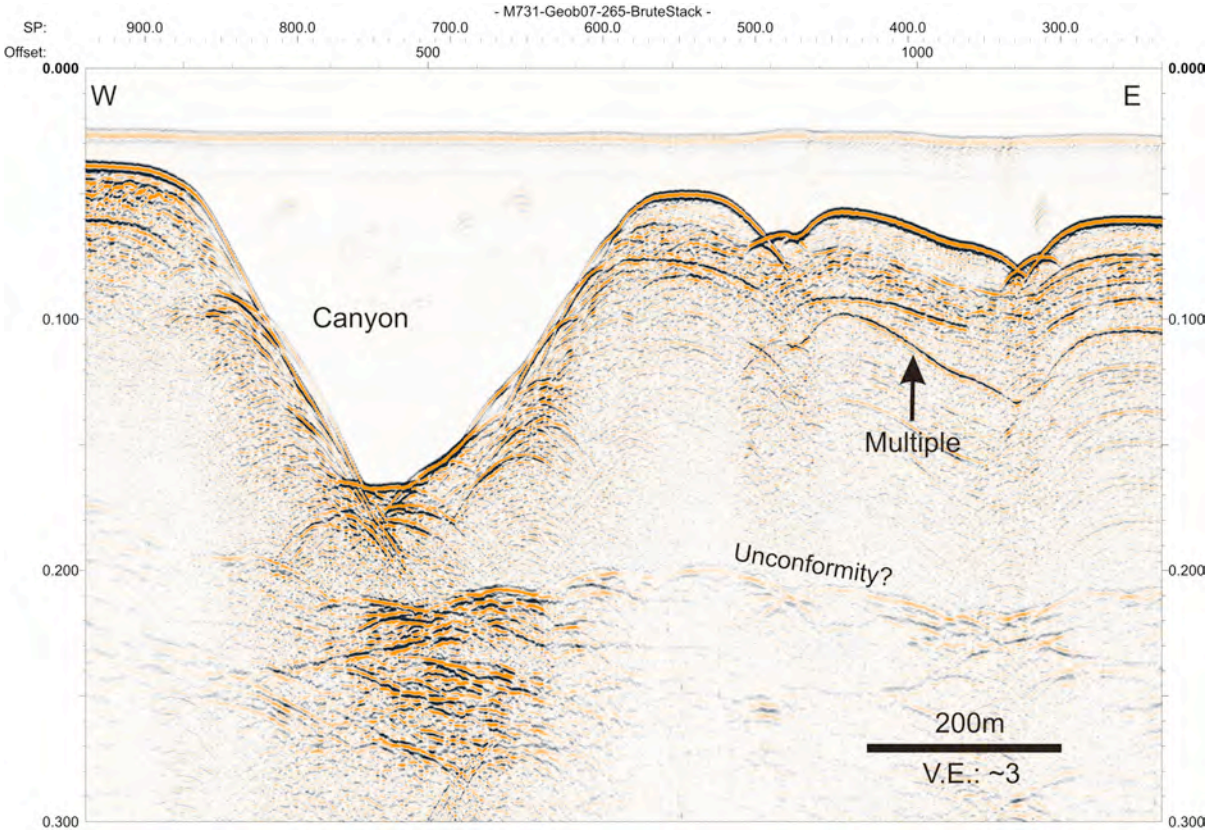

Fig. 40: Brute stack of Line GeoB07-265. See Figure 36 for location of profile.

From profile GeoB07-265 alone it is difficult to decide, if these deposits belong to the Nice Airport Slide. The slide was probably mainly erosive along the profile but a joint analysis of multi-channel seismic, Parasound, and bathymetric data is needed for a detailed image of the Nice Airport Slide. Relatively high amplitude reflectors are imaged at ~200 ms TWT along the entire profile. The reflector most likely represents a major unconformity, which might have formed during a period of a significantly lower sea level.

On the other hand, some interesting features are revealed on a cross-line (Fig. 36), which is running N-S and reaches the headwall area very close to the airport (Fig. 41). Here, a clear distinction between slid sediment and coherently layered underground sediment can be made. A peculiar feature is a southward-dipping lineament close to the airport, which may indicate normal faulting. In deed, sediment north of that lineament seems seismically opaque (i.e. free of coherent signatures) whereas south of it, subhorizontal layering is observed. This latter interval may represent a block of material, which slid southward during the 1979 event

without having been totally displaced. Post-cruise seismic reprocessing will hopefully reveal details regarding the structure of the area and the nature of this lineament.

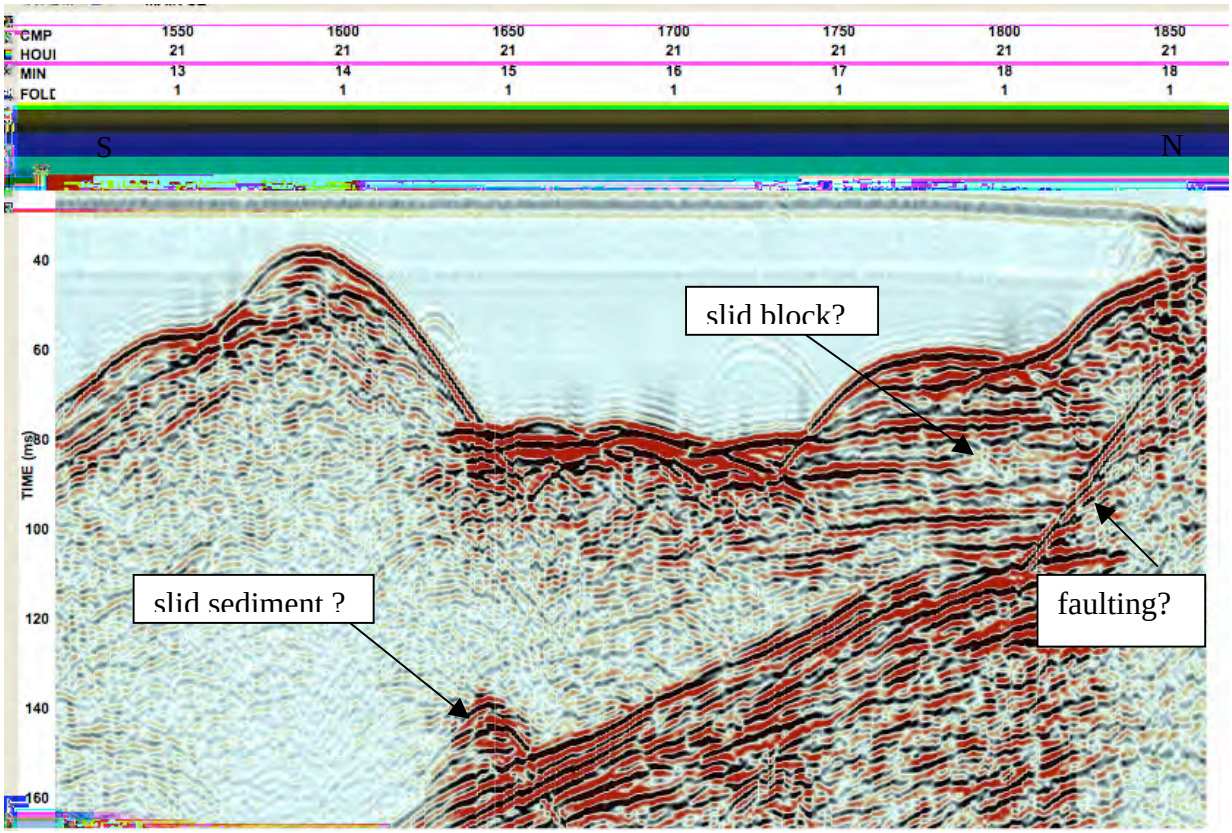

Fig. 41: Brute stack of Line GeoB07-262. See Figure 36 for location of profile.

6.5. Heat flow measurements

(J.F. Metzen, N. Kaul)

Three of the five target areas of cruise M73/1 (see Fig. 24) were successfully covered with heat flow probe penetrations (Fig. 42):

Shallow- and mid-slope region

The mid-slope area is characterised by several small canyons/ gullies, all separated by distinct ridges. It was covered by a South to North (heatflow stations H07-01-ff and continuing profile H07-04-ff.) and a West to East transect (stations H07-02-ff.) (Fig. 43, A1). The shallow-slope area – water depths around 600 m - representing a stable situation, was covered by a transect from S to N, located on a ridge splitting the Var canyon at its proximal part (stations H07-03-ff.) (Fig. 43, A2). This profile, located west of the airport

(and in fact west of the mouth of the Var estuary), is representing a reference slope section to be compared to the Nice Airport landslide area. There, however, no HF surveys could be carried out during cruise M73/1 due to limits of the research permission.

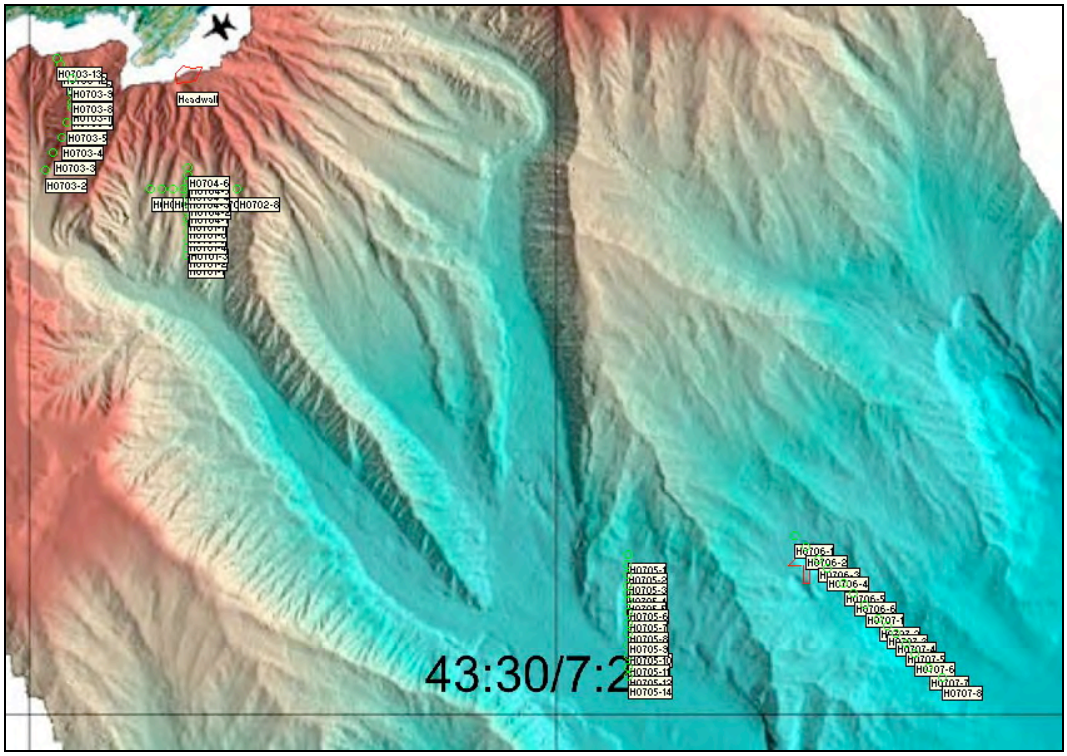

Fig. 42: All heat flow stations measured in the Nice – Var Canyon area during cruise M73/1. Bathymetric background map acquired by S. Migeon, Geosciences Azur, Villefranche-sur-mer, France.

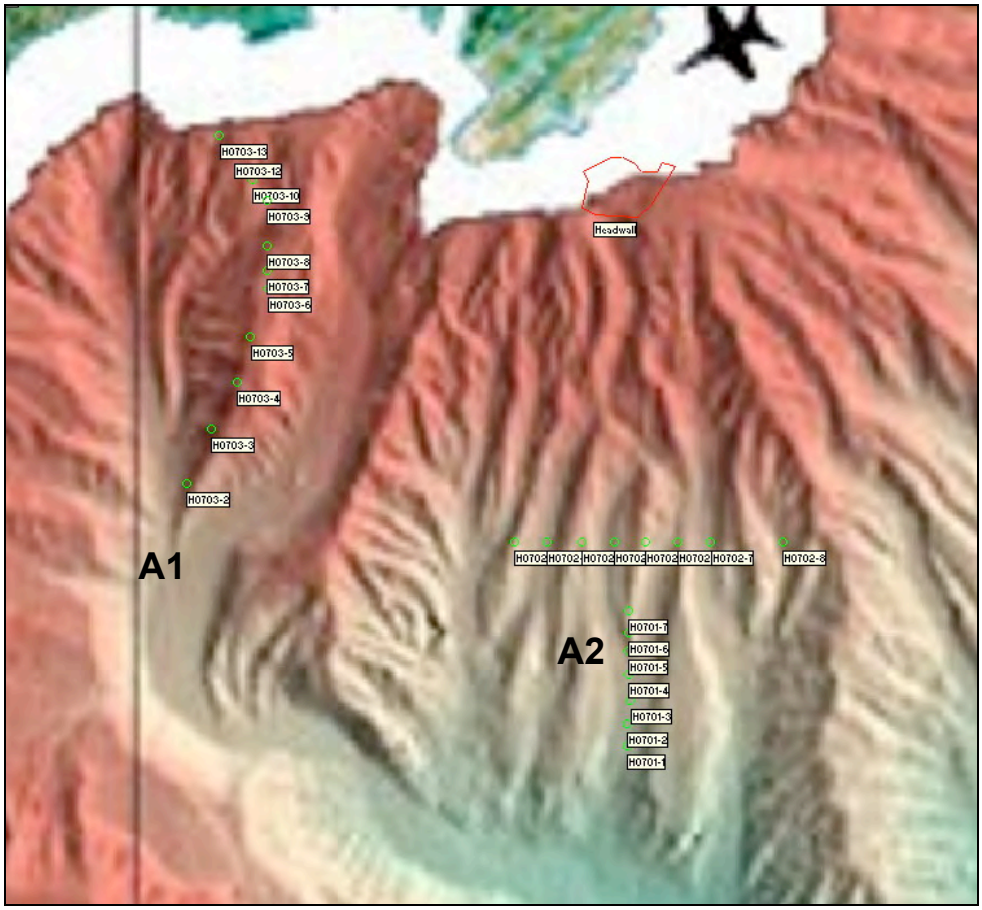

Fig. 43: Map of shallow-slope (A1) and mid-slope (A2) area. Heat flow transects are indicated by their station numbers (c.f. Table 3). The red area marks the headwall of the 1979 Nice Airport slide. Map as above (Fig. 42).

Western and eastern landslides

The two areas of mass wasting, as evidenced from distinct failure scars in the otherwise smooth slope, are located west and east of a pronounced ridge just north of a more distal part of the Var Canyon. The western slide is located on the western flank of the ridge. The HF transect ran N to S from (presumably) undisturbed sediments over the headwall and along the middle of the slide scar axis (stations H07-05-ff.) (Fig. 44, B1). The eastern slide is located E of the ridge in a trough. The transect run from NW to SE, aiming to cover the same (assumed) sediment succession as for area B1 (stations H07-06-ff. and H07-07-ff) (Fig. 44, B2).

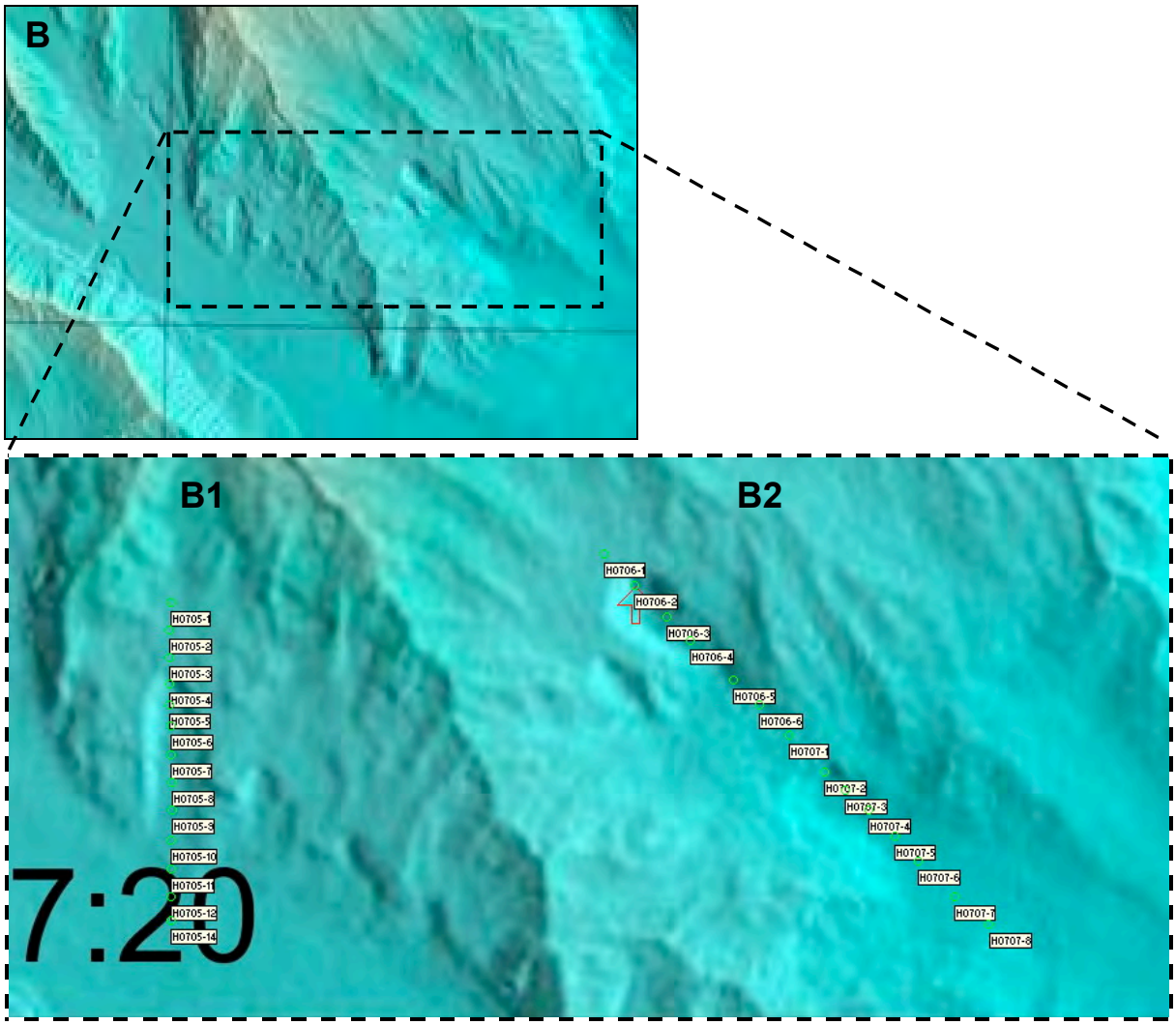

Fig. 44: Overview (B) and detail maps of the western (B1) and eastern (B2) slides. Heatflow transects are indicated by their station numbers (c.f. Table 3). Map as above (Fig. 42).

A prerequisite for reliable temperature gradient measurements is a stable oceanographic situation, which is usually not granted for water depth of 300 – 1000 m as partly encountered in the working areas.

In most of the region the water sensor on the heatflow instrument indicated stable conditions from 13.1 to 13.5°C, with two outliers during stations H0703-12 (~15°C) and -13 (~15.5°C). These values might result from insufficient equilibration time for the sensors prior to penetration. The determination of the geothermal heat flow q requires the knowledge of the vertical temperature gradient, as described above, and the thermal conductivity k, which is a material constant. Values for the thermal conductivity k were not measured on sediment cores taken near/ directly at the HF locations during the cruise. This is planned to be done post-cruise in the laboratories of University Bremen.

Due to the vicinity to the coast at the shallow- and mid-slope region, as well as at the western and eastern slides (located near the Var canyon/ a trough – both locations prone to high sediment transport), a high content of terrestrial input (i.e. quartz and terrestrial derived clay minerals) and comparatively low amounts of pelagic debris can be expected. Therefore, the thermal conductivity k could possibly yield relatively high values (approximately ranging from 0.9 to 1.5 W/m*K) and an assumed k = 1 W/m*K could be used for a first order approximation of the geothermal heat flow q. Figures for the latter parameter are not shown here since the results of the upcoming lab measurements of k should be awaited to gain valid conclusions for q.

In the following, the results in terms of derived temperature gradients are presented by target areas (see also Table 3 for all heat flow locations and additional information).

Shallow-slope area (see Fig. 43, A1)

Figure 45 plots relative temperatures and temperature gradient fits of 5 logger penetrating the sediment and one bottom water temperature logger, always kept out of the sediment. Most of the plots reveal an inverse – or negative – temperature gradient over depth, see penetration 2 – 4 and 11. Penetrations 5 – 7 seem to be transition profiles back to unbiased gradients as penetrations 8 and 9 show. These negative anomalies are due to a strong seasonal signal dominating the absolute temperature of the sediment. The yet (August 2007) still lower sediment than current bottom water temperatures are a remnant of last winter 2006/07. Furthermore, the transect A1 lies in the pathway of Var river, respectively its extension into the submarine Var canyon, thus receiving terrestrial signals and active sediment transport.

Penetration 10 highlights a pitfall of the temperature gradient fit incorporating the bottom water temperature. The linear fit is strongly influenced by latter value, even though sediment temperatures show very uniform values from top down to maximum penetration depth. In principle, this influence holds true for all fitting done throughout the processing of raw absolute temperature data from the loggers. Nevertheless, for ‘normal situation’ showing positive temperature gradients with increasing depth (which also has just slightly higher values at first logger in sediment), the incorporation of the bottom water temperature in the linear fit is inevitable for correct results (e.g. see penetration 9). This is understandable as bottom water temperature is taken as the reference value for calculation of relative temperature anomalies from the different logger depths.

To conclude, the signals shown in temperature gradients might reflect a combination of seasonal influence and, due to the proximity to Var river, active canyon sediment and water mass transport effects rather than normal subbottom heat flow anomalies.

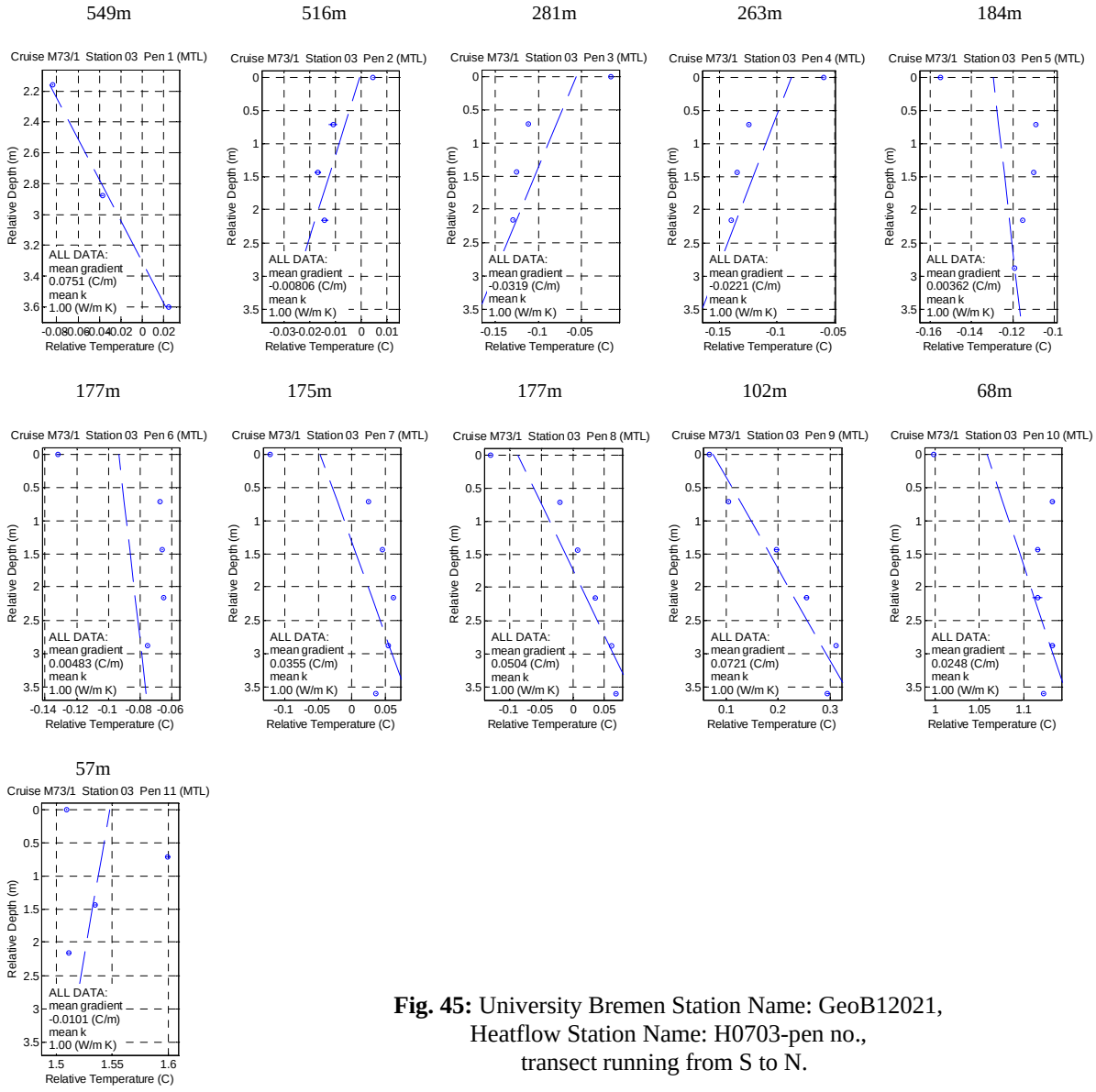

Fig. 45: University Bremen Station Name: GeoB12021, Heatflow Station Name: H0703-pen no., transect running from S to N.

Mid-slope area (Fig 43, A2)

This target region covers the main pathways of sediment transport of the 1979 Nice 'slide event' just south of the airport. Many small scale canyons, resp. gullies, characterise the topography and have previously been interpreted as potential pathways for the wasted mass of the 1979 landslide event (Dan, 2007). As Figure 46 shows, the heat flow transects running from S to N reveal rather heterogeneous sediment temperature gradients – they range from 59.5 to 2.16 mK/m and there is no south-north trend visible. Since most

gradients are positive no seasonal signal should be responsible for the anomalous gradients (c.f. results at area A1, Figs. 43, 45). Only the gradient of H0704-5 is negative and therefore this single site is unlikely to show a seasonal signal. On the other hand, H0704-6 could have penetrated trough (porous) layers, delivering colder freshwater to the area. These groundwater flows have been strongly indicated by the pore water geochemistry. Excluding H0701-1 to -3, which show gradients somewhat adequate for undisturbed marine (hemipelagic) sediments, all other penetrations seem to reflect temperature signals mixed, respectively and possibly induced, by slumping. This would match the 1979 Nice 'slide event' with its pathway directly passing trough this sampled area.

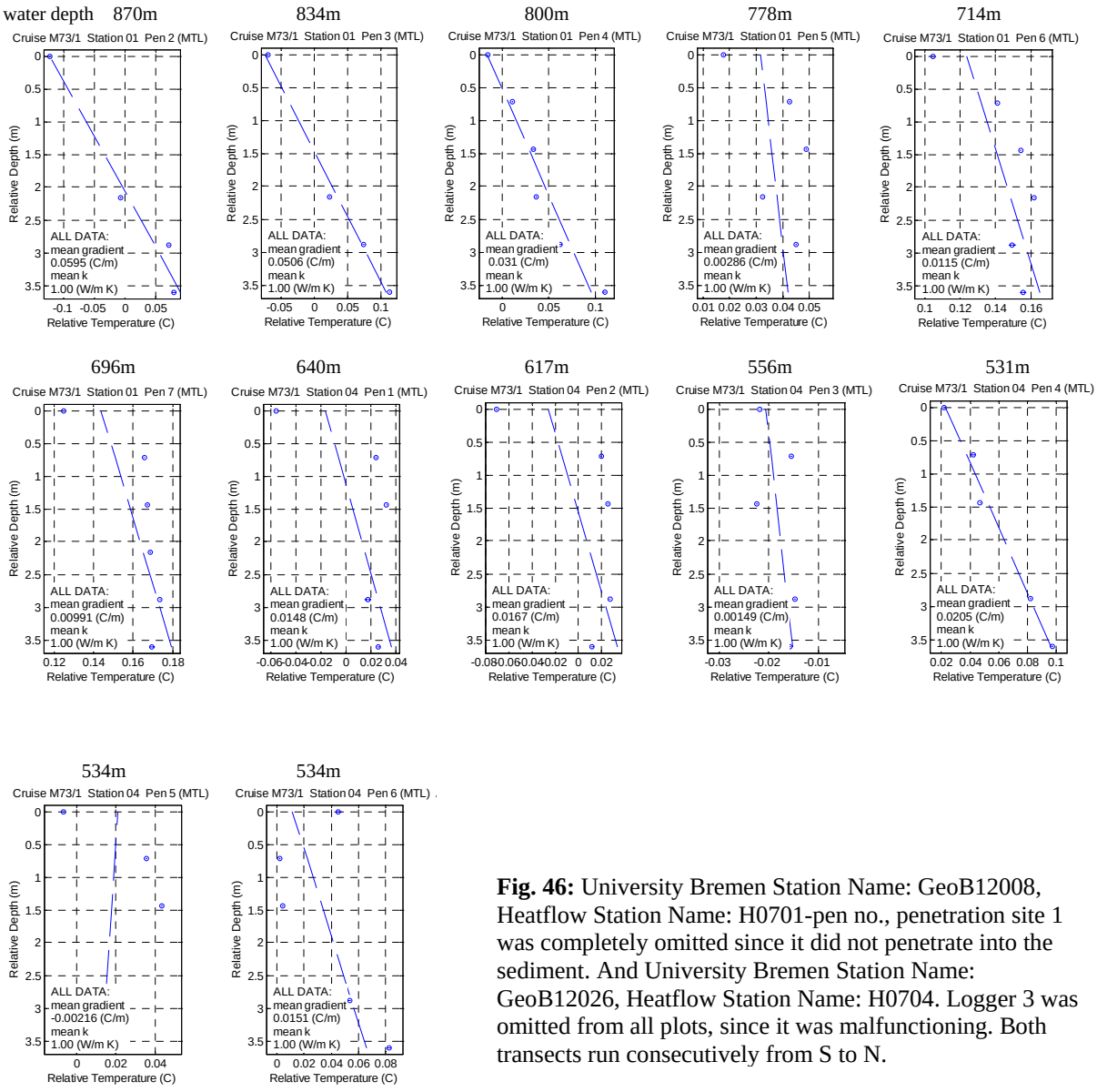

Fig. 46: University Bremen Station Name: GeoB12008, Heatflow Station Name: H0701-pen no., penetration site 1 was completely omitted since it did not penetrate into the sediment. And University Bremen Station Name: GeoB12026, Heatflow Station Name: H0704. Logger 3 was omitted from all plots, since it was malfunctioning. Both transects run consecutively from S to N.

Looking at the West-to-East transect at the mid-slope region, patterns of temperature gradients/ fits are obvious and similar to those described for the S to N transect above (Fig. 47). Again and even more pronounced, the upper 2 to 2.5 m of the sediment show nearly uniform relative temperatures which could possibly be explained by sampling across highly disturbed/ mixed strata. Since the uniform relative temperature values all lie well above the bottom water temperature, influence of a seasonal signal from the previous winter (i.e. 2006/07) can be rejected.

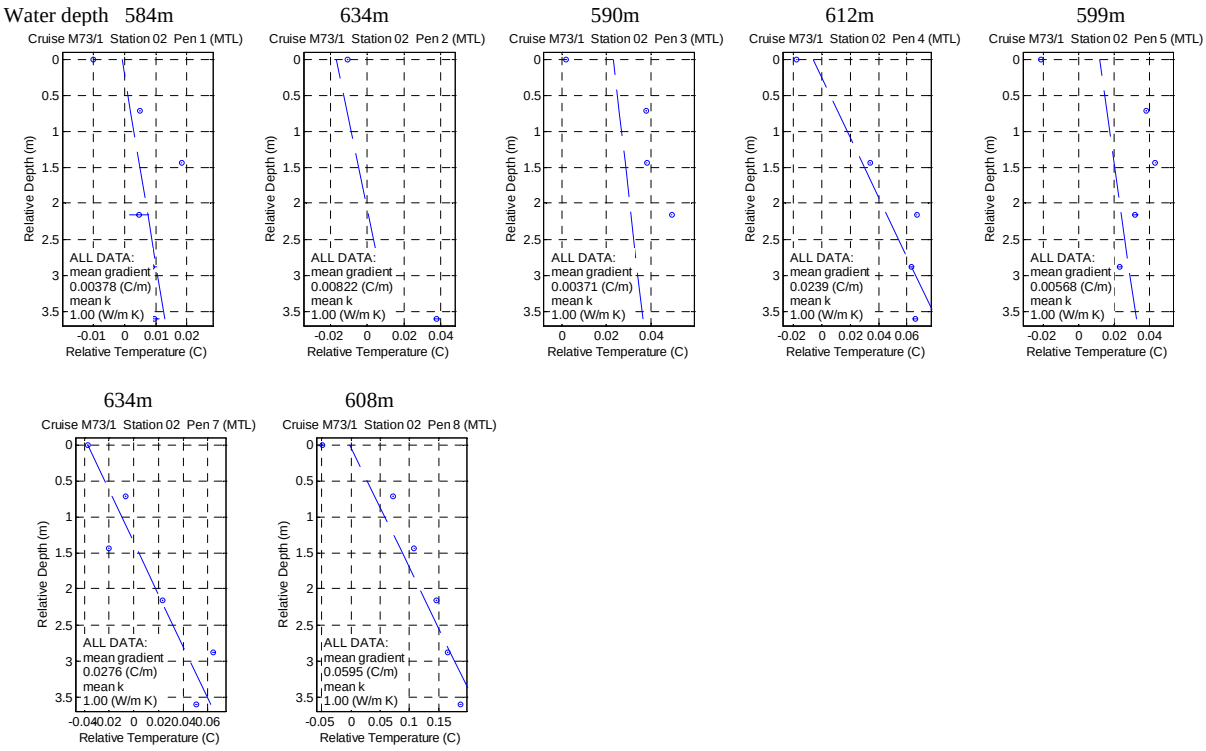

Fig. 47: University Bremen Station Name: GeoB12013, Heatflow Station Name: H0702, Transect running from W to E. Penetration 6 was completely omitted since it did not penetrate into the sediment. At penetration 2 only 2 data points were usable, thus there is no meaningful gradient derivable.

Western landslide area

This target area unexpectedly seems to reveal no particular anomalies which might indicate or show distinct effects of a slide/ slump system (Fig. 48). All linear fits are positive and values are at an expected 'normal' range. At least, gradient values are 15 – 20 mK/m less at todays top of the slide (penetrations 8 – 12) compared to the ones above the slide scar (penetrations 1 – 3). At the headwall, penetration 5 shows a very high temperature gradient of 125 mK/m.

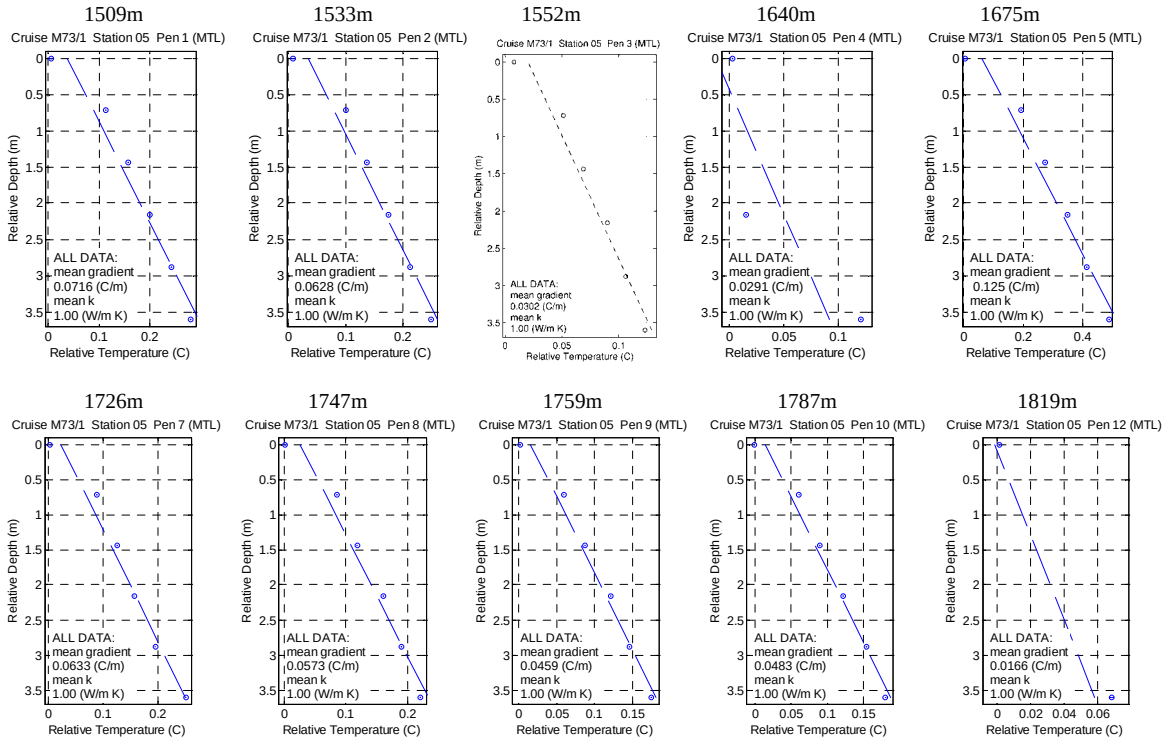

Fig. 48: University Bremen Station Name: GeoB12049, Heatflow Station Name: H0705, transect running from N to S. Penetrations 6, 11, 13 could not be processed until now due to software problems.

Eastern landslide area

Somehow similar to the western-slide, area B2 does reveal unequivocal evidence for sampling a submarine slide region (Fig. 48). However, the observed anomalies of H0706 should be described first: Penetration 1 lies NW of the slide scar in undisturbed hemipelagic sediments and has an expected ‘normal’ temperature gradient of 59 mK/m. Instead, penetration 2 is at the headwall and shows a significant increased gradient of 86 mK/m. The following two penetrations, lying at the outbound slide region, indicate a marked decrease in temp. gradient values. In addition, penetration 4 (which lies directly within the slide area), and 5 as well, show different relative temperatures in the upper 1.5 m than the other locations. From penetration 6 on, the transect further to the southeast reveals a normal gradient pattern again.

Penetration 2 of H0707 has a very high temperature gradient of 122 mK/m, a bit less was measured at penetration 3. At least the former site lies directly at another headwall structure, which might lead to such high values through any process, which could not to be explained with the heat flow method on its own. Following the transect further downslope to the SE, gradients fall and then rise again to ‘normal’ hemipelagic background values again.

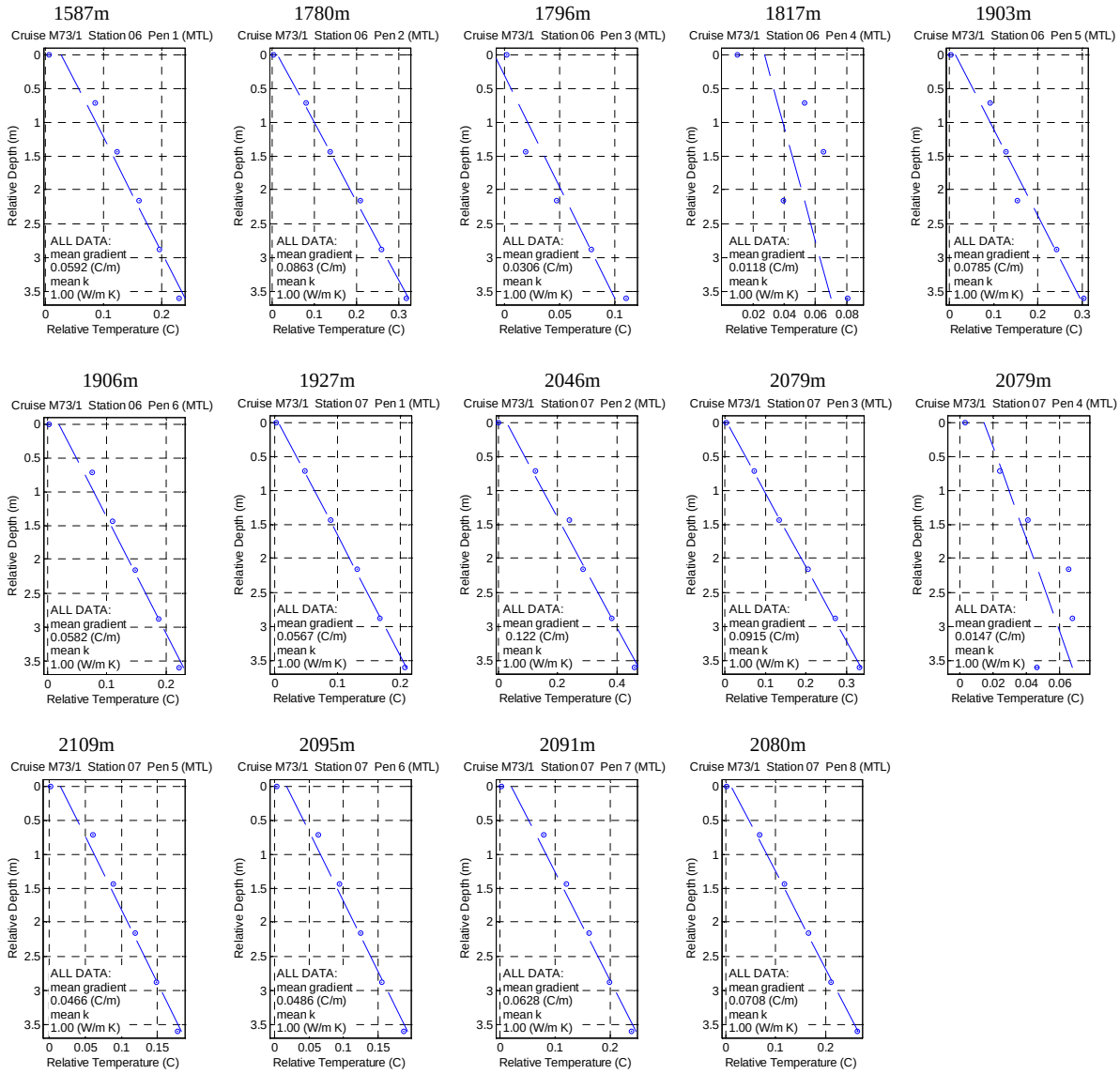

Fig. 49: University Bremen Station Name: GeoB12063, Heatflow Station Name: H0706; University Bremen Station Name: GeoB12078, Heatflow Station Name: H0707, penetration 4 possibly did not penetrate well, thus values might be misleading. Both transects run consecutively from NW to SE.

Table 3: List of all HF Probe penetration sites and deduced temperature gradients and Heatflow values. Since the assumed thermal conductivity k = 1.0 W/m*K, the mean heatflow q equals the numbers of the thermal gradient.

Meteor Station No.		Uni Bremen Station No.	Heatfow Name/ Station No.	Latitude	Longitude	Water Depth	mean temperature gradient dT	Remarks
old nomenclature	new nomenclature	GeoB120-	H07-			[m]	[mK/m]	
ME731/657-1	657	08-1	01-1	43° 36,30' N	7° 12,99' E	898	NaN	Penetration failed
ME731/657-2	658	08-2	01-2	43° 36,40' N	7° 12,99' E	870	59.5	
ME731/657-3	659	08-3	01-3	43° 36,50' N	7° 13,01' E	834	50.6	*Transect runs*
ME731/657-4	661	08-4	01-4	43° 36,62' N	7° 13,00' E	800	31.0	*S to N.*
ME731/657-5	663	08-5	01-5	43° 36,72' N	7° 13,00' E	778	2.86	
ME731/657-6	665	08-6	01-6	43° 36,80' N	7° 13,00' E	714	11.5	
ME731/657-7	667	08-7	01-7	43° 36,90' N	7° 13,00' E	696	9.91	
ME731/663-1	676	13-1	02-1	43° 37,20' N	7° 12,30' E	584	3.87	
ME731/663-2	678	13-2	02-2	43° 37,20' N	7° 12,50' E	634	8.22	
ME731/663-3	680	13-3	02-3	43° 37,20' N	7° 12,71' E	590	3.71	*Transect runs*
ME731/663-4	682	13-4	02-4	43° 37,20' N	7° 12,91' E	612	23.9	*W to E.*
ME731/663-5	683	13-5	02-5	43° 37,20' N	7° 13,10' E	599	56.8	
ME731/663-6	684	13-6	02-6	43° 37,20' N	7° 13,30' E	608	NaN	not penetrated
ME731/663-7	685	13-7	02-7	43° 37,20' N	7° 13,50' E	634	27.6	
no old	ME731/686-1	13-8	02-8	43° 37,20' N	7° 13,94' E	608	59.5	
numbers any	ME731/699-1	21-1f	03-1	43° 37,46' N	7° 10,30' E		NaN	Penetration failed
more	ME731/700-1	21-1	03-2	43° 37,46' N	7° 10,30' E	549	75.1	
	ME731/701-1	21-2	03-3	43° 37,70' N	7° 10,45' E	516	-8.06	
	ME731/702-1	21-3	03-4	43° 37,91' N	7° 10,61' E	281	-31.9	
	ME731/703-1	21-4	03-5	43° 38,11' N	7° 10,69' E	263	-22.1	
	ME731/704-1	21-5	03-6	43° 38,32' N	7° 10,80' E	184	3.62	*Transect runs*
	ME731/705-1	21-6	03-7	43° 38,40' N	7° 10,79' E	177	4.83	*S to N.*
	ME731/706-1	21-7	03-8	43° 38,51' N	7° 10,79' E	175	35.5	
	ME731/707-1	21-8	03-9	43° 38,71' N	7° 10,79' E	177	50.4	
	ME731/708-1	21-9	03-10	43° 38,80' N	7° 10,70' E	102	72.1	
	ME731/709-1	21-10f	03-11	43° 38,91' N	7° 10,59' E		NaN	Penetration failed
	ME731/709-1	21-10	03-12	43° 38,91' N	7° 10,59' E	68	24.8	
	ME731/710-1	21-11	03-13	43° 39,00' N	7° 10,50' E	57	-10.1	
	ME731/716-1	26-1	04-1	43° 37,00' N	7° 13,01' E	640	14.8	
	ME731/718-1	26-2	04-2	43° 37,10' N	7° 13,01' E	617	16.7	*Continuation of*
	ME731/720-1	26-3	04-3	43° 37,20' N	7° 13,00' E	594	1.49	*transect H0701,*
	ME731/722-1	26-4	04-4	43° 37,30' N	7° 13,00' E	556	20.5	*Transect runs*
	ME731/724-1	26-5	04-5	43° 37,40' N	7° 13,01' E	531	-2.16	*S to N.*
	ME731/726-1	26-6	04-6	43° 37,50' N	7° 13,00' E	534	15.1	
	ME731/763-1	49-1	05-1	43° 32,20' N	7° 21,35' E	1509	71.6	
	ME731/765-1	49-2	05-2	43° 32,05' N	7° 21,34' E	1533	62.8	
	ME731/766-1	49-3	05-3	43° 31,91' N	7° 21,34' E	1552	30.2	*Transect runs*
	ME731/767-1	49-4	05-4	43° 31,77' N	7° 21,34' E	1640	29.1	*N to S.*
	ME731/768-1	49-5	05-5	43° 31,66' N	7° 21,34' E	1675	125.0	
	ME731/769-1	49-6	05-6	43° 31,55' N	7° 21,35' E	1691	NaN	processing failed
	ME731/770-1	49-7	05-7	43° 31,40' N	7° 21,35' E	1726	63.3	
	ME731/771-1	49-8	05-8	43° 31,25' N	7° 21,36' E	1747	57.3	
	ME731/772-1	49-9	05-9	43° 31,11' N	7° 21,36' E	1759	45.9	
	ME731/773-1	49-10	05-10	43° 30,95' N	7° 21,35' E	1787	48.3	

	ME731/774-1	49-11	05-11	43° 30,80' N	7° 21,35' E	1796	NaN	processing failed
	ME731/775-1	49-12	05-12	43° 30,65' N	7° 21,35' E	1819	16.6	
	ME731/776-1	49-13-1	05-13	43° 30,53' N	7° 21,35' E	1824	NaN	Penetration failed
	ME731/776-1	49-13-2	05-14	43° 30,53' N	7° 21,35' E	1825	NaN	Penetration failed
	ME731/791-1	63-1	06-1	43° 32,45' N	7° 24,51' E	1587	59.2	
	ME731/792-1	63-2	06-2	43° 32,29' N	7° 24,73' E	1780	86.3	
	ME731/793-1	63-3	06-3	43° 32,12' N	7° 24,97' E	1796	30.6	*Transect runs*
	ME731/794-1	63-4	06-4	43° 32,00' N	7° 25,14' E	1817	11.8	*NW to SW.*
	ME731/795-1	63-5	06-5	43° 31,79' N	7° 25,45' E	1903	78.5	
	ME731/796-1	63-6	06-6	43° 31,66' N	7° 25,64' E	1906	58.2	
	ME731/820-1	78-1	07-1	43° 31,50' N	7° 25,86' E	1927	56.7	
	ME731/821-1	78-2	07-2	43° 31,31' N	7° 26,12' E	2046	122	
	ME731/822-1	78-3	07-3	43° 31,21' N	7° 26,27' E	2079	91.5	*Continuation of*
	ME731/823-1	78-4	07-4	43° 31,11' N	7° 26,44' E	2079	14.7	*transect H0706,*
	ME731/824-1	78-5	07-5	43° 30,97' N	7° 26,63' E	2104	46.6	*Transect runs*
	ME731/825-1	78-6	07-6	43° 30,84' N	7° 26,80' E	2095	48.6	*NW to SW.*
	ME731/826-1	78-7	07-7	43° 30,65' N	7° 27,07' E	2091	62.8	
	ME731/827-1	78-8	07-8	43° 30,51' N	7° 27,32' E	2080	70.8	

6.6. CPT testing

(S. Stegmann, A. Kopf)

During cruise M73/1, 50 free-fall CPT profiles were carried out; these included 19 deployments with the DW-CPT and 31 tests with the SW-CPT. While the first concentrated mostly on the mid-slope region, the first focused on the slide area adjacent to the Nice Airport. A summary map of all 50 deployments is given in Figure 50, which also includes a series of shallow-water tests west of the Var estuary (station GeoB 12020). The wealth of deployments in the Nice Airport vicinity is shown in Figure 51.

As a result of the very stiff sediments in the mid-slope portion of the M73/1 study area (see also unsuccessful coring attempts and low recovery sampling; Ch. 6.7. below), most of the deep-water tests failed and the instrument was finally damaged (Fig 52). In the preliminary cruise report, only the SW-CPT measurements are considered, which position and parameters are summarised in Table 4.

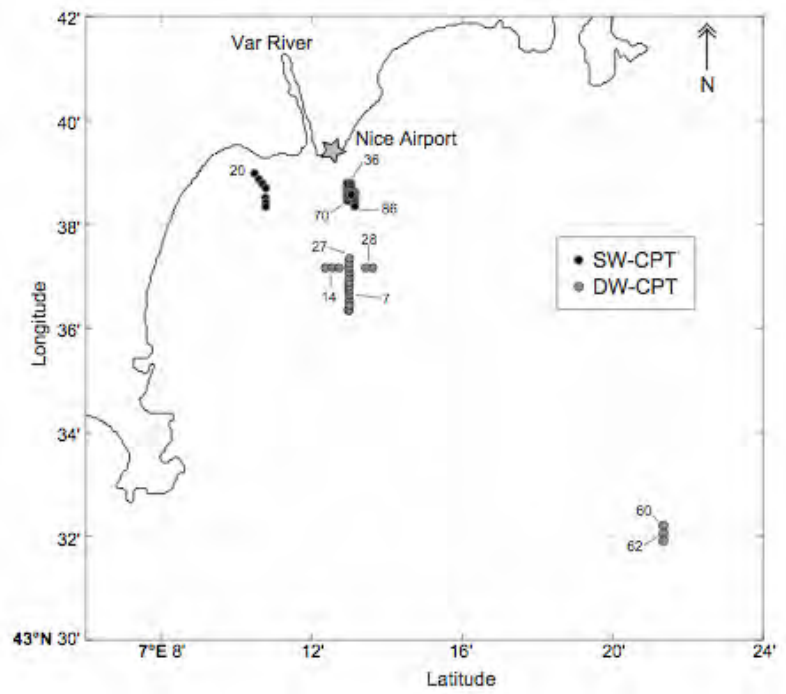

Fig. 50: Map showing all FF-CPT deployments during cruise M73/1. The CPT transects/profiles are here represented with the last two digits of the GeoB nomenclature.

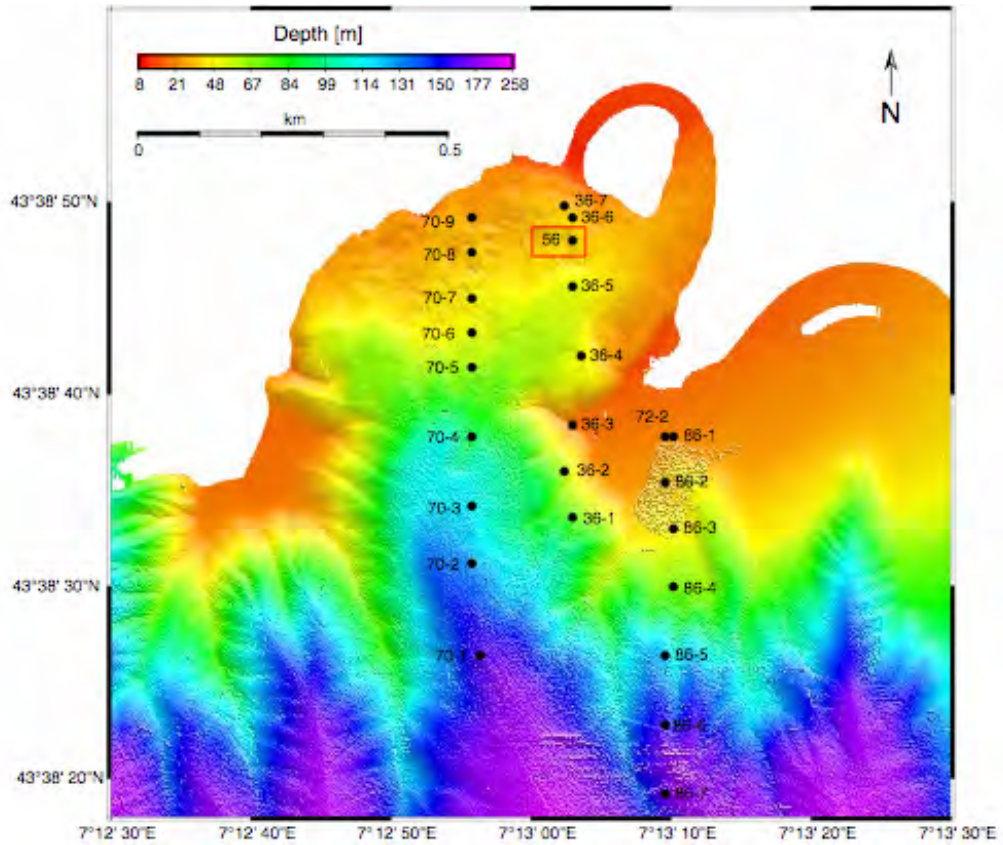

Fig. 51: Map showing all shallow-water FF-CPT deployments near the Nice airport. Red box shows location of long-term CPT experiment shown in Fig. 56.

Fig. 52: Photograph of deep-water FF-CPT probe after having hit hard ground in the mid-slope study area.

The shallow-water instrument was lowered with a winch velocity ranging between 0.5 and 0.9 m/s, before the lance penetrated the sediments with its own momentum. Depending on the sediment, absolute penetration depths between 0.5 and 3.5 m were achieved. As the instrument was heaved to the surface after each drop, stuck sediment on the lance shaft served to check the calculated penetration depth, which is derived by the 2nd integration of the acceleration. Inclination of the instrument was <9° (recommended value for standard CPT Testing [see Lunne et al. 1997]). With respect on the pore pressure evaluation after the impact the lance was remained for ~20 minutes in the sediment. The inclination and acceleration was recorded over this complete duration to detect failure or any other movement during that period. Focussing on the Nice Airport Slide, the SW-FFCPT profile GeoB12070 represents a variety of geotechnical conditions of the superficial sediments. The transect consists of nine individual deployments, which extended in north-south direction from the headwall downslope (for reference see Figure 51). The primary parameters measured (cone resistance q_c, sleeve friction f_s and excess pore pressure u_{exc} [= $u_{measured} - u_{hydrostatic}$]) compiled vs. penetration depth for each measurement are given in Figures 53 and 54**.** Starting in the downslope part of the transect (70-2; 70-3), the stiffness – represented by the cone resistance – is very low with values <400 kPa and homogeneous. Coming closer to the headwall of the slope the cone resistance pointed out distinct layers with increasing strength up to maximum 1200 kPa (Fig. 54, plot 70-8, 70-9). This layer, which was intersected between 20 and 30 cm penetration depth, coincided with cored

coarse-grained sediments (see Ch. 6.8. below; see also Figs. 58 or 66), which are generally more permeable.

Table 4: List of FF-CPT deployments.

GeoB120	Device	Date	Latitude	Longitude	Hydrostatic Pressure [kPa]	Winch-velocity [m/s]	Duration [min]	Penetration depth [m]	Note
20-1	SW CPT	28.07.2007	43° 39,02' N	7° 10,47' E	226.3	0.9	20	0.6	
20-2	SW CPT	28.07.2007	43° 38,89' N	7° 10,60' E	650	0.7	20	2.9	
20-3	SW CPT	28.07.2007	43° 38,80' N	7° 10,70' E	1056	0.7	22	1.28	
20-4	SW CPT	28.07.2007	43° 38,69' N	7° 10,81' E	1838	0.7	25	not possible	movement during measurement
20-5	SW CPT	28.07.2007	43° 38,50' N	7° 10,79' E	1838	0.7	20	2.8	
20-6	SW CPT	28.07.2007	43° 38,40' N	7° 10,80' E	1788	0.7	22	2.2	
20-7	SW CPT	28.07.2007	43° 38,30' N	7° 10,80' E	1984	0.7	22	2.1	
36-1	SW CPT	02.08.2007	43° 38,57' N	7° 13,06' E	813	0.7	20	1.8	movement during measurement
36-2	SW CPT	02.08.2007	43° 38,60' N	7° 13,05' E	549.2	0.5	21	1	movement during measurement
36-3	SW CPT	02.08.2007	43° 38,63' N	7° 13,05' E	193.2	0.5	30	1.6	
36-4	SW CPT	02.08.2007	43° 38,70' N	7° 13,06' E	499	0.8	20	1.8	
36-5	SW CPT	02.08.2007	43° 38,76' N	7° 13,05' E	525.8	0.7	20	1.8	
36-6	SW CPT	02.08.2007	43° 38,80' N	7° 13,05' E	368.7	0.7	27	2.4	
36-7	SW CPT	02.08.2007	43° 38,83' N	7° 13,04' E	262	0.7			failed
56	SW CPT	06.08.2007	43° 32,20' N	7° 21,34' E	380	0.5	321	not possible	
70-1	SW CPT	07.08.2007	43° 38,44' N	7° 12,94' E	1665	0.7	31	1.8	movement during measurement
70-2	SW CPT	07.08.2007	43° 38,52' N	7° 12,93' E	1410	0.5	19	1.9	
70-3	SW CPT	07.08.2007	43° 38,57' N	7° 12,93' E	1180	0.6	20	2	
70-4	SW CPT	07.08.2007	43° 38,63' N	7° 12,93' E	1015	0.7	19	2	
70-5	SW CPT	08.08.2007	43° 38,69' N	7° 12,93' E	746	0.5	21	1	
70-6	SW CPT	08.08.2007	43° 38,72' N	7° 12,93' E	595	0.6	19	0.8	
70-7	SW CPT	08.08.2007	43° 38,75' N	7° 12,93' E	500	0.7	20	1.8	
70-8	SW CPT	08.08.2007	43° 38,79' N	7° 12,93' E	380	0.8	20	1.2	
70-9	SW CPT	08.08.2007	43° 38,82' N	7° 12,93' E	275	0.7	11	1	failed after 15 minutes
72-2	SW CPT	08.08.2007	43° 38,63' N	7° 13,17' E	225.6	0.9	87	2.6	
86-1	SW CPT	09.08.2007	43° 38,62' N	7° 13,16' E	200.6	0.7	22	2.6	
86-2	SW CPT	09.08.2007	43° 38,59' N	7° 13,16' E	242.5	0.5	20	2	
86-3	SW CPT	09.08.2007	43° 38,55' N	7° 13,17' E	480.6	0.5	19	3.5	
86-4	SW CPT	09.08.2007	43° 38,50' N	7° 13,17' E	741.1	0.5	21	2.2	
86-5	SW CPT	09.08.2007	43° 38,44' N	7° 13,16' E	1270	0.5	21	2.4	
86-6	SW CPT	10.08.2007	43° 38,38' N	7° 13,16' E	1637	0.6	21	0.5	failed
86-7	SW CPT	10.08.2007	43° 38,32' N	7° 13,16' E	1609	0.5	21	1.4	

Pore pressure data should be handled with care, because during the impact of the lance an arteficial signal is created due to the displacement and expulsion of the fluid as well as solid particles. A crucial parameter for this very complex stress-strain-relationship as a response of dynamic penetration is the penetration velocity and sediment physical properties (e.g. grain size, stiffness) (Dayal and Allen, 1975; Clayton et al., 1985). This means, pore pressure during penetration may reflect a typical response of sediments (Seifert et al. 2008; Stegmann et al. 2007) and can be used as a hint for different pore pressure regimes. The background (excess) pore pressure value is achieved by the decay depending on the permeability of the sediment. All individual pore pressure profiles of GeoB12070 are characterised by a significant decrease in the pressure signal of up to maximum -100 kPa during the penetration. Fluctuations in the pressure reponse apparently coincide with changes in cone resistance (e.g. 70-5 – 70-9; Figs. 53 and 54). At the final absolute penetration depth, the pore pressure signal usually ranges around zero kPa.

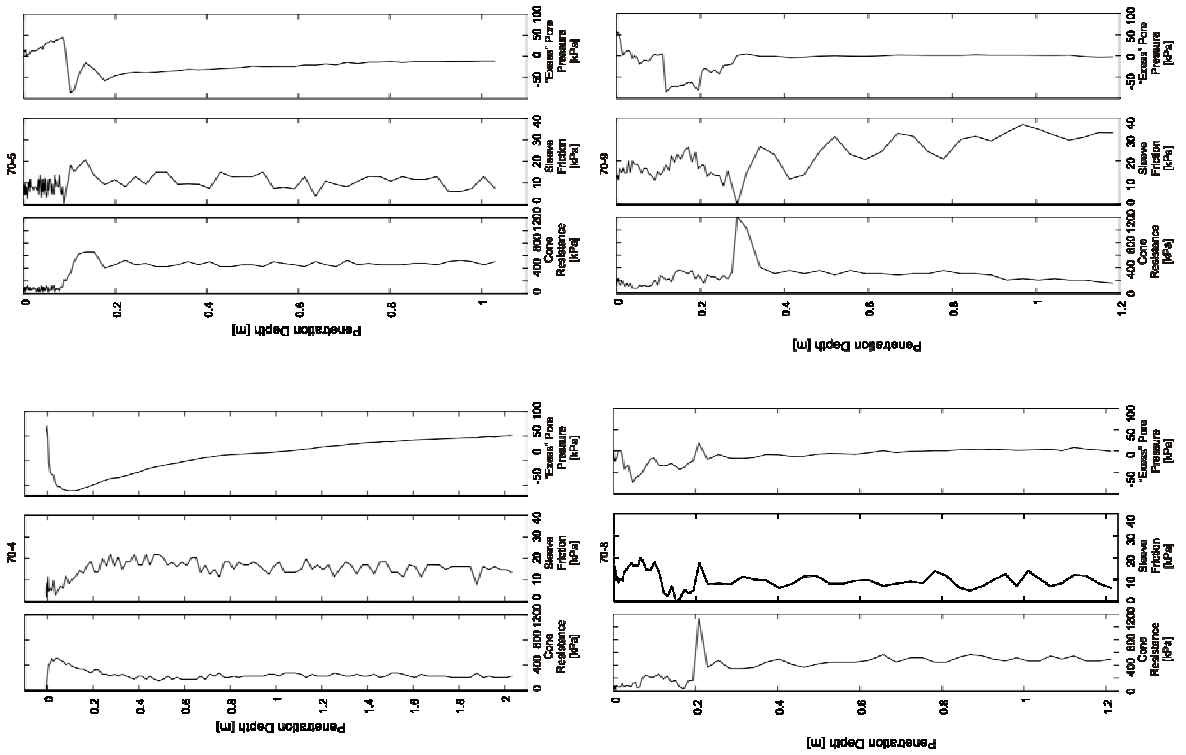

Fig. 53: Results from FF-CPT deployments near the Nice airport along transect GeoB 12070 (first part). Shown are tip resistance, sleeve friction, and excess pore pressure from a test near the headwall as well as a test in the lower part of this transect, where undisturbed sediments or amalgamated landslide sediment is expected. For location of individual deployments, see Figure 51.

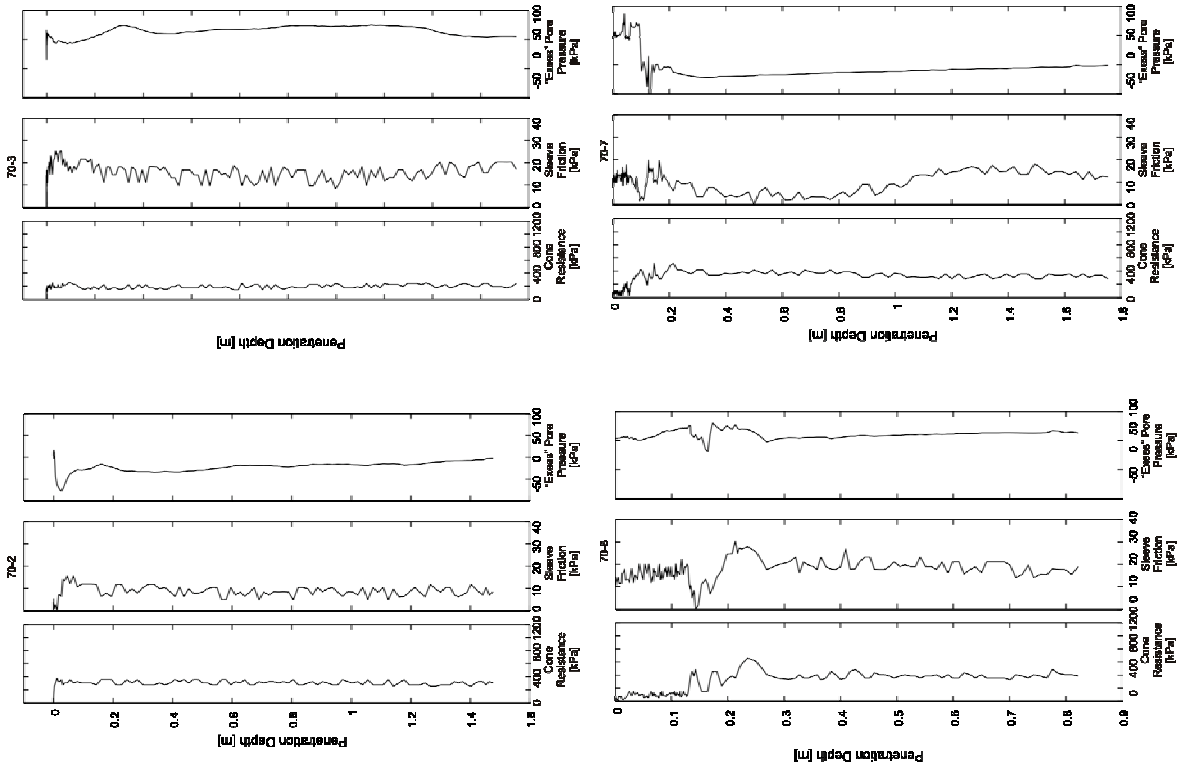

Fig. 54: Results from FF-CPT deployments near the Nice airport along transect GeoB 12070 (second part). Shown are tip resistance, sleeve friction, and excess pore pressure from a test near the headwall as well as a test in the lower part of this transect, where undisturbed sediments or amalgamated landslide sediment is expected. For location of individual deployments, see Figure 51.

When comparing the pore pressure response of transect GeoB12070 with the pressure signal of the more undisturbed GeoB12086 deployments further downslope of the slide (see for reference Fig. 51), the latter ones show a distinct pore pressure signal with a peak due to the impact and a subsequent decrease. Both typical pore pressure curves vs. complete duration of the deployment (~20 min) for two individual profiles are shown in a comparative plot in Figure 55**.** Albeit the absolute values differ by one order of magnitude, profile 70-8, which is located in the headwall, indicates a specific pore pressure regime where the excess pore pressure rose up to 15 kPa maximum. This observation is supported by a long-term test over a period of ~ 4 hours in the headwall area (GeoB12056**,** see Fig. 51), where a continuous ascent was monitored (Fig. 56).

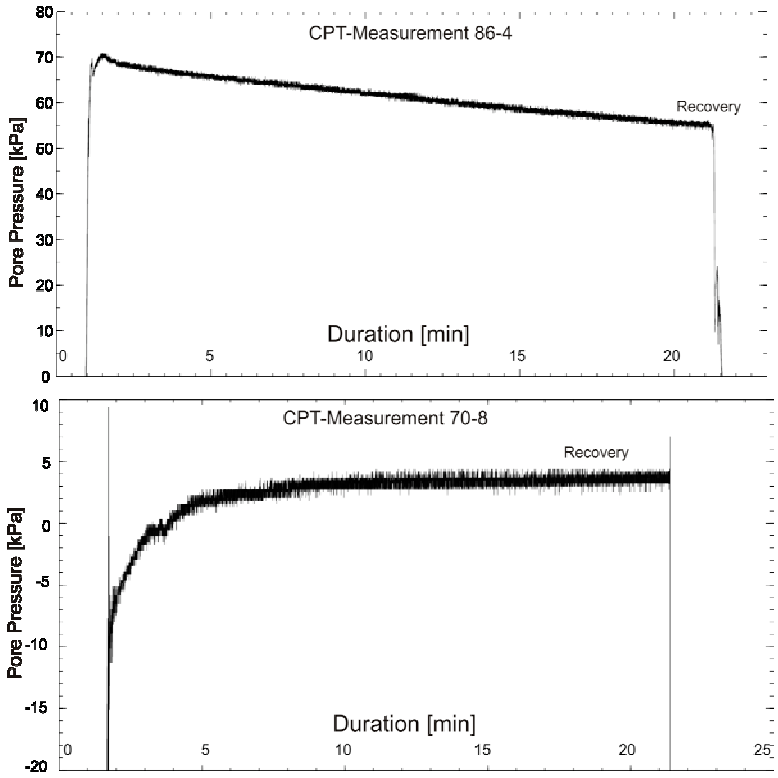

Fig. 55: Comparison of several pore pressure profiles from deployments along transect GeoB 12070 through the slide scar and GeoB 12086 east of the slide scar. See map in Fig. 51 for reference.

As a tentative summary, we propose that the SW-CPT deployments near the Nice Airport show slightly elevated excess pore pressures in the vicinity of the headwall. Those values, which range from a few kPa to maximum 15 kPa, may be a result of either lateral fluid flow through coarse-grained horizons (as also suggested from coring gravel deposits and extracting freshened pore waters from these intervals; see Ch. 6.8 and 6.9 below) or possibly

sealing of the coarser-grained layers by horizons rich in sensitive clay with assumed low permeability. More data will be acquired during post-cruise geotechnical laboratory tests.

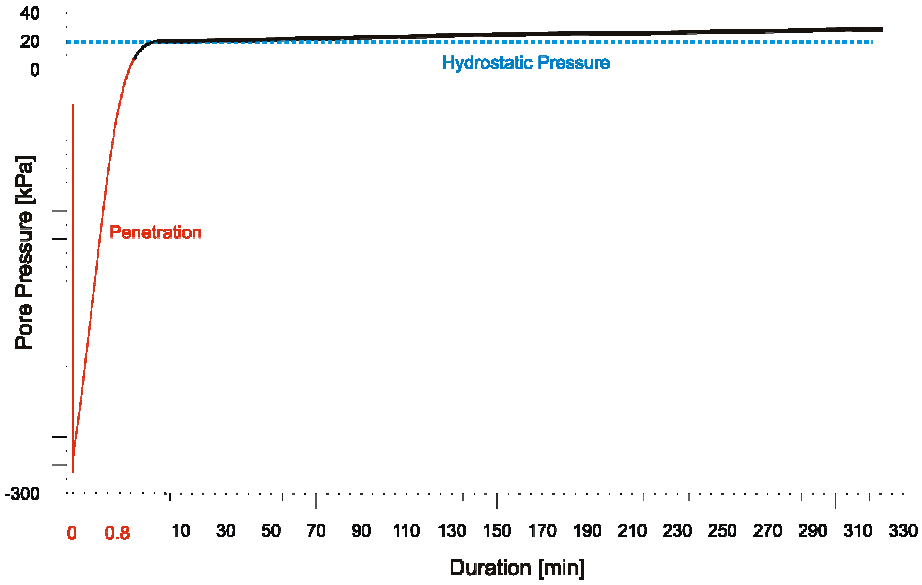

Fig. 56: Pore pressure evolution from FF-CPT deployment at station GeoB 12056, where the probe rested in the sediment overnight. See map in Fig. 51 for reference.

6.7. Gravity coring and sediment description

(B. Dennielou, A. Förster, T. Krumova, F. Girault, M.-A. Meier)

6.7.1. Operations

During the Cruise *LIMO-LAMO* (M73/1), 32 gravity cores of 0.1 m to 5.73 m length and 19 push cores of 0.06 m to 0.89 m length were recovered in five study areas (1: Nice airport, 2: Shallow- and Midslope, 3: Eastern landslide, 4: Western landslides, and 5: Var Canyon turbiditic system; see Fig. 24 above), totalling 100.6 m of core recovery (Fig. 57 and Table 5). Here, the sediments are described and briefly discussed for each study area.

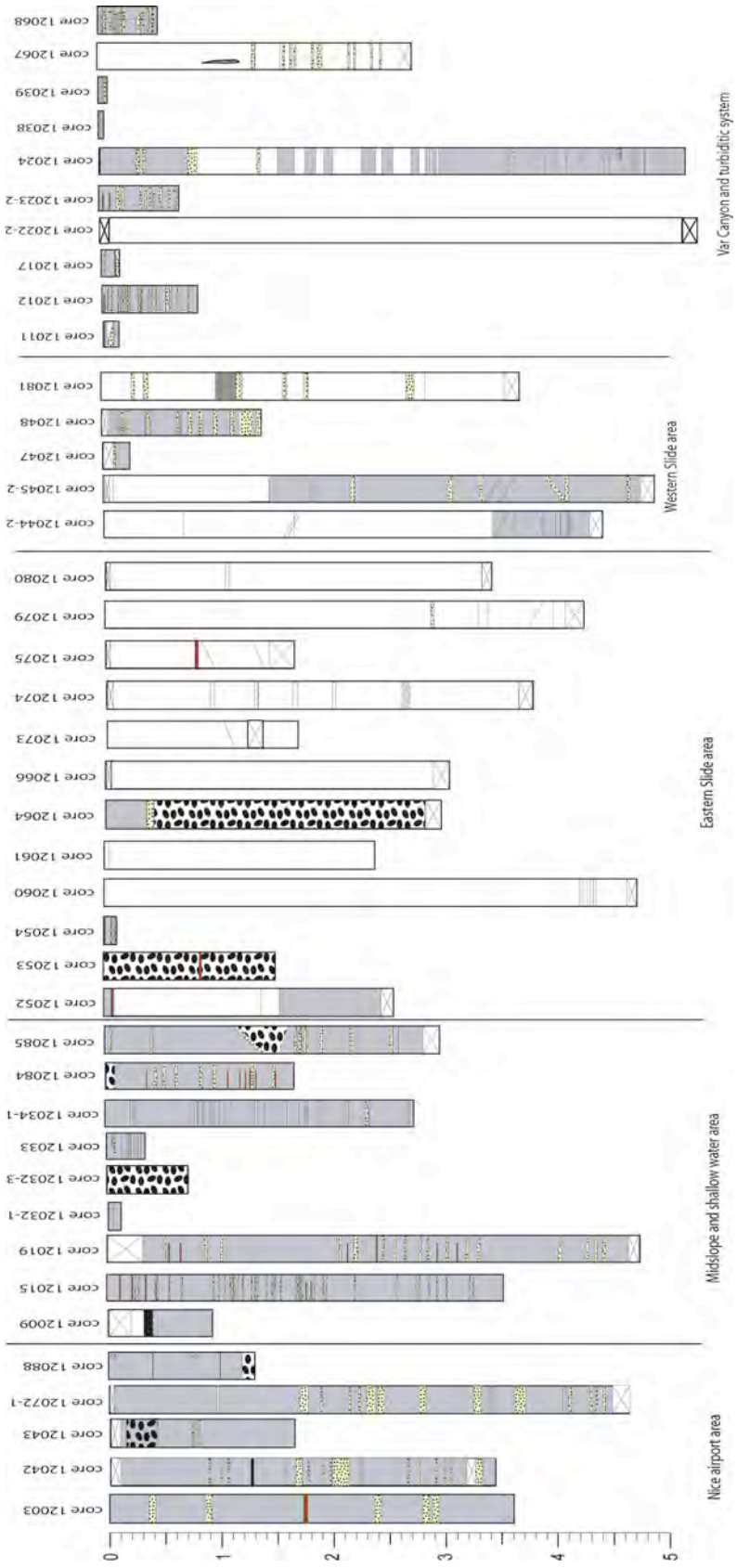

Fig. 57: Compilation and simplified profiles of all cores recovered in the study areas. For legend, see key of symbols above (Fig. 20).

Table 5: Summary of gravity coring (GC) and push coring (PC) information in the study areas.

Study Area	Core #	Date	Latitude	Longitude	Water Depth [m]	Recovery [m]	Type of core
Nice airport	GeoB 12003	26.07.2007	43° 38,80' N	7° 13,15' E	24,4	3,58	GC
	GeoB 12042	03.08.2007	43° 38.83' N	7° 13.05' E	28,4	3,43	GC
	GeoB 12043	03.08.2007	43° 38.84' N	7° 13.05' E	20,2	1,65	GC
	GeoB 12071	08.08.2007	43° 38.73' N	7° 12.93' E	51,2	0,66	PC
	GeoB 12072-1	08.08.2007	43° 38.63' N	7° 13.17' E	19,7	4,65	GC
	GeoB 12088	10.08.2007	43° 38.83' N	7° 12.90' E	15	1,3	GC
Shallow- and midslope area	GeoB 12009	27.07. 2007	43° 36,60' N	7° 13,01' E	807.8	0.93	GC
	GeoB 12015	28.07.	43° 36,90' N	7° 13,00' E	696,5	3,53	GC
	GeoB 12019	28.07.	43° 39,03' N	7° 10,47' E	32,7	4,75	GC
	GeoB 12030	01.08.2007	43° 37,20' N	7° 13,28' E	627,2	0,1	GC
	GeoB 12031-1	01.08.2007	43° 37,22' N	7° 13,50' E	636,3	0	PC
	GeoB 12031-2	01.08.2007	43° 37,20' N	7° 13,52' E	630,2	0	PC
	GeoB 12032-1	01.08.2007	43° 37,20' N	7° 12,82' E	644,4	0,11	PC
	GeoB 12032-2	01.08.2007	43° 37,20' N	7° 12,81' E	643,7	0	GC
	GeoB 12032-3	01.08.2007	43° 37,20' N	7° 12,82' E	643,1	0,73	GC
	GeoB 12033	01.08.2007	43° 37,19' N	7° 12,62' E	570,1	0,33	PC
	GeoB 12034-1	01.08.2007	43° 37,19' N	7° 12,40' E	637	2,76	GC
	GeoB 12034-2	01.08.2007	43° 37,20' N	7° 12,42' E	640,3	0,05	PC
	GeoB 12083	09.08.2007	43° 37.19' N	7° 13.40' E	642,9	0	GC
	GeoB 12084	09.08.2007	43° 37.19' N	7° 13.59' E	605,4	1,5	GC
	GeoB 12085	09.08.2007	43° 37.19' N	7° 13.68' E	573,1	2,99	GC
Eastern Slides	GeoB 12052	05.08.2007	43° 31.79' N	7° 25.45' E	1905.1	2,59	GC
	GeoB 12053	05.08.2007	43° 32.29' N	7° 24.73' E	1760	1,53	GC
	GeoB 12060	06.08.2007	43° 32.50' N	7° 24.51' E	1575	4,76	GC
	GeoB 12061	06.08.2007	43° 31.20' N	7° 26.28' E	2091	2,42	GC
	GeoB 12064	07.08.2007	43° 31.13' N	7° 26.21' E	2100	3	GC
	GeoB 12065	07.08.2007	43° 26.98' N	7° 27.29' E	2068	0	GC
	GeoB 12066	07.08.2007	43° 31.33' N	7° 24.24' E	1636	3,04	GC
	GeoB 12073	08.08.2007	43° 31.63' N	7° 25.71' E	1926	1,705	GC
	GeoB 12074	08.08.2007	43° 31.65' N	7° 25.97' E	1976	3,81	GC
	GeoB 12075	08.08.2007	43° 30.87' N	7° 26.58' E	2101	1,66	GC
	GeoB 12079	09.08.2007	43° 30.25' N	7° 27.61' E	2096	4,29	GC
	GeoB 12080	09.08.2007	43° 31.80' N	7° 24.69' E	1772	3,46	GC
Western Slides	GeoB 12044-2	03.08.2007	43° 32.07' N	7° 21.11' E	1529.1	4,77	GC
	GeoB 12045-2	03.08.2007	43° 31.76' N	7° 21.36' E	1639	5,23	GC
	GeoB 12047	04.08.2007	43° 31.80' N	7° 21.36' E	1614	0,26	GC
	GeoB 12048	04.08.2007	43° 30.65' N	7° 21.39' E	1819	1,51	GC
	GeoB 12081	09.08.2007	43° 31.14' N	7° 21.96' E	1743	4	GC

Var Canyon and turbiditic system	GeoB 12011	27.07. 2007	43° 26,74' N	7° 23,64' E	1971.3	0.15	PC
	GeoB 12012	27.07.2007	43° 28,95' N	7° 21,50' E	1824	0,89	PC
	GeoB 12017	28.07.2007	43° 34,94' N	7° 14,28' E	1226	0,18	PC
	GeoB 12022-2	29.07.2007	43° 37,61' N	7° 23,08' E	929,6	5,73	GC
	GeoB 12022-3	29.07.2007	43° 37,62' N	7° 23,09' E	935,3	0,02	PC
	GeoB 12022-4	29.07.2007	43° 37,62' N	7° 23,09' E	937,6	0	PC
	GeoB 12023-2	29.07.2007	43° 22,10' N	7° 32,85' E	1929	0,77	PC
	GeoB 12024	29.07.2007	43° 22,01' N	7° 31,16' E	1880	5,7	GC
	GeoB 12037	02.08.2007	43° 25.49' N	7° 51,49' E	2373	0	PC
	GeoB 12038	02.08.2007	43° 23.68' N	7° 44.16' E	2293	0,06	PC
	GeoB 12039	02.08.2007	43° 23.46' N	7° 31.51' E	2216	0,06	PC
	GeoB 12054	05.08.2007	43° 30.52' N	7° 22.14' E	1828	0,13	PC
	GeoB 12058	06.08.2007	43° 21.92' N	7° 32.24' E	1929	0,05	PC
	GeoB 12059	06.08.2007	43° 26.97' N	7° 27.27' E	2068	0	PC
	GeoB 12067	07.08.2007	43° 29.20' N	7° 27.08' E	1988	3,3	GC
	GeoB 12068	07.08.2007	43° 32.08' N	7° 17.22' E	1548	0,53	PC
	GeoB 12069	07.08.2007	43° 15.83' N	7° 15.83' E	1433	0,05	PC
	GeoB 12076	08.08.2007	43° 32.08' N	7° 17.21' E	1556	0,88	PC
	GeoB 12077	08.08.2007	43° 30.53' N	7° 22.13' E	1830	0,08	PC
	GeoB 12082-1	09.08.2007	43° 29.87' N	7° 23.59' E	1888	0	GC
	GeoB 12082-2	09.08.2007	43° 29.87' N	7° 23.59' E	1889	0	GC
	GeoB 12089	10.08.2007	43° 29.54' N	7° 20.86' E	1805	0,84	PC
	GeoB 12090	10.08.2007	43° 23.45' N	7° 32.52' E	2247	0,12	PC

6.7.2. Sediment description

Generally, sediments recovered during the entire M73/1 cruise are dominated by a mixture of silty mud to mud with varying portions of clay, silt and sand. Furthermore, low dues of organic matter (e.g. plant debris), pelagic and deltaic oozes and shell fragments (gastropods, pteropods, scaphopods and benthic foraminifera) are contained in the sediments. The facies is typically fine to medium grained with party identifiable sedimentary structures which include burrows from bioturbation, erosive structures and also mass-movement deposits (see below). The colour varies from yellowish brown and light grey in the upper part of the sediments to light grey and olive grey down-section, with distinct reddish (oxidised) grey intervals. In some sediment cores colour-banding from purplish, light beige to grey could be observed (see below).

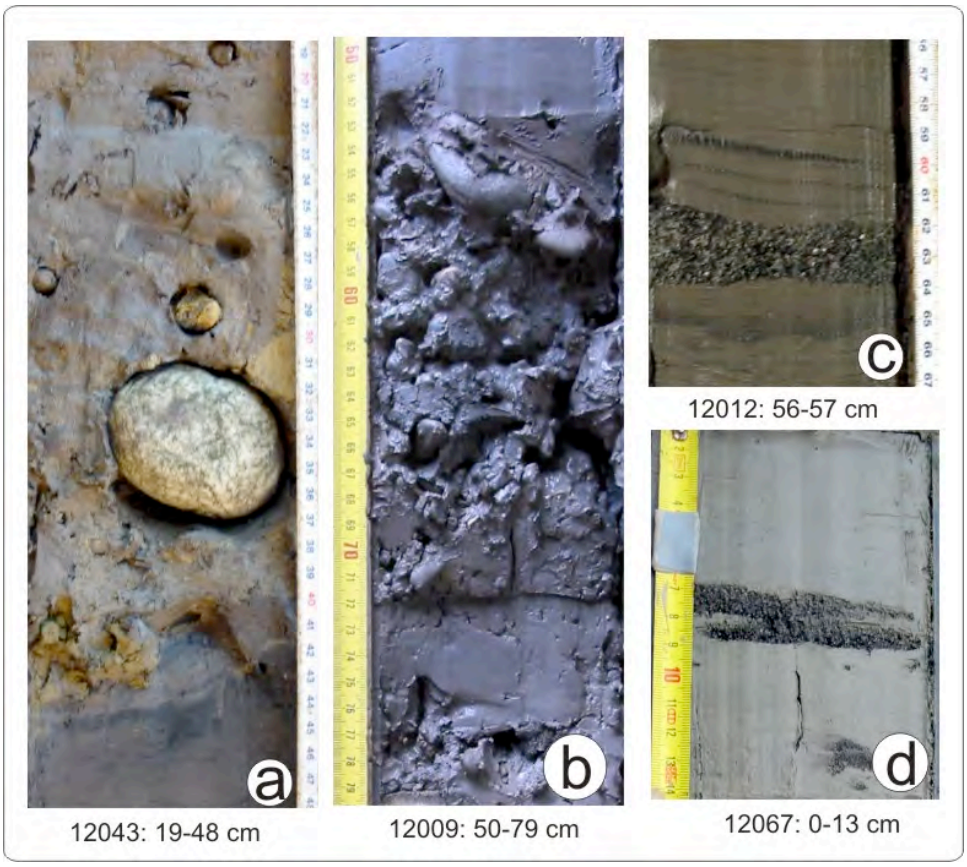

Fig. 58: Collection of core photographs of all research areas; a) debrite with pebbles and mud clasts in a clayey matrix from Nice airport area; b) debrite with pebbles in silt-clay matrix from the midslope area; c) turbidite from the Var Canyon; c) turbidite consisting of shell fragments (white dots) and hydrotrolite.

Before the five study areas (Fig. 24) are described in more detail, a few summary statements regarding debrites and other mass wasting deposits are given, mostly because landsliding and other depositional processes represent a key component in each of the five areas. From a sedimentological point of view, clear evidence for mass-movements such as debrites could be identified in all research areas except the Var Canyon area, where turbidites are evidences for mass movements (see below). Generally, the debrites contain of hard light-coloured clasts, comprising of pebbles and gravel, in a darker silty-clay matrix (Fig. 58a and b). Seismic and bathymetric data indicate major landslide deposits and a lot of smaller and bigger headwall in the research areas. The debrite in the Nice airport area cores (see below and Fig. 57) is tentatively related to the 1979 Nice event.

In contrast to all four other areas, the most common feature observed in the Var Canyon gravity cores were turbidites. The turbidity intervals are more or less abundant silty to sand layers, often with an erosional base (Fig. 58c-d). Otherwise, a content of undefined shell fragments and hydrotrolite (FeS x nH_20) is visible (Fig. 58c). Sometimes spill over deposits

overly the turbidites. Unfortunately, in the seismic data no indications of distinct pathways are visible.

Nice airport area

The primary scientific target in this study area was to identify mass wasting deposits based on the 1979 Nice landslide event. The originated headwall is visible in seismic and bathymetric data and is more or less known from further investigations (IFREMER, Brest). Figure 59 shows the position of the cores surrounded by the boundary of the slide (limite du glissement de 1979). The cores were recovered in very shallow water (15-30 m water depth) except core GeoB12071 (~50 m water depth). Core GeoB12072-1 was located at a proposed IODP (Integrated Ocean Drilling Program) position. This core recovery was primarily a requirement for the IODP proposal 685 (Henry et al., 2005) to provide ground truthing for the site survey panel and environment and safety panel of IODP.

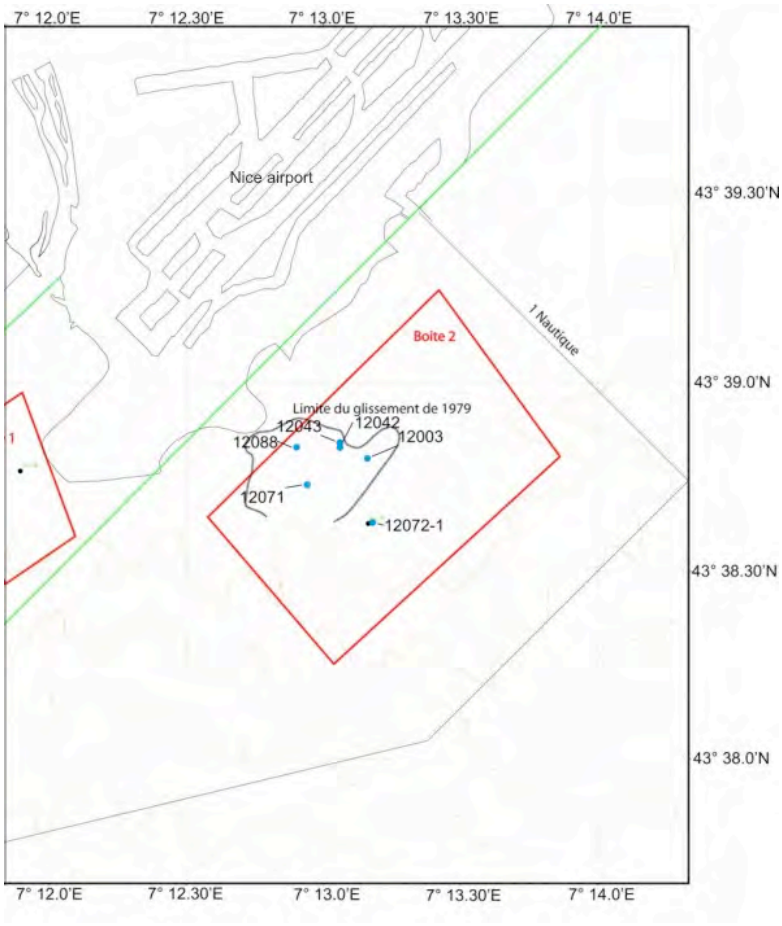

Fig. 59: Core locations surrounded by the boundary of the slide from the 1979 nice event (map provided by IFREMER, Brest).

Normally graded intervals are characteristic for all core described in the Nice airport area except core GeoB12043. Furthermore, sediment structures occur as laminated, colour-banded deltaic deposits of silty clay. In between the deltaic laminae silty to sandy pockets, lenses and layers with erosive bases and tops are frequently found. The colour banding follows a repeated succession of dark, purplish and light beige thin silty clay layers (example in Fig. 61c). The darker base of the sequence is sometimes slightly coarser-grained. Also inversely graded sequences were observed in the cores. The coarsest intervals are silt grained for this research area and fining up to silty clay downwards the core.

Characteristic for the reference core taken outside the 1979 scar (GeoB12072-1) are silty layers with high water contents, additionally releasing gas bubbles when cores were split (Fig. 60a). Such permeable water-rich coarse layers overlain by impermeable clays are candidate planes of sediment failure.

Core GeoB12072 also shows tiltd sediment layers with an inclination of about 15° to 20° (Fig. 60b), which could be related to progressive oversteepening owing to former tectonic movements.

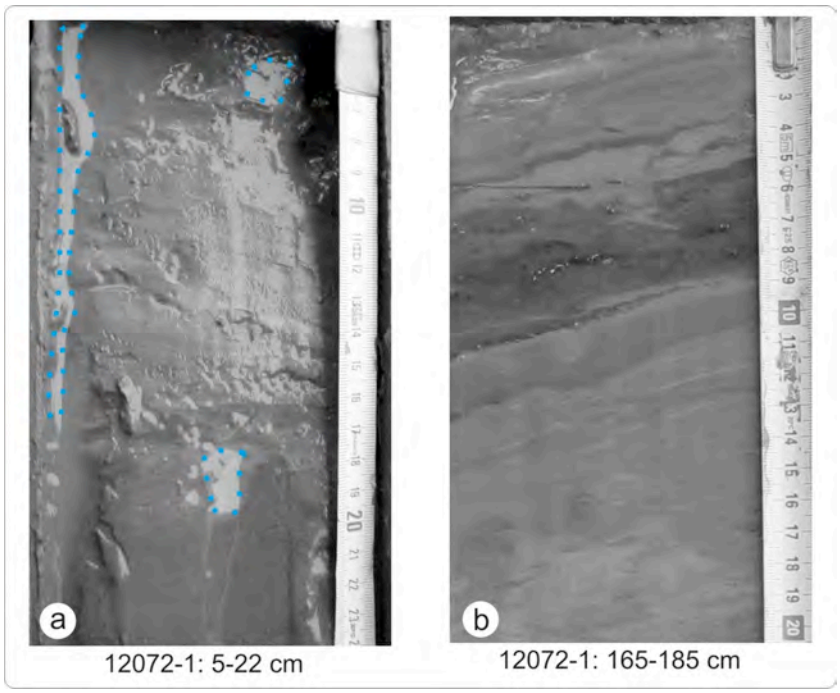

Fig. 60: Silty layers with very high water content (blue dotted lines) from the top of core GeoB 12072-1 in a) and oblique sediment layers from a deeper part of the same core (165-185 cm) in b).

Both headwall cores (GeoB12042 and 12043) contain debrite intervals, one of which could possibly represent the 1979 event. The debrites are composed of gravel-sized shells, shell debris, pebbles, cobbles and beige-green mud clasts in a clayey matrix (Fig. 58a). These debrites provide clear evidence for mass movement. Shell debris intervals are found in the deeper part of the headwall and in cores further east (e.g. GeoB12042, 12003 and 12088). These intervals are very similar in their stiffness, low water content, very dark colour and high abundance of shells, mainly bivalves and gastropods.

An estimate of the age of the material recovered below the debrite of both headwall cores (see location in Fig. 59) was done based on the known sedimentation rate of 11.5 m ky^{-1} for this airport area (given by Dan et al. 2007, Dubar & Antony 1995). Using the thickness of the interval recovered during cruise M73/1, we can estimate the age of the material below the debrite unit to be 183 years (GeoB12042) and 109 years (GeoB12043) (see Table 6).

Table 6: Calculated age of the recovered material from the headwall cores from the Nice.

Core	GeoB12042	GeoB12043
recovery below the debrite (cm)	210	125
sedimentation rate (cm/ky)	1150	1150
age of the debrite (years)	28	28
calculated age of rec. material below debrit (years)	~ 183	~ 109

Shallow- and Midslope area

This research area includes both ridges and gullies where the landslide mass from the 1979 Nice event was supposedly travelling, and is surrounded by some unaffected stable slope regions. The main scientific target was to improve our knowledge about the proposed pathways from landslide mass. For that twelve locations were selected in the shallow-slope region crossing the channels of the Var Canyon (Fig. 61). For description the cores in the channels, the notation of Dan (2007) was used. The recovered cores demonstrate a coarsening of the deposits from west to east in these channels.

Similar to the cores taken in the Nice airport study area, the cores taken from the ridges (GeoB12015, GeoB12033, GeoB12084 and GeoB12085) show also laminated, colour-banded deltaic deposits of silty-clay. In between the deltaic laminas frequently are found silty to sandy pockets, lenses, and layers with erosive bases and tops and with high water content. The attracted core at top of the ridge within channel 3 show sequences of thin layers with silty-clay to clay composition (GeoB12015). In these sequences, colour banding from dark grey by purplish to light beige could be observed (Fig. 62c). Due to the fact that these sequences occur at regular intervals they may represent seasonal events. Similar colour banding was observed in the other study areas (e.g. GeoB12088 - Nice airport area).

Coring in the two western channels (channel 3 and 4) was not very successful because the sediments were very stiff. Fallen gravity corers recovered debrites (Fig. 59b) with cobble-sized gravel (diameter up to 13 cm) in a silty-clay matrix. The sediments at the eastern-most channels (channel 1 and 2 upstream) consist of sequences of soft laminated deltaic deposits of silty-clay with silty and sandy pockets. The interesting features of these locations are the obliquity (30°) of the beds (example Fig. 62b). The tilt could be explained with the actual angle of the slope or with a massive displacement of sediment. The slope angle could be verified with the aid of high-resolution swath bathymetry. Burrows and organic matter are abundant among the oblique deltaic deposits.

The coarsening of the deposits from west to east in the channels in the northern part of the Var Canyon is an evidence for an increase of the energy in the channels in the same direction. Channel 4, therefore receives the highest-energy discharge of the Var River (coarser particles) and the finest particles are deposited in channels 1 and 2. Dan (2007) suggests that the major pathway of the landslide mass was channel 3. With our study we cannot really confirm this hypothesis because debrites were found in both western channels. The only assumption we can make is that the eastern two channels contain no debrites and, therefore, they were obviously somewhat distal pathways for the finer grained material.

The shallow-water core taken near Antibes (GeoB12019), west of the main study area, shows in the upper part of the core undisturbed deltaic deposits of silty clay to clay. The deeper part of the core, however, consists of very porous stiff organic-rich sediments, which suspiciously look like a sapropel (Fig. 62a). Total organic C content as well as other analyses are planned post-cruise.

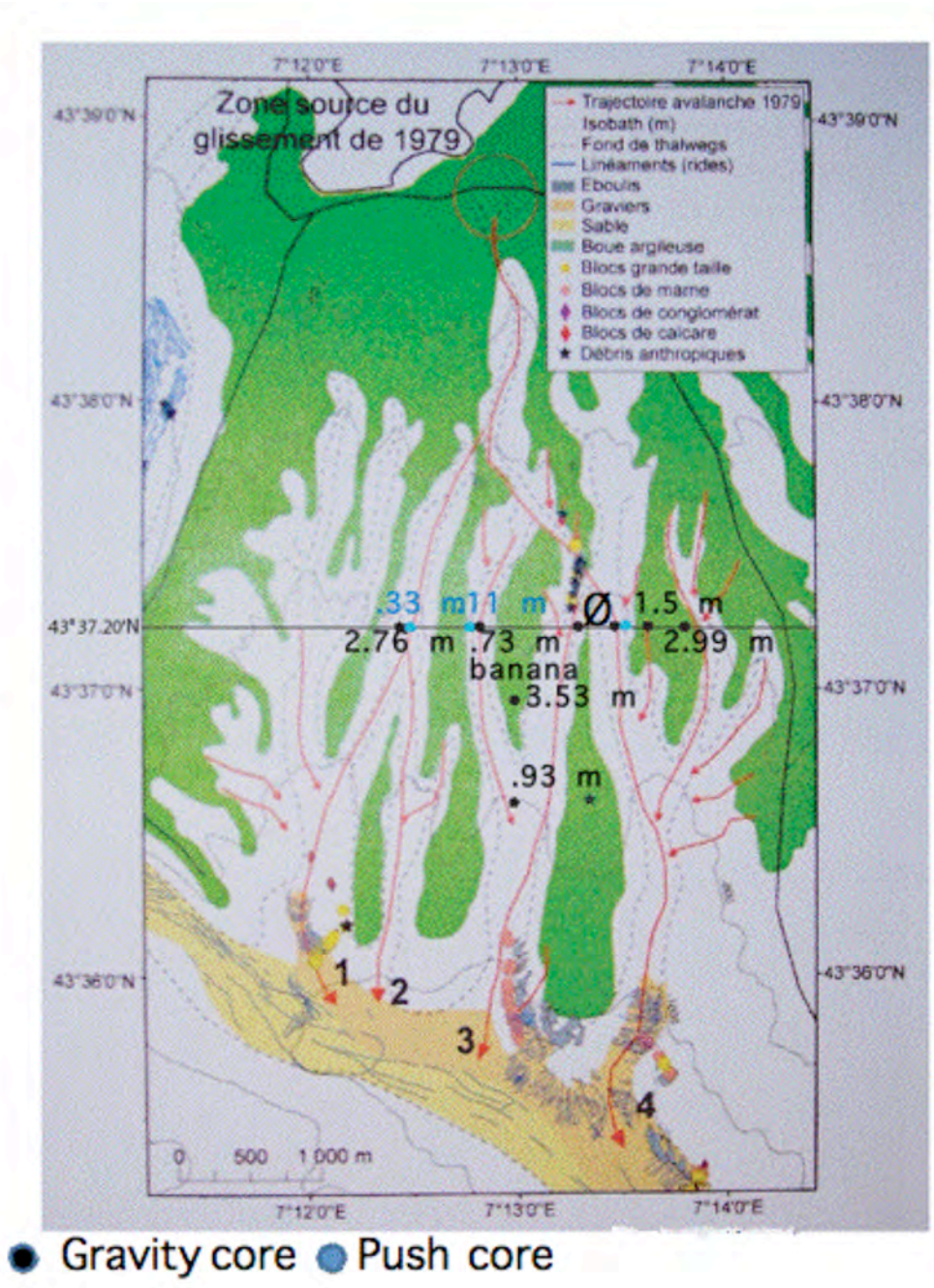

Fig. 61: Map of the northern Var Canyon showing location of push and gravity cores with their recovery. Modified after Dan, 2007.

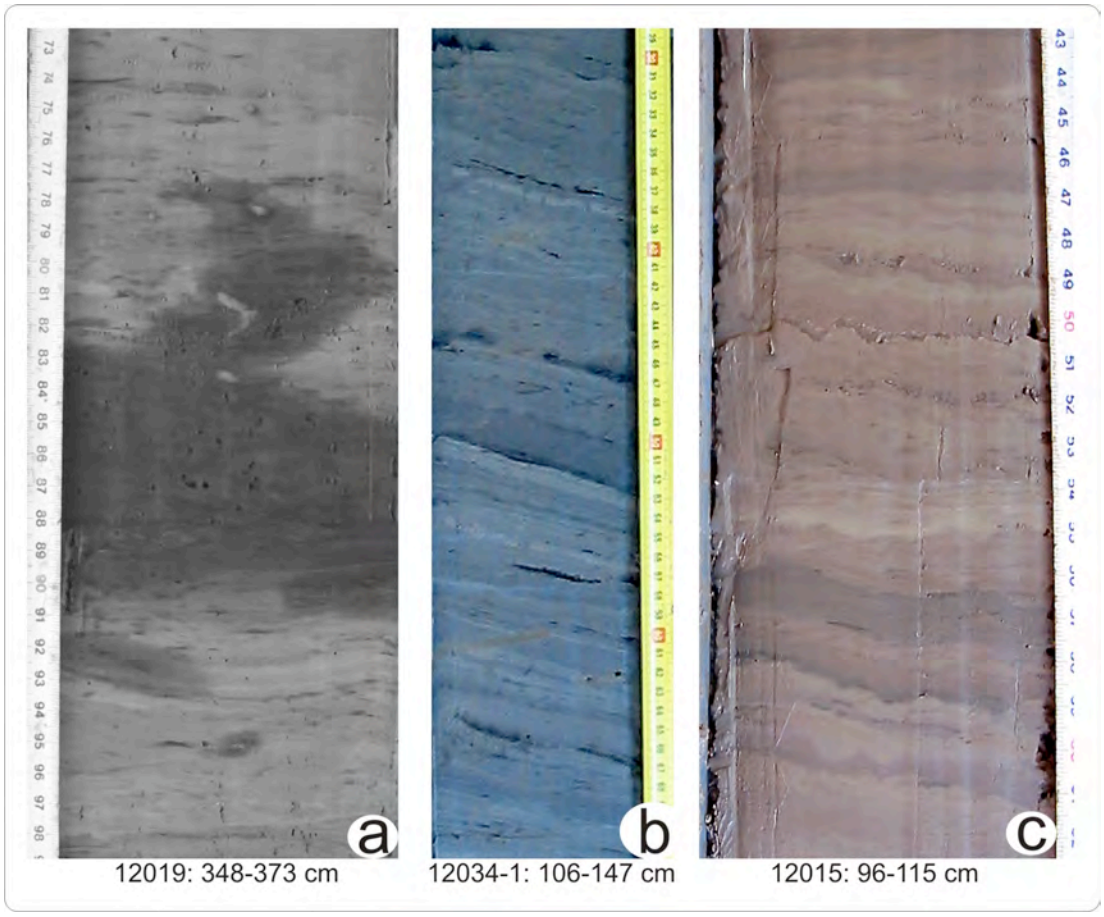

Fig. 62: Collection of core photographs; a) very porous organic-rich sediment from near Antibes; b) obliquity (30°) of the beds in sediments in the eastern most channel 1 (Midslope area); c) colour banding in sequences in sediments on top of a ridge (midslope area).

Western Slide Complex

This study area is affected by landslide scars and talus at the deeper slope (1500-2000 m water depth) and adjoins to the Var Canyon. Figure 63 shows the position of the 5 cores and the supposed scars and pathways of the landslide.

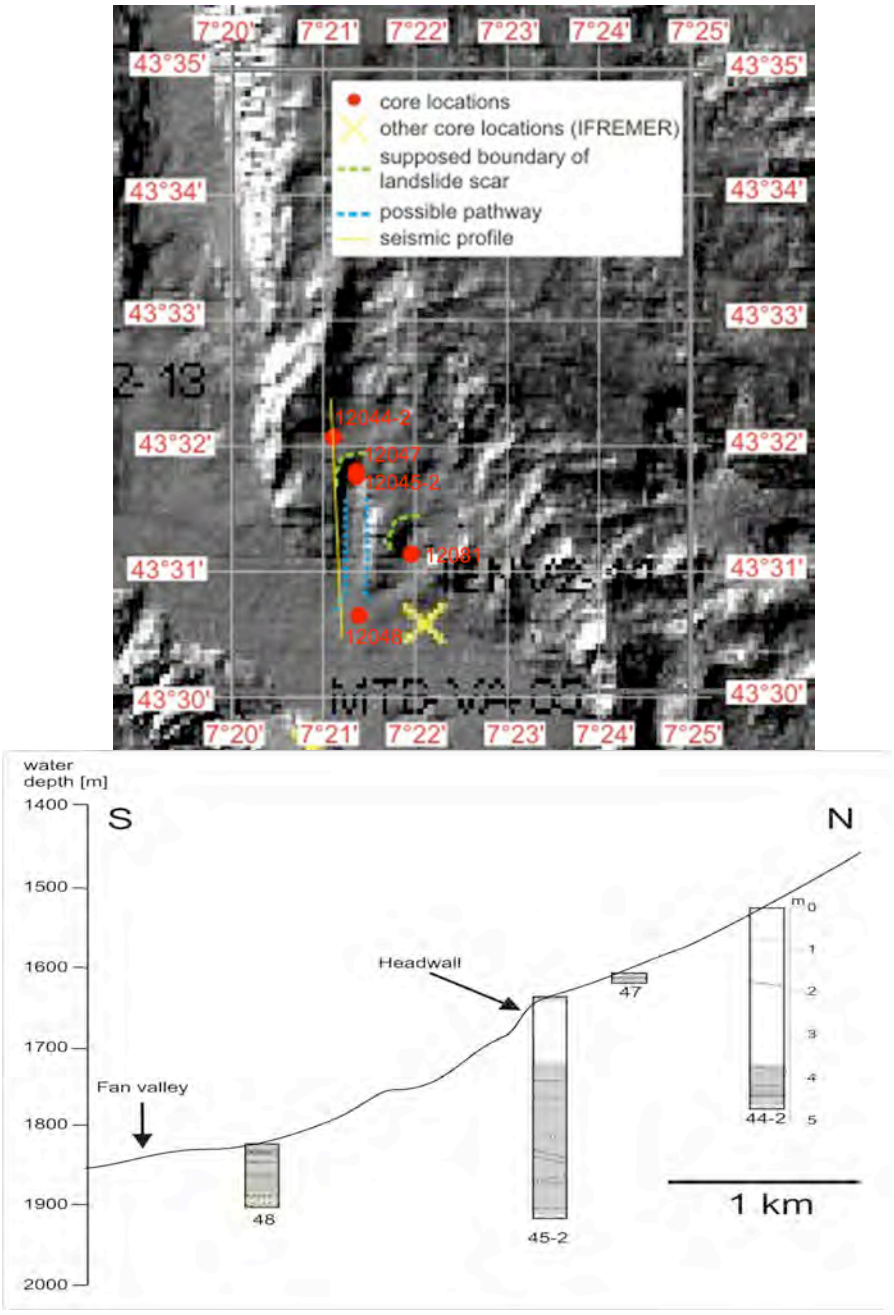

Fig. 63: Core locations of the Western slide research area with supposed scars and pathways of the landslide a); profile (position is shown in upper map; see core lithologs from S to N in lower cross section). [Bathymetry provided by IFREMER, Brest]

Many of the cores in this study area recovered homogenous, highly bioturbated, and fine-grained hemipelagic silty clay. The core upside the main scar (GeoB12044-2) shows

hemipelagic sediment with sharp oblique contacts to the underlying clay and silty-clay sediments (Fig. 63) with shell fragments. The obliquity could be related to the seep slope angle and to an already started and onward creeping of these slope sediments. Core GeoB12081 is located further downslope (location see Fig. 63, top) and consists of hemipelagic sediments, which are much laminated with colour-banding in clayey and silty layers. Furthermore, some pebbles were shown in the silty layers and organic matter and shell debris underlying those.

The core near the headwall (GeoB12045-2) contains displaced and reworked sediment with sandy intervals (Figs. 63 and 64a) which may evidence mass movement. The core is composed of very stiff sediment (see Ch. 6.8. “undrained shear strength”), possibly a result of overconsolidation.

An interesting fact in this area is that the mass movements seem to be multiple events. This could be supported by the already mentioned displaced and reworked sediments as well as by increments of the headwall in the geomorphologic and seismic profiles (Fig. 64b and Ch. 6.4). In the distal part of the supposed pathway (dotted line in Fig. 63) the core GeoB12048-2 is located consisting of silty clay to clay and intermediary silty to sandy layers which up to 10cm thickness (Fig. 64c).

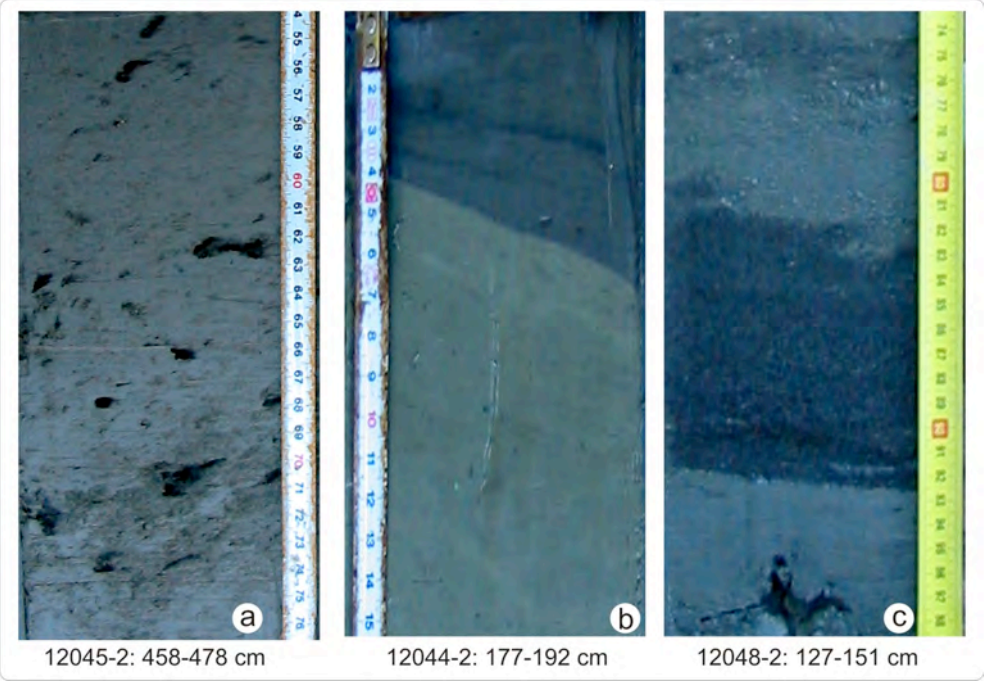

Fig. 64: Collection of core photographs; a) reworked sediments with sandy intervals of GeoB12045-2 (headwall core); b) hemipelagic sediments with sharp oblique contacts from the core upside the scar (GeoB12044-2); c) thick fine-grained sandy and organic rich layer between two mud layers in distal core GeoB12048-2.

Eastern Slide Complex

Eleven locations were selected in the Eastern slide area (Fig. 65), most of which were taken along a NW-SE transect. This research area is defined by a large slide complex further away from the Var Canyon in the east of the western slide area.

Similar to the western slide cores (see above), many of the cores recovered consist of homogenous, highly bioturbated and fine-grained hemipelagic silty clay without turbiditic or mass-wasting events. Instead, the undisturbed hemipelagic sequence is interrupted in several cores by instability features such as spill-over deposits and water-rich silty clay layers. Two of the cores (GeoB12053 and -12064) contain debrites, clasts and pebbles. The debrite of the top-most layer from a core taken near the headwall of the landslide scar (GeoB12053) shows a thick debrite horizon consisting of hard, light-coloured clasts in a darker silty-clay matrix. Figure 66a shows a debrite consisting of soft clasts and well rounded pebbles in a darker silty-clay matrix (GeoB12064, 335-378 cm bsf).

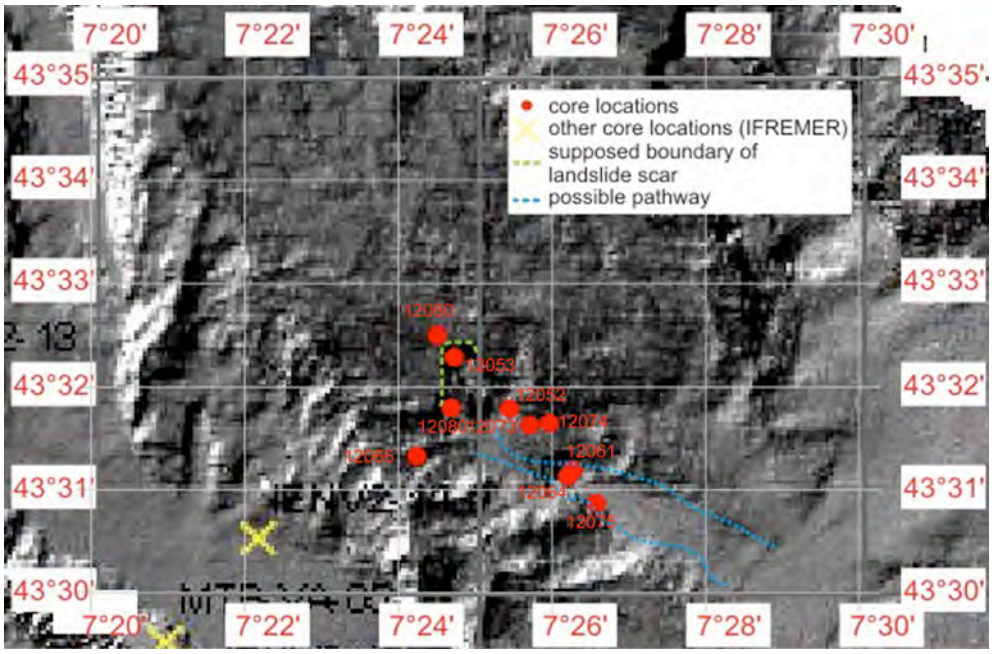

Fig. 65: Core locations of the Eastern slide research area with supposed scars and pathways of the landslide (Bathymetry provided by IFREMER, Brest).

A core taken further downslope (GeoB12075), lying in the projected pathway of the slide, shows sharp oblique contacts between very stiff hemipelagic sediment and the overlying soft hemipelagic sediment which illustrates some instability event (Fig. 66b). The oblique contact is visible between reddish-brown and greyish-green silty-clay. The colouring seems to be a post-depositional feature resultant of a chemical reaction. In the upper part of this

core colour bands (Fig. 66c) are obvious, but are more coherent than the colour bands in the Midslope area (see above). Another chemical reaction could be observed in the core overlying the landslide scar (GeoB12060). In the deeper part of this core (~420-450cm bsf), a pteropod shell debris remineralisation can be observed. FeS_2 (pyrite) occurs as a post-depositional structure in burrows (Fig. 66d).

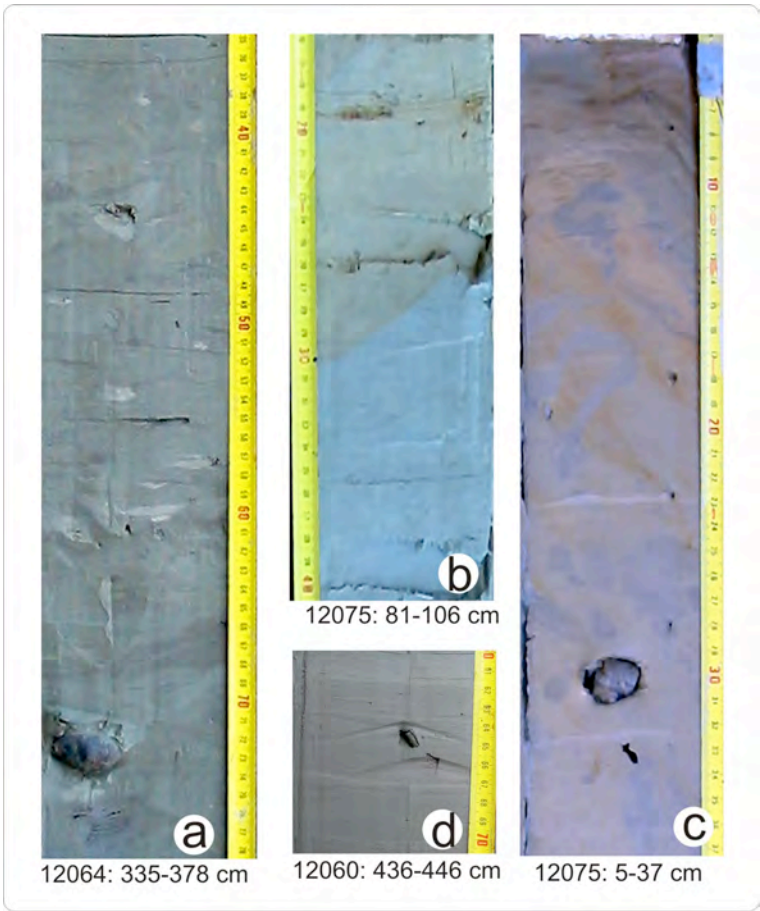

Fig. 66: Collection of core photographs; a) debrite consisting of soft clasts and well rounded pebbles in a darker silty-clay matrix (GeoB12064); b) sharp oblique contact between grey-green hemipelagic sediment and the overlying reddish hemipelagic sediment (GeoB12075); c) merged colour banding of core GeoB12075; d) pteropods shell debris: FeS_2 mineralization.

Var Canyon and turbiditic system

The Var Canyon research area comprises of flanks, terraces and channels in down to ~2500 m water depth (Fig. 67). All of the recovered cores in this study area show evidence of turbidity currents, except for the cores in the open slope where the recovered sediments are hemipelagic. The two open slope cores (GeoB12022-2 and GeoB12022-3) off the coast of Nice, where there is suspected creeping (see IODP proposal 685), yielded homogenous,

highly bioturbated, light coloured fine-grained hemipelagic silty-clay which recorded no turbiditic or mass wasting events.

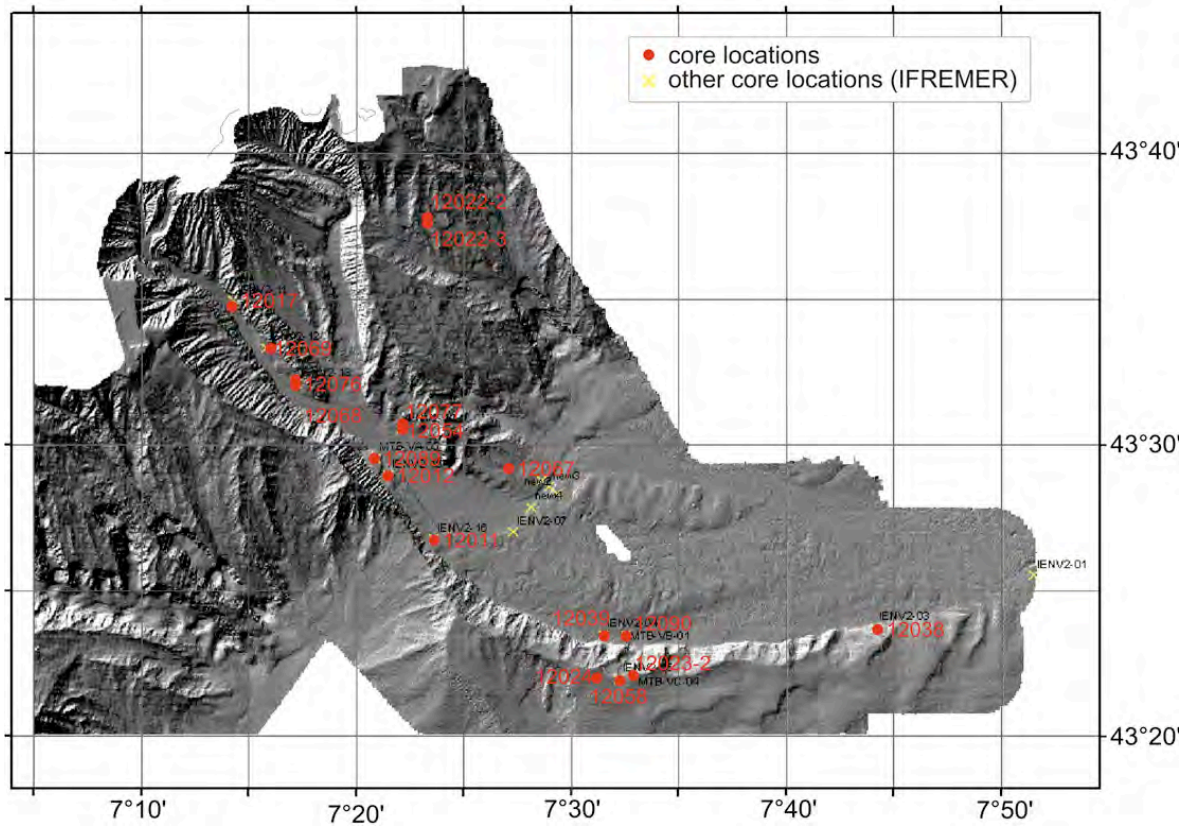

Fig. 67: Core locations of the Var Canyon and turbiditic research area (Bathymetry provided by IFREMER, Brest).

The turbiditic intervals are silty to sandy layers with a thickness of several mm to 6 cm, most of which with erosive bases (examples Figs. 58c-d). Fining-up sequences are also common in the cores recovered from this study area. Otherwise, occasional shell fragments and hydrotrolite (FeS x nH_20; black dots) are visible (Figs. 59d and 68b).

Continuous flow stripping of the upper portion of turbidity currents carries finer grained material, which is deposited as fine spill-over sediment at the top of the levee. In the Var Canyon several cores reveal levee formations, which show a succession of hemipelagic and terrigenous material. Amongst others, spill-over deposits are found in core GeoB12012. It was obtained from a small terrace just in front of the main southern levee of the Var sedimentary ridge, along with another core, GeoB12011 (Fig. 68a), taken further downstream and on a lower elevation of the terrace. The darker intervals in these cores represent conditions of higher terrigenous input (spill over sediment), where only the fined-grained clay particles were carried over the levee. The lighter intervals would correspond to

the background sedimentation of calcareous ooze. The bottom contact of the darker terrigenous sediment with the lighter hemipelagic is sharp, but erosive and with lenses of dark material incorporated into the lighter material. The upper contact of the terrigenous intervals is a gradational transition to hemipelagic sedimentation. The sharpness of the bottom contacts of the terrigenous intervals and their very slightly silty bases, together with the gradual upper transitions indicate clayey turbidite pulses, which start rapidly and steadily decelerate with time.

In core GeoB12067 located on a small ridge at the right side of the Var Canyon (for position see Figure 67), a vertical feature consisting of softer, darker and more water-rich silty clay as the surrounding sediment could be observed (Fig. 68c). Above, the sediments consists of bioturbated, homogenous silty-clay to clay.

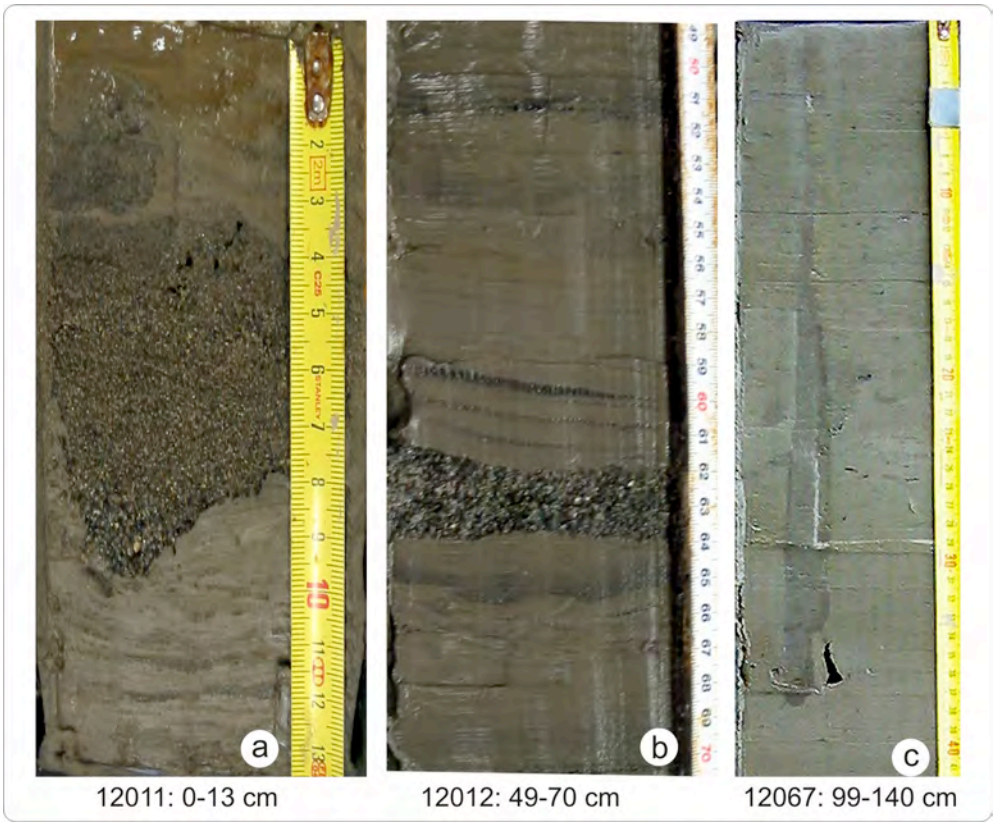

Fig. 68: Collection of core photographs; a) spill over deposits of core GeoB12011; b) turbiditic layer with undefined shell fragments and hydrotrolite (FeS x nH_20; black dots) of core GeoB12012; c) vertical feature consisting of softer, darker and more water rich silty-clay as the surrounding sediment (GeoB12067).

6.8. Physical properties

(A. Förster, T. Krumova, A. Kopf)

The database of physical properties of the LIMO-LAMO cores consists of P-wave velocity, bulk density, magnetic susceptibility and fractional porosity, logged with the GEOTEK multi-sensor core logger (Ch. 5.8.3.), and the undrained shear strength s_U, measured with the fall cone penetrometer (Pen) and the vane shear (Vs) (see Ch. 5.8.1. and 5.8.2.). The properties are described and briefly discussed separately for each study area.

Nice Airport Area

Sediments taken from this area comprise of clay to silty clay mud with several coarser layers and organic carbon-rich layers.

The undrained shear strength values (s_U) from the Vane shear tests of GeoB12042, GeoB12043 (headwall of the slide from 1979) range between 2 and 40 kPa. Strength $s_{U(Pen)}$ shows a strong increase from 2 to 450 kPa. Spikes up to from 600 kPa correlate with the manner of sandy layers. In contrast to these high values the $s_{U(Pen)}$ of the cores east (GeoB12003, GeoB12072-1) of the scar increase linear from 2 to 80 kPa, with higher strength values corresponding to coarser layers. Reddish (oxidised) layers and layers with higher water content are just reflected by low $s_{U(Vs)}$ in all cores. As opposed to the slope sediments, which show average bulk densities of 1.92 to 2.0 g/cm^3, the reference core east of the scar (GeoB12003) shows lower value in bulk density like 1.83 g/cm^3.

Shallow- and Midslope area

Sediments taken from this area comprise of clay to silty clay mud with several silty and sandy layers. The coarsening of the deposits from west to east in the channels in the northern part of the Var Canyon is clearly identifiable. To the northwest of the four channels, core GeoB12019 shows a bulk density similar to the reference core from the Nice Airport area (1.83 g/cm^3). The sediments of the centre of channel 2 (GeoB12034-1) show average densities of 1.94 g/cm^3. The undrained shear strength values $s_{U(Pen)}$ show a linear increase up to 22 kPa. The sediments from core GeoB12009 are similar in density, but show higher $s_{U(Pen)}$ values up to 35 kPa. The average bulk density of the channel 2 sediments show lower

values around 1.86 g/cm^3. The linear increase in $s_{U(Pen)}$ from 4 to 40 kPa may be explained by an obliquity of the beds.

The four cores from the ridges (GeoB12015, 12084, 12085, 12088) show average bulk density values from 1.83 to 1.88 g/cm^3. The undrained shear strength values $s_{U(Pen)}$ of core GeoB12015 show a linear increase to 60 kPa (to 2.15 m) followed by a decrease to 25 kPa, correlating with . higher clay abundance. Reddish (oxidized) layers and layers with higher water content are reflected in lower $s_{U(Vs)}$ values in all cores.

Var Canyon and turbiditic system

All of the recovered cores in the Var Canyon and turbiditic system study area show evidence of turbidity currents with silty to sandy layers with thicknesses of several mm to 6 cm.

The cores in the open slope (GeoB12022) consisting of sediments with clay to silty clay mud show bulk density values of 1.85 g/cm^3 Against these values the sediment cores in the northern (GeoB12022-2) and in the middle part of the canyon (GeoB12067) show lower bulk density values (1.71-1.75 g/cm^3).

For the undrained shear strength values $s_{U(Pen),}$ a linear increase is shown for the cores of the open slope (2-20 kPa) and the northern part of the canyon (1-30 kPa). For core GeoB12067 the $S_{U(Pen)}$ values vary with no visible trend from 4 to 12 kPa. For all cores considered, spots of higher strength values correlate with the manner of coarser layers. For detailed s_U results, see lithological diagrams in Appendix 9.3.

No MSCL data description will be given here, because the measurements were carried out post-cruise and are only available electronically in Appendix 9.4 of this report.

6.9. Pore water chemistry

(J. Blees, K. Bogus, T. Haarmann, M. Hentscher**)**

Most of the total 25 cores analysed can be grouped into three study sites, i.e. the airport area, the eastern landslide and the western landslide, as shown in Table 7 (see also Fig. 24).

Table 7: Position, name and grouping of the cores, depending on their geochemical characteristics.

Group	Core	Longitude	Latitude	Water depth [m]
Airport	03	7° 13,15' E	43° 38,80' N	24.4
	42	7° 13,05' E	43° 38,83' N	28.4
	43	7° 13,05' E	43° 38,84' N	20.2
	72-1	7° 13,17' E	43° 38,63' N	19.7
	88	7° 13,16' E	43° 36,96' N	15
Eastern slide	52	7° 25,45' E	43° 31,79' N	1905.1
	53	7° 24,73' E	43° 32,29' N	1759.9
	60	7° 24,51' E	43° 32,50' N	1574.9
	61	7° 26,28' E	43° 31,20' N	2091.1
	64	7° 26,21' E	43° 31,12' N	2094.4
	74	7° 25,97' E	43° 31,35' N	1976.3
	75	7° 26,58' E	43° 30,87' N	2100.8
	79	7° 27,61' E	43° 30,25' N	2090.1
Western slide	44-2	7° 21,11' E	43° 32,07' N	1529.1
	45-2	7° 21,36' E	43° 31,76' N	1639
	48	7° 21,39' E	43° 30,65' N	1818.8
	81	7° 21,96' E	43° 31,14' N	1742.9

The cores were grouped based on geographical position and morphology of the sea floor. Geochemically these groups showed distinct characteristics, which will be briefly presented below. Furthermore, Table 8 indicates which analyses were carried out for the specific cores.

Nice airport area

The airport cores were all taken in less than 30 metres water depth. Three of the five cores (GeoB12042, -12043 and -12003) show a distinct decrease in salinity with depth (Figs. 69-70). This decreased salinity is paired with a decrease of iron concentrations. In comparison with cores from the slide complexes the airport cores contain significantly

higher ammonium concentrations and alkalinity values, ranging from 100 - 3000 µM and 30 – 60 mmol(eq)/l respectively. As an example for the cores showing reduced salinity core GeoB 12042 is shown (Fig. 69). In this core salinity falls to zero between one and two metres core depth. Ammonium peaks within that depth range, at around 1.5 m. Freshening of the pore water is attributed to the influence (i.e. inflow) of submarine groundwater from the north.

Cores GeoB12072-1 and GeoB12088 show no signs of decreased salinity. These two cores do contain higher alkalinity and ammonium values than the slide cores.

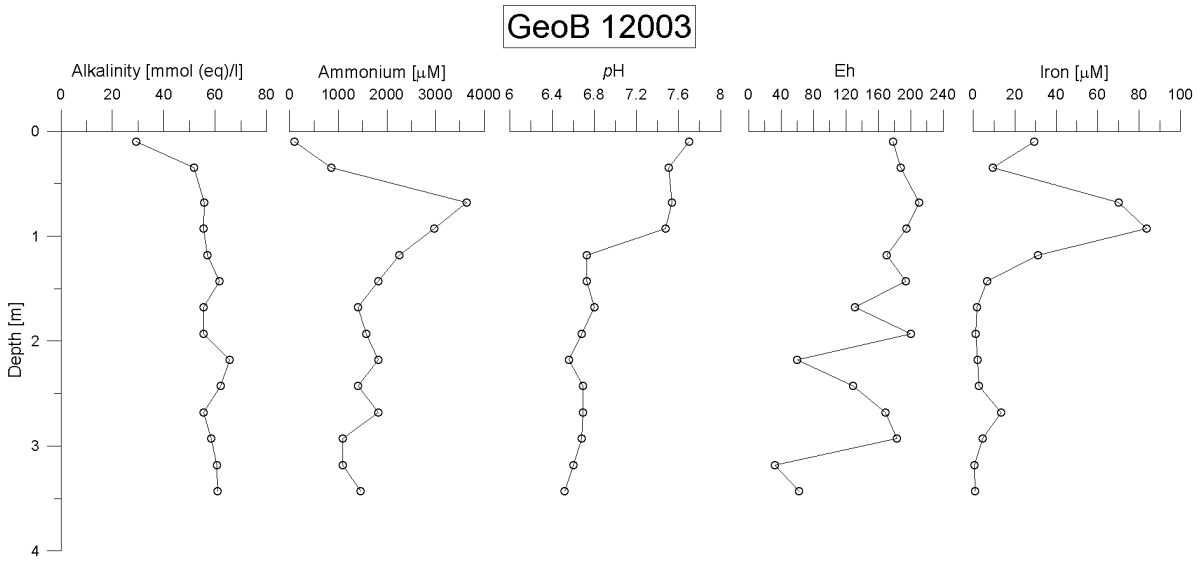

Fig. 69: Pore water concentration profiles of gravity core GeoB12003.

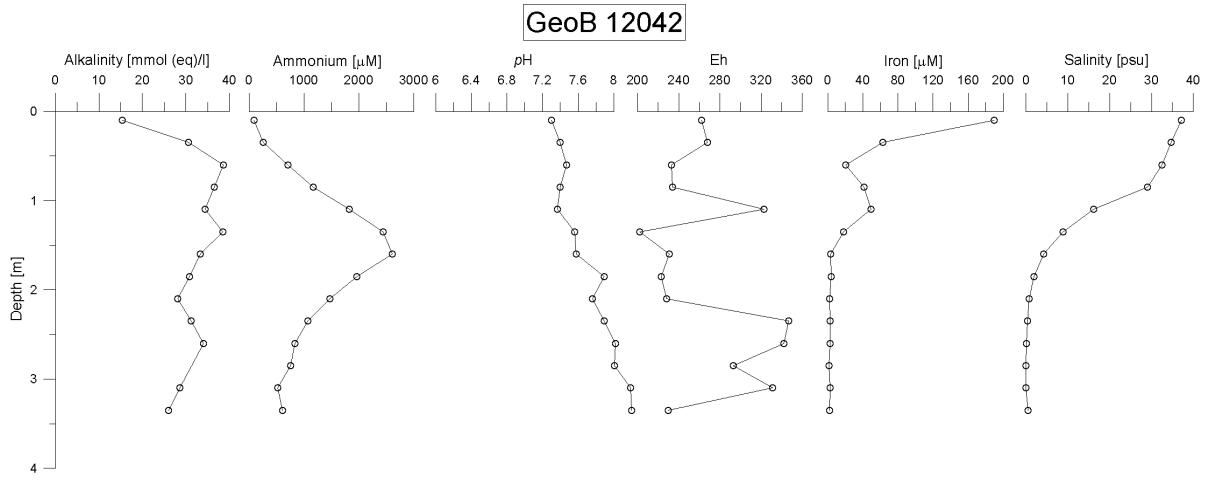

Fig. 70: Pore water concentration profiles of gravity core GeoB12042.

Most interestingly, Cr anomalies are also seen in the freshened pore waters; however, they seem to be restricted to some, but not other freshened areas. As can be seen from Figure 71, adjacent cores GeoB12042 and –43 both show significantly enriched Cr values. On the other hand, those cores are diluted with ground waters from the north, so that it is likely that the Cr is associated with the groundwater flux rather than a marine source.

At this point, it is too early to draw any conclusions regarding the nature and complexity of the hydrology in the Nice airport region. However, earlier workers pointed out that there are several apparently disconnected areas that release freshened fluid into the shallow Ligurian slope (see Guglielmi 1993). Sandy layers with gravel and pebbles, which were cored at the bottom of the failure scar (see above), appear to act as the main aquifer which could influence slope stability conditions off shore of the Var delta (Dan et al. 2007). Post-cruise work will try to shed light to this question.

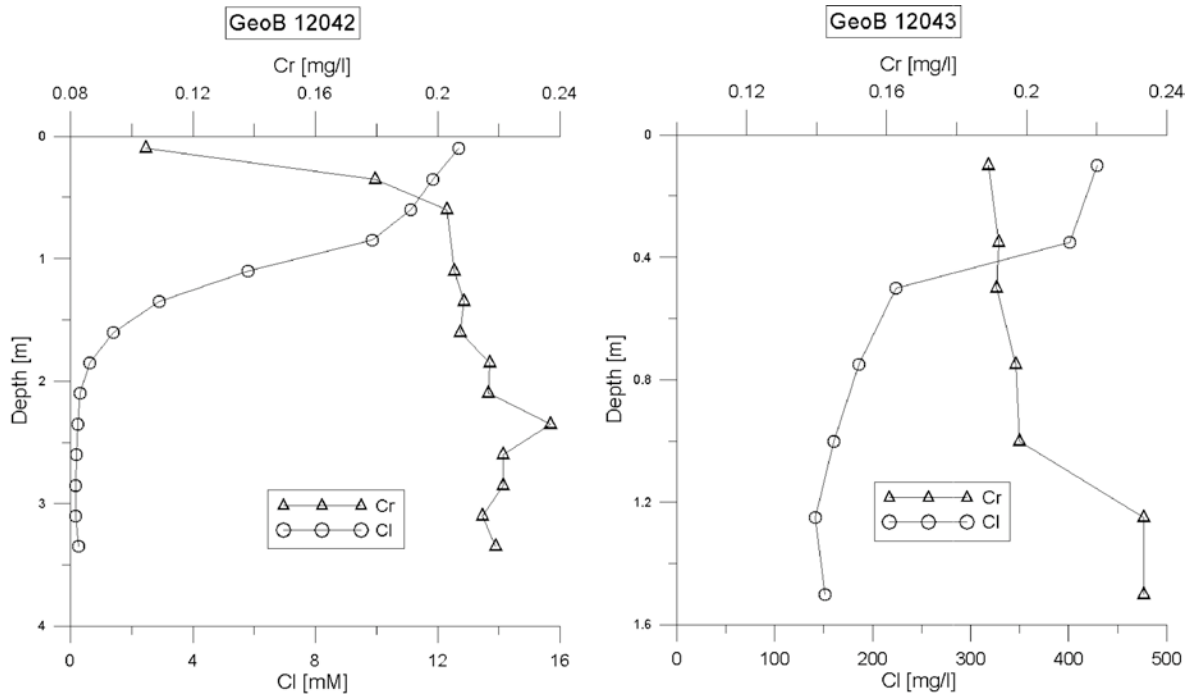

Fig. 71: Examples of elevated Cr values despite significant pore water freshening in gravity cores GeoB12042 and –43. Absence of elevated Cr in otherwise freshened pore waters nearby suggests a complx aquifer system in the Nice airport area. See text.

Eastern and western landslides

Generally the cores taken on both slide complexes show very low ammonium and alkalinity values, ranging from 0 – 400 µM and 15 - 25 mmol(eq)/l respectively. The highest

alkalinity was measured in core Geo12064, peaking at 38 mmol(eq)/l. Geochemically the cores from the slide complexes look similar, with slowly rising alkalinity and ammonium values with depth. Iron concentrations in the pore water were found to be uniform in the entire region, ranging from 30 - 200 µM except in core GeoB12060, where iron concentrations peak at 400 µM at a depth of around 2 metres. Apart from the iron concentrations, core GeoB12060 can be taken as an example for the geochemical trends observed within the pore water of the slide complexes (see Fig. 72).

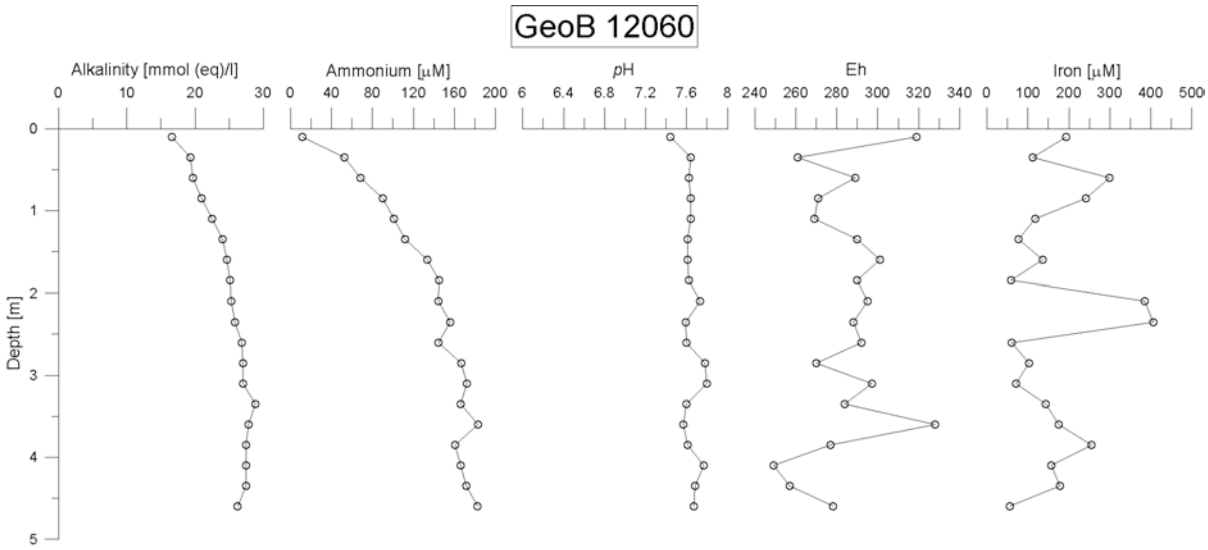

Fig. 72: Pore water concentration profiles of gravity core GeoB 12060.

Table 8: Analyses carried out for the specific cores and, respectively samples taken (for CH_4 and solid phase)

Core name	Longitude	Latitude	Eh	pH	Alk.	Fe^{2+}	NH_4	Salinity	CH_4	Solid phase	HS^-	Cations	SO_4, Cl
GeoB12003	7° 13,15' E	43° 38,80' N	X	X	X	X	X	-	X	-	X	X	X
GeoB 12009	7° 13,01' E	43° 36,60' N	X	X	X	X	X	-	X	-	X	X	-
GeoB 12015	7° 13,00' E	43° 36,90' N	X	X	X	X	X	-	X	-	X	X	X
GeoB 12019	7° 10,47' E	43° 39,03' N	X	X	X	X	X	X	X	-	X	X	-
GeoB 12022	7° 23,08' E	43° 37,61' N	X	X	X	X	X	-	X	-	X	X	-
GeoB 12024	7° 31,16' E	43° 22,01' N	X	X	X	X	X	-	X	X	X	X	X
GeoB 12034	7° 12,40' E	43° 37,19' N	X	X	X	X	X	-	X	X	X	X	-
GeoB 12042	7° 13,05' E	43° 38,83' N	X	X	X	X	X	X	X	X	X	X	-

GeoB 12043	7° 13,05' E	43° 38,84' N	X	X	X	X	X	X	X	X	X	X	-
GeoB12044	7° 21,11' E	43° 32,07' N	X	X	X	X	X	X*	X	X	X	X	-
GeoB 12045	7° 21,36' E	43° 31,76' N	X	X	X	X	X	-	X	X	X	X	-
GeoB 12048	7° 21,39' E	43° 30,65' N	X	X	X	X	X	-	X	X	X	X	-
GeoB 12052	7° 25,45' E	43° 31,79' N	X	X	X	X	X	-	X	X	X	X	-
GeoB 12053	7° 24,73' E	43° 32,29' N	-	-	-	X	X	-	X	X	X	X	-
GeoB 12060	7° 24,51' E	43° 32,50' N	X	X	X	X	X	X*	X	X	X	X	-
GeoB 12061	7° 26,28' E	43° 31,20' N	X	X	X	X	X	-	-	X	X	X	-
GeoB 12064	7° 26,21' E	43° 31,12' N	X	X	X	X	X	-	-	X	X	X	-
GeoB 12066	7° 24,24' E	43° 31,33' N	X	X	X	X	X *	-	-	X	X	X	-
GeoB 12067	7° 27,12' E	43° 29,19' N	X	X	X	X	X*	-	-	X	X	X	-
GeoB 12072	7° 13,17' E	43° 38,63' N	X	X	X	X	X	X*	-	X	X	X	-
GeoB 12074	7° 25,97' E	43° 31,35' N	X	X	X	X	X	-	-	X	X	X	-
GeoB 12075	7° 26,58' E	43° 30,87' N	X	X	X	X	X	-	-	X	X	X	-
GeoB 12079	7° 27,61' E	43° 30,25' N	X	X	X	X	-	-	-	X	X	X	-
GeoB 12081	7° 21,96' E	43° 31,14' N	X	X	X	-	-	-	-	X	X	X	-
GeoB 12085	7° 13,68' E	43° 37,19' N	-	-	-	-	-	X	-	X	X	X	-
GeoB 12088	7° 13,16' E	43° 36,96' N	-	-	-	X	-	-	-	X	X	X	-

*= not measured over the entire length of the core

6.10. Remotely operated vehicle (ROV)

(A. Kopf, H. Hanff, S. Klar, M. Lange)

A total of 5 dives were carried out during the course of expedition M73/1 (see station list, Appendix 9.1). All dives focused on the area near the Nice Airport slide. Both length and water depths covered varied a little from dive to dive. No water depth larger than 80 mbsf was visited; in fact, much of the bottom time was at water depths between 20 and 45 mbsl.

The procedure of the ROV-CTD measurements was similar for all dives. The ROV was positioned as close to the headwall of the Nice Airport landslide as possible. This was achieved by steadying RV *Meteor*'s position in about 50 mbsf, then lowering the ROV to the sea level, and manoeuvre it towards the projected location of the headwall on the sea surface. Once this spot was reached, the ROV was submerged until it had bottom contact (or bottom sight). Once the vehicle was steady on the seafloor, the turbines were switched off for at least 1 minute to minimise disturbance and possible artefacts by ventilating seawater into possible locations of groundwater flux. After this period of quiescence, the ROV was uplifted slightly using the turbines again, and then moved down-slope by ca. 2 meters depth (as seen on the controlling console). We then stopped the turbines again, landed on the seafloor, and repeated the procedure. This way, an incremental downward profile of salinity measurements with reference depth were carried.

In a final step, electrical conductivity data were carefully analysed. However, we fail to observe any signal other than the equivalent of regular Mediterranean seawater. This was surprising given the strong geochemical anomalies (see Ch. 6.9 above) and the fact that we positioned the ship (and ROV) in more or less the same locations as during coring. Also, from the video evidence, we were in areas where gravel was seen on the seafloor, and where water depths of these coarse layers corresponded to a location near the headwall (i.e. ca. 20-25 mbsf). From this we tentatively conclude that there is likely some groundwater discharge through those layers (as attested by the pore water chemistry), but with a very low flow rate. Discharge rates may be enhanced during periods of heavy rainfall, as was reported prior to the October 1979 catastrophic slide event.

7. References

Assier-Rzadkiewicz, S., Heinrich, P., Sabatier, P.C., Savoye, B., and Bourillet, J.F., 2000. Numerical Modelling of a Landslide-generated Tsunami: The 1979 Nice Event, Pure appl. geophys., 157: 1707–1727.

Becker, K., and Davis, E.A., 2003. New evidence for age variation and scale effects of permeabilities of young oceanic crust from borehole thermal and pressure measurements. Earth Planet. Sci. Letts., 210: 499-508.

Bennett, R.H., L. Huon, P.J. Valent, J. Lipkin, M.I. Esrig, 1985. In situ undrained shear strengths and permeabilities derived from piezometer measurements. In: R.C. Chaney & K.R. Demars (eds), Strength Testing of Marine Sediments: Laboratory and In Situ Measurements, American Society for Testing and Materials: 88-100.

Blum, P., 1997. Physical properties handbook: a guide to the shipboard measurement of physical properties of deep-sea cores. Techn. Note 26, ODP.

British Standards Institutions, BS 1377, 1975. Methods of testing soils for civil engineering purposes. London: BSI: 174pp.

Bullard, E.C., 1939. Heat flow in South Africa. Proc, R. Soc. London Series A, 173, 474-503.

Byerlee, J. D., 1978. Friction od rocks. Pure Appl. Geophys., 116: 615-625

Byerlee, J. D., 1990. Friction, overpressure and fault normal compression. Geophys. Res. Lett., 17: 2109-2112

Clayton, C.R.I., Hababa, M.B., and Simons, N.E., 1985. Dynamic penetration resistance and the prediction of the compressibility of a fine-grained sand a laboratory study. Geotechnique, 35/1 : 19-31

Dan, G., 2007. Processus gravitaires et evaluation de la stabilite des pentes: Approches geoloigues et geotechnique. PhD thesis, Univ. Bretagne occidentale, Brest, 364pp.

Dan, G., Sultan, N., and Savoye, B., 2007. The 1979 Nice harbour catastrophe revisited: Trigger mechanism inferred from geotechnical measurements and numerical modelling. Mar. Geology, 245: 40-64.

Dayal, U., and Allen, J.H., 1975. The Effect of Penetration Rate on the Strength of Remolded Clay and Sand Samples. Canadian Geotechnical Journal 12/3: 336-348.

Dubar, M. & Antony, E.J., 1995. Holocene Environmental Change and River-Mouth Sedimentation in the Baie des Anges, French Riviera, Quaternary Research, 43: 329-343

Esrig, M.I., R.C. Kirby, R.G. Bea, 1977. Initial development of a general effective stress method for the prediction of axial capacity for driven piles in clay. Proc. 9th Offshore Technology Conference : 495-501

Gennesseaux, M., Mauffret, A., Pautot, G., 1980. Les glissements sousmarins de la pente continentale niçoise et la rupture des câbles en mer Ligure (Méditerranée occidentale). C.R. Acad. Sc. Paris 290.

Guglielmi, Y., 1993. Hydrogéologie des aquifères Plio-Quaternaires de la Basse Vallée du Var. Thèse d'Etat, Académie d'Aix-Marseille : pp. 170.

Hansbo, S., 1957. A new approach to the determination of the shear strength of clay by the fall-cone test. Royal Swedish Geotechnical Institute Proc., 14, Stockholm.

Hartmann, A., and Villinger, H., 2002. Inversion of marine heat flow measurements by expansion of the temperature decay function. Geophysical Journal International, 148 (3): 628-636.

Henry, P., Person, R., Paull, C.K., Savoye, B., Romanowicz, B., Charvis, P., Kopf, A., 2005. Installation of borehole observatories on the Ligurian Margin. IODP-proposal 685-full, 25 pp.

Hübscher, C. & V. Spieß, 1997. An integrated marine seismic approach for time-efficient high-resolution surveys. J. Petrol. Technology, 49: 492-493.

Kopf, A., Robertson, A.H.F., Screaton, E.J., Mascle, J., Parkes, R.J., Foucher, J.P., DeLange, G.J., Stöckhert, B. & Sakellariou, D., 1999. Backstop hydrogeology of a wide accretionary complex south of Crete, Eastern Mediterranean Sea. Full drilling proposal (#555) for the Ocean Drilling Program, 25p.

Kopf, A., Klaeschen, D. & Mascle, J., 2001. Extreme efficiency of mud volcanism in dewatering accretionary prisms. Earth Planet. Sci. Letters, 189/3-4: 295-313.

Kopf, A., Mascle, J., Klaeschen, D., 2003. The Mediterranean Ridge: A mass balance across the fastest growing accretionary complex on Earth. J. Geophys. Research 108: 2372-2403, doi:10.1029/2001JB000473.

Kopf, A., and Brown, K.M., 2003. The stress state of the Nankai and Barbados subduction thrusts. Mar. Geol. 202: 193-210

Kopf, A., Clennell, M.B. & Brown, K.M., 2005. Physical properties of extruded muds and their relationship to episodic extrusion and seismogenesis. Martinelli, G., and Panahi, B. (Eds.), Mud volcanoes, geodynamics and seismicity. NATO Sci. Ser. IV: Dordrecht (Springer): 263-283.

Kopf, A., Stegmann, S., Krastel, S., Förster, A., Strasser, M, Irving, M., 2007. Marine deep-water Free-fall CPT measurements for landslide characterisation off Crete, Greece (Eastern Mediterranean Sea) --- PART 2: Initial data from the western Cretan Sea. In: Lykousis, V., Sakellariou, D., Locat, J. (eds.), Submarine Mass movements and their consequences. Advances in Natural and Technological Hazards Series, Springer: 199-208.

Logan, J. M., Rauenzahn, K. A., 1987. Frictional dependence of gouge mixtures of quartz and montmorillonite on velocity, composition and fabric. Tectonophysics, 144: 87-108.

Lunne, T., Robertson P.K., Powell, J.J.M., 1997. Cone Penetration Testing in Geotechnical Practice, Blackie Academic & Professional London: pp. 312

Meunier, J., Sultan, N., Jegou, P., Harmegnies, F., 2004. First tests of Penfeld: A new seabed penetrometer. Proc. ISOPE 2004, Toulon, France, 4pp.

Moore, J.C. & Saffer, D., 2001. Updip limit of the seismogenic zone beneath the accretionary prism of southwest Japan: An effect of diagenetic to low-grade metamorphic processes and increasing effective stress. Geology, 29: 183-186

Mulder, T., Savoye, B., Syvitski, J.P.M., 1997. Numerical modelling of a mid-sized gravity flow: the 1979 Nice turbidity current (dynamics, processes, sediment budget and seafloor impact). Sedimentology, 44: 305–326.

Mulder, T., Savoye, B., Piper, D.J.W., Syvitski, J.P.M., 1998. The Var submarine sedimentary system: understanding Holocene sediment delivry processes and their importance to the geological record. In: Stocker, M.S., Evans, D., Cramp, A., Geologcal processes on continental margins: sedimentation, mass wasting and stability. Geol. Soc. London, Spec. Publ., 129: 146-166.

Pfender, M. & H. Villinger, 2002. Miniaturized data logger for deep-sea sediment temperature measurements, Mar. Geol., 186: 557-570.

Rice, J.R.,1992. Fault stress states, pore pressure distributions, and the weakness of the San Andreas Fault. In: Evans, B. & Wong, T.-F., Fault mechanics and transport properties of rocks. London (Acad. Press): 475-503.

Rothwell, R.G., 1989. Identification of Minerals and Mineraloids in Marine Sediments, London/New York (Elsevier).

Saffer, D.M., Frye, K.M., Marone, C., Mair, K., 2001. Laboratory results indicating complex and potentially unstable frictional behavior of smectite clay. Geophys. Res. Letts., 28: 2297-2300

Savoye, B., Rohais, S., Lopez, S., Dan, G., 2005. Revisiting the 1979 submarine avalanche offshore Nice (French Riviera): impacts on the seafloor, flow reconstruction and modelling. Proc. ICG Conf. on Submarine Mass Wasting, NGF, v. 2, p.74.

Scholz, C.H., 1998. Earthquakes and friction laws. Nature, 391: 37-42.

Seifert, A., Stegmann, S., Mörz, T., Lange, M., Wever, T., Kopf, A., 2008. In situ pore-pressure evolution during dynamic CPT measurements in soft sediments of the western Baltic Sea. Geo-Marine Letters, DOI 10.1007/s00367-008-0102-x.

Stegmann, S., Villinger, H, Kopf, A., 2006. Design of a modular, marine free-fall cone penetrometer. Sea Technology, v. 02/2006, 27-33

Stegmann, S., Strasser, M., Anselmetti, F., Kopf, A., 2007. Geotechnical in situ characterization of landslide deposits: The role of pore pressure transients versus frictional strength. Geophys. Res. Lett., 34, doi: 10.1029/2006GL029122.

Stegmann, S., Kopf, A., 2007. Marine deep-water Free-fall CPT measurements for landslide characterisation off Crete, Greece (Eastern Mediterranean Sea) --- PART 1: A new 4000m cone penetrometer. Lykousis, V., Sakellariou, D., Locat, J. (eds.), Submarine Mass movements and their consequences. Advances in Natural and Technological Hazards Series, Springer, 171-177.

Sultan, N., Cochonat, P., Canals, M., Cattaneo, A., Dennielou, B., Haflidason, H., Laberg, J. S., Long, D., Mienert, J. & Trincardi, F., 2004. Triggering mechanisms of slope instability processes and sediment failures on continental margins: a geotechnical approach: Marine Geology, v. 213: 291-321

Weinrebe, W., Schenk, S. (eds.), 2006. FS Meteor Fahrtbericht / Cruise Report M67/1 CHILE-MARGIN-SURVEY Berichte aus dem Leibniz-Institut für Meereswissenschaften an der Christian-Albrechts-Universität zu Kiel. Vol. 7: 112pp.

Wentworth, C.K., 1922. A scale of grade and class terms of clastic sediments. J. Geol., 30: 377-392.

Wood, D. M., 1982. Cone penetrometer and liquid limit. Geotechnique, 32 (2): 152-157.

8. Acknowledgements

We thank Master Walter Bascheck and his officers on the bridge for his willingness to approach shallow portions of the study area, his cooperation, and the patience when negotiating with the French authorities (or scientists). Special thanks go also to the crew of R/V *Meteor* for their friendly support and efficient technical assistance with the various devices used.

Our colleagues in France, namely Nabil Sultan, Sebastien Migeon and Pierre Henry are acknowledged for their discussion of scientific targets during earlier meetings. Jean-Xavier Castrec is thanked for providing crucial hints regarding the local authorities and airport security for receiving a research permission.

Nautilus GmbH, Bremen is thanked for providing us with one of the ANDERAA Seaguard CTD systems for the cruise. Likewise, the Max-Planck-Institution for Marine Microbiology has provided a shallow-water ROV and many hours of technical advice on very short notice. Thanks to Volker Meyer for being so kind!

Partners at RCOM Bremen (Goetz Ruhland, Volker Diekamp) as well as at the *Meteor*-Leitstelle (Michael Berkenheger) have also provided crucial help with expedition planning. Additionally, Klaus Bohn is thanked for his repeated professional logistical assistance.

Thanks go also to the German Science Foundation (DFG) for providing the funds to realise not only cruise *LIMA-LAMO*, but support for coordination of M73 as a whole (KO2108/9-1).

Appendices

9.1. Station list

9.2. List of seismic profiles

9.3. Lithologs and core photographs

9.4. MSCL data logs (electronic version only)

9.5. Group photo

9.6. Press coverage

Appendix 9.1.: Station list

Station: GeoB120-	Date	Time	PositionLat	PositionLong	Water depth [m]	Wind speed [m/s]	Instrument	Comments
01	25.07.2007	14:27	42° 59,16' N	6° 48,09' E	1841,7	NNW 1	CTD	
	25.07.2007	14:50	42° 58,95' N	6° 47,73' E	2044,4	WNW 1	CTD	
	25.07.2007	15:05	43° 38,72' N	7° 11,55' E	142,5	WNW 1	CTD	
02	25.07.2007	19:30	43° 36,50' N	7° 11,27' E	729,2	S 2	Multibeam-Parasound-Profile	
	25.07.2007	19:54	43° 36,75' N	7° 11,80' E	729,3	S 1	Multibeam-Parasound-Profile	Track 1
	25.07.2007	20:44	43° 36,75' N	7° 14,87' E	815,8	WSW 1	Multibeam-Parasound-Profile	
	25.07.2007	21:03	43° 37,10' N	7° 14,97' E	701,7	WSW 1	Multibeam-Parasound-Profile	Track 2
	25.07.2007	22:16	43° 37,01' N	7° 8,85' E	348,4	N 1	Multibeam-Parasound-Profile	
	25.07.2007	22:28	43° 37,25' N	7° 8,95' E	349,1	NNW 2	Multibeam-Parasound-Profile	Track 3
	25.07.2007	23:36	43° 37,26' N	7° 15,06' E	678,9	SSW 0	Multibeam-Parasound-Profile	
	25.07.2007	23:50	43° 37,52' N	7° 15,11' E	650,4	ESE 1	Multibeam-Parasound-Profile	Track 4
	26.07.2007	0:54	43° 37,49' N	7° 9,03' E	361,5	NNE 2	Multibeam-Parasound-Profile	
	26.07.2007	1:08	43° 37,75' N	7° 8,92' E	285,3	NNW 2	Multibeam-Parasound-Profile	Track 5
	26.07.2007	2:20	43° 37,73' N	7° 14,89' E	631,9	N 1	Multibeam-Parasound-Profile	
	26.07.2007	2:42	43° 37,98' N	7° 14,97' E	490,1	NNE 1	Multibeam-Parasound-Profile	Track 6
	26.07.2007	3:57	43° 38,06' N	7° 8,95' E	131,6	WNW 2	Multibeam-Parasound-Profile	
	26.07.2007	4:02	43° 38,22' N	7° 9,01' E	129,1	NW 3	Multibeam-Parasound-Profile	Track 7
	26.07.2007	5:17	43° 38,23' N	7° 15,05' E	494,3	NNE 2	Multibeam-Parasound-Profile	
	26.07.2007	5:30	43° 38,48' N	7° 14,94' E	471,2	N 2	Multibeam-Parasound-Profile	Track 8
	26.07.2007	6:47	0° 0,00' N	0° 0,00' E	0	N 0	Multibeam-Parasound-Profile	
	26.07.2007	7:15	43° 38,72' N	7° 11,55' E	142	N 0	Multibeam-Parasound-Profile	
03	26.07.2007	8:09	43° 38,80' N	7° 13,15' E	24,4	SE 1	Gravity corer	
	26.07.2007	8:09	43° 38,80' N	7° 13,15' E	24,4	SE 1	Gravity corer	
	26.07.2007	8:10	43° 38,80' N	7° 13,15' E	25,6	SE 1	Gravity corer	
04	26.07.2007	8:54	43° 38,63' N	7° 13,15' E	13,4	SE 2	Remote operated vehicle	buoyancy test
	26.07.2007	9:00	43° 38,63' N	7° 13,09' E	13	SE 2	Remote operated vehicle	
05	26.07.2007	9:06	43° 38,64' N	7° 13,09' E	12,6	SE 2	Remote operated vehicle	dive #1
	26.07.2007	9:20	43° 38,64' N	7° 13,11' E	15	SE 2	Remote operated vehicle	several tries
	26.07.2007	10:12	43° 38,51' N	7° 12,85' E	103,1	SE 2	Remote operated vehicle	
06	26.07.2007	10:55	43° 36,77' N	7° 12,84' E	0	N 0	Multibeam-Parasound-Profile	Track 1
	26.07.2007	11:32	43° 36,75' N	7° 9,00' E	0	N 0	Multibeam-Parasound-Profile	
	26.07.2007	11:39	43° 36,52' N	7° 8,93' E	0	N 0	Multibeam-Parasound-Profile	Track 2
	26.07.2007	13:00	43° 36,50' N	7° 15,06' E	899,2	SSW 2	Multibeam-Parasound-Profile	
	26.07.2007	13:12	43° 36,25' N	7° 15,08' E	951,8	S 2	Multibeam-Parasound-Profile	Track 3
	26.07.2007	14:34	43° 36,26' N	7° 8,86' E	380,1	SSE 3	Multibeam-Parasound-Profile	
	26.07.2007	14:47	43° 36,03' N	7° 9,09' E	342,7	S 3	Multibeam-Parasound-Profile	Track 4
	26.07.2007	15:59	43° 35,99' N	7° 15,08' E	1011,6	SSW 3	Multibeam-Parasound-Profile	
07-1f	26.07.2007	17:40	43° 36,29' N	7° 12,98' E	900,5	SSW 4	Deep Water CPT Lance	
	26.07.2007	17:59	43° 36,29' N	7° 12,98' E	901,5	SSW 3	Deep Water CPT Lance	instrument failure
08-1	26.07.2007	18:13	43° 36,30' N	7° 12,99' E	901,9	SW 3	Heat Flow Lance	
	26.07.2007	18:35	43° 36,30' N	7° 12,99' E	898,3	SW 4	Heat Flow Lance	
	26.07.2007	18:42	43° 36,30' N	7° 12,99' E	899	SW 3	Heat Flow Lance	
	26.07.2007	19:07	43° 36,30' N	7° 12,99' E	897,8	SW 3	Heat Flow Lance	
08-2	26.07.2007	19:25	43° 36,40' N	7° 13,00' E	869,4	WSW 3	Heat Flow Lance	
	26.07.2007	19:47	43° 36,40' N	7° 12,99' E	869,6	SW 2	Heat Flow Lance	
	26.07.2007	19:54	43° 36,40' N	7° 12,99' E	870,5	SW 2	Heat Flow Lance	
	26.07.2007	20:13	43° 36,40' N	7° 13,00' E	870,5	SSW 1	Heat Flow Lance	
08-3	26.07.2007	20:27	43° 36,50' N	7° 13,01' E	832,6	S 2	Heat Flow Lance	
	26.07.2007	20:45	43° 36,50' N	7° 13,01' E	833,1	S 2	Heat Flow Lance	
	26.07.2007	20:51	43° 36,50' N	7° 13,01' E	831,2	S 2	Heat Flow Lance	
	26.07.2007	21:35	43° 36,50' N	7° 13,01' E	831,2	SW 2	Heat Flow Lance	
07-3	26.07.2007	22:10	43° 36,50' N	7° 13,01' E	832,2	WSW 1	Deep Water CPT Lance	
	26.07.2007	22:37	43° 36,50' N	7° 13,01' E	830	WNW 1	Deep Water CPT Lance	SLmax 850 m
	26.07.2007	22:38	43° 36,50' N	7° 13,01' E	830,8	WNW 1	Deep Water CPT Lance	
	26.07.2007	23:00	43° 36,50' N	7° 13,01' E	826,6	NW 3	Deep Water CPT Lance	
08-4	26.07.2007	23:14	43° 36,62' N	7° 13,00' E	799	WNW 2	Heat Flow Lance	
	26.07.2007	23:30	43° 36,62' N	7° 13,00' E	798,8	NW 1	Heat Flow Lance	SLmax 807 m
	26.07.2007	23:38	43° 36,62' N	7° 13,00' E	799,2	WNW 2	Heat Flow Lance	Zmax 17,5 kN

	26.07.2007	23:58	43° 36,62' N	7° 13,00' E	797,8	W 1	Heat Flow Lance	
07-4	27.07.2007	0:00	43° 36,62' N	7° 13,00' E	797,6	W 1	Deep Water CPT Lance	
	27.07.2007	0:16	43° 36,62' N	7° 13,00' E	797,4	WNW 2	Deep Water CPT Lance	SLmax 810 m
	27.07.2007	0:20	43° 36,62' N	7° 13,00' E	799,1	NW 2	Deep Water CPT Lance	
	27.07.2007	0:38	43° 36,62' N	7° 13,00' E	800,8	NW 2	Deep Water CPT Lance	
08-5	27.07.2007	0:52	43° 36,72' N	7° 13,00' E	781	WNW 3	Heat Flow Lance	
	27.07.2007	1:07	43° 36,72' N	7° 13,00' E	773,5	WNW 3	Heat Flow Lance	SLmax 782 m
	27.07.2007	1:13	43° 36,72' N	7° 13,00' E	771,6	WNW 2	Heat Flow Lance	SZmax 15,5 kN
	27.07.2007	1:37	43° 36,72' N	7° 13,00' E	771,1	NW 3	Heat Flow Lance	
07-5	27.07.2007	1:38	43° 36,72' N	7° 13,00' E	771,4	NW 3	Deep Water CPT Lance	
	27.07.2007	1:52	43° 36,72' N	7° 13,00' E	771,2	NW 3	Deep Water CPT Lance	SLmax 778 m
	27.07.2007	1:53	43° 36,72' N	7° 13,00' E	772,2	NW 2	Deep Water CPT Lance	
	27.07.2007	2:14	43° 36,72' N	7° 13,00' E	772,4	NNW 3	Deep Water CPT Lance	
08-6	27.07.2007	2:32	43° 36,82' N	7° 12,97' E	752,4	N 3	Heat Flow Lance	
	27.07.2007	2:45	43° 36,80' N	7° 13,00' E	715,6	NNW 2	Heat Flow Lance	SLmax 714 m
	27.07.2007	2:53	43° 36,80' N	7° 13,00' E	718,7	NNW 2	Heat Flow Lance	Zmax 17,4 kN
	27.07.2007	3:00	43° 36,80' N	7° 13,00' E	714,4	NNW 2	Heat Flow Lance	
07-6	27.07.2007	3:12	43° 36,80' N	7° 13,00' E	706,8	NNW 3	Deep Water CPT Lance	
	27.07.2007	3:28	43° 36,80' N	7° 13,00' E	726	NNW 3	Deep Water CPT Lance	SLmax 725 m
	27.07.2007	4:02	43° 36,80' N	7° 13,00' E	716,6	N 2	Deep Water CPT Lance	Zmax 9,3 kN
	27.07.2007	4:21	43° 36,80' N	7° 13,00' E	716,3	N 3	Deep Water CPT Lance	
08-7	27.07.2007	4:38	43° 36,90' N	7° 13,00' E	694,6	N 2	Heat Flow Lance	
	27.07.2007	4:57	43° 36,90' N	7° 13,00' E	694,5	N 2	Heat Flow Lance	SLmax 695 m
	27.07.2007	5:04	43° 36,90' N	7° 13,00' E	693,2	N 3	Heat Flow Lance	Zmax 21,2 kN
	27.07.2007	5:28	43° 36,90' N	7° 13,00' E	693,2	N 2	Heat Flow Lance	
07-7	27.07.2007	5:31	43° 36,90' N	7° 13,00' E	693,4	N 2	Deep Water CPT Lance	
	27.07.2007	5:46	43° 36,90' N	7° 13,00' E	693,3	NNW 2	Deep Water CPT Lance	SLmax 707 m
	27.07.2007	6:18	43° 36,90' N	7° 13,00' E	697,5	N 2	Deep Water CPT Lance	
	27.07.2007	6:34	43° 36,90' N	7° 13,00' E	693,1	NNE 2	Deep Water CPT Lance	
07-1	27.07.2007	7:08	43° 36,30' N	7° 13,00' E	895,9	NNE 0	Deep Water CPT Lance	
	27.07.2007	7:26	43° 36,30' N	7° 13,01' E	894,3	ENE 1	Deep Water CPT Lance	
	27.07.2007	7:42	43° 36,30' N	7° 13,01' E	894,7	ENE 2	Deep Water CPT Lance	
	27.07.2007	7:54	43° 36,30' N	7° 13,01' E	894,6	ENE 1	Deep Water CPT Lance	
07-02	27.07.2007	8:04	43° 36,40' N	7° 13,01' E	863,1	ENE 1	Deep Water CPT Lance	
	27.07.2007	8:21	43° 36,40' N	7° 13,01' E	862,6	E 1	Deep Water CPT Lance	
	27.07.2007	8:24	43° 36,40' N	7° 13,01' E	863,2	E 2	Deep Water CPT Lance	
	27.07.2007	8:27	43° 36,40' N	7° 13,01' E	864,1	E 1	Deep Water CPT Lance	
	27.07.2007	8:33	43° 36,40' N	7° 13,01' E	862,8	E 1	Deep Water CPT Lance	
	27.07.2007	8:57	43° 36,49' N	7° 12,99' E	841,5	ESE 3	Deep Water CPT Lance	
09	27.07.2007	9:18	43° 36,60' N	7° 13,01' E	805,9	ESE 3	Gravity corer	
	27.07.2007	9:42	43° 36,60' N	7° 13,01' E	807,8	E 3	Gravity corer	
	27.07.2007	9:42	43° 36,60' N	7° 13,01' E	807,8	E 3	Gravity corer	
	27.07.2007	10:04	43° 36,60' N	7° 13,01' E	808	ESE 3	Gravity corer	
10	27.07.2007	11:00	43° 35,56' N	7° 13,29' E	1140,1	E 6	Multibeam-Parasound-Profile	
	27.07.2007	14:20	43° 25,94' N	7° 24,45' E	2012,8	S 2	Multibeam-Parasound-Profile	
11	27.07.2007	14:46	43° 26,64' N	7° 23,59' E	1967	SE 2	Pushcorer	PC#1
	27.07.2007	15:48	43° 26,74' N	7° 23,64' E	1971,3	S 1	Pushcorer	SLmax 1997 m, Zmax 10,7 kN
	27.07.2007	16:43	43° 26,74' N	7° 23,64' E	1971,5	SSE 2	Pushcorer	
12	27.07.2007	17:18	43° 28,90' N	7° 21,55' E	1818,7	ESE 2	Pushcorer	PC#2
	27.07.2007	17:51	43° 28,95' N	7° 21,50' E	1824,1	E 2	Pushcorer	SLmax 1833 m
	27.07.2007	18:33	43° 28,95' N	7° 21,50' E	1825,9	ENE 2	Pushcorer	
	27.07.2007	18:59	43° 31,11' N	7° 20,01' E	1750	ENE 4	Multibeam-Parasound-Profile	
	27.07.2007	20:05	43° 37,44' N	7° 12,17' E	610,4	E 4	Multibeam-Parasound-Profile	
13-1	27.07.2007	20:34	43° 37,20' N	7° 12,30' E	570,8	E 4	Heat Flow Lance	
	27.07.2007	20:52	43° 37,20' N	7° 12,30' E	588,3	E 4	Heat Flow Lance	
	27.07.2007	20:59	43° 37,20' N	7° 12,30' E	583,8	E 4	Heat Flow Lance	
	27.07.2007	21:13	43° 37,20' N	7° 12,30' E	579,7	E 3	Heat Flow Lance	
14-1	27.07.2007	21:17	43° 37,20' N	7° 12,30' E	584,3	E 3	Deep Water CPT Lance	
	27.07.2007	21:47	43° 37,20' N	7° 12,30' E	578,8	E 3	Deep Water CPT Lance	
	27.07.2007	22:16	43° 37,20' N	7° 12,30' E	587,3	ENE 3	Deep Water CPT Lance	
	27.07.2007	22:36	43° 37,20' N	7° 12,30' E	580,5	E 3	Deep Water CPT Lance	
13-2	27.07.2007	22:50	43° 37,19' N	7° 12,52' E	632,2	E 3	Heat Flow Lance	
	27.07.2007	23:05	43° 37,20' N	7° 12,50' E	636,3	E 3	Heat Flow Lance	SLmax=636m

	27.07.2007	23:12	43° 37,20' N	7° 12,50' E	633,4	E 3	Heat Flow Lance	SZmax=24,7 KN
	27.07.2007	23:33	43° 37,20' N	7° 12,50' E	633,2	E 2	Heat Flow Lance	
14-2	27.07.2007	23:55	43° 37,20' N	7° 12,50' E	634,2	ESE 2	Deep Water CPT Lance	
	28.07.2007	0:13	43° 37,19' N	7° 12,50' E	633,3	ENE 2	Deep Water CPT Lance	SLmax=646m
	28.07.2007	0:44	43° 37,20' N	7° 12,50' E	633,2	NW 2	Deep Water CPT Lance	
	28.07.2007	1:00	43° 37,20' N	7° 12,50' E	634,2	NNW 2	Deep Water CPT Lance	
13-3	28.07.2007	1:15	43° 37,21' N	7° 12,70' E	592	NNW 2	Heat Flow Lance	
	28.07.2007	1:26	43° 37,20' N	7° 12,71' E	594,7	NW 2	Heat Flow Lance	SLmax=594m
	28.07.2007	1:32	43° 37,20' N	7° 12,71' E	594,8	NNW 2	Heat Flow Lance	SZmax=20,9 Kn
	28.07.2007	1:50	43° 37,20' N	7° 12,71' E	595,5	NNW 2	Heat Flow Lance	
14-3	28.07.2007	1:53	43° 37,20' N	7° 12,71' E	595,8	NNW 2	Deep Water CPT Lance	instrument failure, no data
	28.07.2007	2:20	43° 37,20' N	7° 12,70' E	594,3	NNW 2	Deep Water CPT Lance	
	28.07.2007	2:23	43° 37,20' N	7° 12,70' E	594,5	NNW 3	Deep Water CPT Lance	2nd try
	28.07.2007	2:36	43° 37,20' N	7° 12,70' E	593,4	NNW 2	Deep Water CPT Lance	
	28.07.2007	2:38	43° 37,20' N	7° 12,70' E	596,4	NW 2	Deep Water CPT Lance	3rd try
	28.07.2007	2:46	43° 37,20' N	7° 12,70' E	596,1	NNW 2	Deep Water CPT Lance	
13-4	28.07.2007	3:09	43° 37,20' N	7° 12,91' E	614,3	NNW 2	Heat Flow Lance	
	28.07.2007	3:24	43° 37,20' N	7° 12,91' E	606,9	NW 2	Heat Flow Lance	SLmax 623 m
	28.07.2007	3:32	43° 37,20' N	7° 12,91' E	612,8	NNW 2	Heat Flow Lance	Zmax 19,3 kN
	28.07.2007	3:47	43° 37,20' N	7° 12,91' E	613,1	NNW 3	Heat Flow Lance	
13-5	28.07.2007	3:57	43° 37,19' N	7° 13,13' E	613,5	NW 4	Heat Flow Lance	
	28.07.2007	4:13	43° 37,20' N	7° 13,10' E	593	NNW 3	Heat Flow Lance	SLmax 569 m
	28.07.2007	4:21	43° 37,20' N	7° 13,10' E	587,5	NNW 4	Heat Flow Lance	Zmax 23,5 kN
	28.07.2007	4:35	43° 37,20' N	7° 13,10' E	595,5	NNW 4	Heat Flow Lance	
13-6	28.07.2007	4:44	43° 37,20' N	7° 13,32' E	607,9	NNW 3	Heat Flow Lance	
	28.07.2007	5:01	43° 37,20' N	7° 13,30' E	611,1	NNW 3	Heat Flow Lance	SLmax 620 m
	28.07.2007	5:08	43° 37,20' N	7° 13,30' E	609,4	NNW 3	Heat Flow Lance	Zmax 14,1 kN
	28.07.2007	5:25	43° 37,20' N	7° 13,30' E	614	NNW 3	Heat Flow Lance	
13-7	28.07.2007	5:33	43° 37,19' N	7° 13,50' E	640,7	NNW 3	Heat Flow Lance	
	28.07.2007	5:52	43° 37,20' N	7° 13,50' E	648,5	NNW 3	Heat Flow Lance	SLmax 644 m
	28.07.2007	6:00	43° 37,20' N	7° 13,50' E	634,5	N 3	Heat Flow Lance	Zmax 14,3 kN
13-8	28.07.2007	6:30	43° 37,19' N	7° 13,94' E	598,1	N 1	Heat Flow Lance	
	28.07.2007	6:47	43° 37,20' N	7° 13,94' E	618,1	NNW 1	Heat Flow Lance	SL max 638
	28.07.2007	6:55	43° 37,20' N	7° 13,94' E	621,3	NNW 1	Heat Flow Lance	Zmax 6,9kn
	28.07.2007	7:14	43° 37,20' N	7° 13,94' E	611,7	NNE 0	Heat Flow Lance	
15	28.07.2007	7:39	43° 36,90' N	7° 12,99' E	697,8	SE 1	Gravity corer	
	28.07.2007	8:01	43° 36,90' N	7° 13,00' E	696,5	SSE 1	Gravity corer	Sl 688m
	28.07.2007	8:01	43° 36,90' N	7° 13,00' E	696,5	SSE 1	Gravity corer	SZmax 42,3kn
	28.07.2007	8:22	43° 36,90' N	7° 13,00' E	697,6	SE 2	Gravity corer	
16	28.07.2007	8:30	43° 36,76' N	7° 12,83' E	756,8	SE 2	Multibeam-Parasound-Profile	speed 3kn 180°-1,3nm
	28.07.2007	8:54	43° 35,45' N	7° 13,00' E	1138,7	SE 2	Multibeam-Parasound-Profile	121,4° - 1,1kn
	28.07.2007	9:23	43° 34,91' N	7° 14,23' E	1244	SE 3	Multibeam-Parasound-Profile	150° - 1,1nm
	28.07.2007	9:43	43° 34,03' N	7° 14,86' E	1374,6	ESE 4	Multibeam-Parasound-Profile	
17	28.07.2007	10:37	43° 34,93' N	7° 14,29' E	1215,6	SE 4	Pushcorer	PC#3
	28.07.2007	11:20	43° 34,94' N	7° 14,28' E	1226,4	ESE 4	Pushcorer	SLmax=1239m, SZmax=7,5 KN
	28.07.2007	12:03	43° 34,94' N	7° 14,28' E	1216,3	ESE 4	Pushcorer	
18	28.07.2007	12:20	43° 34,90' N	7° 13,62' E	1205,8	ESE 4	Multibeam-Parasound-Profile	
19	28.07.2007	16:38	43° 39,03' N	7° 10,47' E	32,5	SSE 0	Gravity corer	
	28.07.2007	16:38	43° 39,03' N	7° 10,47' E	32,5	SSE 0	Multibeam-Parasound-Profile	
	28.07.2007	16:41	43° 39,03' N	7° 10,47' E	32,7	SSE 1	Gravity corer	SLmax 52 m
	28.07.2007	16:42	43° 39,03' N	7° 10,47' E	31	SSE 1	Gravity corer	Zmax 36,9 kN
	28.07.2007	16:52	43° 39,02' N	7° 10,47' E	30,1	SSE 1	Gravity corer	
20-1	28.07.2007	17:05	43° 39,02' N	7° 10,47' E	35,2	SSE 1	Shallow water CPT Lance	
	28.07.2007	17:29	43° 39,02' N	7° 10,47' E	32,1	SE 1	Shallow water CPT Lance	SLmax 21 m
	28.07.2007	17:49	43° 39,02' N	7° 10,47' E	35,2	SSE 1	Shallow water CPT Lance	Zmax 2,3 kN
	28.07.2007	17:52	43° 39,02' N	7° 10,47' E	32,9	S 0	Shallow water CPT Lance	
20-2	28.07.2007	18:05	43° 38,89' N	7° 10,60' E	76,1	S 1	Shallow water CPT Lance	
	28.07.2007	18:11	43° 38,89' N	7° 10,60' E	70,4	SE 1	Shallow water CPT Lance	SLmax: 68m
	28.07.2007	18:30	43° 38,89' N	7° 10,60' E	76,6	SE 1	Shallow water CPT Lance	SZmax:2kn
	28.07.2007	18:33	43° 38,89' N	7° 10,60' E	69,8	ESE 1	Shallow water CPT Lance	
20-3	28.07.2007	18:42	43° 38,80' N	7° 10,70' E	130,5	SE 1	Shallow water CPT Lance	
	28.07.2007	18:49	43° 38,80' N	7° 10,70' E	125,9	E 1	Shallow water CPT Lance	SLmax: 124m
	28.07.2007	19:09	43° 38,80' N	7° 10,70' E	127,4	ESE 0	Shallow water CPT Lance	SZmax: 1,7kn

	28.07.2007	19:15	43° 38,80' N	7° 10,70' E	121,8	SSE 0	Shallow water CPT Lance	
20-4	28.07.2007	19:28	43° 38,70' N	7° 10,80' E	182,4	ESE 0	Shallow water CPT Lance	
	28.07.2007	19:34	43° 38,69' N	7° 10,81' E	179,5	NE 0	Shallow water CPT Lance	SLmax: 196m
	28.07.2007	19:54	43° 38,69' N	7° 10,81' E	180	E 0	Shallow water CPT Lance	SZmax: 2,8kn
	28.07.2007	20:01	43° 38,70' N	7° 10,81' E	179,7	ESE 0	Shallow water CPT Lance	
20-5	28.07.2007	20:21	43° 38,50' N	7° 10,79' E	157,2	SE 0	Shallow water CPT Lance	
	28.07.2007	20:26	43° 38,50' N	7° 10,79' E	163,7	NNE 1	Shallow water CPT Lance	SLmax: 185m
	28.07.2007	20:45	43° 38,50' N	7° 10,79' E	159,2	NNW 2	Shallow water CPT Lance	SZmax: 3,6kn
	28.07.2007	20:50	43° 38,50' N	7° 10,79' E	162,3	NNE 1	Shallow water CPT Lance	
20-6	28.07.2007	21:00	43° 38,39' N	7° 10,80' E	177	NW 1	Shallow water CPT Lance	
	28.07.2007	21:06	43° 38,40' N	7° 10,80' E	178,9	NW 2	Shallow water CPT Lance	SLmax:179m
	28.07.2007	21:23	43° 38,40' N	7° 10,80' E	177,8	NW 2	Shallow water CPT Lance	SZmax: 3,9kn
	28.07.2007	21:29	43° 38,40' N	7° 10,80' E	180,6	NW 2	Shallow water CPT Lance	
20-7	28.07.2007	21:38	43° 38,30' N	7° 10,80' E	197,2	NW 2	Shallow water CPT Lance	
	28.07.2007	21:44	43° 38,30' N	7° 10,80' E	198,1	NNW 2	Shallow water CPT Lance	SLmax: 197m
	28.07.2007	22:05	43° 38,30' N	7° 10,80' E	195,7	NNW 2	Shallow water CPT Lance	SZmax: 2,5KN
	28.07.2007	22:14	43° 38,30' N	7° 10,80' E	195,7	N 2	Shallow water CPT Lance	
21-1f	28.07.2007	22:52	43° 37,46' N	7° 10,31' E	543,6	NNW 2	Heat Flow Lance	
	28.07.2007	23:08	43° 37,46' N	7° 10,30' E	546,2	NNW 1	Heat Flow Lance	SLmax=599m, no bottom contact
	29.07.2007	0:08	43° 37,46' N	7° 10,30' E	547,1	NW 2	Heat Flow Lance	SZmax=10,3 KN
	29.07.2007	0:12	43° 37,46' N	7° 10,30' E	546,4	NNW 2	Heat Flow Lance	
21-1	29.07.2007	0:15	43° 37,46' N	7° 10,30' E	548,2	NW 3	Heat Flow Lance	
	29.07.2007	0:24	43° 37,46' N	7° 10,30' E	550,3	NW 2	Heat Flow Lance	SLmax=549m
	29.07.2007	0:32	43° 37,46' N	7° 10,30' E	550,2	NW 3	Heat Flow Lance	SZmax=21,7KN
	29.07.2007	0:47	43° 37,46' N	7° 10,31' E	535,6	NW 3	Heat Flow Lance	
21-2	29.07.2007	1:00	43° 37,69' N	7° 10,45' E	398,1	NW 3	Heat Flow Lance	
	29.07.2007	1:11	43° 37,70' N	7° 10,45' E	410,3	NW 3	Heat Flow Lance	SLmax=393m
	29.07.2007	1:18	43° 37,70' N	7° 10,45' E	413,8	NW 3	Heat Flow Lance	SZmax= 20,5KN
	29.07.2007	1:28	43° 37,70' N	7° 10,46' E	397,2	NW 3	Heat Flow Lance	
21-3	29.07.2007	1:43	43° 37,91' N	7° 10,61' E	284,2	NW 3	Heat Flow Lance	
	29.07.2007	1:51	43° 37,91' N	7° 10,61' E	293,7	NW 3	Heat Flow Lance	SLmax=274m
	29.07.2007	2:00	43° 37,91' N	7° 10,61' E	282,3	NNW 3	Heat Flow Lance	SZmax= 18,7 KN
	29.07.2007	2:05	43° 37,91' N	7° 10,61' E	283,8	NNW 3	Heat Flow Lance	
21-4	29.07.2007	2:20	43° 38,12' N	7° 10,69' E	272,9	NNW 1	Heat Flow Lance	
	29.07.2007	2:27	43° 38,11' N	7° 10,69' E	260,2	NNW 2	Heat Flow Lance	SLmax 250 m
	29.07.2007	2:33	43° 38,11' N	7° 10,69' E	268,4	NNW 2	Heat Flow Lance	Zmax17,8 kN
	29.07.2007	2:40	43° 38,11' N	7° 10,69' E	262,9	NW 3	Heat Flow Lance	
21-5	29.07.2007	2:54	43° 38,32' N	7° 10,79' E	187,6	NW 2	Heat Flow Lance	
	29.07.2007	3:06	43° 38,32' N	7° 10,80' E	183,9	NW 3	Heat Flow Lance	SLmax 201 m
	29.07.2007	3:13	43° 38,32' N	7° 10,80' E	184,3	NW 4	Heat Flow Lance	Zmax 17,9 kN
	29.07.2007	3:21	43° 38,32' N	7° 10,80' E	183,5	NW 3	Heat Flow Lance	
21-6	29.07.2007	3:31	43° 38,40' N	7° 10,78' E	176,8	NW 3	Heat Flow Lance	
	29.07.2007	3:40	43° 38,40' N	7° 10,79' E	177,1	NW 3	Heat Flow Lance	SLmax 184 m
	29.07.2007	3:47	43° 38,40' N	7° 10,79' E	177,1	NW 3	Heat Flow Lance	Zmax 18,8 kN
	29.07.2007	3:53	43° 38,40' N	7° 10,79' E	177,2	NW 4	Heat Flow Lance	
21-7	29.07.2007	4:04	43° 38,51' N	7° 10,79' E	182,9	NNW 3	Heat Flow Lance	
	29.07.2007	4:12	43° 38,51' N	7° 10,79' E	176,3	NW 2	Heat Flow Lance	SLmax 179 m
	29.07.2007	4:20	43° 38,51' N	7° 10,79' E	176,4	NNW 2	Heat Flow Lance	Zmax 19,3 kN
	29.07.2007	4:26	43° 38,51' N	7° 10,79' E	180,7	NNW 1	Heat Flow Lance	
21-8	29.07.2007	4:39	43° 38,71' N	7° 10,79' E	181,5	NNW 2	Heat Flow Lance	
	29.07.2007	4:46	43° 38,71' N	7° 10,79' E	177,3	NW 1	Heat Flow Lance	SLmax 184 m
	29.07.2007	4:53	43° 38,71' N	7° 10,79' E	181,9	NW 2	Heat Flow Lance	Zmax 18,5 kN
	29.07.2007	4:59	43° 38,71' N	7° 10,79' E	177,3	NW 2	Heat Flow Lance	
21-9	29.07.2007	5:14	43° 38,80' N	7° 10,70' E	102,3	NW 2	Heat Flow Lance	
	29.07.2007	5:20	43° 38,80' N	7° 10,70' E	101,9	NW 2	Heat Flow Lance	SLmax 134 m
	29.07.2007	5:28	43° 38,80' N	7° 10,70' E	102,3	NNW 2	Heat Flow Lance	Zmax 21,8 kN
	29.07.2007	5:33	43° 38,80' N	7° 10,70' E	107,4	NNW 2	Heat Flow Lance	
21-10f	29.07.2007	5:42	43° 38,91' N	7° 10,59' E	67,3	NW 2	Heat Flow Lance	no bottom contact
	29.07.2007	5:47	43° 38,91' N	7° 10,59' E	63,5	NW 2	Heat Flow Lance	SLmax 46 m
	29.07.2007	5:54	43° 38,91' N	7° 10,59' E	59,4	NNW 2	Heat Flow Lance	hieven, bei SL 15 m Stopp und Widerholung des Versuchs
21-10	29.07.2007	6:01	43° 38,91' N	7° 10,59' E	67,8	NW 2	Heat Flow Lance	SLmax 76 m
	29.07.2007	6:09	43° 38,91' N	7° 10,59' E	59,2	NNW 1	Heat Flow Lance	SZmax: 16,5kn

	29.07.2007	6:18	43° 38,90' N	7° 10,59' E	68,1	NNE 0	Heat Flow Lance	
21-11	29.07.2007	6:30	43° 39,00' N	7° 10,50' E	58,1	NW 1	Heat Flow Lance	
	29.07.2007	6:35	43° 39,00' N	7° 10,50' E	57,7	WNW 1	Heat Flow Lance	SLmax:64m
	29.07.2007	6:41	43° 39,00' N	7° 10,50' E	57,8	WNW 1	Heat Flow Lance	SZmax: 12,2kn
	29.07.2007	6:54	43° 38,94' N	7° 10,55' E	58,6	S 2	Heat Flow Lance	
22-2	29.07.2007	8:35	43° 37,62' N	7° 23,07' E	930,4	S 2	Gravity corer	GeoB12022-1 = Parasound approach
	29.07.2007	9:09	43° 37,61' N	7° 23,08' E	929,6	SSE 3	Gravity corer	SLmax: 929m
	29.07.2007	9:09	43° 37,61' N	7° 23,08' E	929,6	SSE 3	Gravity corer	SZmax: 51,1kn
	29.07.2007	9:32	43° 37,61' N	7° 23,08' E	928,8	SSE 3	Gravity corer	
22-3	29.07.2007	9:36	43° 37,62' N	7° 23,08' E	934,7	SSE 3	Pushcorer	PC#4
	29.07.2007	10:07	43° 37,62' N	7° 23,09' E	935,3	SSE 3	Pushcorer	SLmax: 941m
	29.07.2007	10:33	43° 37,62' N	7° 23,09' E	930,7	SE 3	Pushcorer	
22-4	29.07.2007	11:02	43° 37,62' N	7° 23,10' E	933,9	ESE 3	Pushcorer	no recovery
	29.07.2007	11:24	43° 37,62' N	7° 23,09' E	937,6	SE 2	Pushcorer	SLmax=938m, SZmax=6,8KN
	29.07.2007	11:53	43° 37,62' N	7° 23,08' E	928,8	SE 2	Pushcorer	
23-2	29.07.2007	13:50	43° 22,11' N	7° 32,83' E	1932,7	S 2	Pushcorer	PC#5; GeoB12023-1 = Parasound approach
	29.07.2007	14:39	43° 22,10' N	7° 32,85' E	1929,1	SSE 4	Pushcorer	SLmax 1932 m, Zmax 9,9 kN
	29.07.2007	15:55	43° 22,10' N	7° 32,85' E	1928,6	SSW 8	Pushcorer	
24	29.07.2007	16:25	43° 22,01' N	7° 31,15' E	1880,3	S 5	Gravity corer	W 11
	29.07.2007	17:03	43° 22,01' N	7° 31,16' E	1879,9	SW 1	Gravity corer	SLmax 1877 m
	29.07.2007	17:06	43° 22,01' N	7° 31,15' E	1883,5	SSW 0	Gravity corer	Zmax 56,3 kN
	29.07.2007	17:51	43° 22,01' N	7° 31,15' E	1883,8	S 1	Gravity corer	
26-1	29.07.2007	20:16	43° 37,01' N	7° 13,01' E	656,6	WNW 1	Heat Flow Lance	GeoB12025 = Parasound approach
	29.07.2007	20:39	43° 37,00' N	7° 13,01' E	656,3	NW 1	Heat Flow Lance	SLmax: 658m
	29.07.2007	20:46	43° 37,00' N	7° 13,01' E	654,2	NW 1	Heat Flow Lance	SZmax: 24,2kn
	29.07.2007	21:03	43° 37,00' N	7° 13,01' E	654,5	NW 2	Heat Flow Lance	
27-1	29.07.2007	21:04	43° 37,00' N	7° 13,01' E	654,3	NW 1	Deep Water CPT Lance	
	29.07.2007	21:23	43° 37,00' N	7° 13,01' E	651	NNW 3	Deep Water CPT Lance	SLmax: 650m
	29.07.2007	21:49	43° 37,00' N	7° 13,01' E	653,7	NNW 3	Deep Water CPT Lance	SZmax: 4,7kn
	29.07.2007	22:06	43° 37,00' N	7° 13,01' E	654,9	NW 2	Deep Water CPT Lance	
26-2	29.07.2007	22:24	43° 37,10' N	7° 13,01' E	617,8	NNW 4	Heat Flow Lance	
	29.07.2007	22:37	43° 37,10' N	7° 13,01' E	618,4	NNW 4	Heat Flow Lance	SLmax=613m
	29.07.2007	22:46	43° 37,10' N	7° 13,01' E	618,1	N 4	Heat Flow Lance	Smax=19.0KN
	29.07.2007	23:02	43° 37,10' N	7° 13,01' E	617,3	NW 4	Heat Flow Lance	
27-2	29.07.2007	23:06	43° 37,10' N	7° 13,01' E	617,2	NNW 4	Deep Water CPT Lance	
	29.07.2007	23:19	43° 37,10' N	7° 13,01' E	617,8	NNW 4	Deep Water CPT Lance	SLmax=610m
	29.07.2007	23:38	43° 37,10' N	7° 13,01' E	621,5	NW 3	Deep Water CPT Lance	SZmax=8,0KN
	29.07.2007	23:53	43° 37,10' N	7° 13,01' E	615,9	NW 3	Deep Water CPT Lance	
26-3	30.07.2007	0:08	43° 37,20' N	7° 13,00' E	594,5	NNW 2	Heat Flow Lance	
	30.07.2007	0:20	43° 37,20' N	7° 13,00' E	594,9	NW 2	Heat Flow Lance	SLmax=569m
	30.07.2007	0:27	43° 37,20' N	7° 13,00' E	593,9	WNW 1	Heat Flow Lance	SZmax=13,7KN
	30.07.2007	0:43	43° 37,20' N	7° 13,00' E	591,7	WNW 2	Heat Flow Lance	
27-3	30.07.2007	0:44	43° 37,20' N	7° 13,00' E	601,3	WNW 2	Deep Water CPT Lance	
	30.07.2007	0:57	43° 37,20' N	7° 13,00' E	599,5	N 2	Deep Water CPT Lance	SLmax=589m
	30.07.2007	1:30	43° 37,20' N	7° 13,00' E	595	NNE 2	Deep Water CPT Lance	SZmax=7,5KN
	30.07.2007	1:44	43° 37,20' N	7° 13,00' E	596,6	E 2	Deep Water CPT Lance	
26-4	30.07.2007	2:00	43° 37,29' N	7° 12,99' E	568,1	ENE 6	Heat Flow Lance	
	30.07.2007	2:18	43° 37,30' N	7° 13,00' E	554,5	E 6	Heat Flow Lance	SLmax 573 m
	30.07.2007	2:25	43° 37,30' N	7° 13,00' E	556,2	E 6	Heat Flow Lance	Zmax 22,5 kN
	30.07.2007	2:40	43° 37,30' N	7° 13,00' E	555,8	E 5	Heat Flow Lance	
27-4	30.07.2007	2:42	43° 37,30' N	7° 13,00' E	555,9	E 5	Deep Water CPT Lance	
	30.07.2007	2:55	43° 37,30' N	7° 13,00' E	555,4	E 5	Deep Water CPT Lance	SLmax 566 m
	30.07.2007	3:26	43° 37,30' N	7° 13,00' E	556,5	E 5	Deep Water CPT Lance	Zmax 4,8 kN
	30.07.2007	3:41	43° 37,30' N	7° 13,00' E	558	ESE 5	Deep Water CPT Lance	
26-5	30.07.2007	3:54	43° 37,40' N	7° 13,01' E	527,1	ESE 5	Heat Flow Lance	
	30.07.2007	4:06	43° 37,40' N	7° 13,01' E	530,3	ESE 4	Heat Flow Lance	SLmax 540 m
	30.07.2007	4:15	43° 37,40' N	7° 13,01' E	532,9	ESE 4	Heat Flow Lance	Zmax 24,0 kN
	30.07.2007	4:29	43° 37,40' N	7° 13,01' E	530,4	SE 3	Heat Flow Lance	
27-5	30.07.2007	4:31	43° 37,40' N	7° 13,01' E	532,2	ESE 3	Deep Water CPT Lance	
	30.07.2007	4:43	43° 37,40' N	7° 13,01' E	533,4	SSE 2	Deep Water CPT Lance	SLmax 554 m
	30.07.2007	5:12	43° 37,40' N	7° 13,01' E	533,3	WSW 2	Deep Water CPT Lance	Zmax 8,3 kN
	30.07.2007	5:35	43° 37,40' N	7° 13,01' E	530,4	WSW 2	Deep Water CPT Lance	

26-6	30.07.2007	5:47	43° 37,51' N	7° 13,01' E	530	W 2	Heat Flow Lance	
	30.07.2007	6:01	43° 37,50' N	7° 13,00' E	533	NW 2	Heat Flow Lance	SLmax 526 m
	30.07.2007	6:10	43° 37,50' N	7° 13,00' E	534,1	WNW 2	Heat Flow Lance	SZmax: 15,4m
	30.07.2007	6:31	43° 37,55' N	7° 13,21' E	519,1	WNW 2	Heat Flow Lance	
28-1	30.07.2007	9:45	43° 37,20' N	7° 13,70' E	545,1	ESE 6	Deep Water CPT Lance	
	30.07.2007	9:59	43° 37,19' N	7° 13,70' E	560,3	ESE 6	Deep Water CPT Lance	SLmax:596m
	30.07.2007	10:39	43° 37,19' N	7° 13,69' E	562,2	E 5	Deep Water CPT Lance	SZmax=8,0KN
	30.07.2007	10:55	43° 37,19' N	7° 13,69' E	561,7	ESE 5	Deep Water CPT Lance	
28-2	30.07.2007	11:18	43° 37,20' N	7° 13,49' E	643,4	E 5	Deep Water CPT Lance	
	30.07.2007	11:32	43° 37,20' N	7° 13,50' E	646	E 6	Deep Water CPT Lance	SLmax=647m
	30.07.2007	11:57	43° 37,20' N	7° 13,48' E	636,4	E 6	Deep Water CPT Lance	
29	30.07.2007	16:54	43° 36,92' N	7° 13,26' E	652,1	ESE 2	Seismic reflection profile	buoy to water, 3 kn
	30.07.2007	17:28	43° 35,16' N	7° 13,23' E	1152,5	E 2	Seismic reflection profile	600 m Streamer
	30.07.2007	17:33	43° 34,90' N	7° 13,23' E	1081,8	E 3	Seismic reflection profile	
	30.07.2007	17:49	43° 34,11' N	7° 13,25' E	991,1	E 2	Seismic reflection profile	start firing, system check
	30.07.2007	17:55	43° 33,74' N	7° 13,26' E	1017,7	E 2	Seismic reflection profile	compressor off
	30.07.2007	18:41	43° 31,23' N	7° 13,27' E	659,9	ENE 2	Seismic reflection profile	system check on board
	30.07.2007	20:13	43° 27,87' N	7° 13,07' E	1332,1	NNE 2	Seismic reflection profile	
	30.07.2007	20:35	43° 26,67' N	7° 13,25' E	1502,4	N 2	Seismic reflection profile	start firing, system check
	30.07.2007	21:22	43° 23,95' N	7° 13,02' E	2140,6	NNE 2	Seismic reflection profile	approach 730 profil
	30.07.2007	22:15	43° 26,59' N	7° 12,51' E	1733,5	N 2	Seismic reflection profile	060°- 14,6nm
	31.07.2007	1:13	43° 33,09' N	7° 28,44' E	1904,3	NNE 2	Seismic reflection profile	rwK=170
	31.07.2007	2:00	43° 30,01' N	7° 29,37' E	2150,5	N 2	Seismic reflection profile	rwK 237°
	31.07.2007	4:06	43° 24,65' N	7° 18,05' E	2086,5	E 10	Seismic reflection profile	rwK 135°
	31.07.2007	4:48	43° 22,47' N	7° 19,29' E	2148,2	ENE 13	Seismic reflection profile	rwK 053°
	31.07.2007	6:24	43° 26,04' N	7° 27,64' E	2087,6	ENE 10	Seismic reflection profile	180°-4nm
	31.07.2007	7:11	43° 22,17' N	7° 28,12' E	1971,5	ENE 12	Seismic reflection profile	090°-4nm
	31.07.2007	8:17	43° 22,05' N	7° 33,39' E	1966,1	ENE 12	Seismic reflection profile	180°- 0,8
	31.07.2007	8:32	43° 21,07' N	7° 33,10' E	2006,7	ENE 12	Seismic reflection profile	270° - 4,0nm
	31.07.2007	9:13	43° 21,29' N	7° 27,92' E	2071,6	ENE 11	Seismic reflection profile	090° - 4,0nm
	31.07.2007	10:37	43° 22,00' N	7° 33,61' E	1978	E 12	Seismic reflection profile	rwK=210
	31.07.2007	11:28	43° 20,03' N	7° 31,09' E	2078,4	E 8	Seismic reflection profile	rwK=360
	31.07.2007	13:05	43° 27,76' N	7° 31,12' E	2125,5	E 9	Seismic reflection profile	rwk=328
	31.07.2007	13:55	43° 31,46' N	7° 28,01' E	2056,5	E 7	Seismic reflection profile	rwK=326
	31.07.2007	14:19	43° 32,88' N	7° 26,40' E	1680,1	E 6	Seismic reflection profile	rwK 240°
	31.07.2007	14:54	43° 31,41' N	7° 23,09' E	1545,9	ESE 5	Seismic reflection profile	rwK 147°
	31.07.2007	15:06	43° 30,90' N	7° 23,63' E	1582,4	ESE 6	Seismic reflection profile	rwK 060°
	31.07.2007	15:45	43° 32,35' N	7° 27,15' E	1834,2	ESE 4	Seismic reflection profile	rwK 326°
	31.07.2007	15:53	43° 32,74' N	7° 26,56' E	1712,6	ESE 3	Seismic reflection profile	rwK 240°
	31.07.2007	16:38	43° 30,99' N	7° 22,10' E	1726,9	SE 3	Seismic reflection profile	rwK 270°
	31.07.2007	17:02	43° 30,99' N	7° 19,52' E	1745,7	SSE 3	Seismic reflection profile	rwK 354°
	31.07.2007	17:15	43° 31,79' N	7° 19,58' E	1696,4	S 2	Seismic reflection profile	rwK 092°
	31.07.2007	17:47	43° 31,66' N	7° 22,89' E	1525,4	SW 2	Seismic reflection profile	rwK 171°
	31.07.2007	17:53	43° 31,38' N	7° 22,79' E	1568,9	SSW 3	Seismic reflection profile	rwK 270°
	31.07.2007	19:05	43° 31,40' N	7° 14,74' E	901,3	WSW 5	Seismic reflection profile	2. Airgun
	31.07.2007	19:34	43° 31,35' N	7° 12,72' E	685,4	SW 4	Seismic reflection profile	system check
	31.07.2007	19:44	43° 31,47' N	7° 11,93' E	636,7	WSW 4	Seismic reflection profile	052° - 9,7nm
	31.07.2007	22:06	43° 38,60' N	7° 24,66' E	832,7	W 5	Seismic reflection profile	rwk=312
	31.07.2007	22:29	43° 40,01' N	7° 22,86' E	377,4	W 4	Seismic reflection profile	rwK=262
	31.07.2007	22:47	43° 39,81' N	7° 20,78' E	284,1	WNW 4	Seismic reflection profile	rwK=142
	01.08.2007	0:50	43° 39,82' N	7° 22,15' E	313	WNW 2	Seismic reflection profile	rwk=234
	01.08.2007	1:45	43° 37,62' N	7° 17,14' E	941,6	NNW 6	Seismic reflection profile	RWK=144
	01.08.2007	2:00	43° 36,73' N	7° 17,83' E	1158,6	NNW 5	Seismic reflection profile	rwK053
	01.08.2007	3:06	43° 39,63' N	7° 23,83' E	582,4	NNE 4	Seismic reflection profile	rwK 140°
	01.08.2007	3:12	43° 39,25' N	7° 24,16' E	636,5	NE 4	Seismic reflection profile	rwK 232°
	01.08.2007	3:48	43° 37,28' N	7° 20,85' E	804,4	NE 4	Seismic reflection profile	rwK 140°
	01.08.2007	4:08	43° 36,44' N	7° 22,14' E	971,1	ENE 5	Seismic reflection profile	rwK 052°
	01.08.2007	4:43	43° 38,11' N	7° 25,31' E	985,4	ENE 5	Seismic reflection profile	rwK 124°
	01.08.2007	4:53	43° 37,74' N	7° 26,10' E	1202	ENE 4	Seismic reflection profile	rwK 234°
	01.08.2007	5:22	43° 36,29' N	7° 23,31' E	1188,9	E 3	Seismic reflection profile	rwK 322°
	01.08.2007	6:00	43° 38,46' N	7° 20,48' E	705,7	ENE 4	Seismic reflection profile	rwK 243°
	01.08.2007	6:32	43° 37,19' N	7° 16,85' E	1000	E 5	Seismic reflection profile	270° - 5,3nm
	01.08.2007	7:28	43° 37,21' N	7° 10,02' E	614,9	ESE 4	Seismic reflection profile	take in airguns and streamer

	01.08.2007	7:40	43° 36,86' N	7° 10,08' E	695,2	ESE 3	Seismic reflection profile	total: 161 nm
	01.08.2007	8:40	43° 36,82' N	7° 13,12' E	740,5	ESE 3	Seismic reflection profile	
30	01.08.2007	9:12	43° 37,24' N	7° 13,53' E	614,5	ESE 4	Gravity corer	
	01.08.2007	9:52	43° 37,20' N	7° 13,28' E	627,2	E 5	Gravity corer	SLmax: 611m
	01.08.2007	9:53	43° 37,20' N	7° 13,28' E	629,5	E 5	Gravity corer	SZ max:26,3kn
	01.08.2007	10:15	43° 37,20' N	7° 13,28' E	632	ESE 5	Gravity corer	
31-1	01.08.2007	10:45	43° 37,21' N	7° 13,49' E	635,2	ESE 5	Pushcorer	PC#6
	01.08.2007	11:04	43° 37,22' N	7° 13,50' E	636,3	ESE 4	Pushcorer	SLmax= 618m
	01.08.2007	11:21	43° 37,20' N	7° 13,52' E	629,7	ESE 6	Pushcorer	
31-2	01.08.2007	11:27	43° 37,20' N	7° 13,51' E	636,7	ESE 6	Pushcorer	PC#7
	01.08.2007	11:43	43° 37,20' N	7° 13,52' E	630,2	ESE 5	Pushcorer	SLmax=640m
	01.08.2007	12:00	43° 37,20' N	7° 13,51' E	623,9	ESE 5	Pushcorer	
32-1	01.08.2007	12:34	43° 37,19' N	7° 12,80' E	636,2	ESE 5	Pushcorer	
	01.08.2007	12:47	43° 37,20' N	7° 12,82' E	644,4	ESE 4	Pushcorer	SLmax=638m
	01.08.2007	13:05	43° 37,20' N	7° 12,81' E	644	SE 4	Pushcorer	
32-2	01.08.2007	13:17	43° 37,20' N	7° 12,82' E	644	ESE 4	Gravity corer	
	01.08.2007	13:28	43° 37,20' N	7° 12,81' E	643,7	ESE 4	Gravity corer	SLmax=633m, SZmax=24,4KN
	01.08.2007	13:47	43° 37,20' N	7° 12,82' E	642,9	SE 4	Gravity corer	
32-3	01.08.2007	13:53	43° 37,20' N	7° 12,82' E	643,7	SE 4	Gravity corer	
	01.08.2007	14:06	43° 37,20' N	7° 12,82' E	643,1	SE 4	Gravity corer	SLmax=632m, SZmax=27,5KN
	01.08.2007	14:32	43° 37,20' N	7° 12,81' E	641,7	SE 3	Gravity corer	banana
33	01.08.2007	15:05	43° 37,19' N	7° 12,62' E	570,1	SE 3	Pushcorer	PC#9
	01.08.2007	15:19	43° 37,19' N	7° 12,62' E	570,1	SE 2	Pushcorer	SLmax 581 m, Zmax 4,9 kN
	01.08.2007	15:37	43° 37,19' N	7° 12,62' E	574,8	SSE 2	Pushcorer	
34-1	01.08.2007	16:23	43° 37,19' N	7° 12,40' E	636,7	SE 2	Gravity corer	GC 3 m
	01.08.2007	16:36	43° 37,19' N	7° 12,40' E	637	S 2	Gravity corer	SLmax 625 m
	01.08.2007	16:36	43° 37,19' N	7° 12,40' E	637	SSE 2	Gravity corer	Zmax 37,5 kN
	01.08.2007	17:01	43° 37,19' N	7° 12,40' E	636,1	S 2	Gravity corer	
34-2	01.08.2007	17:06	43° 37,19' N	7° 12,40' E	634,6	S 2	Pushcorer	PC#10
	01.08.2007	17:43	43° 37,20' N	7° 12,42' E	640,3	S 2	Pushcorer	SLmax 628 m, Zmax 6,3 kN
	01.08.2007	18:00	43° 37,20' N	7° 12,42' E	640,9	SSW 2	Pushcorer	
35	01.08.2007	18:13	43° 37,19' N	7° 12,43' E	640,9	SSW 2	Seismic reflection profile	Streamer 75m
	01.08.2007	18:29	43° 37,11' N	7° 11,60' E	551	S 2	Seismic reflection profile	
	01.08.2007	18:31	43° 37,13' N	7° 11,47' E	506,2	S 2	Seismic reflection profile	
	01.08.2007	19:34	43° 36,96' N	7° 14,61' E	674,5	WSW 1	Seismic reflection profile	270°-2,0nm
	01.08.2007	20:27	43° 36,72' N	7° 13,11' E	772,4	WSW 1	Seismic reflection profile	360°-202
	01.08.2007	21:18	43° 38,87' N	7° 13,06' E	15,9	NW 3	Seismic reflection profile	180°
	01.08.2007	21:25	43° 38,81' N	7° 13,18' E	18,4	NNW 3	Seismic reflection profile	223°
	01.08.2007	21:39	43° 38,32' N	7° 12,53' E	180,4	NNW 5	Seismic reflection profile	180°
	01.08.2007	21:42	43° 38,20' N	7° 12,54' E	249,1	NNW 4	Seismic reflection profile	45°
	01.08.2007	22:03	43° 38,76' N	7° 13,42' E	17,8	NNW 4	Seismic reflection profile	
	01.08.2007	22:16	43° 38,58' N	7° 12,89' E	116	N 5	Seismic reflection profile	
	01.08.2007	22:36	43° 38,45' N	7° 13,39' E	140,9	NW 4	Seismic reflection profile	
	01.08.2007	22:50	43° 38,75' N	7° 12,96' E	45,6	WNW 4	Seismic reflection profile	
	01.08.2007	23:20	43° 37,59' N	7° 13,19' E	495,6	WNW 4	Seismic reflection profile	
	01.08.2007	23:35	43° 38,34' N	7° 13,26' E	165,8	NNW 5	Seismic reflection profile	total 15 nm
	01.08.2007	23:45	43° 38,67' N	7° 13,28' E	15,2	N 5	Seismic reflection profile	
	01.08.2007	23:45	43° 38,65' N	7° 13,28' E	15,5	NNW 5	Seismic reflection profile	
36-1	02.08.2007	0:35	43° 38,57' N	7° 13,06' E	67,8	NNW 6	Shallow water CPT Lance	
	02.08.2007	0:48	43° 38,56' N	7° 13,05' E	75,5	NNW 5	Shallow water CPT Lance	SLmax=86
	02.08.2007	1:07	43° 38,55' N	7° 13,05' E	83,4	NNW 5	Shallow water CPT Lance	
	02.08.2007	1:13	43° 38,55' N	7° 13,05' E	74,6	N 5	Shallow water CPT Lance	
36-2	02.08.2007	1:20	43° 38,60' N	7° 13,05' E	48,1	NNW 5	Shallow water CPT Lance	
	02.08.2007	1:23	43° 38,60' N	7° 13,04' E	57,4	N 5	Shallow water CPT Lance	SLmax=62m
	02.08.2007	1:43	43° 38,60' N	7° 13,05' E	50,6	N 4	Shallow water CPT Lance	
	02.08.2007	1:46	43° 38,60' N	7° 13,05' E	53,3	NNW 4	Shallow water CPT Lance	
36-3	02.08.2007	1:53	43° 38,63' N	7° 13,05' E	20	N 4	Shallow water CPT Lance	
	02.08.2007	2:00	43° 38,64' N	7° 13,05' E	22,3	NNW 4	Shallow water CPT Lance	
	02.08.2007	2:24	43° 38,64' N	7° 13,05' E	21,1	NNW 3	Shallow water CPT Lance	SLmax 67 m
	02.08.2007	2:31	43° 38,64' N	7° 13,05' E	20,1	NNW 3	Shallow water CPT Lance	
36-4	02.08.2007	2:42	43° 38,70' N	7° 13,06' E	50,1	NW 4	Shallow water CPT Lance	
	02.08.2007	2:44	43° 38,70' N	7° 13,06' E	53,1	NW 4	Shallow water CPT Lance	SLmax 57 m
	02.08.2007	3:03	43° 38,70' N	7° 13,06' E	50,6	NNW 5	Shallow water CPT Lance	Zmax 2,3 kN

	02.08.2007	3:07	43° 38,70' N	7° 13,06' E	50	NNW 5	Shallow water CPT Lance	
36-5	02.08.2007	3:20	43° 38,76' N	7° 13,05' E	48,2	N 5	Shallow water CPT Lance	
	02.08.2007	3:22	43° 38,76' N	7° 13,05' E	47,7	N 4	Shallow water CPT Lance	SLmax 58 m
	02.08.2007	3:41	43° 38,76' N	7° 13,06' E	46,5	NNW 5	Shallow water CPT Lance	Zmax 2,4 kN
	02.08.2007	3:47	43° 38,76' N	7° 13,06' E	49,5	NNW 4	Shallow water CPT Lance	
36-6	02.08.2007	3:50	43° 38,80' N	7° 13,05' E	31,8	NNW 5	Shallow water CPT Lance	
	02.08.2007	3:56	43° 38,82' N	7° 13,05' E	37	NNW 5	Shallow water CPT Lance	
	02.08.2007	4:22	43° 38,82' N	7° 13,05' E	37	NNW 5	Shallow water CPT Lance	
	02.08.2007	4:26	43° 38,82' N	7° 13,05' E	36,8	NNW 6	Shallow water CPT Lance	
36-7	02.08.2007	4:39	43° 38,83' N	7° 13,04' E	24,5	NNW 6	Shallow water CPT Lance	
	02.08.2007	4:41	43° 38,83' N	7° 13,04' E	25	NNW 6	Shallow water CPT Lance	SLmax 32 m
	02.08.2007	4:58	43° 38,84' N	7° 13,04' E	23,7	NNW 6	Shallow water CPT Lance	
	02.08.2007	5:00	43° 38,83' N	7° 13,04' E	30,3	NNW 6	Shallow water CPT Lance	
37	02.08.2007	9:03	43° 25,48' N	7° 51,45' E	2369	SW 3	Pushcorer	PC#11
	02.08.2007	9:49	43° 25,49' N	7° 51,49' E	2373,1	SW 3	Pushcorer	SLmax 2379m
	02.08.2007	10:47	43° 25,49' N	7° 51,48' E	2371,8	WSW 3	Pushcorer	
38	02.08.2007	11:35	43° 23,71' N	7° 44,16' E	2299,7	WSW 4	Pushcorer	PC#12
	02.08.2007	12:19	43° 23,68' N	7° 44,16' E	2292,5	SE 4	Pushcorer	SLmax 2300m, Zmax 11,4 KN
	02.08.2007	13:23	43° 23,66' N	7° 43,46' E	2310	S 4	Pushcorer	
39	02.08.2007	14:29	43° 23,46' N	7° 31,51' E	2217,4	S 3	Pushcorer	PC #13
	02.08.2007	15:20	43° 23,46' N	7° 31,51' E	2215,9	S 5	Pushcorer	SLmax 2224 m, Zmax 11.1 kN
	02.08.2007	16:07	43° 23,46' N	7° 31,50' E	2216,6	S 5	Pushcorer	
40	02.08.2007	18:26	43° 38,99' N	7° 10,09' E	73,2	S 2	Seismic reflection profile	75m
	02.08.2007	18:39	43° 38,72' N	7° 10,83' E	170,1	SSE 2	Seismic reflection profile	
	02.08.2007	18:39	43° 38,72' N	7° 10,83' E	170,1	SSE 2	Seismic reflection profile	195°
	02.08.2007	19:08	43° 37,44' N	7° 10,31' E	543,3	SSE 4	Seismic reflection profile	232°
	02.08.2007	19:24	43° 36,95' N	7° 9,41' E	440,2	SSE 2	Seismic reflection profile	090°
	02.08.2007	20:30	43° 36,89' N	7° 12,99' E	698,4	S 3	Seismic reflection profile	360°
	02.08.2007	21:14	43° 38,79' N	7° 13,08' E	3241	SE 2	Seismic reflection profile	180°
	02.08.2007	21:32	43° 38,30' N	7° 12,60' E	119,3	E 2	Seismic reflection profile	
	02.08.2007	21:33	43° 38,26' N	7° 12,61' E	118,8	ESE 2	Seismic reflection profile	
	02.08.2007	21:39	43° 38,06' N	7° 12,63' E	136,7	E 1	Seismic reflection profile	
41-1	02.08.2007	21:49	43° 37,80' N	7° 12,65' E	8,4	E 2	Multibeam-Parasound-Profile	
	02.08.2007	22:32	43° 37,46' N	7° 13,03' E	498,5	ENE 1	Multibeam-Parasound-Profile	
	02.08.2007	23:02	43° 38,67' N	7° 12,85' E	81,7	N 2	Multibeam-Parasound-Profile	
	03.08.2007	1:00	43° 38,68' N	7° 13,42' E	28,7	ENE 5	Multibeam-Parasound-Profile	
41-2	03.08.2007	2:10	43° 38,82' N	7° 12,93' E	26,9	ENE 4	Remote operated vehicle	dive #2
	03.08.2007	2:21	43° 38,82' N	7° 12,93' E	28,5	NE 4	Remote operated vehicle	
	03.08.2007	3:11	43° 38,81' N	7° 12,93' E	28,2	NNW 2	Remote operated vehicle	
	03.08.2007	3:30	43° 38,79' N	7° 12,93' E	36,8	NNW 2	Remote operated vehicle	
	03.08.2007	4:00	43° 38,79' N	7° 12,93' E	36,9	NW 3	Remote operated vehicle	
	03.08.2007	4:05	43° 38,79' N	7° 12,93' E	37	NW 3	Remote operated vehicle	
42	03.08.2007	4:26	43° 38,83' N	7° 13,05' E	28,4	NW 3	Gravity corer	
	03.08.2007	4:27	43° 38,83' N	7° 13,05' E	28,4	NW 3	Gravity corer	SLmax 37 m
	03.08.2007	4:29	43° 38,83' N	7° 13,05' E	28,8	NW 3	Gravity corer	Zmax 34.0 kN
	03.08.2007	4:34	43° 38,83' N	7° 13,05' E	28,7	NNW 3	Gravity corer	
43	03.08.2007	5:10	43° 38,84' N	7° 13,05' E	19,9	NNW 4	Gravity corer	
	03.08.2007	5:12	43° 38,84' N	7° 13,05' E	20,2	NNW 3	Gravity corer	SLmax 24 m
	03.08.2007	5:12	43° 38,84' N	7° 13,05' E	20,2	NNW 3	Gravity corer	Zmax 25,5 kN
	03.08.2007	5:18	43° 38,84' N	7° 13,05' E	20,3	NNW 4	Gravity corer	
44-1	03.08.2007	6:49	43° 32,27' N	7° 21,19' E	1485,3	NE 4	Multibeam-Parasound-Profile	180deg
	03.08.2007	7:24	43° 30,50' N	7° 21,31' E	1822,9	NE 4	Multibeam-Parasound-Profile	
44-2	03.08.2007	8:09	43° 32,07' N	7° 21,11' E	1527,4	ENE 5	Gravity corer	
	03.08.2007	8:35	43° 32,07' N	7° 21,11' E	1529,1	ENE 6	Gravity corer	SLmax 1521m
	03.08.2007	8:35	43° 32,07' N	7° 21,11' E	1529,1	ENE 6	Gravity corer	SYmax. 45.7kn
	03.08.2007	9:18	43° 32,07' N	7° 21,10' E	1527,7	E 5	Gravity corer	
45-1	03.08.2007	10:55	43° 31,19' N	7° 21,36' E	1753	E 2	Multibeam-Parasound-Profile	
	03.08.2007	11:20	43° 32,28' N	7° 21,30' E	1487,5	E 3	Multibeam-Parasound-Profile	
45-2	03.08.2007	11:47	43° 31,76' N	7° 21,35' E	1636,7	ESE 2	Gravity corer	
	03.08.2007	12:21	43° 31,76' N	7° 21,36' E	1639	ENE 2	Gravity corer	SLmax 1630m, SZmax 46,7KN
	03.08.2007	13:02	43° 31,76' N	7° 21,39' E	1625,6	E 1	Gravity corer	
46	03.08.2007	13:12	43° 31,86' N	7° 21,35' E	1565,5	SSE 0	Seismic reflection profile	600 m Streamer
	03.08.2007	13:38	43° 32,43' N	7° 21,34' E	1465,2	WNW 1	Seismic reflection profile	

	03.08.2007	15:02	43° 32,44' N	7° 21,26' E	1432,6	NW 3	Seismic reflection profile	rwK 180 °, FüG 4 kn
	03.08.2007	15:37	43° 30,16' N	7° 21,43' E	1848,6	NNW 2	Seismic reflection profile	KÄ rwK 355°
	03.08.2007	15:54	43° 30,18' N	7° 22,11' E	1856,2	NNE 2	Seismic reflection profile	rwK 355°
	03.08.2007	16:22	43° 32,13' N	7° 21,90' E	1482,1	ENE 2	Seismic reflection profile	KÄ rwK 178°
	03.08.2007	16:39	43° 32,20' N	7° 21,23' E	1494,8	ENE 1	Seismic reflection profile	rwK 178°
	03.08.2007	17:05	43° 30,37' N	7° 21,35' E	1833,8	ENE 2	Seismic reflection profile	KÄ rwk 090°
	03.08.2007	17:29	43° 30,29' N	7° 22,70' E	1854,3	E 1	Seismic reflection profile	rwK 356°
	03.08.2007	17:55	43° 32,12' N	7° 22,54' E	1383,3	NNE 1	Seismic reflection profile	Kä rwK 178°
	03.08.2007	18:16	43° 32,21' N	7° 21,39' E	1510,8	NNW 2	Seismic reflection profile	178°
	03.08.2007	19:01	43° 28,97' N	7° 21,55' E	1834	N 2	Seismic reflection profile	
	03.08.2007	19:27	43° 28,88' N	7° 21,47' E	1838,1	NNW 2	Seismic reflection profile	070°
	03.08.2007	19:55	43° 29,43' N	7° 23,53' E	1915,4	NNW 1	Seismic reflection profile	
	03.08.2007	20:13	43° 29,39' N	7° 23,60' E	1926,7	N 1	Seismic reflection profile	307°
	03.08.2007	21:05	43° 31,51' N	7° 19,80' E	1724,5	NW 1	Seismic reflection profile	090°
	03.08.2007	21:42	43° 31,62' N	7° 22,62' E	1583,8	NW 0	Seismic reflection profile	
	03.08.2007	22:00	43° 31,14' N	7° 22,77' E	1626,8	E 1	Seismic reflection profile	270deg
	03.08.2007	22:23	43° 31,17' N	7° 20,31' E	1753,3	NNE 1	Seismic reflection profile	
	03.08.2007	22:48	43° 31,57' N	7° 20,39' E	1717,8	NE 1	Seismic reflection profile	
	03.08.2007	23:16	43° 31,53' N	7° 23,09' E	1546	ENE 2	Seismic reflection profile	
	03.08.2007	23:30	43° 31,08' N	7° 22,75' E	1631,6	ESE 2	Seismic reflection profile	
	04.08.2007	0:00	43° 31,10' N	7° 19,73' E	1747,1	ESE 4	Seismic reflection profile	
	04.08.2007	0:17	43° 31,48' N	7° 20,33' E	1727,8	ESE 3	Seismic reflection profile	
	04.08.2007	0:47	43° 31,46' N	7° 23,29' E	1515	ESE 2	Seismic reflection profile	
	04.08.2007	1:00	43° 30,88' N	7° 22,92' E	1645	E 2	Seismic reflection profile	
	04.08.2007	1:32	43° 30,91' N	7° 19,79' E	1766,5	ENE 2	Seismic reflection profile	
	04.08.2007	1:53	43° 31,31' N	7° 20,36' E	1743,6	NE 3	Seismic reflection profile	
	04.08.2007	2:25	43° 31,25' N	7° 23,46' E	1530,9	NNE 4	Seismic reflection profile	rwK 059°
	04.08.2007	3:02	43° 32,53' N	7° 26,37' E	1704,4	NNE 4	Seismic reflection profile	Kä rwK 240°
	04.08.2007	3:22	43° 31,99' N	7° 27,27' E	1923,4	NE 4	Seismic reflection profile	rwK 240°
	04.08.2007	3:49	43° 31,07' N	7° 24,83' E	1700,4	NNE 4	Seismic reflection profile	KÄ rwK 325°
	04.08.2007	4:18	43° 31,75' N	7° 23,68' E	1472,2	NE 2	Seismic reflection profile	rwK 061°
	04.08.2007	4:47	43° 32,68' N	7° 26,03' E	1627,9	E 2	Seismic reflection profile	KÄ rwK 144°
	04.08.2007	5:00	43° 32,39' N	7° 26,74' E	1791	ENE 2	Seismic reflection profile	rwK 241°
	04.08.2007	5:29	43° 31,38' N	7° 24,39' E	1699,8	ENE 2	Seismic reflection profile	KÄ rwK 060°
	04.08.2007	5:50	43° 31,64' N	7° 23,95' E	1564,1	NNE 1	Seismic reflection profile	rwK 060°
	04.08.2007	6:19	43° 32,57' N	7° 26,30' E	1689,7	N 2	Seismic reflection profile	
	04.08.2007	6:36	43° 32,18' N	7° 26,64' E	1786,7	N 2	Seismic reflection profile	241°
	04.08.2007	7:05	43° 31,25' N	7° 24,27' E	1667,7	NE 2	Seismic reflection profile	
	04.08.2007	7:30	43° 31,46' N	7° 24,05' E	1605,3	NE 2	Seismic reflection profile	061°
	04.08.2007	8:06	43° 32,43' N	7° 26,42' E	1731,5	E 2	Seismic reflection profile	
	04.08.2007	8:25	43° 32,11' N	7° 26,66' E	1802	E 2	Seismic reflection profile	241°
	04.08.2007	8:46	43° 31,30' N	7° 24,74' E	1786	E 2	Seismic reflection profile	019°
	04.08.2007	9:25	43° 32,97' N	7° 25,28' E	1519,3	ESE 2	Seismic reflection profile	
	04.08.2007	9:41	43° 33,02' N	7° 25,24' E	1517,8	ESE 2	Seismic reflection profile	277°
	04.08.2007	10:00	43° 33,15' N	7° 23,29' E	1351,8	ESE 3	Seismic reflection profile	
	04.08.2007	10:17	43° 33,14' N	7° 23,53' E	1398,9	ESE 4	Seismic reflection profile	134°
	04.08.2007	11:10	43° 30,48' N	7° 27,31' E	2092,8	SE 3	Seismic reflection profile	
	04.08.2007	11:20	43° 30,17' N	7° 27,16' E	1971,1	ESE 4	Seismic reflection profile	
	04.08.2007	11:45	43° 30,00' N	7° 25,95' E	1786,8	ESE 4	Seismic reflection profile	total length: 76nm
47	04.08.2007	12:34	43° 31,79' N	7° 21,36' E	1627,1	ESE 3	Gravity corer	W11
	04.08.2007	12:59	43° 31,80' N	7° 21,36' E	1613,7	ESE 2	Gravity corer	SLmax 1620m, 40,5 KN
	04.08.2007	13:41	43° 31,80' N	7° 21,36' E	1595,3	SE 2	Gravity corer	
48	04.08.2007	14:30	43° 30,65' N	7° 21,39' E	1816,6	SE 2	Gravity corer	
	04.08.2007	14:58	43° 30,65' N	7° 21,39' E	1818,8	SSE 2	Gravity corer	SLmax 1806 m
	04.08.2007	14:59	43° 30,65' N	7° 21,39' E	1818,9	SSE 2	Gravity corer	Zmax 40.5 kN
	04.08.2007	15:40	43° 30,65' N	7° 21,39' E	1817,7	SSE 2	Gravity corer	
49-1	04.08.2007	16:28	43° 32,20' N	7° 21,35' E	1512,8	SW 2	Heat Flow Lance	
	04.08.2007	16:56	43° 32,20' N	7° 21,35' E	1509,6	SW 2	Heat Flow Lance	SLmax 1495 m
	04.08.2007	17:04	43° 32,20' N	7° 21,35' E	1509,4	WSW 2	Heat Flow Lance	Zmax 29,3 kN
	04.08.2007	17:28	43° 32,20' N	7° 21,35' E	1509,6	WSW 2	Heat Flow Lance	
50-1f	04.08.2007	17:30	43° 32,20' N	7° 21,35' E	1511,9	WSW 2	Deep Water CPT Lance	
	04.08.2007	17:35	43° 32,20' N	7° 21,35' E	1515,1	WSW 3	Deep Water CPT Lance	SLmax 100 m, instrument failure
	04.08.2007	17:43	43° 32,20' N	7° 21,35' E	1509,9	WSW 3	Deep Water CPT Lance	

49-2	04.08.2007	17:54	43° 32,05' N	7° 21,34' E	1528,8	WSW 2	Heat Flow Lance	
	04.08.2007	18:21	43° 32,05' N	7° 21,35' E	1528,3	W 3	Heat Flow Lance	SLmax 1517m
	04.08.2007	18:27	43° 32,05' N	7° 21,35' E	1528	W 4	Heat Flow Lance	SYmax 30kn
	04.08.2007	18:31	43° 32,05' N	7° 21,34' E	1534	W 3	Heat Flow Lance	
49-3	04.08.2007	18:53	43° 31,91' N	7° 21,34' E	1553,9	W 3	Heat Flow Lance	
	04.08.2007	18:55	43° 31,91' N	7° 21,34' E	1550,7	W 3	Heat Flow Lance	SL max 1533m
	04.08.2007	19:04	43° 31,90' N	7° 21,35' E	1549,7	W 3	Heat Flow Lance	SZmax 30.2kn
	04.08.2007	19:07	43° 31,90' N	7° 21,35' E	1552,1	W 3	Heat Flow Lance	
49-4	04.08.2007	19:29	43° 31,77' N	7° 21,34' E	1642,2	W 4	Heat Flow Lance	
	04.08.2007	19:36	43° 31,77' N	7° 21,35' E	1643,3	W 3	Heat Flow Lance	SLmax 1605m
	04.08.2007	19:39	43° 31,77' N	7° 21,35' E	1643,1	W 4	Heat Flow Lance	SZmax 26.9kn
	04.08.2007	20:15	43° 31,71' N	7° 21,35' E	1660,6	W 2	Heat Flow Lance	
49-5	04.08.2007	20:45	43° 31,66' N	7° 21,34' E	1679,1	W 3	Heat Flow Lance	
	04.08.2007	21:10	43° 31,66' N	7° 21,34' E	1676,9	W 3	Heat Flow Lance	SLmax 1656m
	04.08.2007	21:17	43° 31,66' N	7° 21,34' E	1675,8	W 3	Heat Flow Lance	SZmax 30.3kn
	04.08.2007	21:23	43° 31,65' N	7° 21,34' E	1677,9	W 2	Heat Flow Lance	
49-6	04.08.2007	21:44	43° 31,55' N	7° 21,35' E	1694,6	W 4	Heat Flow Lance	
	04.08.2007	21:52	43° 31,55' N	7° 21,35' E	1689,8	W 3	Heat Flow Lance	SLmax 1681m
	04.08.2007	22:00	43° 31,55' N	7° 21,35' E	1690	WNW 3	Heat Flow Lance	Szmax30,5 KN
	04.08.2007	22:06	43° 31,55' N	7° 21,35' E	1688,1	WNW 3	Heat Flow Lance	
49-7	04.08.2007	22:30	43° 31,40' N	7° 21,35' E	1725,5	WNW 3	Heat Flow Lance	
	04.08.2007	22:36	43° 31,40' N	7° 21,36' E	1724,1	WNW 3	Heat Flow Lance	SLmax 1714m
	04.08.2007	22:45	43° 31,41' N	7° 21,36' E	1720,4	NW 2	Heat Flow Lance	SZmax 31 KN
	04.08.2007	22:48	43° 31,41' N	7° 21,36' E	1718,7	NW 2	Heat Flow Lance	
49-8	04.08.2007	23:10	43° 31,25' N	7° 21,36' E	1748,5	NW 2	Heat Flow Lance	
	04.08.2007	23:16	43° 31,25' N	7° 21,36' E	1747,3	WNW 3	Heat Flow Lance	SLmax 1736m
	04.08.2007	23:25	43° 31,25' N	7° 21,36' E	1747	NW 4	Heat Flow Lance	Sz max 31,2 KN
	04.08.2007	23:30	43° 31,25' N	7° 21,36' E	1745	WNW 4	Heat Flow Lance	
49-9	04.08.2007	23:52	43° 31,11' N	7° 21,36' E	1761,1	NW 3	Heat Flow Lance	
	04.08.2007	23:56	43° 31,10' N	7° 21,36' E	1760,5	WNW 3	Heat Flow Lance	SLmax 1 756m
	05.08.2007	0:06	43° 31,10' N	7° 21,36' E	1759,3	WNW 3	Heat Flow Lance	SZ max 24,7KN
	05.08.2007	0:12	43° 31,10' N	7° 21,36' E	1761	WNW 3	Heat Flow Lance	
49-10	05.08.2007	0:31	43° 30,95' N	7° 21,35' E	1787,1	WNW 3	Heat Flow Lance	
	05.08.2007	0:36	43° 30,95' N	7° 21,35' E	1788,3	WNW 3	Heat Flow Lance	SLmax 1778m
	05.08.2007	0:45	43° 30,95' N	7° 21,36' E	1789,7	WNW 3	Heat Flow Lance	Sz max 32,0 KN
	05.08.2007	0:48	43° 30,95' N	7° 21,36' E	1786	NW 3	Heat Flow Lance	
49-11	05.08.2007	1:20	43° 30,80' N	7° 21,35' E	1800,2	NW 3	Heat Flow Lance	
	05.08.2007	1:22	43° 30,80' N	7° 21,35' E	1798,9	NW 3	Heat Flow Lance	SLmax 1785m
	05.08.2007	1:30	43° 30,80' N	7° 21,35' E	1798,5	NW 3	Heat Flow Lance	SZmax 33,7KN
	05.08.2007	2:10	43° 30,65' N	7° 21,35' E	1818,9	NW 3	Heat Flow Lance	
49-12	05.08.2007	2:11	43° 30,65' N	7° 21,35' E	1819,2	NW 2	Heat Flow Lance	
	05.08.2007	2:43	43° 30,65' N	7° 21,35' E	1818,9	NW 3	Heat Flow Lance	SLmax 1807 m
	05.08.2007	2:50	43° 30,65' N	7° 21,35' E	1820	NW 2	Heat Flow Lance	Zmax 26.8 kN
	05.08.2007	2:55	43° 30,65' N	7° 21,35' E	1819,8	WNW 1	Heat Flow Lance	
49-13	05.08.2007	3:27	43° 30,53' N	7° 21,35' E	1824,6	NNE 2	Heat Flow Lance	failed
	05.08.2007	3:30	43° 30,53' N	7° 21,35' E	1824,4	NNE 2	Heat Flow Lance	SLmax 1808 m
	05.08.2007	3:40	43° 30,53' N	7° 21,35' E	1824,3	ENE 1	Heat Flow Lance	
	05.08.2007	3:47	43° 30,53' N	7° 21,35' E	1824,9	ESE 2	Heat Flow Lance	failed
	05.08.2007	3:49	43° 30,53' N	7° 21,35' E	1823,5	SE 3	Heat Flow Lance	SLmax 1810 m
	05.08.2007	4:00	43° 30,53' N	7° 21,35' E	1823,2	S 1	Heat Flow Lance	
	05.08.2007	4:41	43° 30,53' N	7° 21,35' E	1823,4	NNE 2	Heat Flow Lance	
51	05.08.2007	4:52	43° 30,51' N	7° 20,83' E	1823,4	NE 2	Seismic reflection profile	buoy to water, 2.5 kn
	05.08.2007	5:14	43° 30,30' N	7° 19,06' E	1566,1	ENE 2	Seismic reflection profile	600 m Streamer
	05.08.2007	5:15	43° 30,29' N	7° 18,98' E	1541,4	ENE 2	Seismic reflection profile	airgun out
	05.08.2007	5:23	43° 30,29' N	7° 18,33' E	1381,3	E 2	Seismic reflection profile	
	05.08.2007	6:05	43° 30,44' N	7° 21,72' E	1832	ENE 5	Seismic reflection profile	rwK 126°
	05.08.2007	6:17	43° 29,93' N	7° 22,75' E	1875,3	ENE 5	Seismic reflection profile	
	05.08.2007	6:28	43° 29,53' N	7° 23,50' E	1905,5	E 5	Seismic reflection profile	117°
	05.08.2007	6:50	43° 28,80' N	7° 25,57' E	1989,9	ENE 2	Seismic reflection profile	
	05.08.2007	7:08	43° 29,36' N	7° 26,02' E	1921,9	E 4	Seismic reflection profile	295°
	05.08.2007	7:10	43° 29,43' N	7° 25,81' E	1906,7	E 3	Seismic reflection profile	
	05.08.2007	7:49	43° 30,56' N	7° 22,69' E	1802	E 5	Seismic reflection profile	
	05.08.2007	7:55	43° 30,71' N	7° 22,24' E	1801,4	E 4	Seismic reflection profile	

	05.08.2007	8:16	43° 30,31' N	7° 21,93' E	1840,3	E 5	Seismic reflection profile	126°
	05.08.2007	8:48	43° 28,91' N	7° 24,66' E	1970,3	E 4	Seismic reflection profile	006°
	05.08.2007	9:34	43° 30,77' N	7° 24,89' E	1700,3	E 5	Seismic reflection profile	
	05.08.2007	10:05	43° 29,69' N	7° 24,09' E	1691,5	E 4	Seismic reflection profile	114°
	05.08.2007	10:32	43° 28,88' N	7° 26,52' E	1970,4	E 4	Seismic reflection profile	
	05.08.2007	10:47	43° 29,53' N	7° 26,56' E	1961,9	E 4	Seismic reflection profile	rwk 294
	05.08.2007	11:11	43° 30,25' N	7° 24,33' E	1586,1	E 4	Seismic reflection profile	
	05.08.2007	11:26	43° 30,65' N	7° 24,87' E	1668,9	E 4	Seismic reflection profile	rwk 061
	05.08.2007	12:20	43° 32,78' N	7° 24,87' E	1505,9	E 3	Seismic reflection profile	rwk 241
	05.08.2007	12:23	43° 32,66' N	7° 24,60' E	1560,5	E 3	Seismic reflection profile	stb
	05.08.2007	12:40	43° 32,09' N	7° 23,10' E	1380,4	E 4	Seismic reflection profile	
	05.08.2007	12:44	43° 31,96' N	7° 22,75' E	1503,9	E 4	Seismic reflection profile	
	05.08.2007	13:05	43° 31,62' N	7° 21,83' E	1605	E 4	Seismic reflection profile	total length = 30nm
52	05.08.2007	13:46	43° 31,79' N	7° 25,45' E	1903,9	ESE 4	Gravity corer	
	05.08.2007	14:14	43° 31,79' N	7° 25,45' E	1905,1	ESE 3	Gravity corer	SLmax 1891 m
	05.08.2007	14:14	43° 31,79' N	7° 25,45' E	1905,1	ESE 3	Gravity corer	Zmax 43.5 kN
	05.08.2007	14:57	43° 31,79' N	7° 25,45' E	1903,9	ESE 2	Gravity corer	
53	05.08.2007	15:45	43° 32,29' N	7° 24,73' E	1754,2	SE 1	Gravity corer	
	05.08.2007	16:11	43° 32,29' N	7° 24,73' E	1759,9	SE 2	Gravity corer	SLmax 1744 m
	05.08.2007	16:12	43° 32,29' N	7° 24,73' E	1760,8	SE 2	Gravity corer	Zmax 45.1 kN
	05.08.2007	16:57	43° 32,29' N	7° 24,73' E	1757,6	S 1	Gravity corer	banana
54	05.08.2007	17:33	43° 30,50' N	7° 22,12' E	1829,7	S 1	Pushcorer	PC #14
	05.08.2007	18:12	43° 30,52' N	7° 22,14' E	1828,3	SW 0	Pushcorer	SLmax 1822m
	05.08.2007	18:57	43° 30,52' N	7° 22,14' E	1828,6	SW 2	Pushcorer	
55	05.08.2007	20:05	43° 36,42' N	7° 12,68' E	802,9	S 2	Seismic reflection profile	
	05.08.2007	20:11	43° 36,68' N	7° 12,66' E	778,8	SSE 2	Seismic reflection profile	75m
	05.08.2007	20:28	43° 37,47' N	7° 12,73' E	513,1	S 1	Seismic reflection profile	360°
	05.08.2007	20:42	43° 38,13' N	7° 12,72' E	273,8	S 1	Seismic reflection profile	352°
	05.08.2007	20:53	43° 38,64' N	7° 12,65' E	17,4	SSW 1	Seismic reflection profile	047°
	05.08.2007	21:01	43° 38,83' N	7° 12,96' E	27,6	SW 2	Seismic reflection profile	120°
	05.08.2007	21:10	43° 38,69' N	7° 13,36' E	22,4	SW 1	Seismic reflection profile	221°
	05.08.2007	21:25	43° 38,26' N	7° 12,98' E	226,7	WSW 2	Seismic reflection profile	314°
	05.08.2007	21:34	43° 38,36' N	7° 12,64' E	139,8	W 2	Seismic reflection profile	046°
	05.08.2007	21:50	43° 38,81' N	7° 13,18' E	24,2	NNW 3	Seismic reflection profile	222°
	05.08.2007	22:00	43° 38,55' N	7° 13,20' E	62,2	NNW 2	Seismic reflection profile	rwk 222
	05.08.2007	22:21	43° 38,37' N	7° 12,75' E	186	NNW 2	Seismic reflection profile	46
	05.08.2007	22:30	43° 38,67' N	7° 13,14' E	16,9	NW 3	Seismic reflection profile	
	05.08.2007	22:35	43° 38,63' N	7° 13,35' E	31,5	NW 3	Seismic reflection profile	rwk 180
	05.08.2007	22:48	43° 38,02' N	7° 13,36' E	335,8	NNW 3	Seismic reflection profile	
	05.08.2007	23:00	43° 37,40' N	7° 13,38' E	584,5	N 1	Seismic reflection profile	total length 7 nm
56	05.08.2007	23:42	43° 38,80' N	7° 13,05' E	41,2	NNE 2	Shallow water CPT Lance	long-term test with surface buoy
57	06.08.2007	0:52	43° 38,80' N	7° 13,20' E	22,3	NE 2	Remote operated vehicle	dive #3
	06.08.2007	3:22	43° 38,80' N	7° 13,20' E	20,1	N 1	Remote operated vehicle	
	06.08.2007	4:07	43° 38,69' N	7° 12,93' E	69	NE 3	Remote operated vehicle	dive #4
	06.08.2007	4:52	43° 38,69' N	7° 12,93' E	70,7	E 4	Remote operated vehicle	
	06.08.2007	4:58	43° 38,69' N	7° 12,93' E	68	E 5	Remote operated vehicle	
56	06.08.2007	5:18	43° 38,79' N	7° 13,01' E	33,5	NE 3	Shallow water CPT Lance	
	06.08.2007	5:24	43° 38,77' N	7° 12,98' E	38,5	ENE 2	Shallow water CPT Lance	
58	06.08.2007	10:48	43° 21,92' N	7° 32,24' E	1930	E 2	Pushcorer	PC #15
	06.08.2007	11:31	43° 21,92' N	7° 32,24' E	1928,7	SSE 1	Pushcorer	SLmax=1926m
	06.08.2007	12:20	43° 21,92' N	7° 32,24' E	1930,7	SSW 2	Pushcorer	
59	06.08.2007	13:17	43° 26,97' N	7° 27,27' E	2067,7	SSE 2	Pushcorer	PC #16
	06.08.2007	14:00	43° 26,98' N	7° 27,30' E	2067,7	S 3	Pushcorer	SLmax=2082m
	06.08.2007	14:47	43° 26,98' N	7° 27,30' E	2067,7	SSW 1	Pushcorer	
60	06.08.2007	15:57	43° 32,47' N	7° 24,51' E	1585,8	SSW 1	Gravity corer	
	06.08.2007	16:22	43° 32,50' N	7° 24,51' E	1574,9	SSW 4	Gravity corer	SLmax 1564 m
	06.08.2007	16:23	43° 32,50' N	7° 24,51' E	1575,2	SSW 3	Gravity corer	Zmax 51,3 kN
	06.08.2007	16:59	43° 32,50' N	7° 24,51' E	1576,1	WSW 5	Gravity corer	
61	06.08.2007	17:54	43° 31,20' N	7° 26,28' E	2089,6	WSW 4	Gravity corer	
	06.08.2007	18:28	43° 31,20' N	7° 26,28' E	2091,1	SW 3	Gravity corer	SLmax 2083m
	06.08.2007	18:29	43° 31,20' N	7° 26,28' E	2089,8	WSW 3	Gravity corer	SZmax 39.8kn
62-1	06.08.2007	19:12	43° 31,20' N	7° 26,28' E	2090,6	SW 2	Gravity corer	
	06.08.2007	19:55	43° 32,21' N	7° 21,33' E	1510,4	SW 2	Deep Water CPT Lance	

	06.08.2007	20:27	43° 32,20' N	7° 21,34' E	1506,2	WSW 4	Deep Water CPT Lance	SLmax 1490m
	06.08.2007	20:30	43° 32,20' N	7° 21,34' E	1505,9	SW 4	Deep Water CPT Lance	SZ max 11.3kn
	06.08.2007	21:10	43° 32,05' N	7° 21,31' E	1534,2	SW 4	Deep Water CPT Lance	
62-2	06.08.2007	21:21	43° 32,05' N	7° 21,35' E	1530,5	SSW 4	Deep Water CPT Lance	
	06.08.2007	21:44	43° 32,05' N	7° 21,35' E	1532,6	SW 6	Deep Water CPT Lance	SLmax 1514m
	06.08.2007	22:10	43° 32,05' N	7° 21,35' E	1530	WSW 4	Deep Water CPT Lance	SZmax 12,7 KN
	06.08.2007	22:52	43° 32,05' N	7° 21,35' E	1533,1	W 3	Deep Water CPT Lance	
62-3	06.08.2007	23:13	43° 31,91' N	7° 21,35' E	1549,5	WNW 2	Deep Water CPT Lance	
	06.08.2007	23:29	43° 31,91' N	7° 21,36' E	1550,5	NNW 3	Deep Water CPT Lance	
	06.08.2007	23:51	43° 31,91' N	7° 21,36' E	1545,7	WNW 2	Deep Water CPT Lance	
63-1	07.08.2007	0:45	43° 32,45' N	7° 24,51' E	1590,7	NW 2	Heat Flow Lance	
	07.08.2007	1:20	43° 32,45' N	7° 24,50' E	1588,4	N 2	Heat Flow Lance	SLmax 1579 m
	07.08.2007	1:30	43° 32,45' N	7° 24,51' E	1585,9	N 2	Heat Flow Lance	Szmax 30,6KN
	07.08.2007	1:34	43° 32,45' N	7° 24,50' E	1585,4	NNW 2	Heat Flow Lance	
63-2	07.08.2007	2:15	43° 32,29' N	7° 24,73' E	1799,1	NE 3	Heat Flow Lance	pogo-style
	07.08.2007	2:22	43° 32,28' N	7° 24,73' E	1785,4	NE 4	Heat Flow Lance	SLmax 1753 m
	07.08.2007	2:29	43° 32,29' N	7° 24,73' E	1761,6	NE 3	Heat Flow Lance	Zmax 33.4 kN
	07.08.2007	3:08	43° 32,29' N	7° 24,73' E	1723,3	ENE 4	Heat Flow Lance	
63-3	07.08.2007	3:37	43° 32,12' N	7° 24,97' E	1803	ENE 4	Heat Flow Lance	
	07.08.2007	4:09	43° 32,13' N	7° 24,97' E	1797,9	ENE 6	Heat Flow Lance	SLmax 1788 m
	07.08.2007	4:16	43° 32,13' N	7° 24,97' E	1799,1	ENE 6	Heat Flow Lance	Zmax 27.7 kN
	07.08.2007	4:20	43° 32,13' N	7° 24,97' E	1795,1	ENE 7	Heat Flow Lance	
63-4	07.08.2007	4:46	43° 32,00' N	7° 25,14' E	1857,5	NE 7	Heat Flow Lance	
	07.08.2007	4:51	43° 32,00' N	7° 25,14' E	1816,2	NE 8	Heat Flow Lance	SLmax 1831 m
	07.08.2007	4:58	43° 32,00' N	7° 25,14' E	1816	NE 8	Heat Flow Lance	Zmax 36.0 kN
	07.08.2007	5:01	43° 32,00' N	7° 25,14' E	1819,5	NE 8	Heat Flow Lance	
63-5	07.08.2007	5:44	43° 31,79' N	7° 25,45' E	1903,9	E 4	Heat Flow Lance	
	07.08.2007	5:48	43° 31,79' N	7° 25,45' E	1905,9	E 4	Heat Flow Lance	SLmax 1893 m
	07.08.2007	5:54	43° 31,79' N	7° 25,45' E	1905	E 4	Heat Flow Lance	Zmax 27.7 kN
	07.08.2007	5:59	43° 31,79' N	7° 25,45' E	1907,3	E 3	Heat Flow Lance	
63-6	07.08.2007	6:21	43° 31,67' N	7° 25,63' E	1910,7	E 2	Heat Flow Lance	
	07.08.2007	6:29	43° 31,67' N	7° 25,64' E	1906,5	ENE 2	Heat Flow Lance	SLmax 1919m
	07.08.2007	6:40	43° 31,67' N	7° 25,64' E	1904,2	ENE 2	Heat Flow Lance	SZmax 32.4kn
	07.08.2007	7:31	43° 31,67' N	7° 25,64' E	1903,6	E 2	Heat Flow Lance	
64	07.08.2007	7:57	43° 31,11' N	7° 26,20' E	2094,1	ESE 2	Gravity corer	
	07.08.2007	8:31	43° 31,12' N	7° 26,21' E	2094,4	E 2	Gravity corer	SLmax 2094m, SZmax 50.1
	07.08.2007	9:32	43° 31,06' N	7° 26,19' E	2089,4	ESE 2	Gravity corer	
65	07.08.2007	10:50	43° 26,98' N	7° 27,29' E	2068,4	S 2	Gravity corer	
	07.08.2007	11:26	43° 26,98' N	7° 27,29' E	2068,6	S 2	Gravity corer	SLmax 2054m Szmax 38,1 KN
	07.08.2007	12:21	43° 26,98' N	7° 27,29' E	2068	S 3	Gravity corer	
66	07.08.2007	13:26	43° 31,33' N	7° 24,24' E	1636,8	S 4	Gravity corer	
	07.08.2007	13:58	43° 31,33' N	7° 24,24' E	1638	SSW 5	Gravity corer	SLmax 1644 Zmax 48,3kN
	07.08.2007	14:41	43° 31,32' N	7° 24,24' E	1632,9	S 2	Gravity corer	
67	07.08.2007	15:30	43° 29,22' N	7° 27,07' E	1987,6	SSW 4	Gravity corer	
	07.08.2007	16:04	43° 29,19' N	7° 27,12' E	1987,7	SW 3	Gravity corer	SLmax 1993 m, Zmax 45.9 kN
	07.08.2007	16:58	43° 29,19' N	7° 27,12' E	1988,5	SSW 2	Gravity corer	
68	07.08.2007	17:54	43° 32,12' N	7° 17,24' E	1550,1	SSE 2	Pushcorer	PC#17
	07.08.2007	18:20	43° 32,08' N	7° 17,23' E	1553,1	S 2	Pushcorer	SLmax 1556m
	07.08.2007	19:04	43° 32,09' N	7° 17,23' E	1552,2	SSE 4	Pushcorer	
69	07.08.2007	19:33	43° 33,31' N	7° 15,84' E	1433,2	SSW 4	Pushcorer	PC#18
	07.08.2007	19:57	43° 33,31' N	7° 15,83' E	1434,2	SSE 2	Pushcorer	SLmax 1445m
	07.08.2007	20:39	43° 33,31' N	7° 15,83' E	1435,1	SW 1	Pushcorer	
70-1	07.08.2007	21:39	43° 38,44' N	7° 12,94' E	166,1	SSE 1	Shallow water CPT Lance	
	07.08.2007	21:50	43° 38,44' N	7° 12,94' E	161,3	ESE 1	Shallow water CPT Lance	SLmax 171m
	07.08.2007	22:10	43° 38,44' N	7° 12,94' E	167,4	NE 0	Shallow water CPT Lance	
	07.08.2007	22:17	43° 38,44' N	7° 12,94' E	165,5	ENE 1	Shallow water CPT Lance	
70-2	07.08.2007	22:29	43° 38,52' N	7° 12,93' E	130,6	ENE 1	Shallow water CPT Lance	
	07.08.2007	22:33	43° 38,52' N	7° 12,93' E	135,6	ENE 1	Shallow water CPT Lance	SLmax 141m
	07.08.2007	22:52	43° 38,52' N	7° 12,93' E	133,4	ENE 1	Shallow water CPT Lance	
	07.08.2007	22:58	43° 38,52' N	7° 12,93' E	132,8	E 0	Shallow water CPT Lance	
70-3	07.08.2007	23:07	43° 38,57' N	7° 12,93' E	117	E 1	Shallow water CPT Lance	
	07.08.2007	23:10	43° 38,57' N	7° 12,93' E	117,7	E 0	Shallow water CPT Lance	SLmax 120m
	07.08.2007	23:30	43° 38,57' N	7° 12,93' E	117	WNW 1	Shallow water CPT Lance	

	07.08.2007	23:34	43° 38,57' N	7° 12,93' E	117,2	WSW 1	Shallow water CPT Lance	
70-4	07.08.2007	23:44	43° 38,63' N	7° 12,93' E	92,1	WNW 0	Shallow water CPT Lance	
	07.08.2007	23:47	43° 38,63' N	7° 12,93' E	91	W 1	Shallow water CPT Lance	
	08.08.2007	0:05	43° 38,63' N	7° 12,93' E	92,2	WNW 2	Shallow water CPT Lance	
	08.08.2007	0:10	43° 38,63' N	7° 12,93' E	92,3	NW 2	Shallow water CPT Lance	
70-5	08.08.2007	0:19	43° 38,69' N	7° 12,93' E	62,9	NW 2	Shallow water CPT Lance	
	08.08.2007	0:22	43° 38,69' N	7° 12,93' E	64,1	NW 2	Shallow water CPT Lance	SLmax 81m
	08.08.2007	0:42	43° 38,69' N	7° 12,93' E	64,2	NW 2	Shallow water CPT Lance	
	08.08.2007	0:46	43° 38,69' N	7° 12,93' E	64,6	NW 3	Shallow water CPT Lance	
70-6	08.08.2007	0:57	43° 38,72' N	7° 12,93' E	53,5	NW 2	Shallow water CPT Lance	
	08.08.2007	1:00	43° 38,72' N	7° 12,93' E	52,8	NW 3	Shallow water CPT Lance	SLmax 62m
	08.08.2007	1:17	43° 38,72' N	7° 12,93' E	55,3	NNW 4	Shallow water CPT Lance	
	08.08.2007	1:20	43° 38,72' N	7° 12,93' E	53,7	NNW 3	Shallow water CPT Lance	
70-7	08.08.2007	1:30	43° 38,75' N	7° 12,93' E	47,4	NNW 4	Shallow water CPT Lance	
	08.08.2007	1:32	43° 38,75' N	7° 12,93' E	47,7	NNW 4	Shallow water CPT Lance	SLmax 52m
	08.08.2007	1:50	43° 38,75' N	7° 12,93' E	47,7	NNW 4	Shallow water CPT Lance	
	08.08.2007	1:55	43° 38,75' N	7° 12,93' E	47,4	NNW 4	Shallow water CPT Lance	
70-8	08.08.2007	2:03	43° 38,79' N	7° 12,93' E	32,8	NW 3	Shallow water CPT Lance	
	08.08.2007	2:05	43° 38,79' N	7° 12,93' E	34,2	NW 4	Shallow water CPT Lance	SLmax 38m
	08.08.2007	2:23	43° 38,79' N	7° 12,93' E	34,4	NNW 3	Shallow water CPT Lance	
	08.08.2007	2:25	43° 38,79' N	7° 12,93' E	34	NW 3	Shallow water CPT Lance	
70-9	08.08.2007	2:34	43° 38,82' N	7° 12,93' E	24,9	NNW 3	Shallow water CPT Lance	
	08.08.2007	2:35	43° 38,82' N	7° 12,93' E	25,1	NNW 3	Shallow water CPT Lance	SLmax 28m
	08.08.2007	2:55	43° 38,82' N	7° 12,93' E	23	NNW 4	Shallow water CPT Lance	
	08.08.2007	3:00	43° 38,82' N	7° 12,93' E	24,5	NNW 4	Shallow water CPT Lance	
71	08.08.2007	3:17	43° 38,73' N	7° 12,93' E	49,7	NNW 4	Pushcorer	PC#19
	08.08.2007	3:20	43° 38,73' N	7° 12,93' E	51,2	NNW 4	Pushcorer	SLmax 54
	08.08.2007	3:26	43° 38,73' N	7° 12,93' E	50,8	NNW 4	Pushcorer	
72-1	08.08.2007	3:53	43° 38,63' N	7° 13,17' E	20,9	NNW 5	Gravity corer	
	08.08.2007	3:57	43° 38,63' N	7° 13,17' E	19,7	NNW 5	Gravity corer	SLmax 20m
	08.08.2007	3:57	43° 38,63' N	7° 13,17' E	19,7	NNW 5	Gravity corer	Zmax 32,1kN
	08.08.2007	4:10	43° 38,63' N	7° 13,17' E	19	NNW 4	Gravity corer	
72-2	08.08.2007	4:12	43° 38,63' N	7° 13,17' E	18	NNW 4	Shallow water CPT Lance	
	08.08.2007	4:12	43° 38,63' N	7° 13,17' E	18	NNW 4	Shallow water CPT Lance	SLmax 28m
	08.08.2007	5:42	43° 38,63' N	7° 13,17' E	20	N 3	Shallow water CPT Lance	
	08.08.2007	5:48	43° 38,63' N	7° 13,17' E	18,3	NNW 4	Shallow water CPT Lance	
73	08.08.2007	7:17	43° 31,64' N	7° 25,71' E	1921,3	SSE 1	Gravity corer	
	08.08.2007	7:55	43° 31,63' N	7° 25,71' E	1926,3	SSW 4	Gravity corer	SLmax 1915m
	08.08.2007	7:56	43° 31,63' N	7° 25,71' E	1926,2	SSW 4	Gravity corer	SZmax 37.8kn
	08.08.2007	8:39	43° 31,63' N	7° 25,71' E	1925,6	SW 1	Gravity corer	
74	08.08.2007	10:00	43° 31,35' N	7° 25,97' E	2001,7	WSW 6	Gravity corer	
	08.08.2007	10:40	43° 31,35' N	7° 25,97' E	1976,3	SW 8	Gravity corer	SLmax 1955m, SZmax 46,1 KN
	08.08.2007	11:27	43° 31,36' N	7° 25,97' E	1974,5	WSW 7	Gravity corer	
75	08.08.2007	12:20	43° 30,87' N	7° 26,57' E	2101,6	W 11	Gravity corer	
	08.08.2007	12:57	43° 30,87' N	7° 26,58' E	2100,8	W 9	Gravity corer	SLmax 2084m, SZmax 37,3 KN
	08.08.2007	13:50	43° 30,87' N	7° 26,57' E	2101,2	SW 12	Gravity corer	
76	08.08.2007	15:54	43° 32,08' N	7° 17,25' E	1556,5	SW 15	Pushcorer	PC#20
	08.08.2007	16:19	43° 32,08' N	7° 17,21' E	1555,7	WSW 15	Pushcorer	SLmax 1549 m, hieven, Zmax 8.2 kN
	08.08.2007	17:00	43° 32,08' N	7° 17,22' E	1556,2	W 14	Pushcorer	
77	08.08.2007	17:50	43° 30,51' N	7° 22,15' E	1830,7	W 13	Pushcorer	PC#21
	08.08.2007	18:19	43° 30,53' N	7° 22,13' E	1830,4	WNW 14	Pushcorer	SLmax 1820m
78-1	08.08.2007	19:03	43° 30,53' N	7° 22,13' E	1830	W 10	Pushcorer	
	08.08.2007	19:56	43° 31,50' N	7° 25,86' E	1937,8	WSW 13	Heat Flow Lance	
	08.08.2007	20:38	43° 31,50' N	7° 25,86' E	1937,7	WSW 16	Heat Flow Lance	SLmax 1927m
	08.08.2007	20:49	43° 31,50' N	7° 25,86' E	1939,8	WSW 14	Heat Flow Lance	SZmax 34.7kn
78-2	08.08.2007	21:35	43° 31,34' N	7° 26,16' E	1987,7	WSW 17	Heat Flow Lance	
	08.08.2007	22:13	43° 31,31' N	7° 26,12' E	2044,4	WSW 12	Heat Flow Lance	
	08.08.2007	22:56	43° 31,31' N	7° 26,12' E	2059,7	W 9	Heat Flow Lance	SLmax 2046m
	08.08.2007	23:03	43° 31,31' N	7° 26,12' E	2063	W 8	Heat Flow Lance	Szmax 36,5 KN
	08.08.2007	23:53	43° 31,31' N	7° 26,12' E	2061,2	W 14	Heat Flow Lance	
78-3	09.08.2007	0:13	43° 31,21' N	7° 26,26' E	2097,7	W 12	Heat Flow Lance	
	09.08.2007	0:55	43° 31,21' N	7° 26,27' E	2079,6	WNW 9	Heat Flow Lance	SL max 2079m
	09.08.2007	1:03	43° 31,21' N	7° 26,27' E	2095,5	WNW 8	Heat Flow Lance	Szmax 30.1 KN

	09.08.2007	1:50	43° 31,21' N	7° 26,27' E	2077,5	WNW 7	Heat Flow Lance	
78-4	09.08.2007	2:13	43° 31,11' N	7° 26,43' E	2095,2	NW 5	Heat Flow Lance	
	09.08.2007	2:53	43° 31,11' N	7° 26,44' E	2108	N 4	Heat Flow Lance	SLmax 2079 m
	09.08.2007	3:00	43° 31,11' N	7° 26,44' E	2107	N 5	Heat Flow Lance	Zmax 28.6 kN
	09.08.2007	3:05	43° 31,10' N	7° 26,44' E	2106,3	NNE 5	Heat Flow Lance	
78-5	09.08.2007	3:31	43° 30,97' N	7° 26,63' E	2099,3	NNE 7	Heat Flow Lance	
	09.08.2007	3:46	43° 30,97' N	7° 26,63' E	2099,2	NNE 7	Heat Flow Lance	SLmax 2104 m
	09.08.2007	3:55	43° 30,97' N	7° 26,63' E	2098,7	NNE 7	Heat Flow Lance	Zmax 34.1 kN
	09.08.2007	4:00	43° 30,97' N	7° 26,63' E	2100,1	NNE 6	Heat Flow Lance	
78-6	09.08.2007	4:22	43° 30,84' N	7° 26,80' E	2096,8	NNE 6	Heat Flow Lance	
	09.08.2007	4:31	43° 30,84' N	7° 26,80' E	2099,3	NE 6	Heat Flow Lance	SLmax 2095 m
	09.08.2007	4:39	43° 30,84' N	7° 26,80' E	2097,4	NE 5	Heat Flow Lance	Zmax 35.2 kN
	09.08.2007	4:44	43° 30,84' N	7° 26,80' E	2097,7	NE 6	Heat Flow Lance	
78-7	09.08.2007	5:11	43° 30,65' N	7° 27,07' E	2091,9	NE 7	Heat Flow Lance	
	09.08.2007	5:21	43° 30,65' N	7° 27,07' E	2094,3	NE 6	Heat Flow Lance	SLmax 2091 m
	09.08.2007	5:30	43° 30,65' N	7° 27,07' E	2093,9	NE 7	Heat Flow Lance	Zmax 33.7 kN
	09.08.2007	5:39	43° 30,64' N	7° 27,08' E	2093,8	NE 6	Heat Flow Lance	
78-8	09.08.2007	6:05	43° 30,51' N	7° 27,32' E	2095,1	NE 5	Heat Flow Lance	
	09.08.2007	6:12	43° 30,51' N	7° 27,32' E	2097,4	NE 5	Heat Flow Lance	SLmax 2080m
	09.08.2007	6:19	43° 30,51' N	7° 27,32' E	2094,7	ENE 4	Heat Flow Lance	SZmax 33.3kn
	09.08.2007	7:09	43° 30,26' N	7° 27,61' E	2095,2	NE 2	Heat Flow Lance	
79	09.08.2007	7:38	43° 30,25' N	7° 27,61' E	2091,4	E 3	Gravity corer	
	09.08.2007	8:14	43° 30,25' N	7° 27,61' E	2090,1	E 3	Gravity corer	SLmax 2072m
	09.08.2007	8:15	43° 30,25' N	7° 27,61' E	2096	E 3	Gravity corer	SZXmax 53.0
	09.08.2007	9:05	43° 30,47' N	7° 27,46' E	2105,1	E 4	Gravity corer	
80	09.08.2007	9:45	43° 31,80' N	7° 24,69' E	1776,4	ESE 3	Gravity corer	
	09.08.2007	10:14	43° 31,80' N	7° 24,69' E	1771,8	ESE 3	Gravity corer	SL max 1756m, SZmax 44,1 KN
	09.08.2007	10:56	43° 31,79' N	7° 24,69' E	1799,9	ESE 3	Gravity corer	
81	09.08.2007	11:37	43° 31,14' N	7° 21,96' E	1741,3	SE 4	Gravity corer	
	09.08.2007	12:05	43° 31,14' N	7° 21,96' E	1742,9	SE 4	Gravity corer	SL max 1725m, SZmax 46,1 KN
	09.08.2007	12:55	43° 31,14' N	7° 21,96' E	1732,4	SE 5	Gravity corer	
82-1	09.08.2007	13:33	43° 29,87' N	7° 23,59' E	1888,7	ESE 4	Gravity corer	
	09.08.2007	14:04	43° 29,87' N	7° 23,59' E	1888,3	SE 4	Gravity corer	SLmax 1873m, SZmax 31,1 KN
	09.08.2007	14:48	43° 29,87' N	7° 23,59' E	1890	SE 3	Gravity corer	empty liner
82-2	09.08.2007	15:05	43° 29,88' N	7° 23,59' E	1889,8	ESE 3	Gravity corer	
	09.08.2007	15:33	43° 29,87' N	7° 23,59' E	1888,5	E 4	Gravity corer	SLmax 1874 Zmax 36,28kN
	09.08.2007	16:16	43° 29,84' N	7° 23,61' E	1891,4	E 6	Gravity corer	
83	09.08.2007	17:32	43° 37,19' N	7° 13,40' E	640,6	ENE 7	Gravity corer	
	09.08.2007	17:43	43° 37,19' N	7° 13,40' E	642,9	ENE 8	Gravity corer	SLmax 635 m
	09.08.2007	17:44	43° 37,19' N	7° 13,40' E	638,2	ENE 8	Gravity corer	Zmax 23.2 kN
	09.08.2007	18:02	43° 37,20' N	7° 13,40' E	638,5	ENE 8	Gravity corer	
84	09.08.2007	18:27	43° 37,19' N	7° 13,59' E	601,8	ENE 8	Gravity corer	
	09.08.2007	18:37	43° 37,19' N	7° 13,59' E	605,4	ENE 8	Gravity corer	SLmax 611m
	09.08.2007	18:39	43° 37,19' N	7° 13,59' E	607	ENE 8	Gravity corer	SZmax 35.2kn
	09.08.2007	18:57	43° 37,19' N	7° 13,59' E	618,6	ENE 8	Gravity corer	
85	09.08.2007	19:28	43° 37,19' N	7° 13,68' E	579,3	E 6	Gravity corer	
	09.08.2007	19:40	43° 37,19' N	7° 13,68' E	573,1	ENE 6	Gravity corer	SLmax 576m
	09.08.2007	19:40	43° 37,19' N	7° 13,68' E	573,1	ENE 6	Gravity corer	SZmax 38.4kn
	09.08.2007	19:58	43° 37,19' N	7° 13,68' E	573,9	E 6	Gravity corer	
86-1	09.08.2007	20:41	43° 38,62' N	7° 13,17' E	21,7	ENE 7	Shallow water CPT Lance	
	09.08.2007	20:54	43° 38,63' N	7° 13,16' E	20,5	NE 5	Shallow water CPT Lance	20min im boden. SLmax 20m
	09.08.2007	21:15	43° 38,63' N	7° 13,16' E	20,6	N 3	Shallow water CPT Lance	
	09.08.2007	21:16	43° 38,63' N	7° 13,16' E	19	NNW 2	Shallow water CPT Lance	
86-2	09.08.2007	21:29	43° 38,59' N	7° 13,16' E	28,5	NNW 3	Shallow water CPT Lance	
	09.08.2007	21:32	43° 38,59' N	7° 13,16' E	31,2	N 3	Shallow water CPT Lance	SLmax 27m
	09.08.2007	21:53	43° 38,60' N	7° 13,15' E	23	NNW 2	Shallow water CPT Lance	
	09.08.2007	21:55	43° 38,60' N	7° 13,14' E	23,8	NNW 2	Shallow water CPT Lance	
86-3	09.08.2007	22:16	43° 38,55' N	7° 13,17' E	47,3	NNW 5	Shallow water CPT Lance	
	09.08.2007	22:19	43° 38,55' N	7° 13,17' E	47,7	NNW 5	Shallow water CPT Lance	SLmax 54m
	09.08.2007	22:33	43° 38,54' N	7° 13,16' E	47	NNE 5	Shallow water CPT Lance	
	09.08.2007	22:38	43° 38,54' N	7° 13,16' E	47,8	NNE 8	Shallow water CPT Lance	
86-4	09.08.2007	22:51	43° 38,50' N	7° 13,17' E	69,6	NNE 5	Shallow water CPT Lance	
	09.08.2007	22:54	43° 38,50' N	7° 13,17' E	68,5	NNE 7	Shallow water CPT Lance	SL max 81m

	09.08.2007	23:13	43° 38,50' N	7° 13,16' E	73,5	N 4	Shallow water CPT Lance	
	09.08.2007	23:20	43° 38,50' N	7° 13,16' E	71,9	N 3	Shallow water CPT Lance	
86-5	09.08.2007	23:35	43° 38,44' N	7° 13,16' E	117,2	NNE 4	Shallow water CPT Lance	
	09.08.2007	23:40	43° 38,44' N	7° 13,16' E	115,4	N 4	Shallow water CPT Lance	SLmax 134m
	10.08.2007	0:00	43° 38,44' N	7° 13,16' E	112,3	N 5	Shallow water CPT Lance	
	10.08.2007	0:05	43° 38,44' N	7° 13,16' E	124,4	N 4	Shallow water CPT Lance	
86-6	10.08.2007	0:20	43° 38,38' N	7° 13,16' E	149,9	NNW 3	Shallow water CPT Lance	
	10.08.2007	0:26	43° 38,38' N	7° 13,16' E	158,5	NNE 2	Shallow water CPT Lance	SLmax 163m
	10.08.2007	0:46	43° 38,38' N	7° 13,16' E	159,1	NNE 5	Shallow water CPT Lance	
	10.08.2007	0:52	43° 38,38' N	7° 13,16' E	167,6	NNE 7	Shallow water CPT Lance	
86-7	10.08.2007	1:07	43° 38,32' N	7° 13,16' E	179,4	NW 1	Shallow water CPT Lance	
	10.08.2007	1:17	43° 38,32' N	7° 13,16' E	183,8	NE 3	Shallow water CPT Lance	SLmax 172m
	10.08.2007	1:37	43° 38,32' N	7° 13,16' E	179	ENE 4	Shallow water CPT Lance	
	10.08.2007	1:46	43° 38,32' N	7° 13,16' E	180	ENE 5	Shallow water CPT Lance	
87	10.08.2007	2:37	43° 38,84' N	7° 13,08' E	15,8	WNW 3	Remote operated vehicle	dive #5
	10.08.2007	4:00	43° 38,84' N	7° 13,08' E	15,8	NNW 1	Remote operated vehicle	
88	10.08.2007	4:22	43° 36,96' N	7° 13,16' E	15	N 0	Gravity corer	
	10.08.2007	4:24	43° 36,96' N	7° 13,16' E	15	N 0	Gravity corer	SLmax 27m, hieven, Zmax24.3 kN
	10.08.2007	4:27	43° 36,96' N	7° 13,16' E	15	N 0	Gravity corer	
89	10.08.2007	6:16	43° 29,54' N	7° 20,87' E	1803,6	SE 2	Pushcorer	PC#22
	10.08.2007	6:41	43° 29,54' N	7° 20,86' E	1805	S 4	Pushcorer	SLmax 1793m
	10.08.2007	7:28	43° 29,55' N	7° 20,87' E	1803,7	SW 4	Pushcorer	
90	10.08.2007						Pushcorer	PC23
91	10.08.2007						Parasound/Multibeam	

Appendix 9.2.: List of seismic reflection profiles

Profile	Start FFN	End FFN	Start Time		End Time		Start		End	
							[Latitude]	[Longitude]	[Latitude]	[Longitude]
M731-GeoB07-224	0002034	0004466	30.07.2007	22:10.00	31.07.2007	01:13.00	43° 46,10'N	07° 10,10'E	43°33.01'N	07°28.45'E
M731-GeoB07-225	0004500	0004974	31.07.2007	01:16.00	31.07.2007	01:51.00	43°32.97'N	07°28.69'E	43°30.46'N	07°29.66'E
M731-GeoB07-226	0005039	0006581	31.07.2007	01:57.00	31.07.2007	04:05.00	43°30.01N	07°29.61'E	43°24,650'N	07°18,060'E
M731-GeoB07-227	0006725	0007064	31.07.2007	04:19.00	31.07.2007	04:48.00	43°23,850'N	07°17,450'E	43°22,460'N	07°19,310'E
M731-GeoB07-228	0007137	0008165	31.07.2007	04:54.00	31.07.2007	06:21.00	43°22,560'N	07°19,610'E	43°26,093'N	07°27,580'E
M731-GeoB07-229	0008420	~0008670	31.07.2007	06:42.00	31.07.2007	07:06.00	43°24,557'N	07°27,998'E	43°22,436'N	07°27,918'E
M731-GeoB07-230	0000001	0000545	31.07.2007	07:39.00	31.07.2007	08:18.00	43°22,172'N	07°30,406'E	43°22,000'N	07°33,450'E
M731-GeoB07-231	0000745	0001222	31.07.2007	08:34.55	31.07.2007	09:14.41	43°21,069'N	07°32,656'E	43°21,298'N	07°27,722'E
M731-GeoB07-232	0001398	0002254	31.07.2007	09:29.21	31.07.2007	10:40.42	43°21,995'N	07°26,961'E	43°22,003'N	07°33,960'E
M731-GeoB07-233	0002301	0002751	31.07.2007	10:46.00	31.07.2007	11:22.00	43°21.65N	07°33.71E	43°19,600N	7°31,390E
M731-GeoB07-234	0002823	0003973	31.07.2007	11:28.08	31.07.2007	13:04.04	43°20,037'N	07°31,087'E	43°27,691'N	07°31,187'E
M731-GeoB07-235	0003974	0004865	31.07.2007	13:04.09	31.07.2007	14:18.25	43°27,697'N	07°31,181'E	43°32,871'N	07°26,467'E
M731-GeoB07-236	0004911	0005251	31.07.2007	14:22.15	31.07.2007	14:50.36	43°32,809'N	07°26,087'E	43°31,642'N	07°23,240'E
M731-GeoB07-237	0005324	0005479	31.07.2007	14:56.41	31.07.2007	15:09.36	43°31,256'N	07°23,131'E	43°30,883'N	07°23,961'E
M731-GeoB07-238	0005497	0005871	31.07.2007	15:11.06	31.07.2007	15:42.17	43°30,920'N	07°24,090'E	43°32,158'N	07°27,017'E
M731-GeoB07-239	0006017	0006525	31.07.2007	15:54.27	31.07.2007	16:36.45	43°32,712'N	07°26,417'E	43°31,016'N	07°22,237'E
M731-GeoB07-240	0006554	0006810	31.07.2007	16:39.10	31.07.2007	17:00.31	43°30,978'N	07°21,978'E	43°30,956'N	07°19,648'E
M731-GeoB07-241	0006861	0006977	31.07.2007	17:04.46	31.07.2007	17:14.43	43°31,131'N	07°19,444'E	43°31,776'N	07°19,569'E
M731-GeoB07-242	0007005	0007349	31.07.2007	17:17.06	31.07.2007	17:46.21	43°31,844'N	07°19,729'E	43°31,675'N	07°22,828'E
M731-GeoB07-243	0007423	0008680	31.07.2007	17:52.38	31.07.2007	19:39.52	43°31,381'N	07°22,826'E	43°31,340'N	07°12,242'E
M731-GeoB07-244	0008822	0010432	31.07.2007	19:51.42	31.07.2007	22:05.54	43°31,702'N	07°12,506'E	43°38,589'N	07°24,665'E
M731-GeoB07-245	0010499	0010736	31.07.2007	22:11.29	31.07.2007	22:27.49	43°38,985'N	07°24,340'E	43°39,969'N	07°22,988'E
M731-GeoB07-246	0010790	0011066	31.07.2007	22:31.06	31.07.2007	22:44.54	43°40,034'N	07°22,633'E	43°39,868'N	07°20,998'E
M731-GeoB07-247	0011202	0011779	31.07.2007	22:55.53	31.07.2007	23:43.59	43°39,326'N	07°21,247'E	43°36,508'N	07°24,190'E
M731-GeoB07-248	0011889	0011996	31.07.2007	23:53.09	01.08.2007	00:02.04	43°36,356'N	07°24,775'E	43°36,791'N	07°25,468'E
M731-GeoB07-249	0012045	0012644	01.08.2007	00:06.10	01.08.2007	00:53.55	43°37,086'N	07°25,323'E	43°40,044'N	07°21,847'E
M731-GeoB07-250	0012689	0013301	01.08.2007	00:56.55	01.08.2007	01:42.35	43°40,017'N	07°21,533'E	43°37,799'N	07°17,231'E
M731-GeoB07-251	0013374	0013536	01.08.2007	01:48.40	01.08.2007	02:02.11	43°37,341'N	07°17,143'E	43°36,720'N	07°17,975'E
M731-GeoB07-252	0013561	0014268	01.08.2007	02:04.16	01.08.2007	03:03.12	43°36,747'N	07°18,111'E	43°39,678'N	07°23,583'E
M731-GeoB07-253	0014396	0014799	01.08.2007	03:13.52	01.08.2007	03:47.27	43°39,122'N	07°24,063'E	43°37,315'N	07°20,882'E
M731-GeoB07-254	0014839	0015014	01.08.2007	03:50.47	01.08.2007	04:05.23	43°37,134'N	07°20,857'E	43°36,370'N	07°21,913'E
M731-GeoB07-255	0015036	0015558	01.08.2007	04:08.31	01.08.2007	04:43.20	43°36,458'N	07°22,176'E	43°38,110'N	07°25,343'E
M731-GeoB07-256	0015715	0016139	01.08.2007	04:53.48	01.08.2007	05:22.05	43°37,683'N	07°26,064'E	43°36,287'N	07°23,306'E
M731-GeoB07-257	0016175	0016657	01.08.2007	05:24.53	01.08.2007	05:57.01	43°36,368'N	07°23,007'E	43°38,424'N	07°20,803'E
M731-GeoB07-258	0016705	0017058	01.08.2007	06:01.40	01.08.2007	06:31.05	43°38,405'N	07°20,318'E	43°37,206'N	07°16,964'E
M731-GeoB07-259	0017071	0017757	01.08.2007	06:32.10	01.08.2007	07:29.21	43°37,190'N	07°16,833'E	43°37,204'N	07°09,865'E
M731-GeoB07-260	0000477	0001749	01.08.2007	18:46.04	01.08.2007	19:28.29	43°37,202'N	07°11,583'E	43°37,187'N	07°14,586'E
M731-GeoB07-262	0002010	0003158	01.08.2007	19:37.11	01.08.2007	20:15.29	43°36,857'N	07°14,537'E	43°37,242'N	07°13,169'E
M731-GeoB07-262a	0003687	0005381	01.08.2007	20:33.07	01.08.2007	21:18.56	43°36,706'N	07°12,968'E	43°38,882'N	07°13,063'E
M731-GeoB07-263	0005614	0006624	01.08.2007	21:22.50	01.08.2007	21:39.41	43°38,906'N	07°13,189'E	43°38,314'N	07°12,529'E
M731-GeoB07-264	0007047	0007955	01.08.2007	21:46.46	01.08.2007	22:01.55	43°38,185'N	07°12,683'E	43°38,751'N	07°13,340'E
M731-GeoB07-265	0008175	0009048	01.08.2007	22:05.37	01.08.2007	22:20.11	43°38,727'N	07°13,474'E	43°38,574'N	07°12,635'E
M731-GeoB07-266	0009414	0010008	01.08.2007	22:26.18	01.08.2007	22:36.13	43°38,424'N	07°12,657'E	43°38,441'N	07°13,371'E
M731-GeoB07-267	0010286	0010901	01.08.2007	22:40.51	01.08.2007	22:51.08	43°38,552'N	07°13,447'E	43°38,760'N	07°12,934'E

M731-GeoB07-268	0011097	0012289	01.08.2007	22:54.26	01.08.2007	23:14.19	43°38,680'N	07°12,830'E	43°37,640'N	07°12,853'E
M731-GeoB07-269	0000125	0001590	02.08.2007	18:41.26	02.08.2007	19:08.21	43°38,657'N	07°10,825'E	43°37,434'N	07°10,303'E
M731-GeoB07-270	0001595	0002271	02.08.2007	19:08.29	02.08.2007	19:25.26	43°37,430'N	07°10,298'E	43°36,904'N	07°09,339'E
M731-GeoB07-271	0002853	0004450	02.08.2007	19:40.00	02.08.2007	20:31.00	43°36,920'N	07°09,360'E	43°36,930'N	07°13,140'E
M731-GeoB07-272	0004569	0006186	02.08.2007	20:34.43	02.08.2007	21:16.03	43°36,987'N	07°13,153'E	43°38,793'N	07°13,016'E
M731-GeoB07-273	0006191	0007364	02.08.2007	21:16.00	02.08.2007	21:35.00	43°38,790'N	07°13,010'E	43°38,190'N	07°12,620'E
M731-GeoB07-274	0000841	0001597	03.08.2007	14:49.22	03.08.2007	15:39.47	43°33,287'N	07°21,296'E	43°29,986'N	07°21,438'E
M731-GeoB07-275	0001777	0002263	03.08.2007	15:51.47	03.08.2007	16:24.10	43°30,025'N	07°22,149'E	43°32,265'N	07°21,882'E
M731-GeoB07-276	0002437	0002930	03.08.2007	16:35.46	03.08.2007	17:08.38	43°32,390'N	07°21,221'E	43°30,122'N	07°21,374'E
M731-GeoB07-277	0002986	0003157	03.08.2007	17:12.22	03.08.2007	17:23.47	43°30,000'N	07°21,596'E	43°30,024'N	07°22,536'E
M731-GeoB07-278	0003219	0003694	03.08.2007	17:27.55	03.08.2007	17:59.35	43°30,223'N	07°22,717'E	43°32,439'N	07°22,505'E
M731-GeoB07-279	0003740	0003899	03.08.2007	18:02.39	03.08.2007	18:13.16	43°32,577'N	07°22,305'E	43°32,382'N	07°21,415'E
M731-GeoB07-280	0003900	0004654	03.08.2007	18:13.20	03.08.2007	19:03.36	43°32,378'N	07°21,414'E	43°28,787'N	07°21,562'E
M731-GeoB07-281	0004944	0005463	03.08.2007	19:22.57	03.08.2007	19:57.33	43°28,786'N	07°21,205'E	43°29,478'N	07°23,718'E
M731-GeoB07-282	0005716	0006480	03.08.2007	20:14.26	03.08.2007	21:05.23	43°29,454'N	07°23,540'E	43°31,525'N	07°19,776'E
M731-GeoB07-283	0006627	0007116	03.08.2007	21:15.11	03.08.2007	21:47.47	43°31,621'N	07°20,253'E	43°31,618'N	07°23,125'E
M731-GeoB07-284	0007271	0007649	03.08.2007	21:58.08	03.08.2007	22:23.20	43°31,143'N	07°22,933'E	43°31,172'N	07°20,309'E
M731-GeoB07-285	0007832	0007861	03.08.2007	22:35.32	03.08.2007	22:37.28	43°31,391'N	07°19,557'E	43°31,470'N	07°19,582'E
M731-GeoB07-285-1	0007918	0008482	03.08.2007	22:41.16	03.08.2007	23:18.53	43°31,557'N	07°19,783'E	43°31,515'N	07°23,312'E
M731-GeoB07-286	0008612	0009107	03.08.2007	23:27.33	04.08.2007	00:00.34	43°31,070'N	07°23,076'E	43°31,098'N	07°19,728'E
M731-GeoB07-287	0009244	0009810	04.08.2007	00:09.42	04.08.2007	00:47.27	43°31,451'N	07°19,653'E	43°31,458'N	07°23,262'E
M731-GeoB07-288	0009965	0010500	04.08.2007	00:57.47	04.08.2007	01:33.28	43°30,870'N	07°23,205'E	43°30,918'N	07°19,731'E
M731-GeoB07-289	0010658	0011306	04.08.2007	01:44.00	04.08.2007	02:27.13	43°31,301'N	07°19,598'E	43°31,283'N	07°23,559'E
M731-GeoB07-290	0011310	0011855	04.08.2007	02:27.29	04.08.2007	03:03.49	43°31,294'N	07°23,573'E	43°32,592'N	07°26,507'E
M731-GeoB07-291	0011907	0012080	04.08.2007	03:07.17	04.08.2007	03:18.50	43°32,719'N	07°26,797'E	43°32,139'N	07°27,434'E
M731-GeoB07-292	0012125	0012643	04.08.2007	03:21.50	04.08.2007	03:56.22	43°31,998'N	07°27,284'E	43°30,820'N	07°24,238'E
M731-GeoB07-293	0012714	0012856	04.08.2007	04:01.06	04.08.2007	04:10.35	43°30,874'N	07°23,910'E	43°31,427'N	07°23,395'E
M731-GeoB07-294	0012979	0013464	04.08.2007	04:18.47	04.08.2007	04:51.07	43°31,781'N	07°23,739'E	43°32,808'N	07°26,356'E
M731-GeoB07-295	0013524	0013592	04.08.2007	04:55.07	04.08.2007	04:59.40	43°32,695'N	07°26,596'E	43°32,416'N	07°26,742'E
M731-GeoB07-296	0013633	0014127	04.08.2007	05:02.24	04.08.2007	05:35.20	43°32,281'N	07°26,588'E	43°31,187'N	07°23,863'E
M731-GeoB07-297	0014341	0014856	04.08.2007	05:49.36	04.08.2007	06:23.57	43°31,626'N	07°23,917'E	43°32,720'N	07°26,677'E
M731-GeoB07-298	0014891	0014963	04.08.2007	06:26.17	04.08.2007	06:31.05	43°32,672'N	07°26,824'E	43°32,404'N	07°27,014'E
M731-GeoB07-299	0014996	0015543	04.08.2007	06:33.17	04.08.2007	07:09.46	43°32,279'N	07°26,923'E	43°31,097'N	07°23,890'E
M731-GeoB07-300	0015802	0016460	04.08.2007	07:27.02	04.08.2007	08:10.55	43°31,412'N	07°23,870'E	43°32,576'N	07°26,772'E
M731-GeoB07-301	0016621	0016999	04.08.2007	08:21.39	04.08.2007	08:46.52	43°32,210'N	07°26,925'E	43°31,275'N	07°24,667'E
M731-GeoB07-302	0017106	0017629	04.08.2007	08:54.00	04.08.2007	09:28.53	43°31,428'N	07°24,457'E	43°33,182'N	07°25,395'E
M731-GeoB07-303	0017811	0018111	04.08.2007	09:41.01	04.08.2007	10:01.01	43°33,022'N	07°25,236'E	43°33,163'N	07°23,181'E
M731-GeoB07-304	0018280	0019149	04.08.2007	10:12.17	04.08.2007	11:10.14	43°33,340'N	07°23,208'E	43°30,470'N	07°27,320'E
M731-GeoB07-305	0000554	0000986	05.08.2007	05:58.45	05.08.2007	06:27.33	43°30,747'N	07°21,038'E	43°29,551'N	07°23,442'E
M731-GeoB07-306	0001014	0001372	05.08.2007	06:29.25	05.08.2007	06:53.18	43°29,500'N	07°23,606'E	43°28,709'N	07°25,843'E
M731-GeoB07-307	0001570	0002379	05.08.2007	07:06.37	05.08.2007	08:00.48	43°29,324'N	07°26,164'E	43°30,856'N	07°21,704'E
M731-GeoB07-308	0002516	0002920	05.08.2007	08:10.00	05.08.2007	08:37.01	43°30,512'N	07°21,554'E	43°29,413'N	07°23,677'E
M731-GeoB07-309	0002921	0003085	05.08.2007	08:37.05	05.08.2007	08:48.01	43°29,409'N	07°23,682'E	43°28,910'N	07°24,654'E
M731-GeoB07-310	0003303	0003749	05.08.2007	09:02.33	05.08.2007	09:32.18	43°28,658'N	07°24,524'E	43°30,646'N	07°24,868'E
M731-GeoB07-311	0004096	0004672	05.08.2007	09:55.26	05.08.2007	10:33.51	43°29,935'N	07°23,415'E	43°28,833'N	07°26,689'E
M731-GeoB07-312	0004830	0005263	05.08.2007	10:44.23	05.08.2007	11:13.16	43°29,437'N	07°26,808'E	43°30,340'N	07°24,188'E
M731-GeoB07-313	0005355	0005835	05.08.2007	11:19.24	05.08.2007	11:51.24	43°30,461'N	07°24,372'E	43°31,489'N	07°26,919'E
M731-GeoB07-314	0005874	0006233	05.08.2007	11:54.00	05.08.2007	12:17.57	43°31,635'N	07°26,852'E	43°32,801'N	07°25,063'E
M731-GeoB07-315	0006270	0006567	05.08.2007	12:20.00	05.08.2007	12:40.00	43°32,760'N	07°24,810'E	43°32,060'N	07°23,020'E
M731-GeoB07-316	0000101	0001444	05.08.2007	20:16.18	05.08.2007	20:43.44	43°36,885'N	07°12,673'E	43°38,209'N	07°12,723'E
M731-GeoB07-317	0001449	0002142	05.08.2007	20:43.49	05.08.2007	20:55.23	43°38,214'N	07°12,723'E	43°38,699'N	07°12,720'E

M731-GeoB07-318	0002147	0002494	05.08.2007	20:55.28	05.08.2007	21:01.15	43°38,700'N	07°12,724'E	43°38,833'N	07°12,965'E
M731-GeoB07-319	0002498	0003105	05.08.2007	21:01.19	05.08.2007	21:11.27	43°38,833'N	07°12,968'E	43°38,652'N	07°13,385'E
M731-GeoB07-320	0003109	0004074	05.08.2007	21:11.31	05.08.2007	21:27.35	43°38,651'N	07°13,386'E	43°38,207'N	07°12,869'E
M731-GeoB07-321	0004079	0004581	05.08.2007	21:27.40	05.08.2007	21:36.04	43°38,206'N	07°12,865'E	43°38,438'N	07°12,603'E
M731-GeoB07-322	0004592	0005396	05.08.2007	21:36.15	05.08.2007	21:49.39	43°38,444'N	07°12,604'E	43°38,816'N	07°13,164'E
M731-GeoB07-323	0005408	0005716	05.08.2007	21:49.51	05.08.2007	21:55.00	43°38,816'N	07°13,172'E	43°38,691'N	07°13,326'E
M731-GeoB07-324	0005718	0006891	05.08.2007	21:55.02	05.08.2007	22:14.36	43°38,690'N	07°13,326'E	43°38,207'N	07°12,655'E
M731-GeoB07-325	0006894	0008058	05.08.2007	22:14.39	05.08.2007	22:34.04	43°38,208'N	07°12,654'E	43°38,658'N	07°13,323'E
M731-GeoB07-326	0008059	0009151	05.08.2007	22:35.00	05.08.2007	22:52.00	43°38,658'N	07°13,323'E	43°37,760'N	07°16,360'E

Appendix 9.3.: Lithologs and core photographs

The lithological sheets for each core are listed by study area, not chronologically! They appear in the following order:

- **Nice Airport slide (5)**
- **Shallow to Mid-slope area (9)**
- **Eastern Landslide Complex (12)**
- **Western Landslide Complex (5)**
- **Var Canyon turbiditic system (14)**

Nice Airport Slide

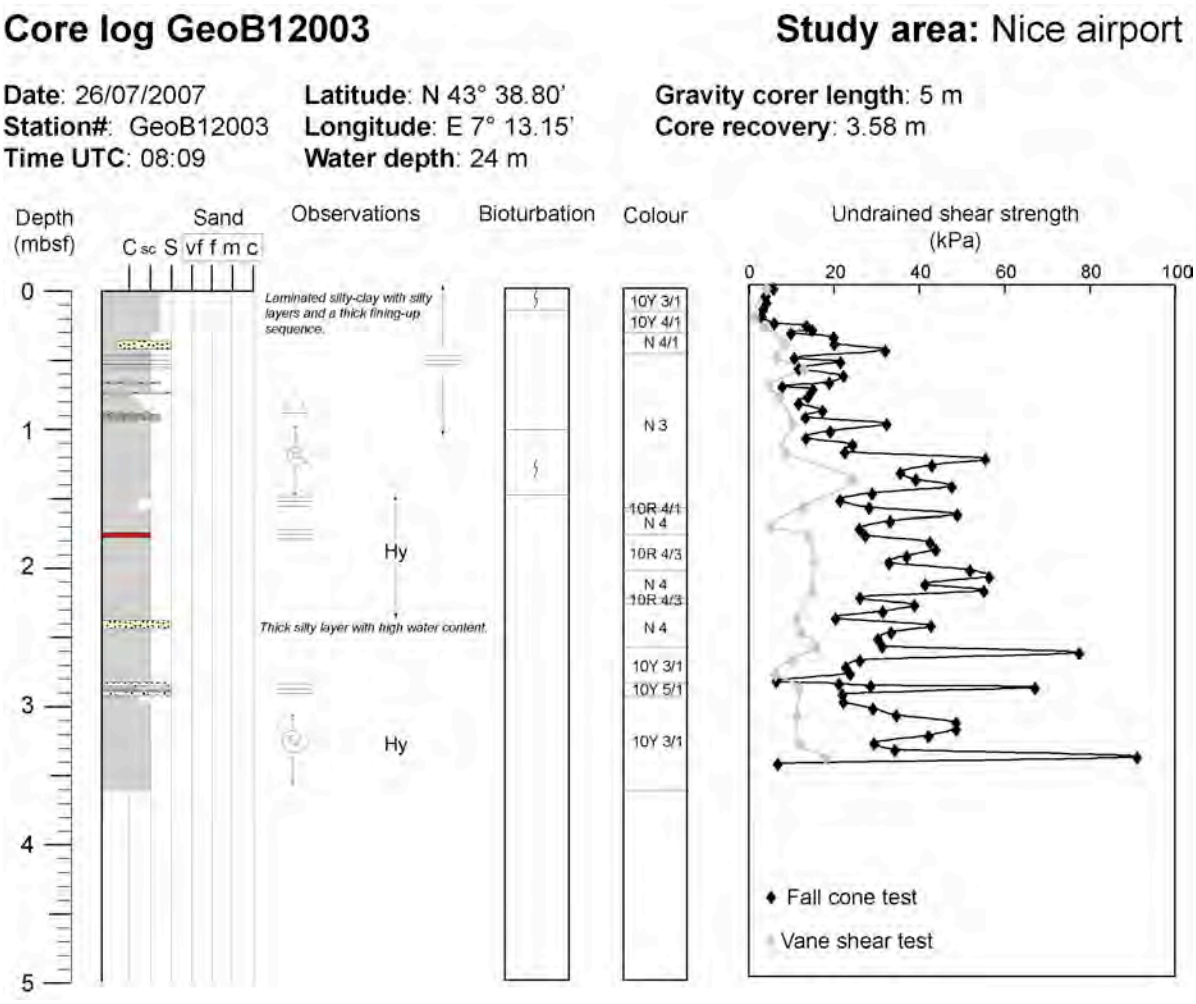

Nice Airport Slide

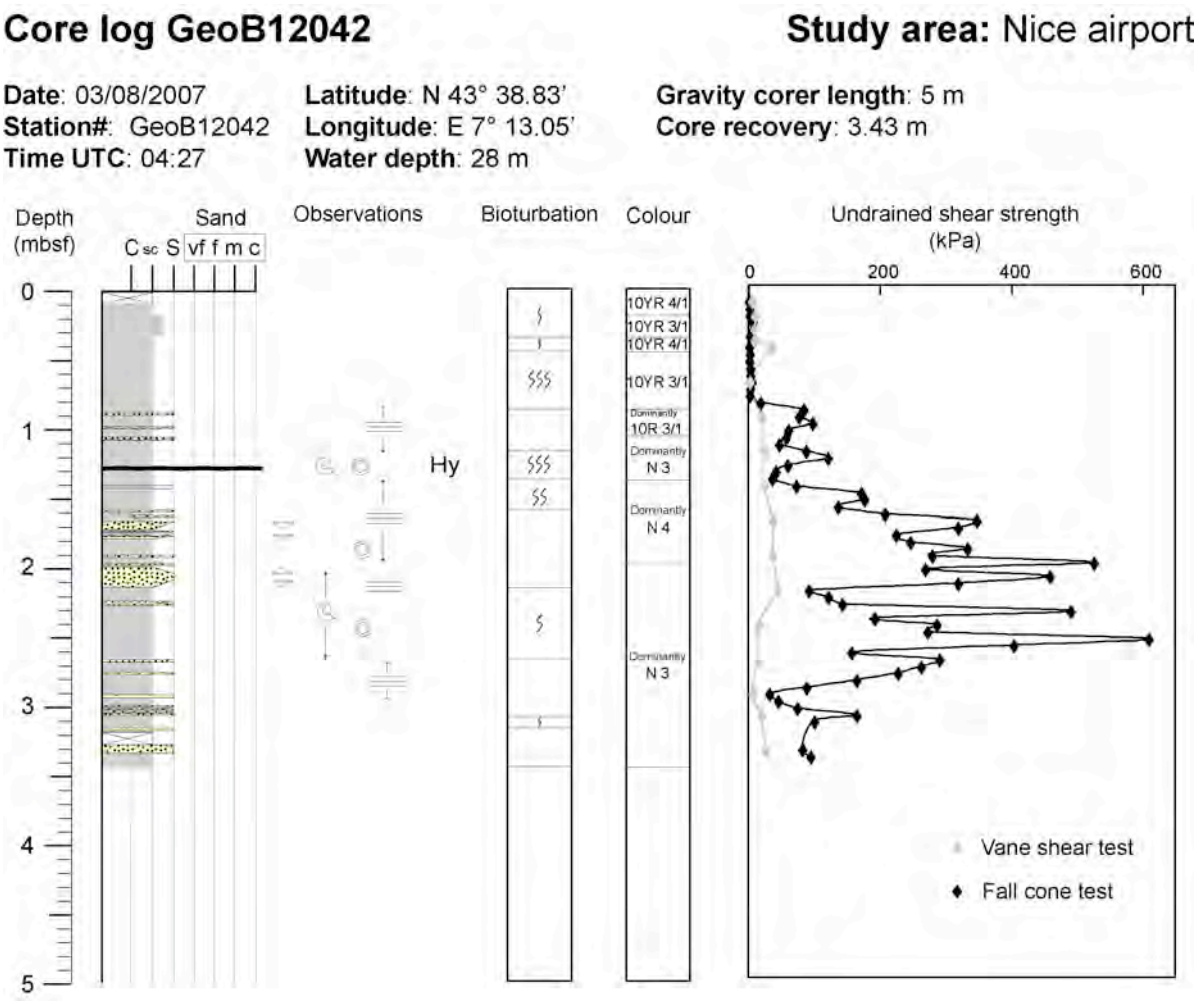

Nice Airport Slide

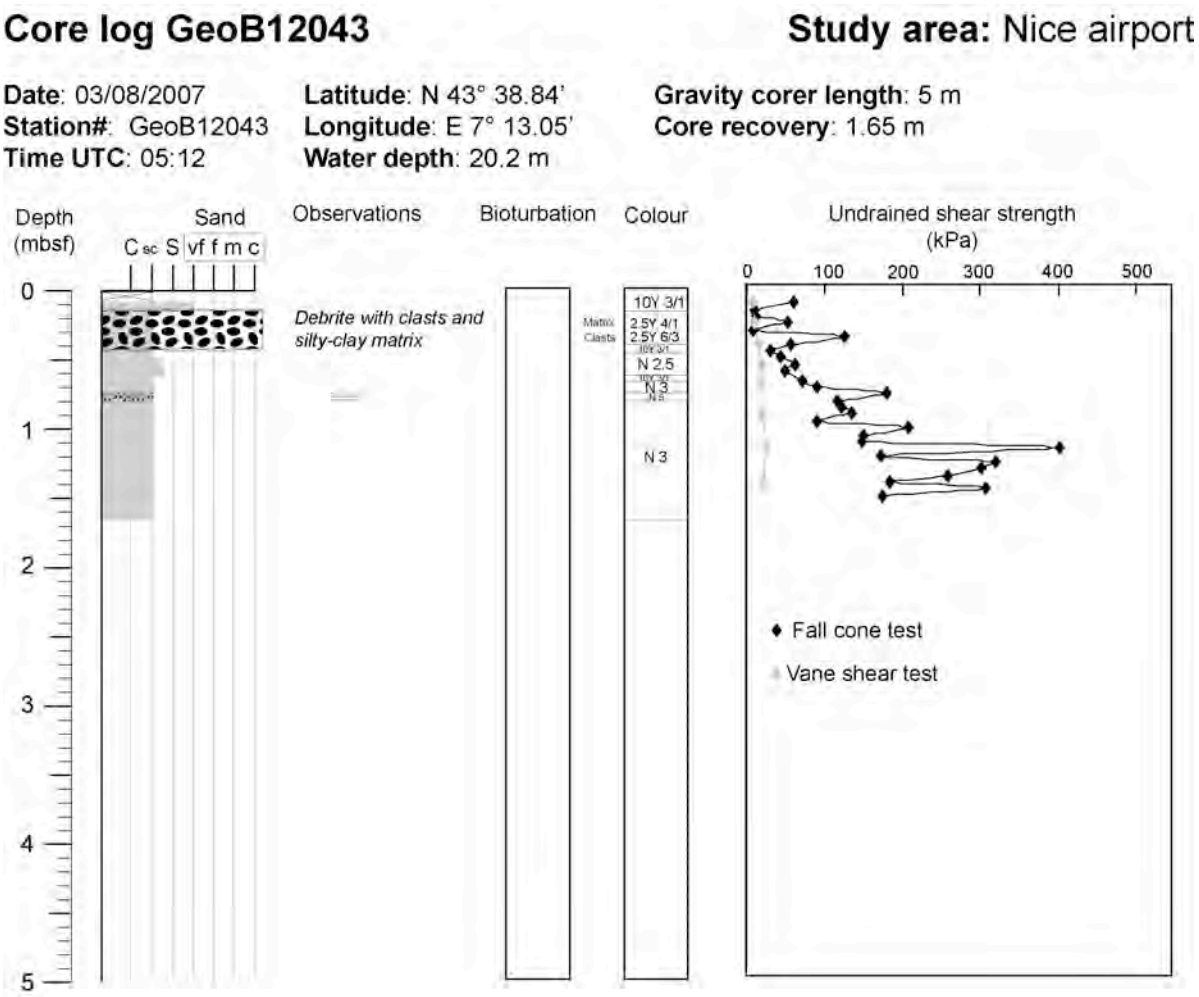

Nice Airport Slide

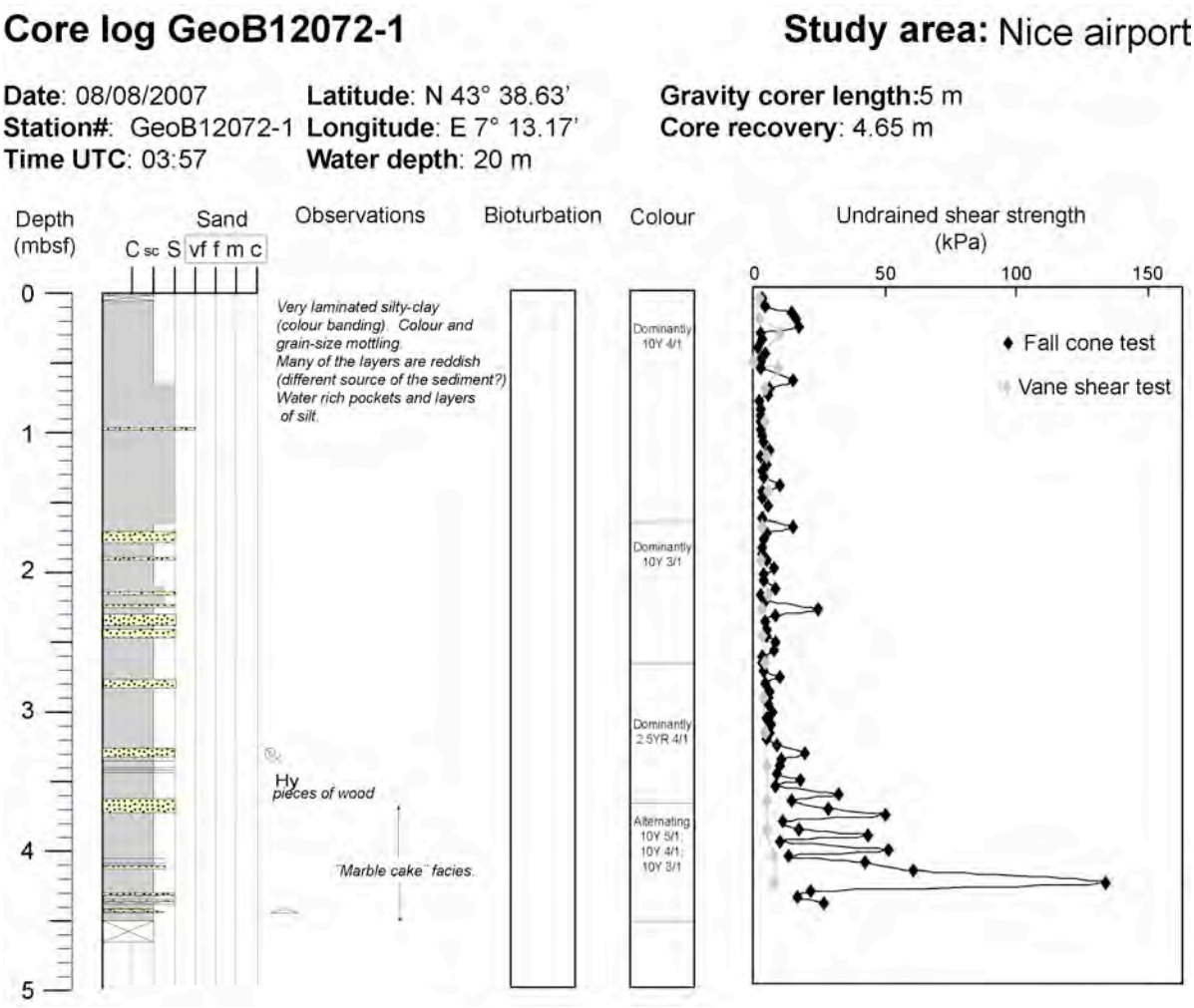

Nice Airport Slide

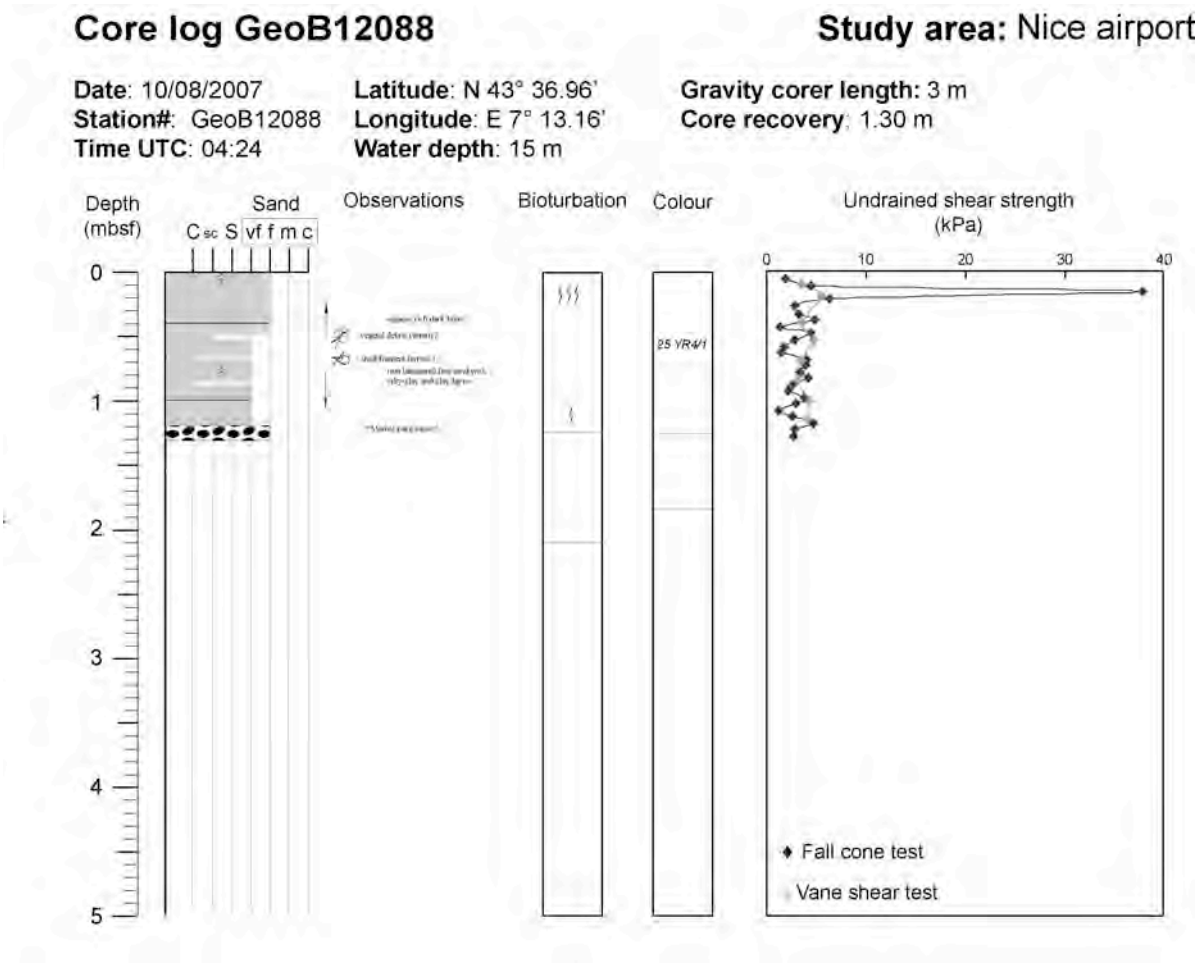

Shallow to Mid-slope area

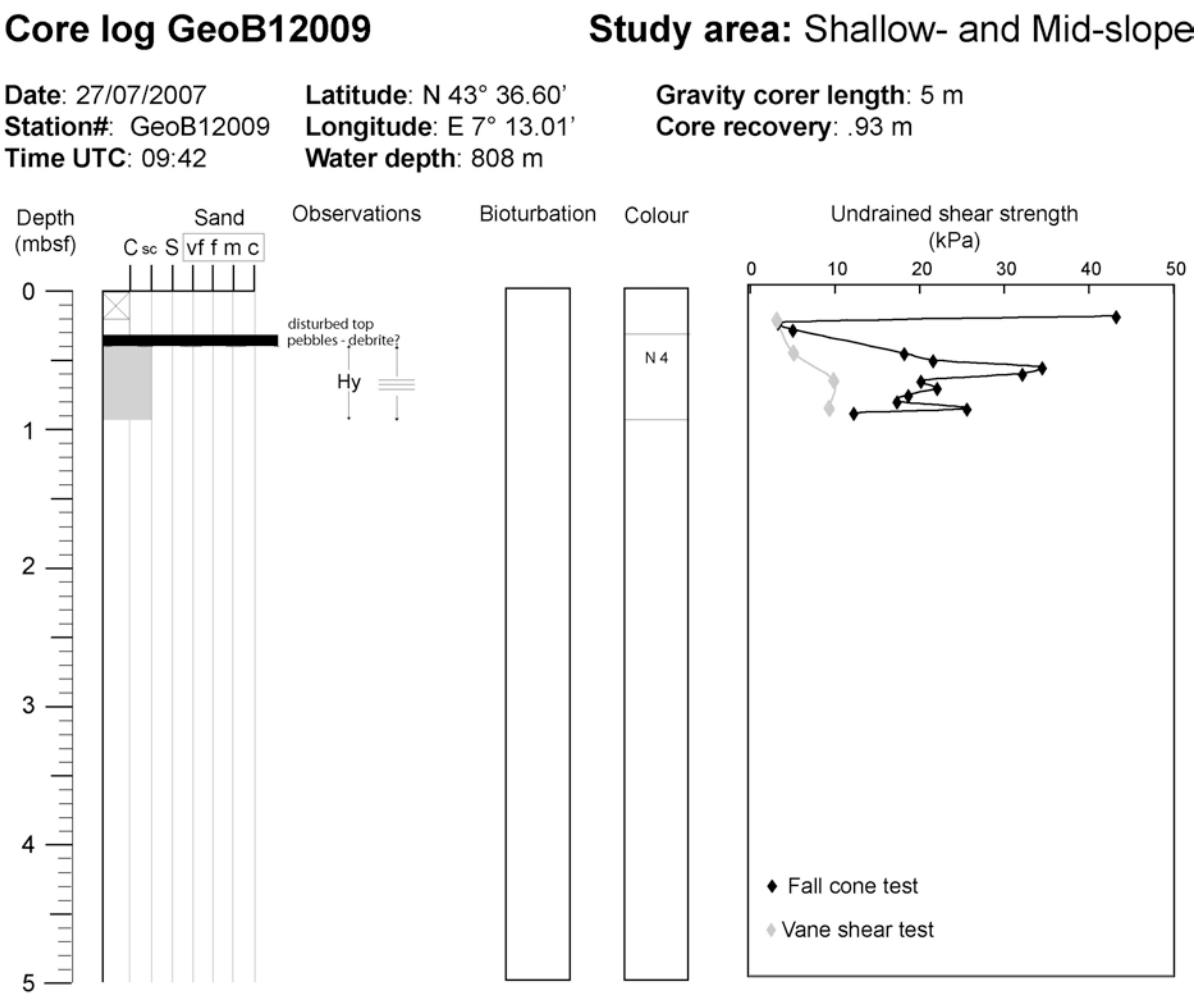

Shallow to Mid-slope area

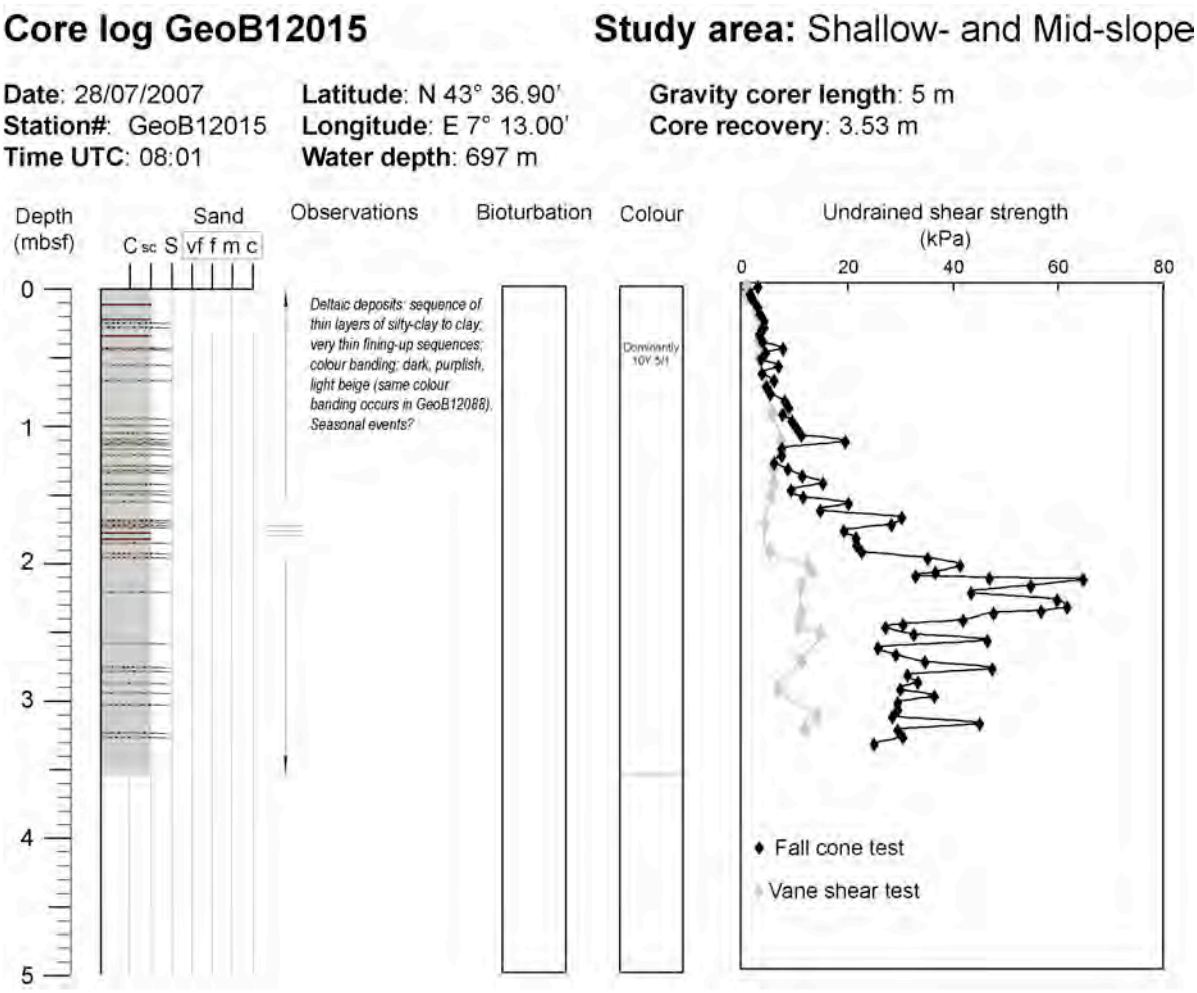

Shallow to Mid-slope area

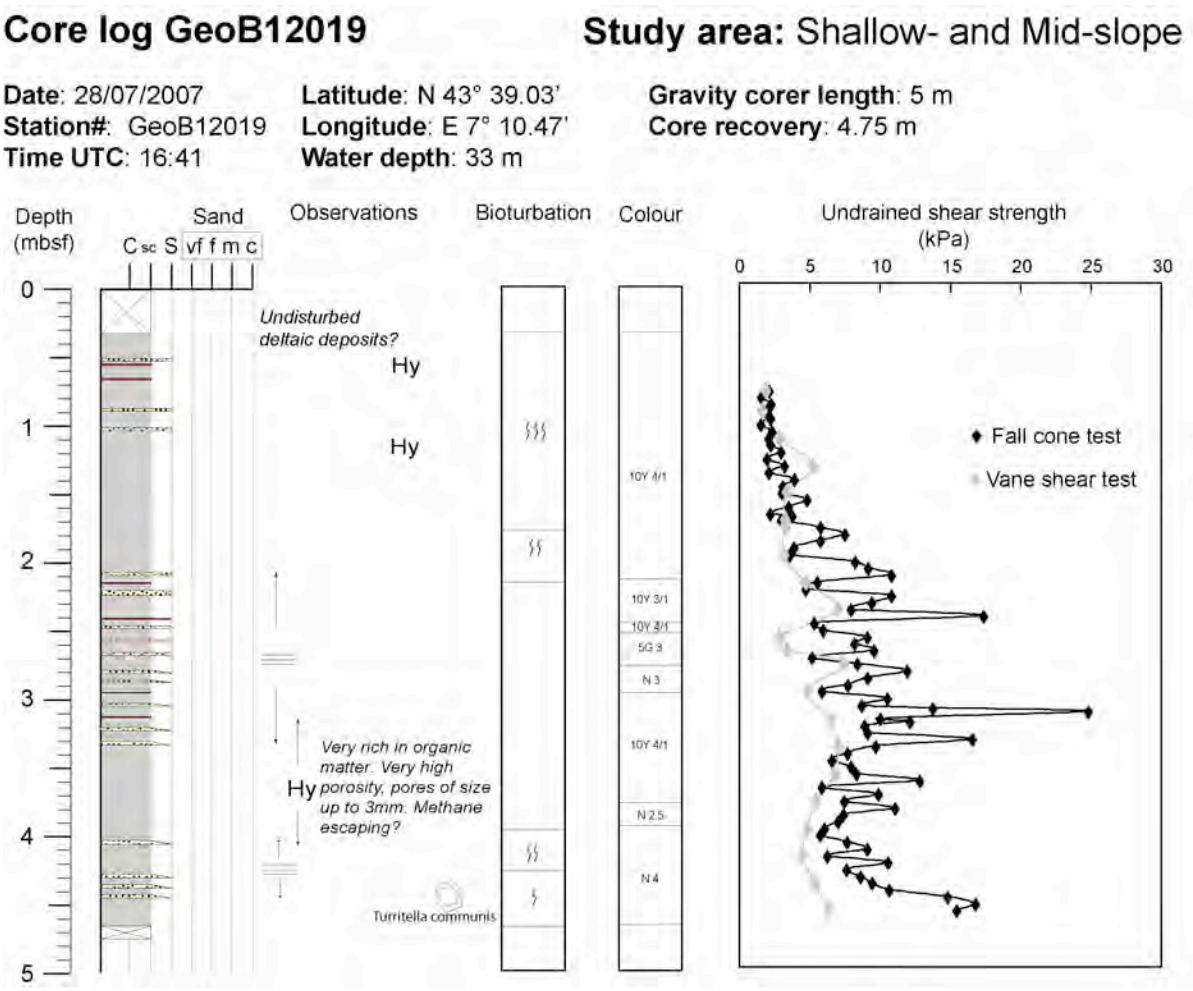

Shallow to Mid-slope area

Core log GeoB12032-1 **Study area:** Shallow- and Mid-slope

Date: 01/08/2007 **Latitude**: N 43° 37.20' **Push corer length**: 1 m
Station#: GeoB12023-2 **Longitude**: E 7° 12.82' **Core recovery**: 0.11 m
Time UTC: 12:47 **Water depth**: 644 m

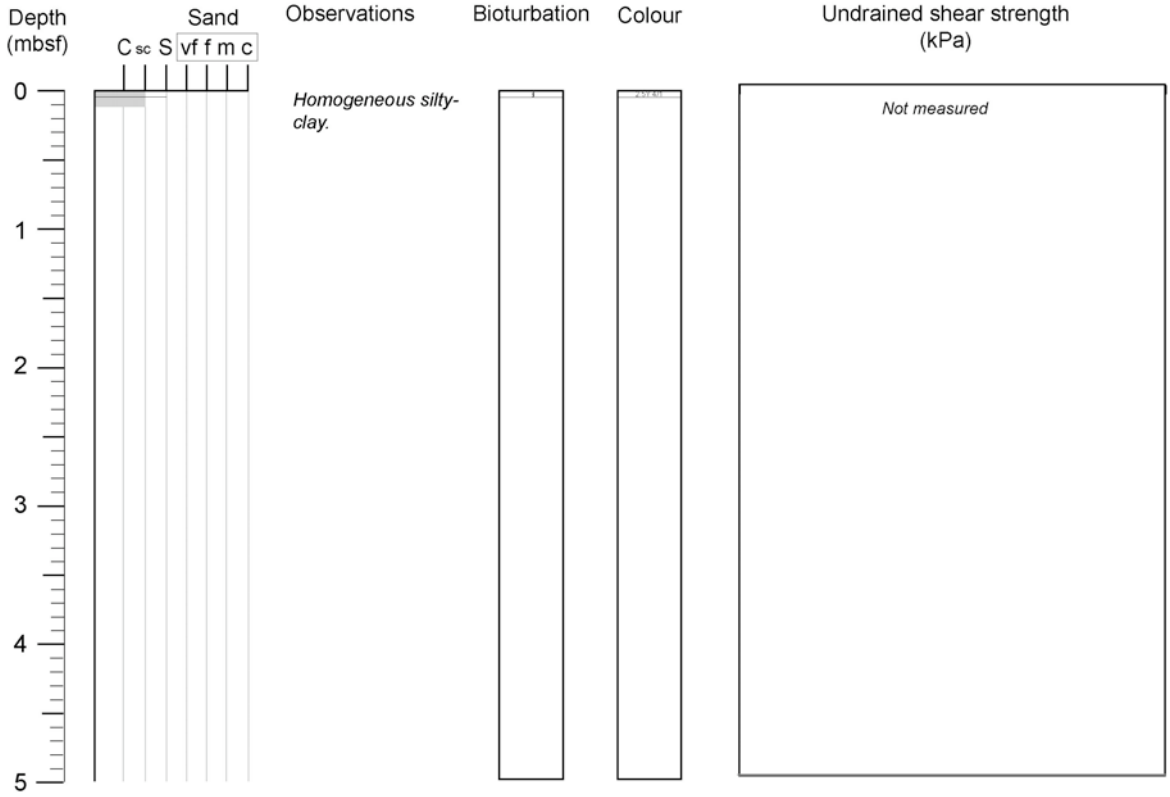

Shallow to Mid-slope area

Core log GeoB12032-3 **Study area:** Shallow- and Mid-slope

Date: 01/08/2007 **Latitude**: N 43° 37.20' **Gravity corer length**: 3 m
Station#: GeoB12032-3 **Longitude**: E 7° 12.82' **Core recovery**: 0.73 m
Time UTC: 14:06 **Water depth**: 643 m

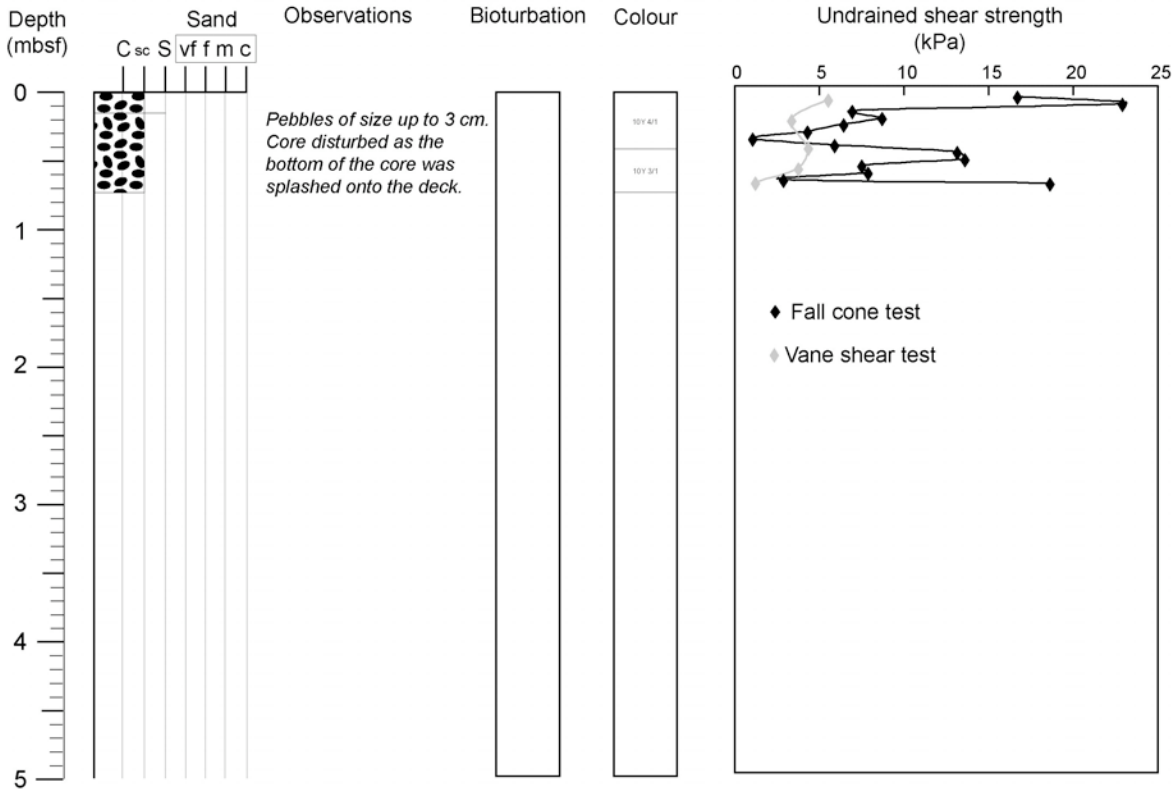

Shallow to Mid-slope area

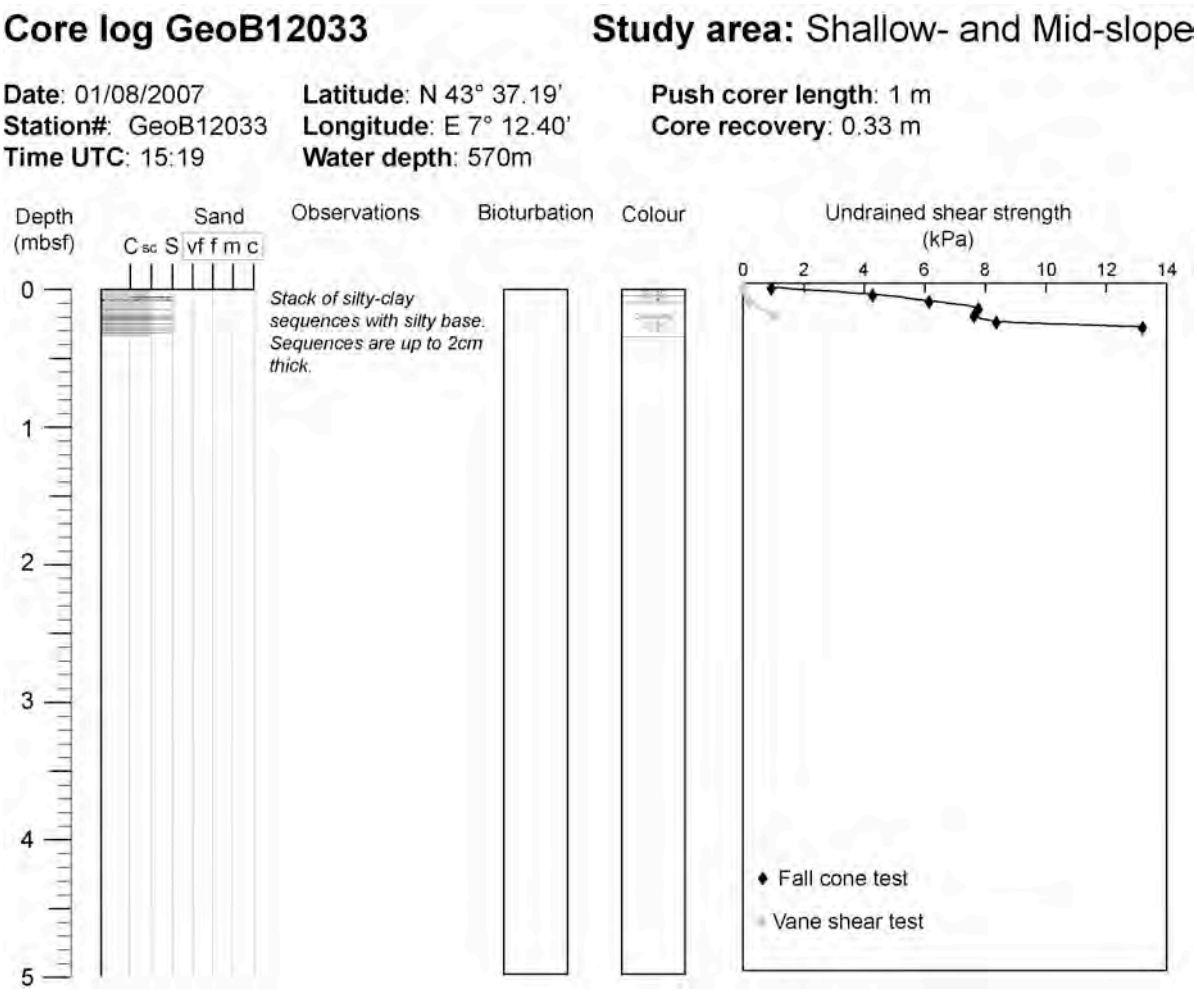

Shallow to Mid-slope area

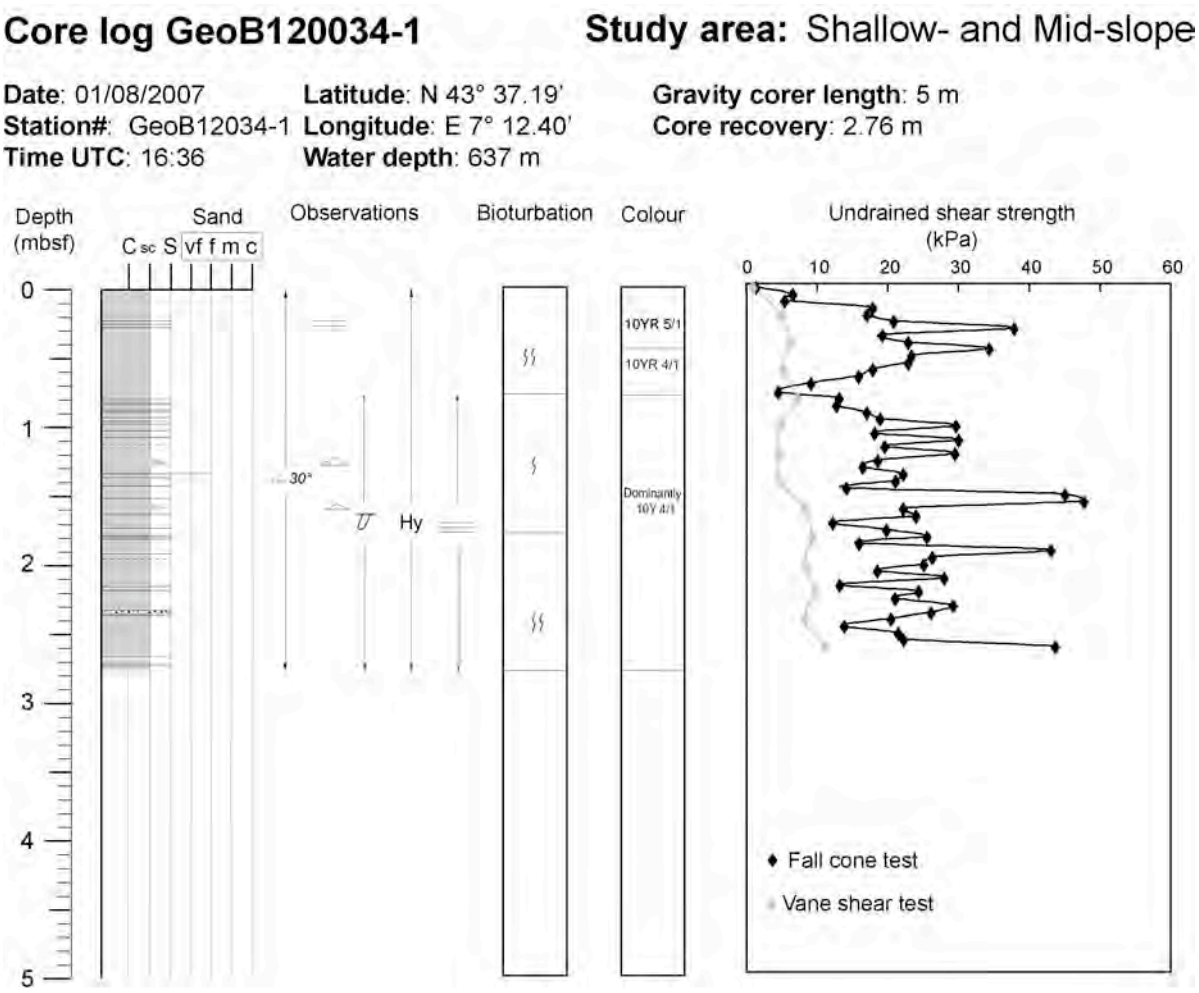

Shallow to Mid-slope area

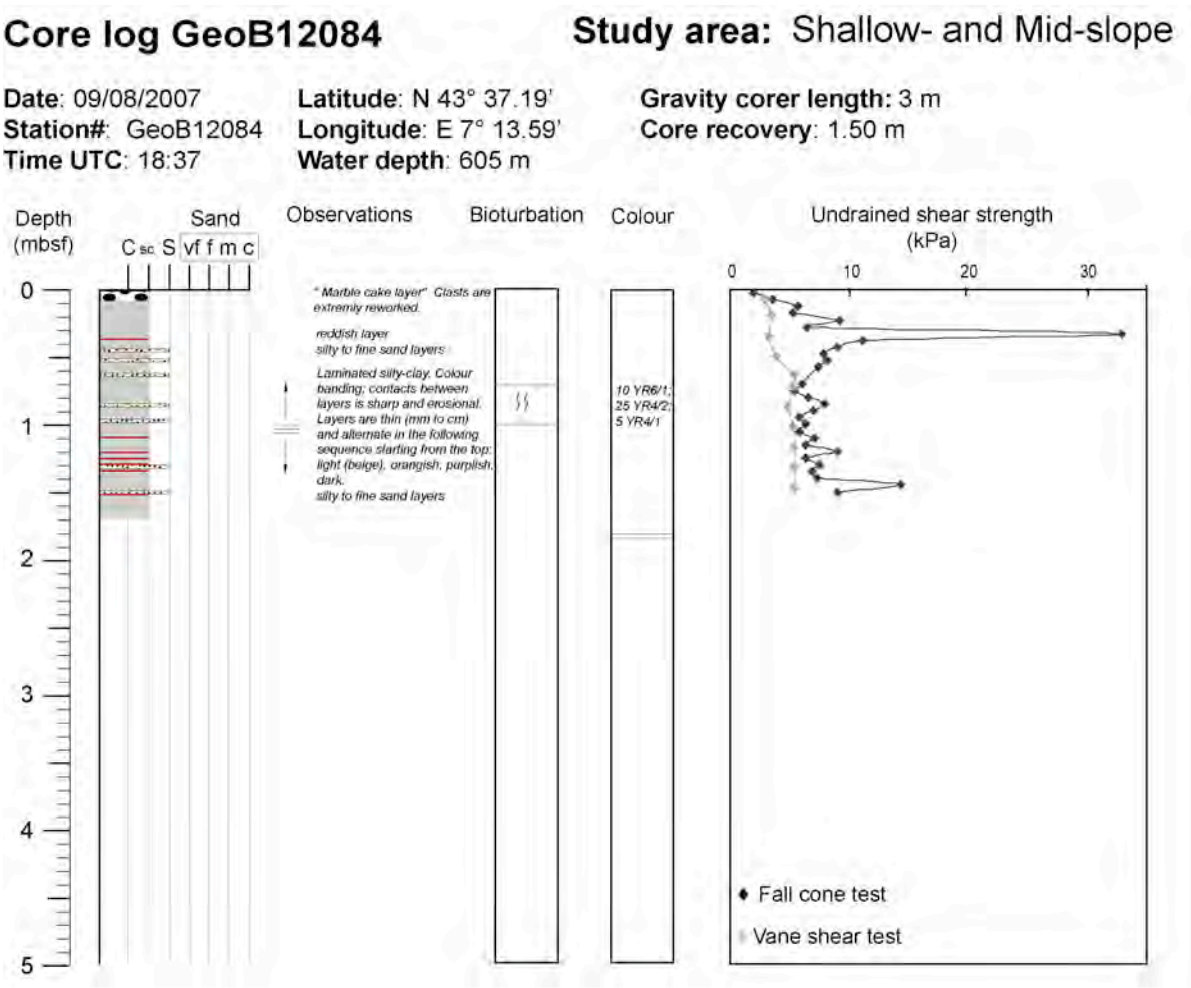

Shallow to Mid-slope area

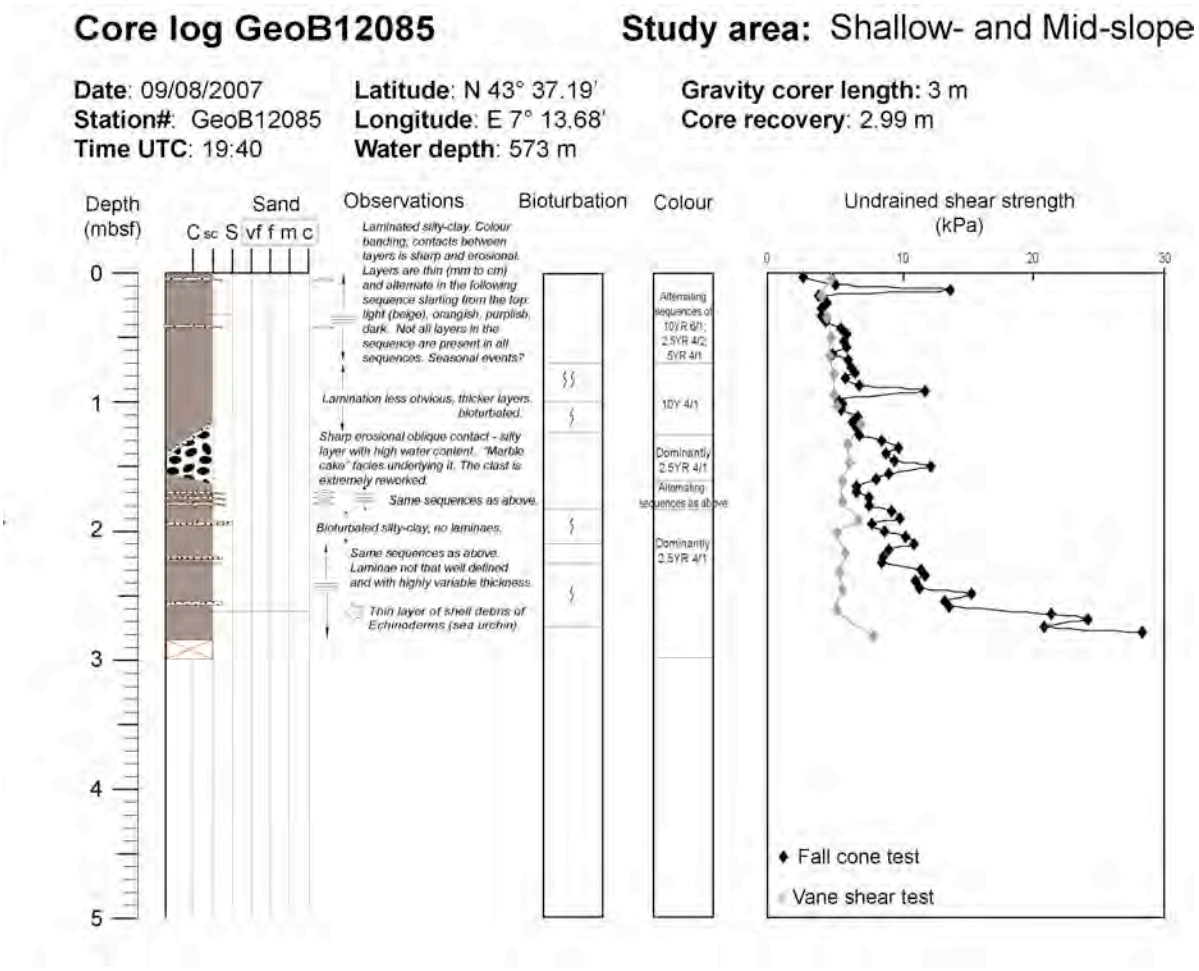

Eastern Landslide Complex

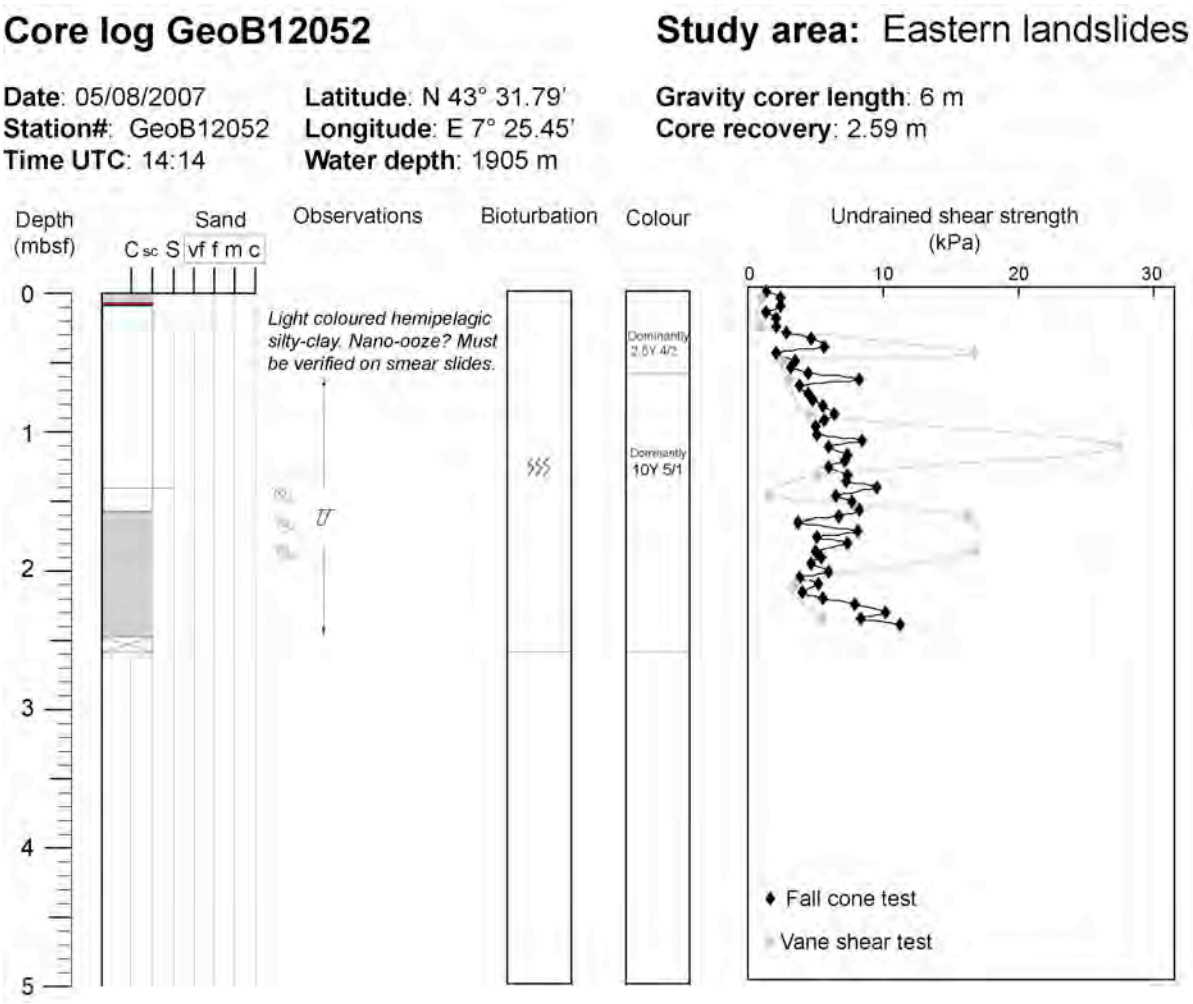

Eastern Landslide Complex

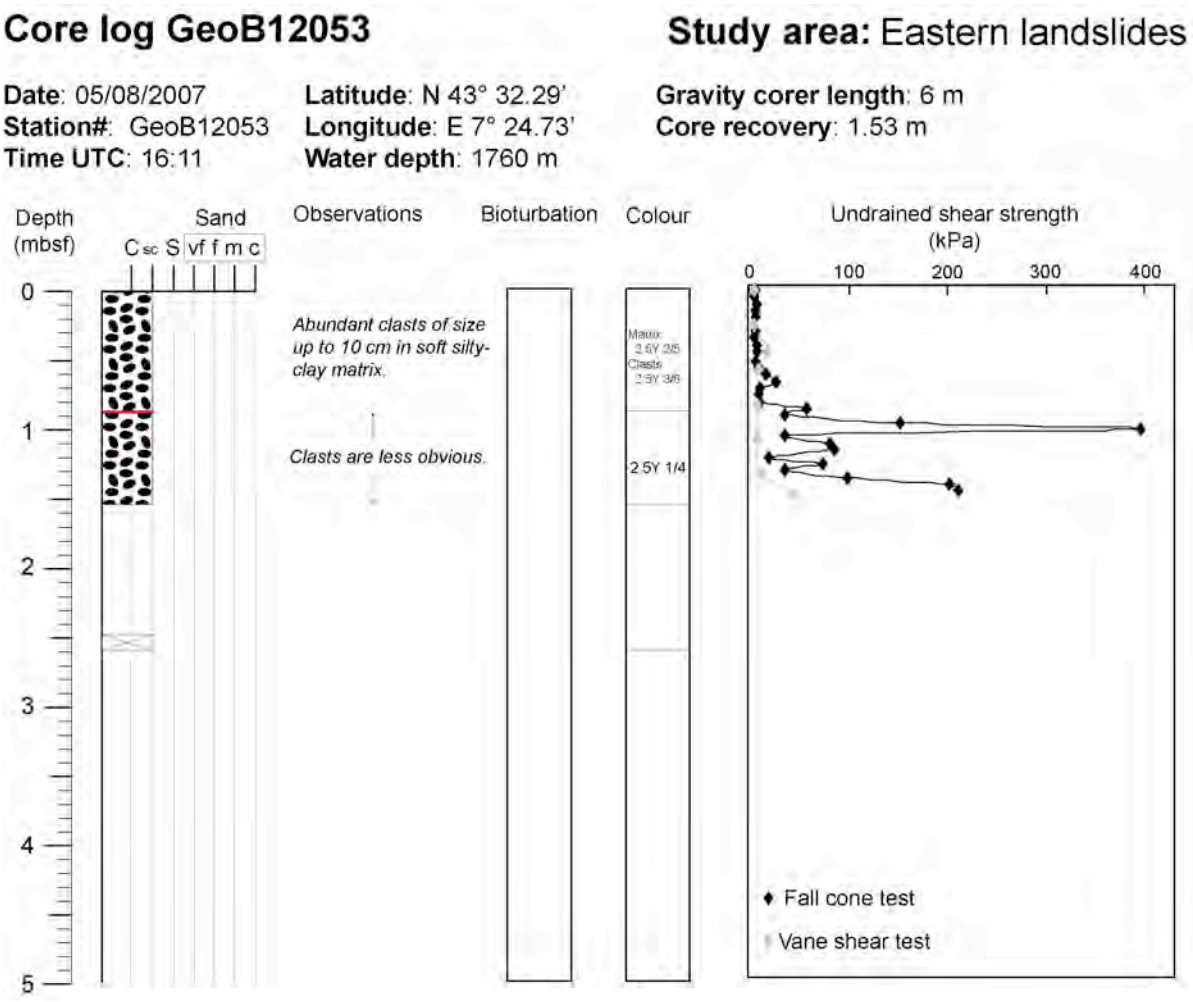

Eastern Landslide Complex

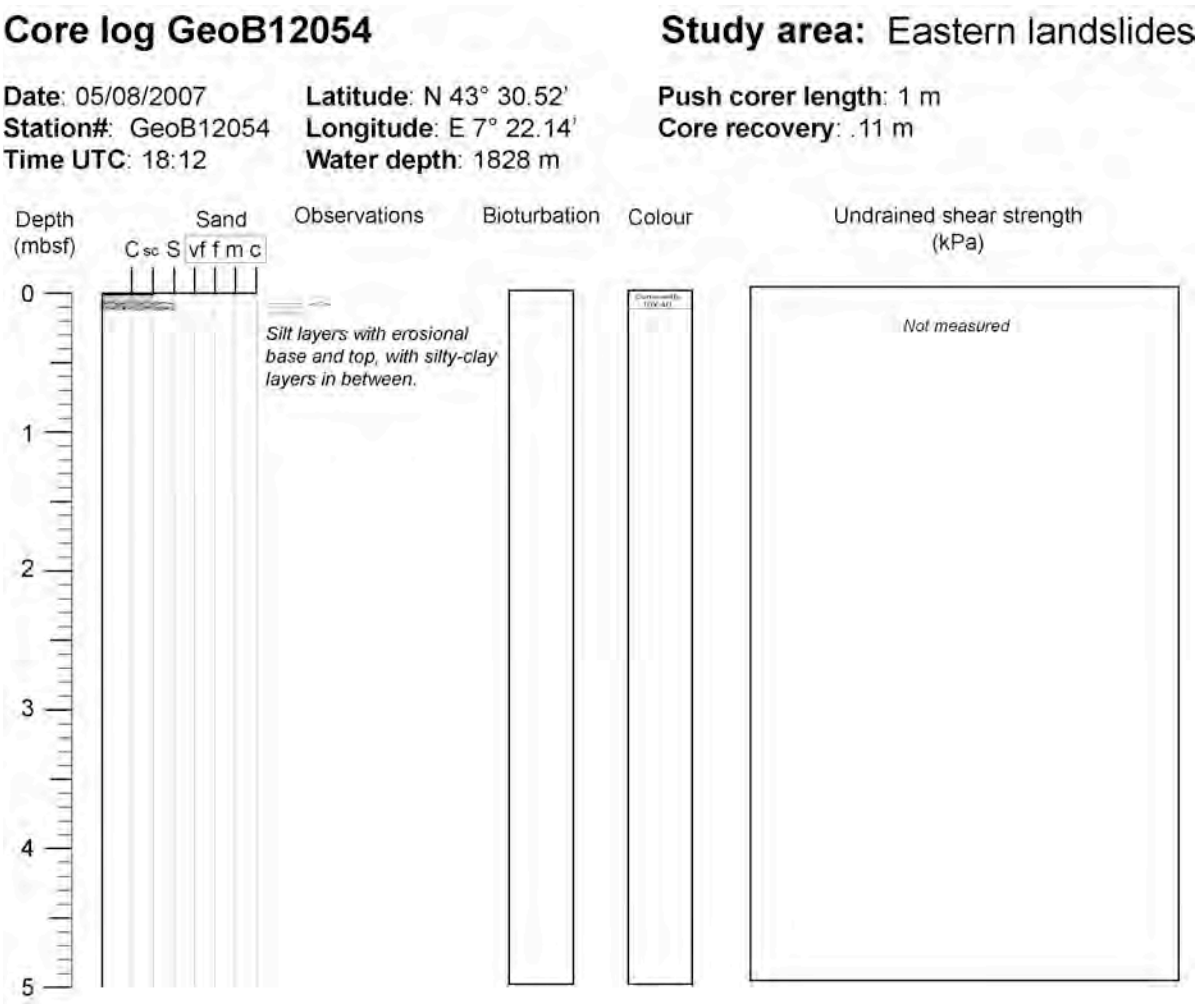

Eastern Landslide Complex

Core log GeoB12060 **Study area:** Eastern landslides

Date: 06/08/2007
Station#: GeoB12060
Time UTC: 11:31

Latitude: N 43° 32.50'
Longitude: E 7° 24.51'
Water depth: 1575 m

Gravity corer length: 5 m
Core recovery: 4.76 m

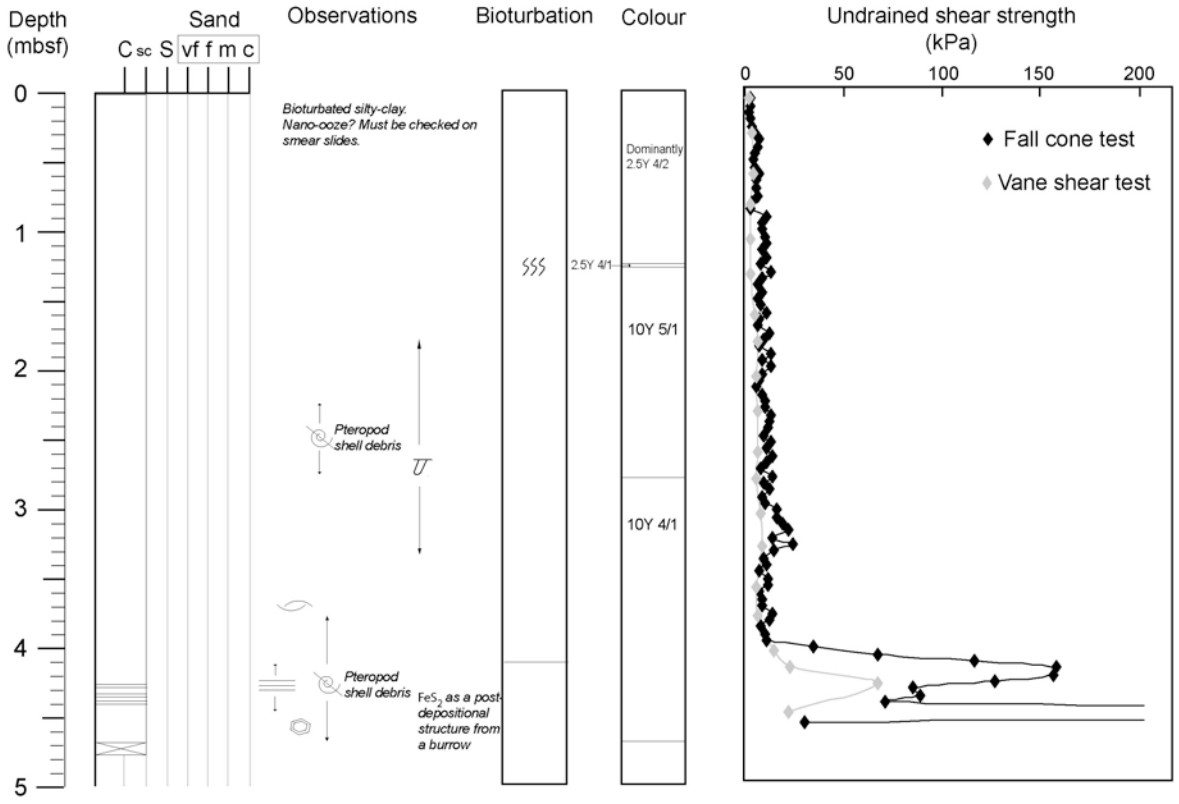

Eastern Landslide Complex

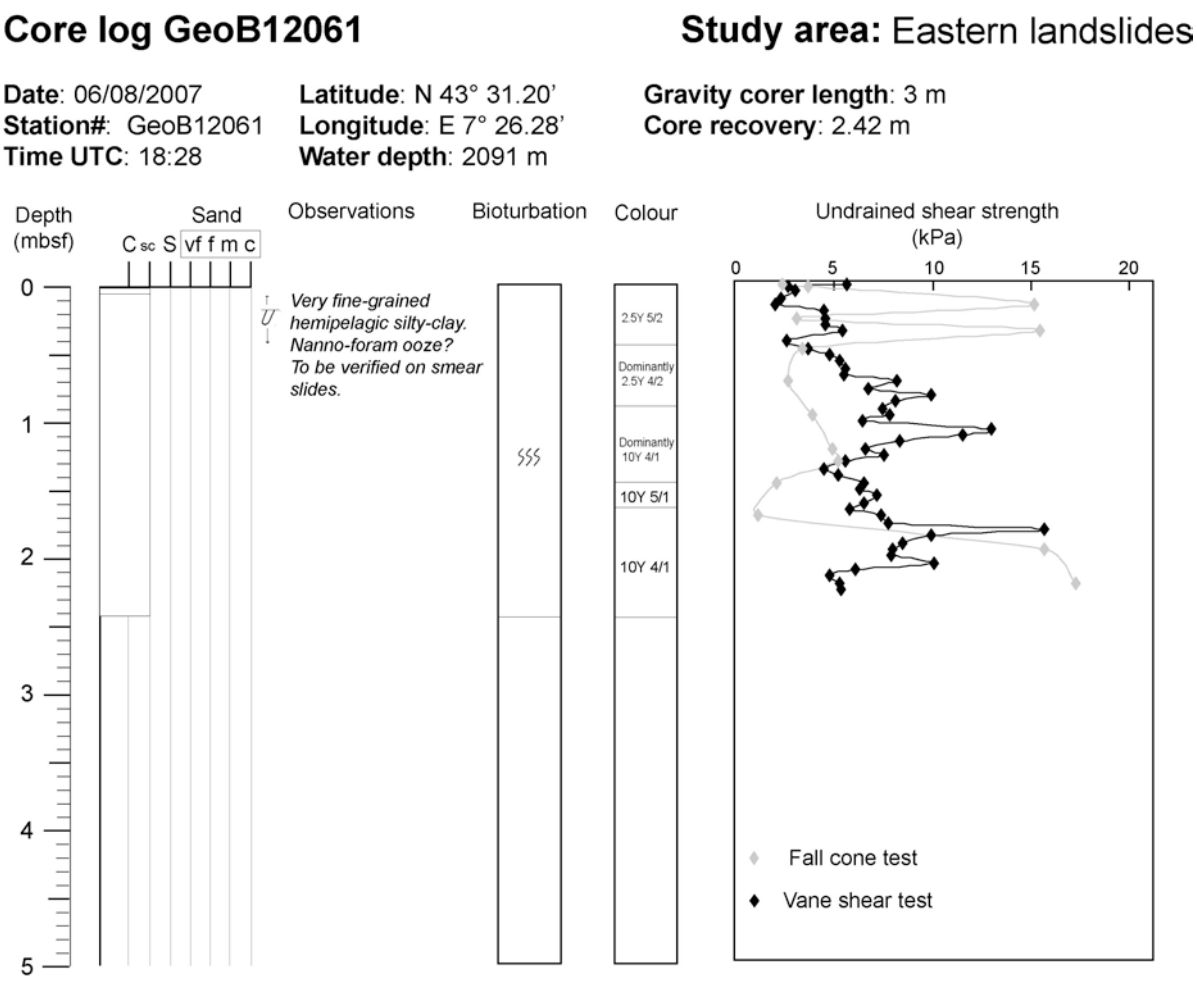

Eastern Landslide Complex

Core log GeoB12064 **Study area:** Eastern landslides

Date: 07/08/2007 **Latitude**: N 43° 31.13' **Gravity corer length**: 3 m
Station#: GeoB12064 **Longitude**: E 7° 26.21' **Core recovery**: 3 m
Time UTC: 08:32 **Water depth**: 2100 m

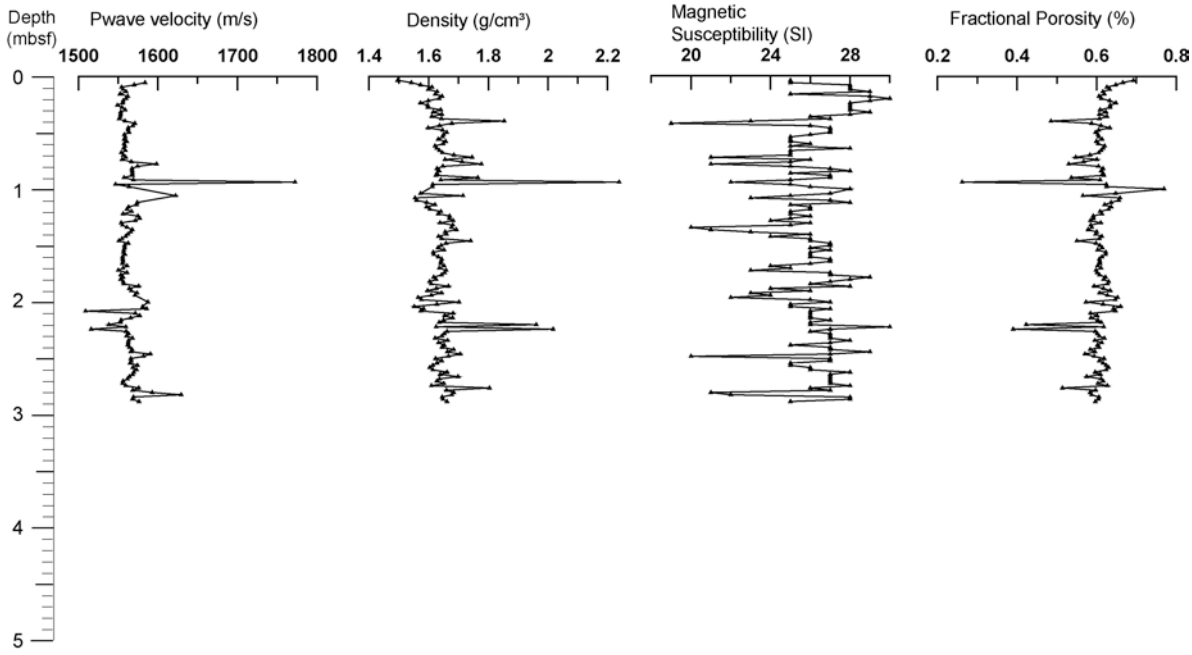

Eastern Landslide Complex

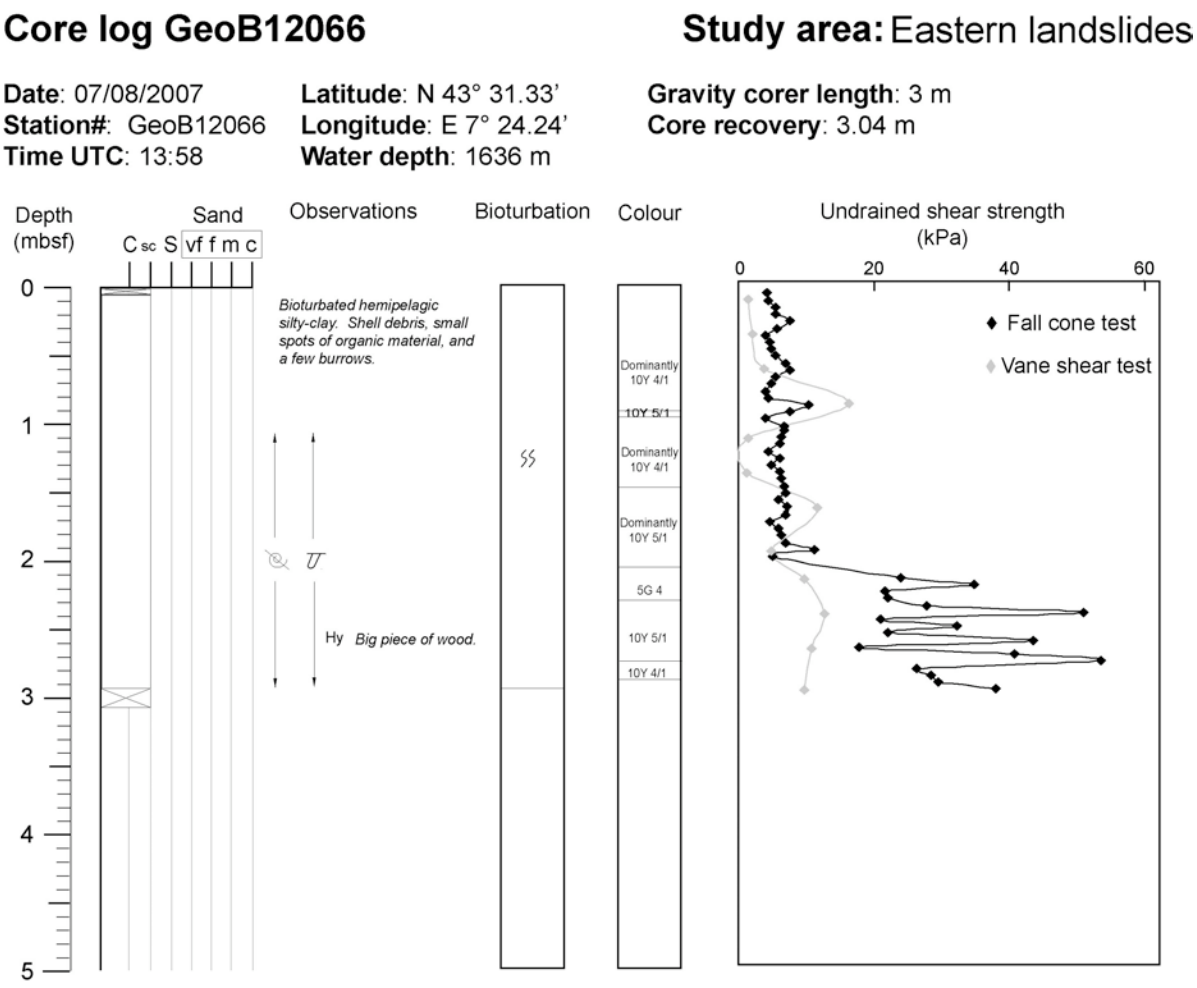

Eastern Landslide Complex

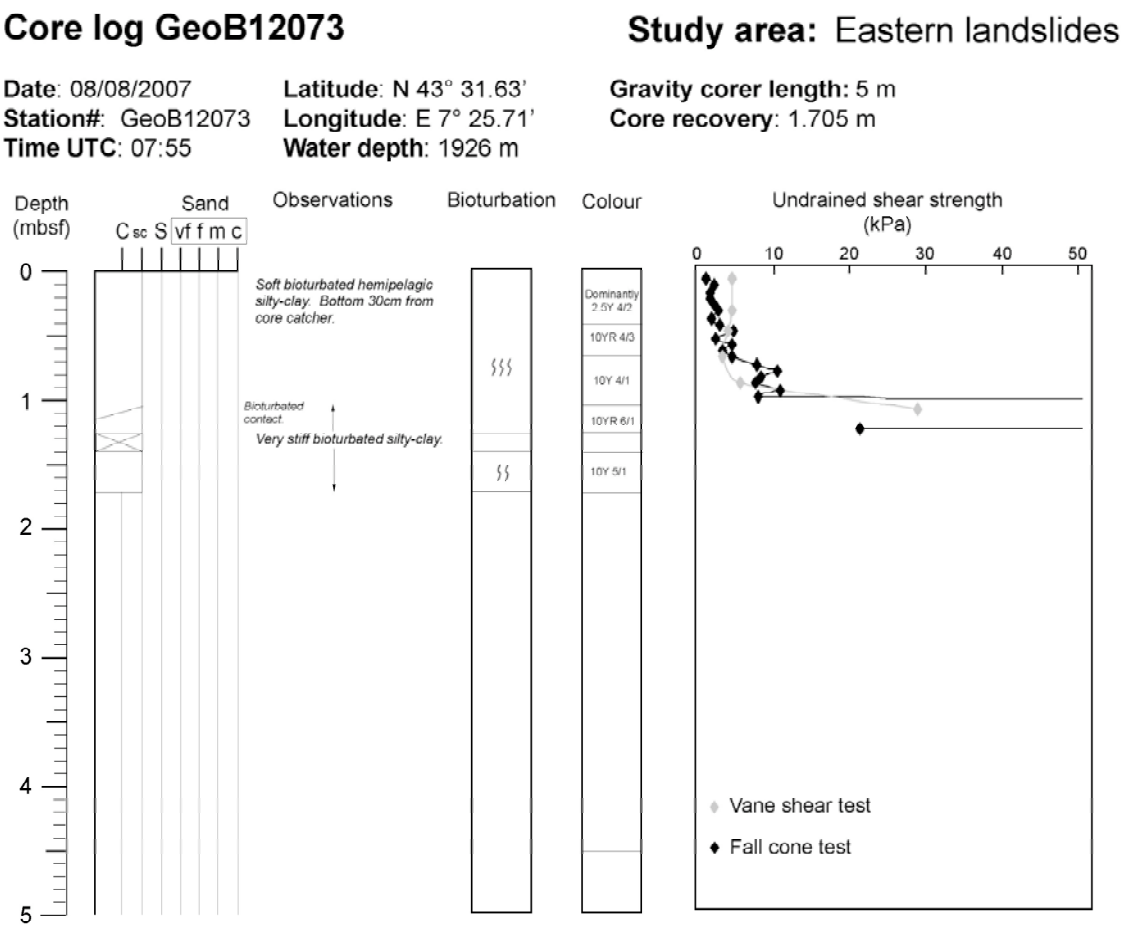

Eastern Landslide Complex

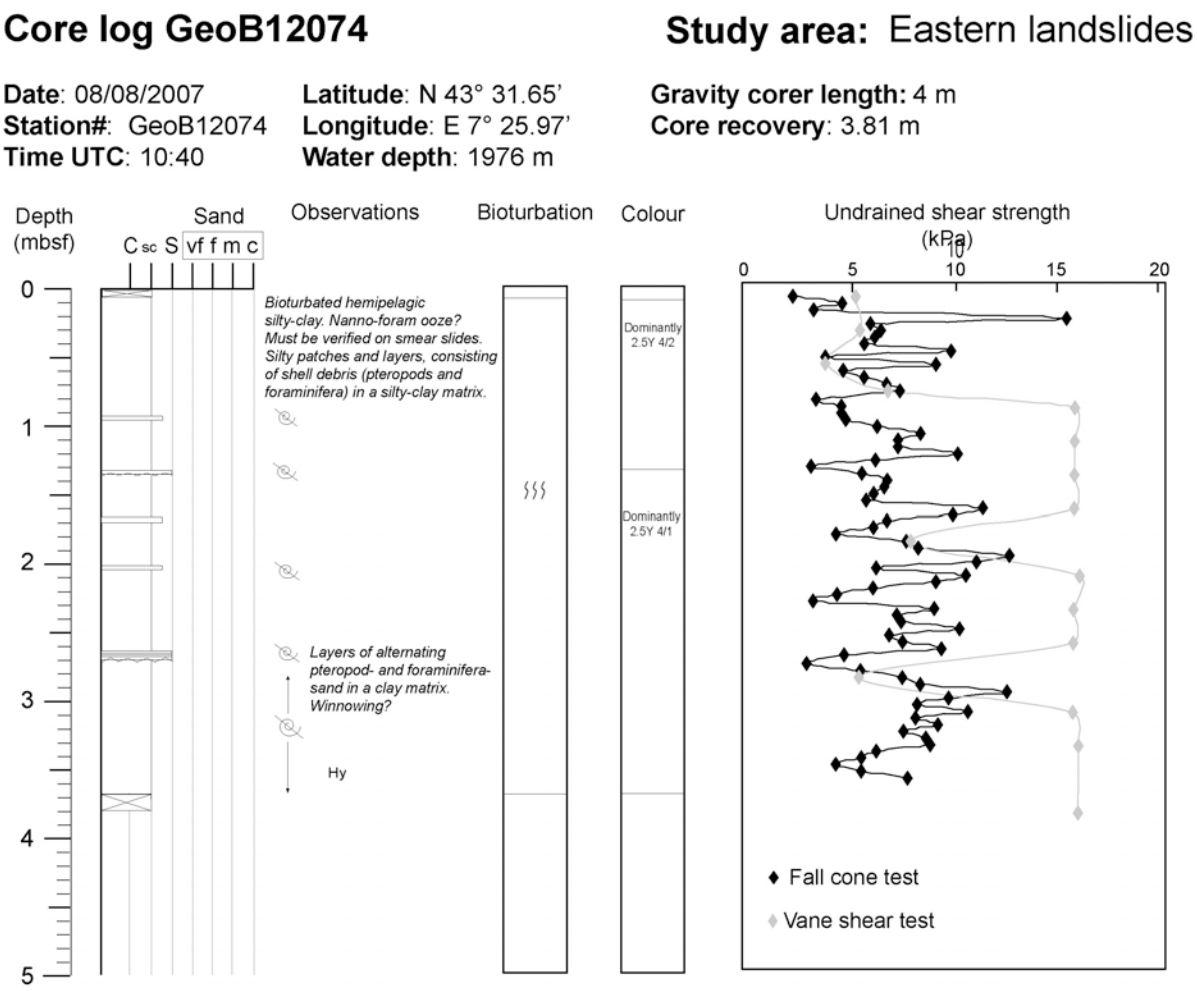

Eastern Landslide Complex

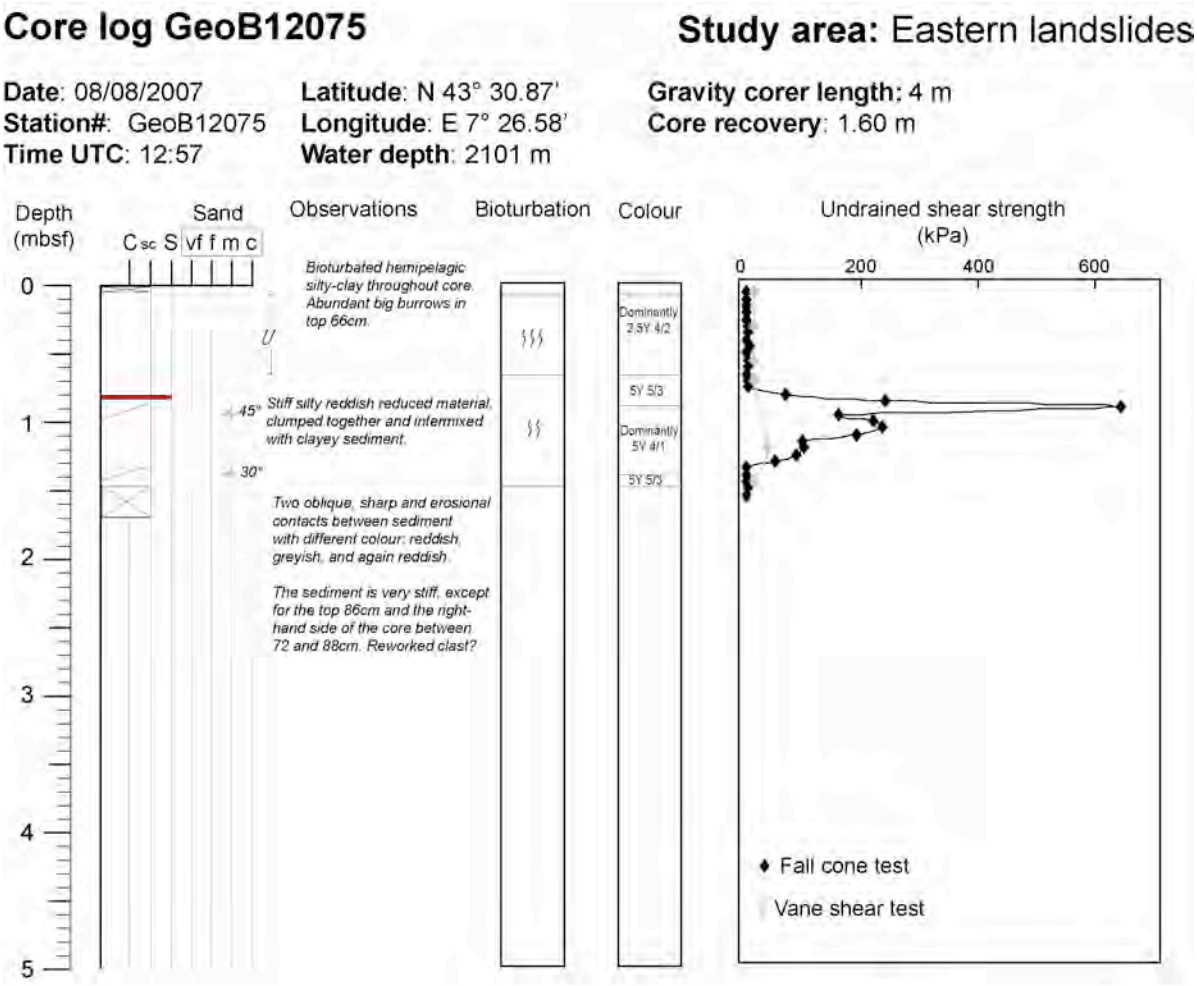

Eastern Landslide Complex

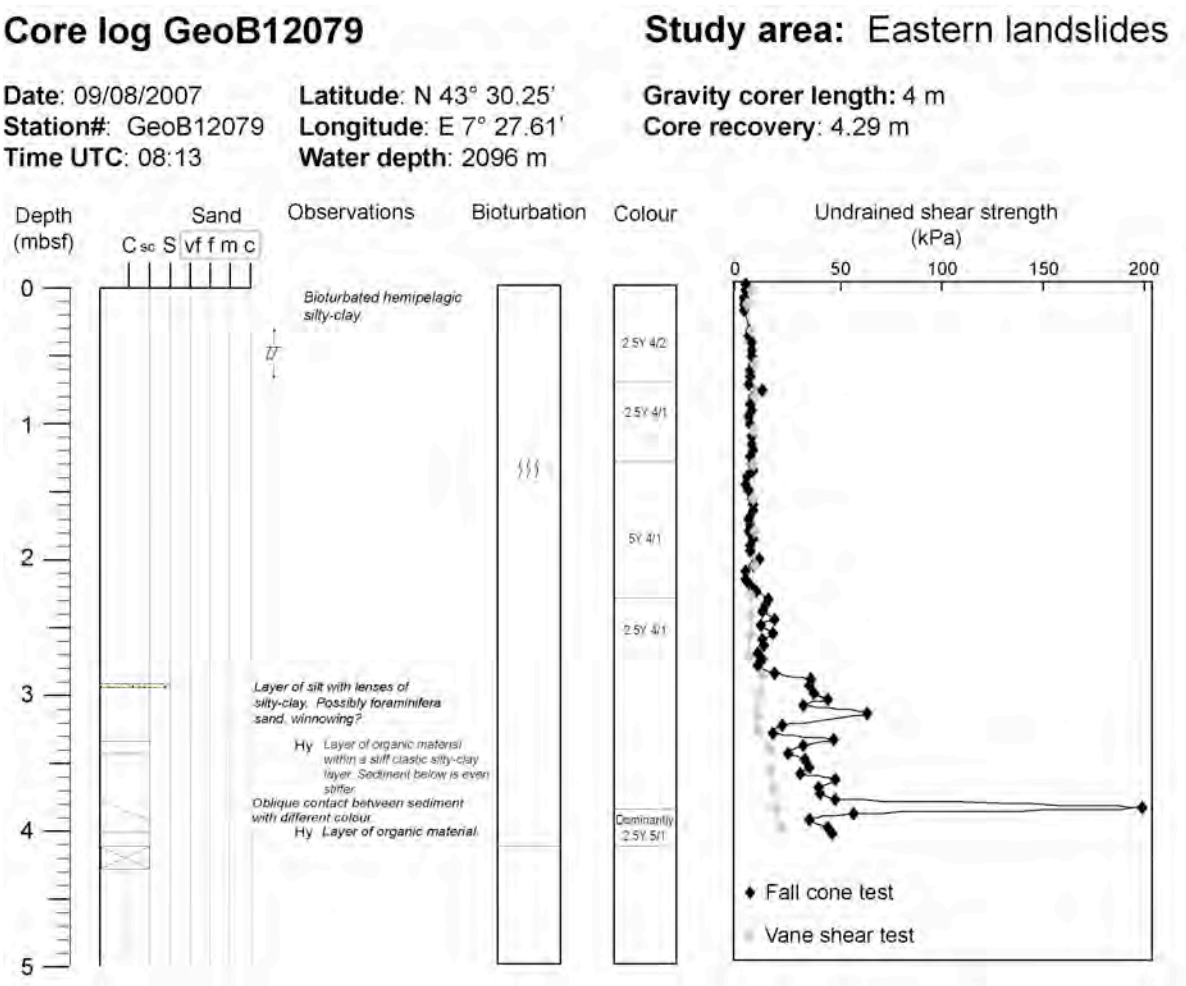

Eastern Landslide Complex

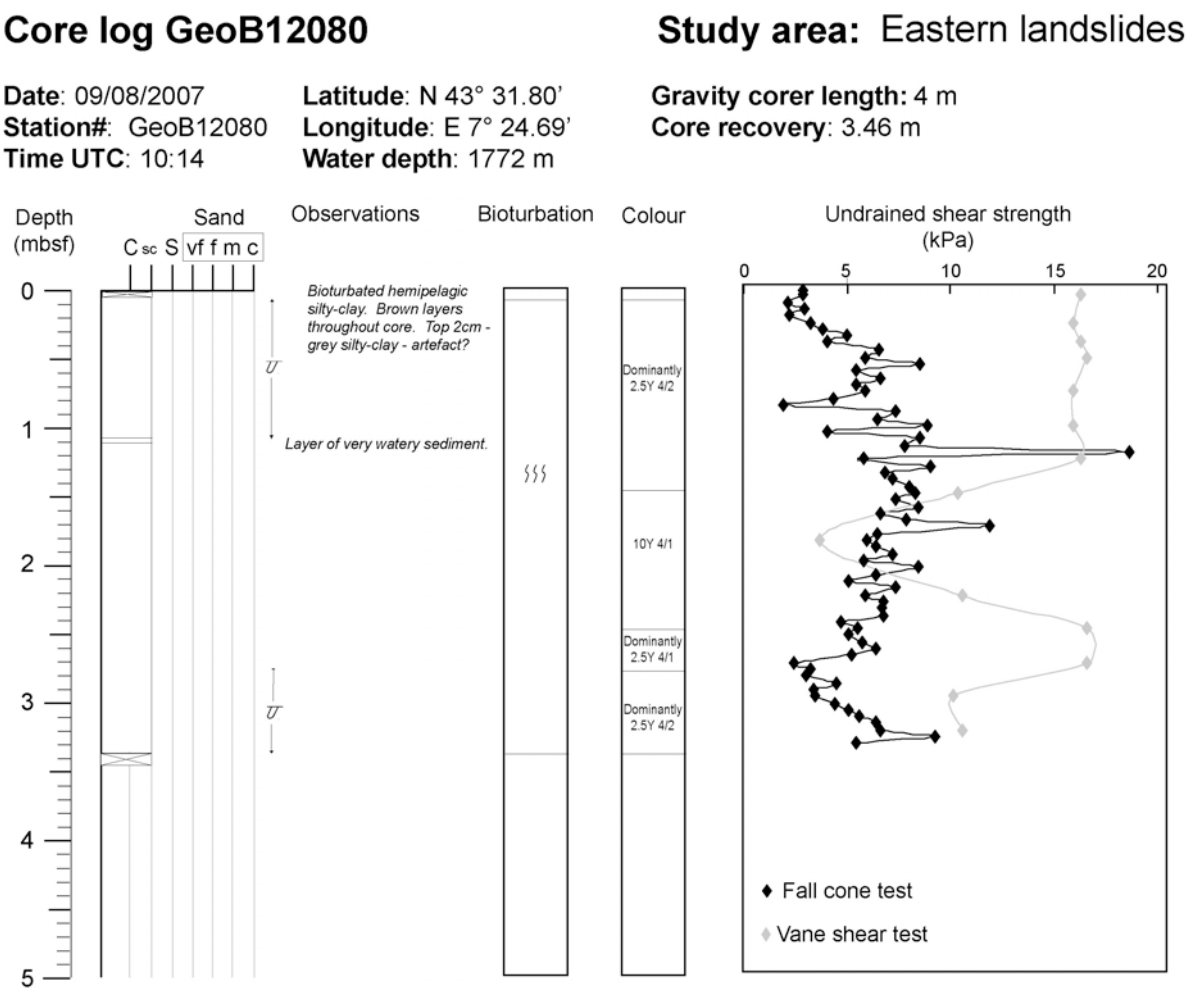

Western Landslide Complex

Core log GeoB12044-2

Study area: Western landslides

Date: 03/08/2007 **Latitude**: N 43° 32.07'
Station#: GeoB12044-2 **Longitude**: E 7° 21.11'
Time UTC: 08:35 **Water depth**: 1529 m

Gravity corer length: 5 m
Core recovery: 4.77 m

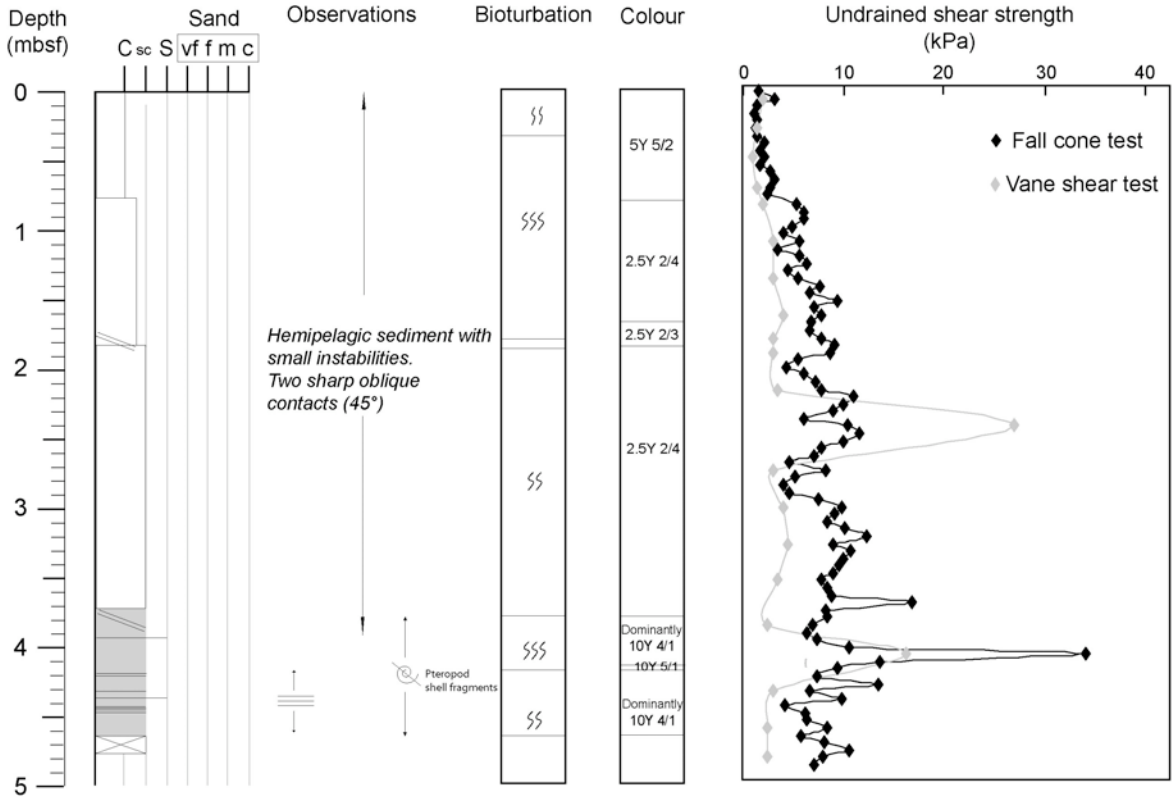

Western Landslide Complex

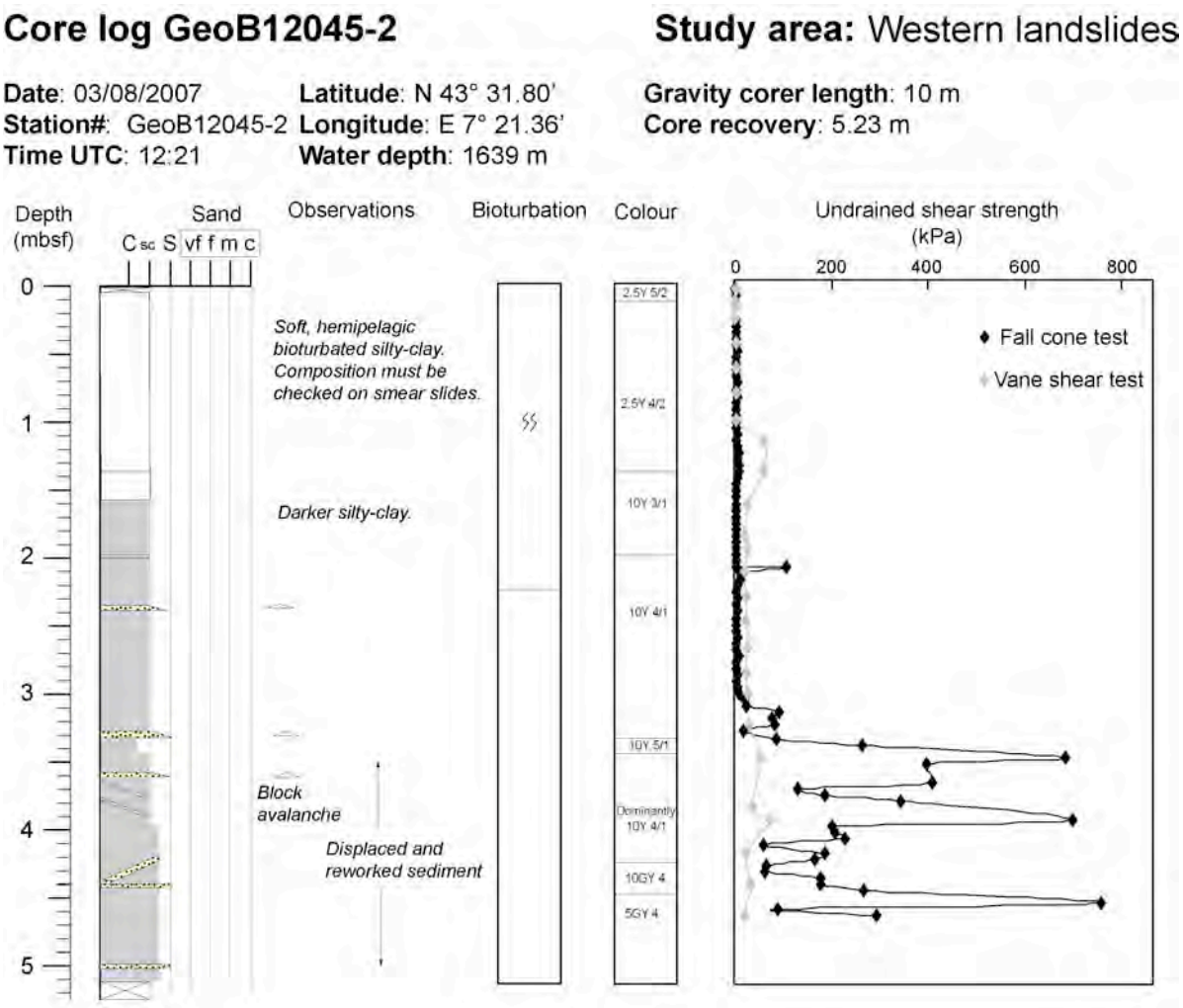

Western Landslide Complex

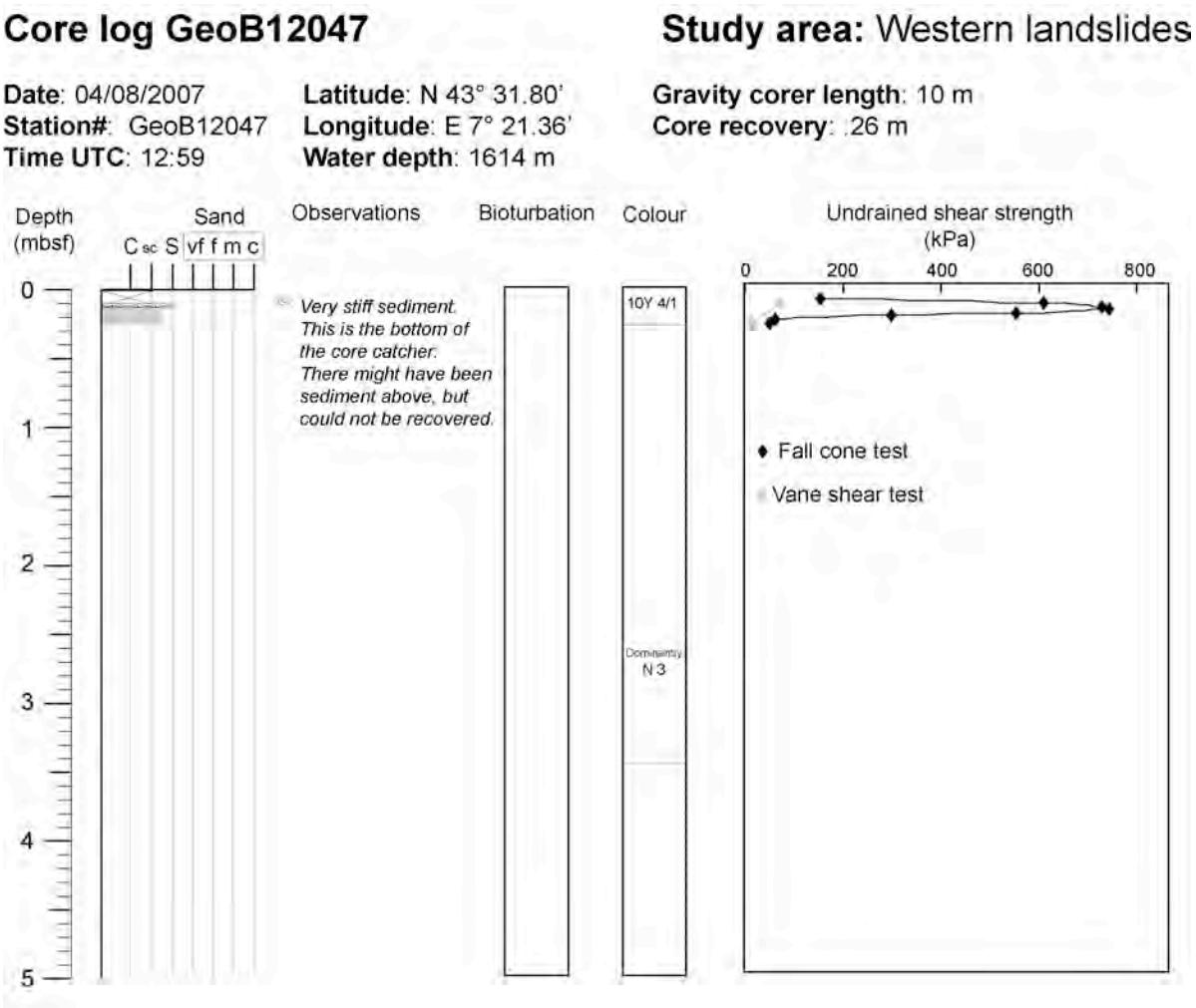

Western Landslide Complex

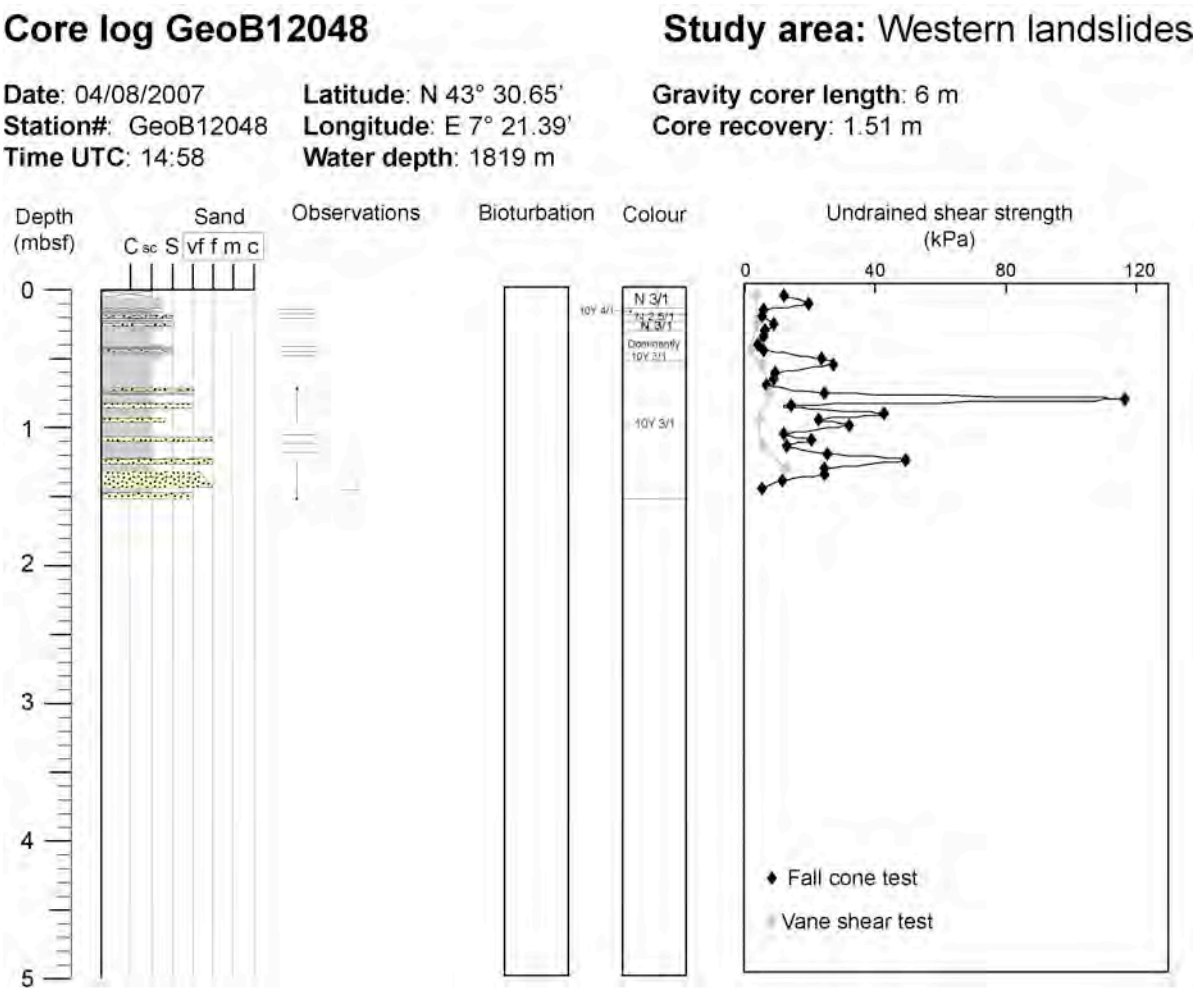

Western Landslide Complex

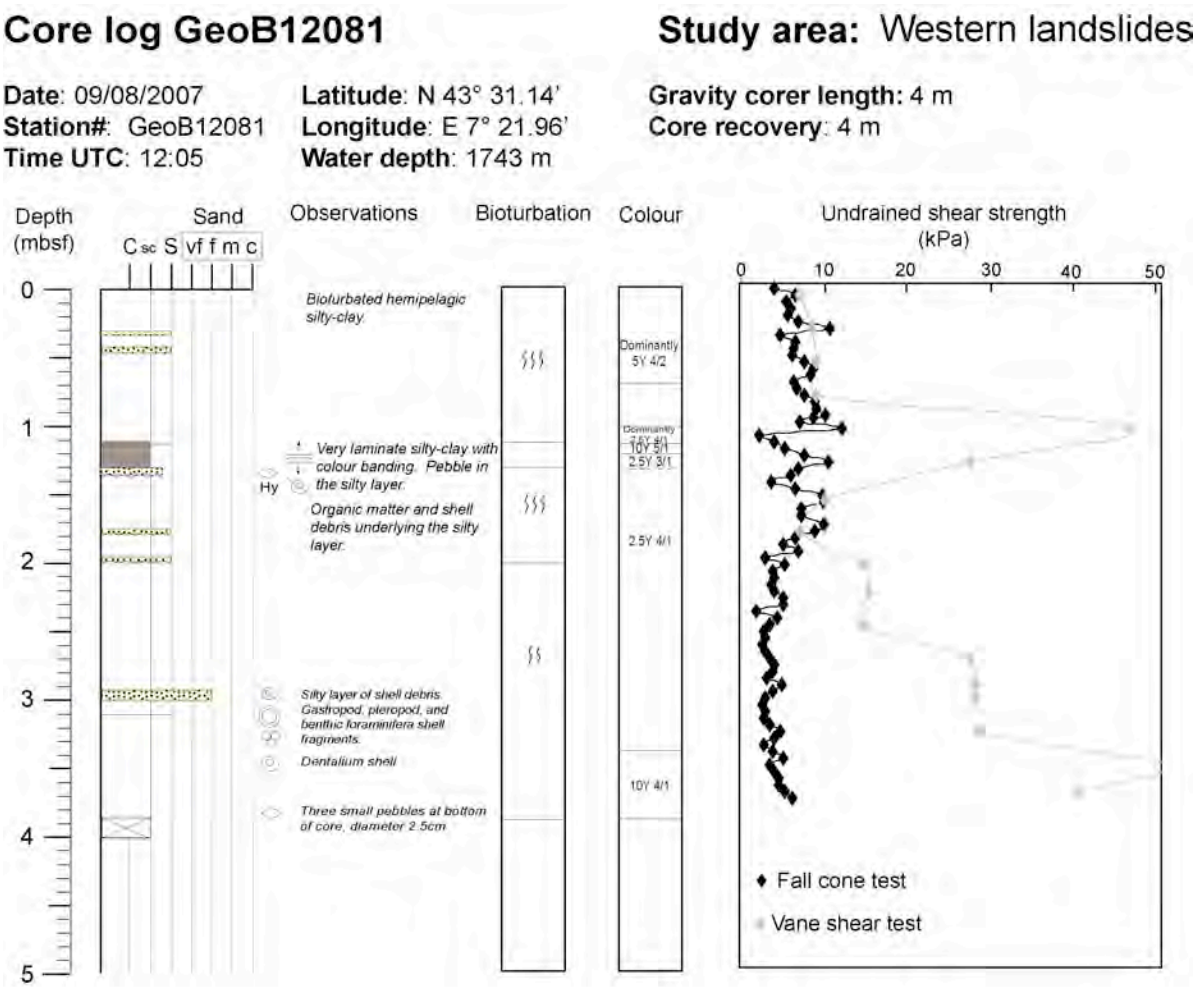

Var Canyon turbiditic system

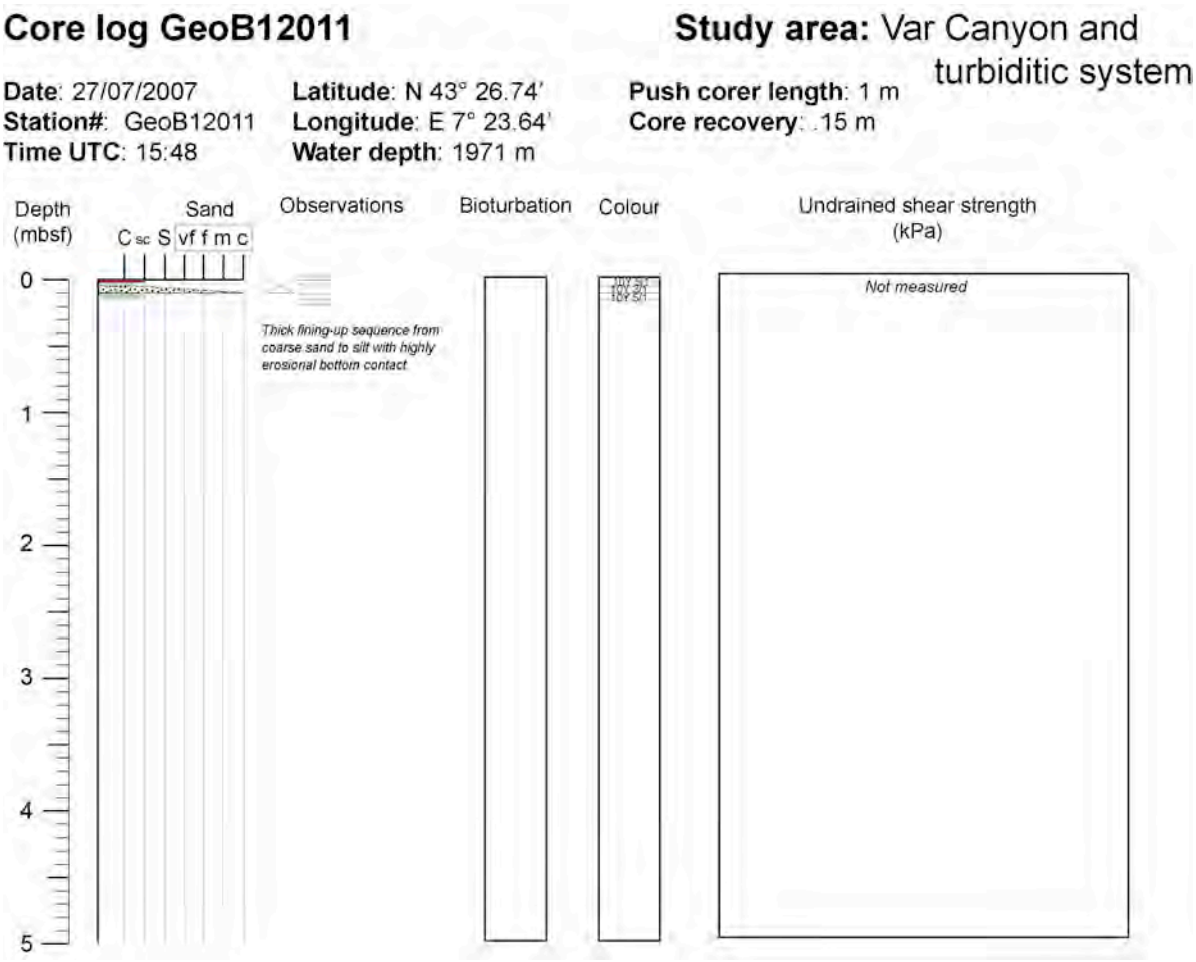

Var Canyon turbiditic system

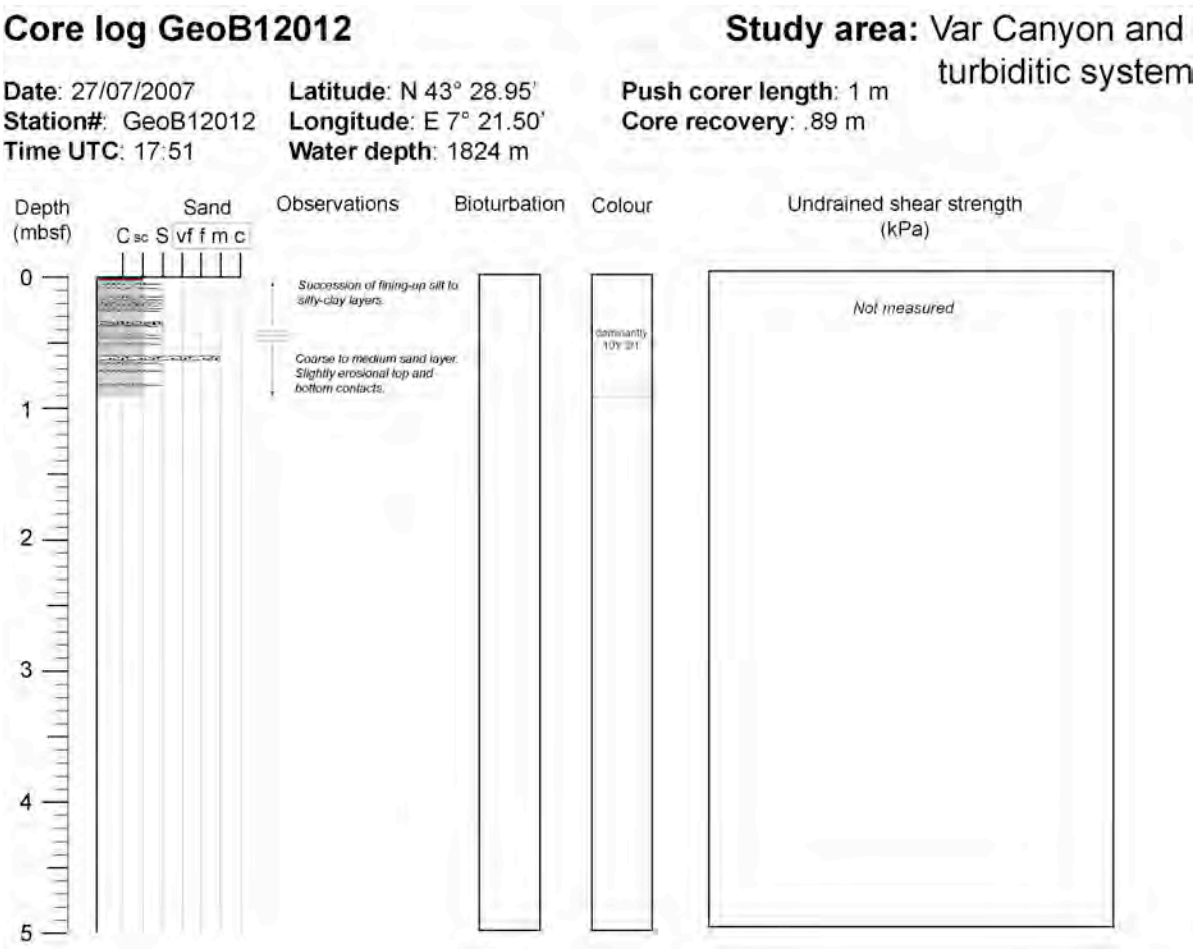

Var Canyon turbiditic system

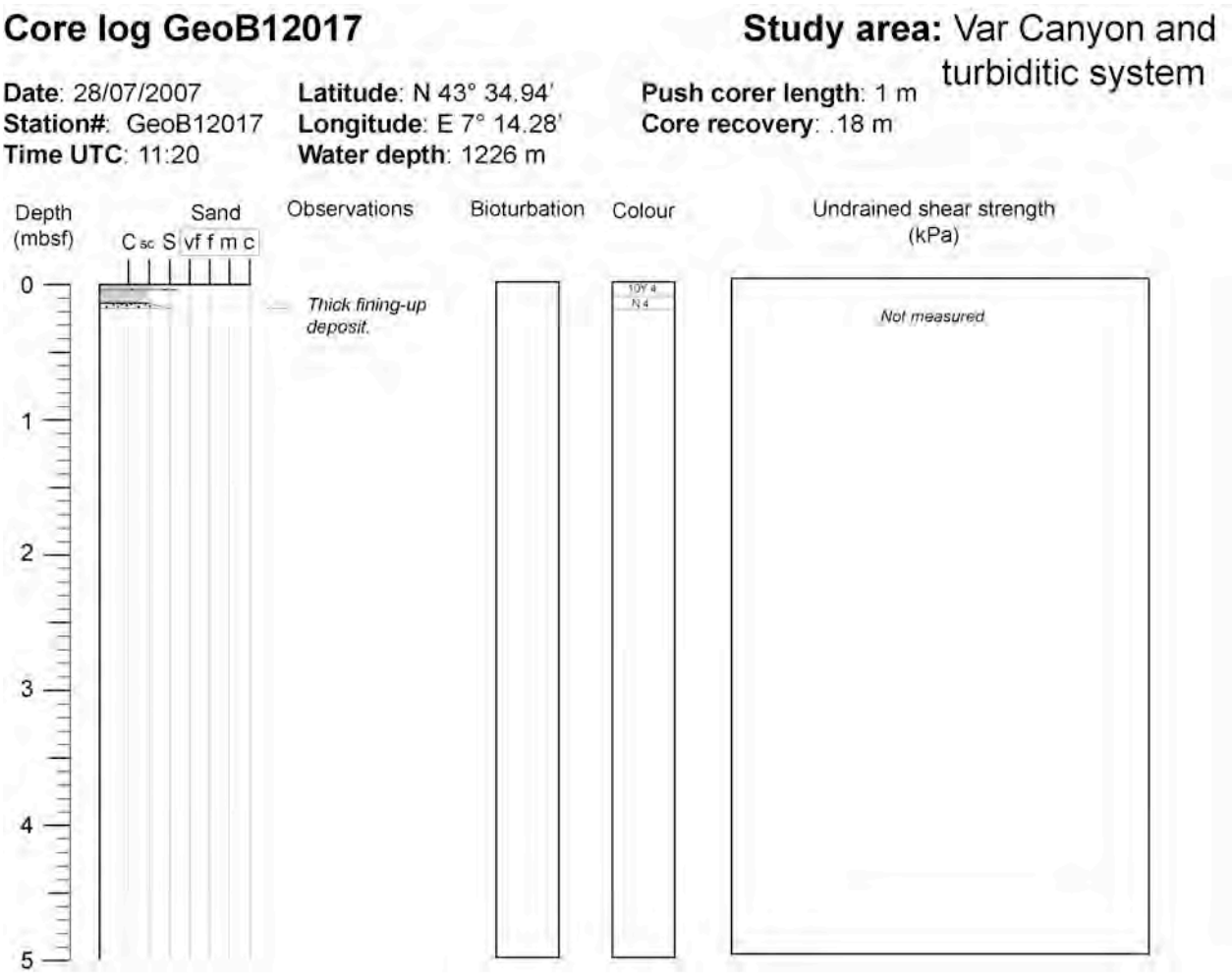

Var Canyon turbiditic system

Core log GeoB12022-2 **Study area:** Var Canyon and turbiditic system

Date: 29/07/2007 **Latitude**: N 43° 37.61' **Gravity corer length**: 10 m
Station#: GeoB12022-2 **Longitude**: E 7° 23.08' **Core recovery**: 5.73 m
Time UTC: 09:09 **Water depth**: 930 m

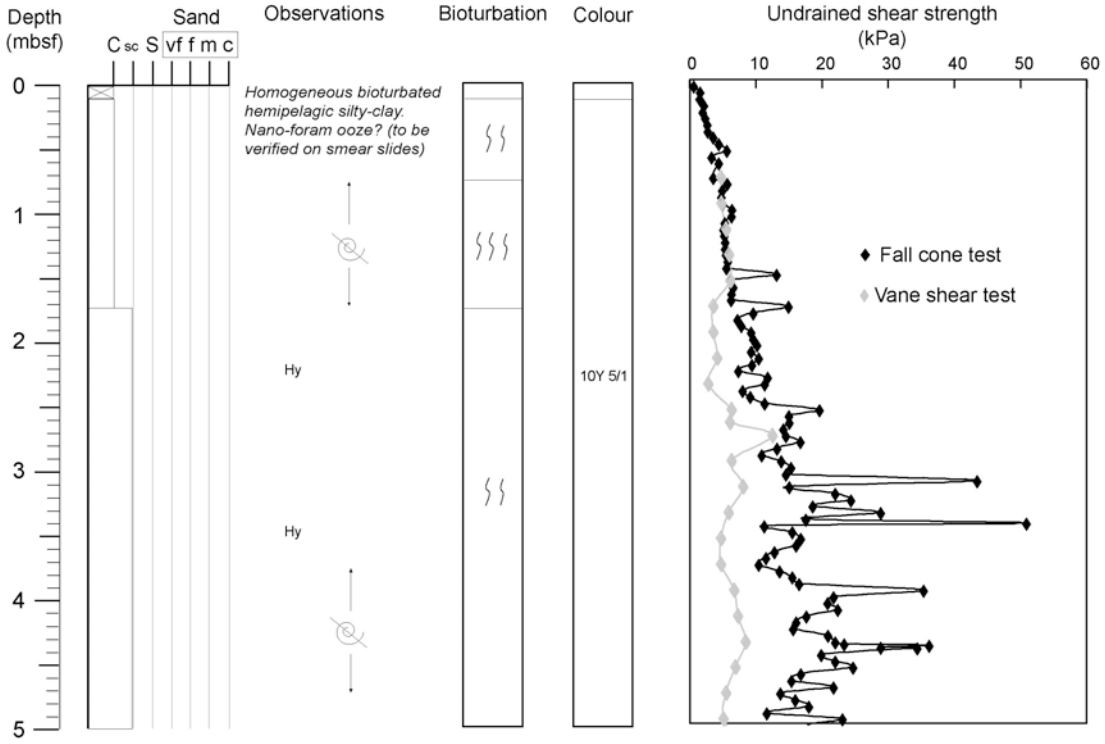

Var Canyon turbiditic system

Core log GeoB12022-2

Study area: Var Canyon and turbiditic system

Date: 29/07/2007 **Latitude**: N 43° 37.61' **Gravity corer length**: 10 m
Station#: GeoB12022-2 **Longitude**: E 7° 23.08' **Core recovery**: 5.73 m
Time UTC: 09:09 **Water depth**: 930 m

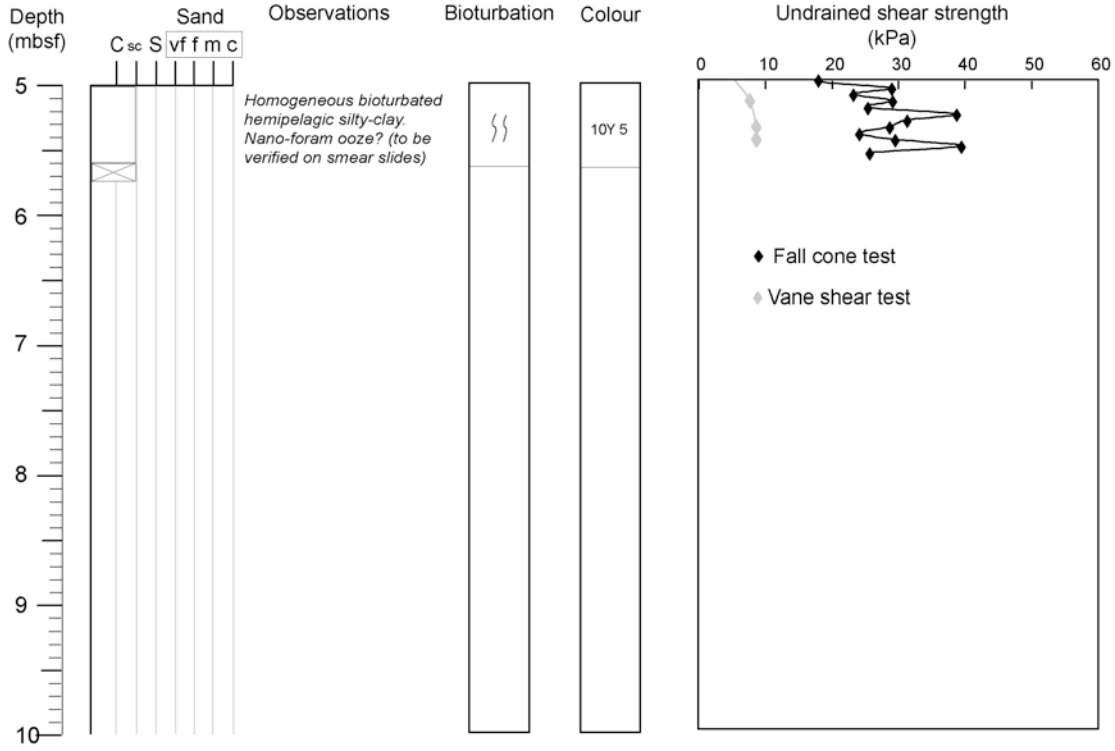

Var Canyon turbiditic system

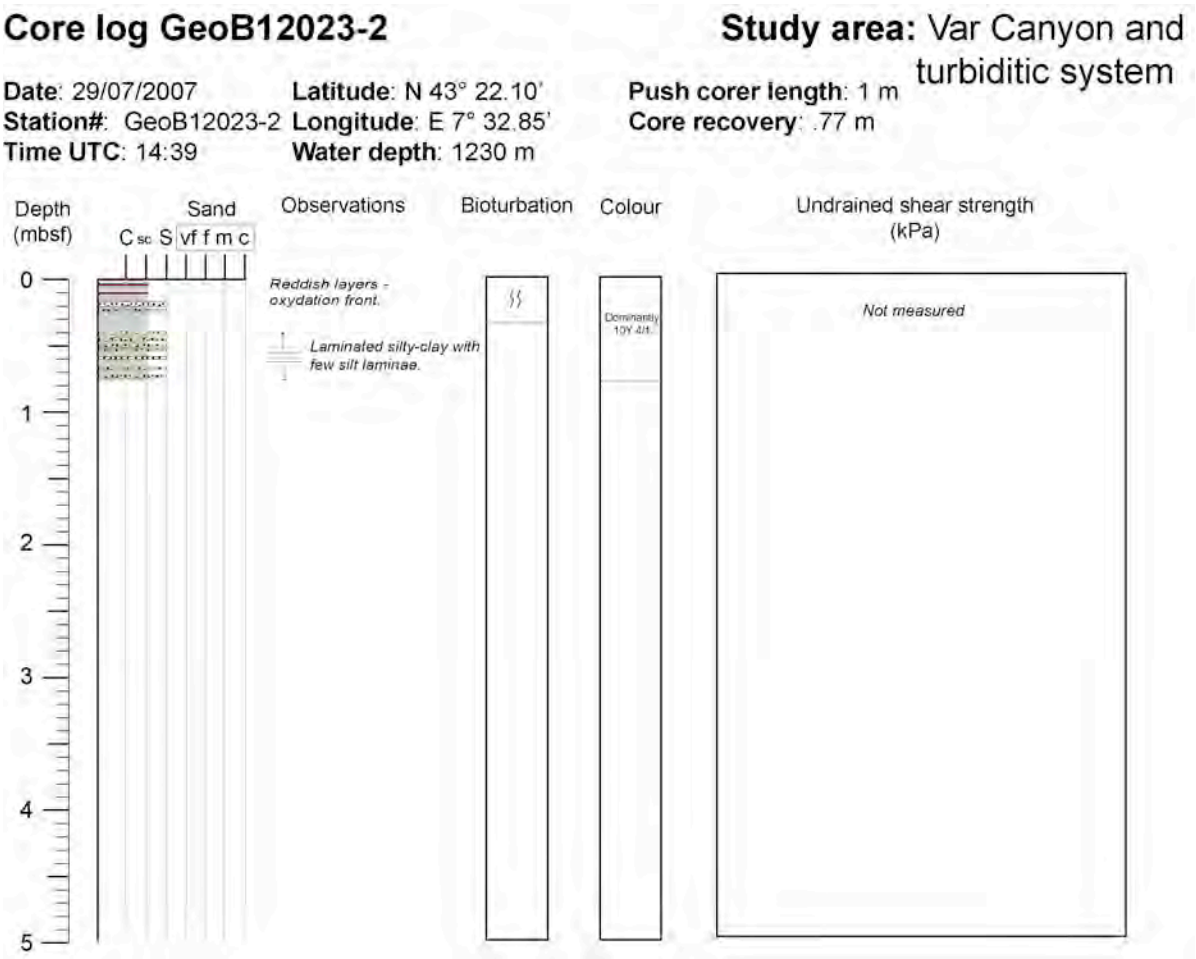

Var Canyon turbiditic system

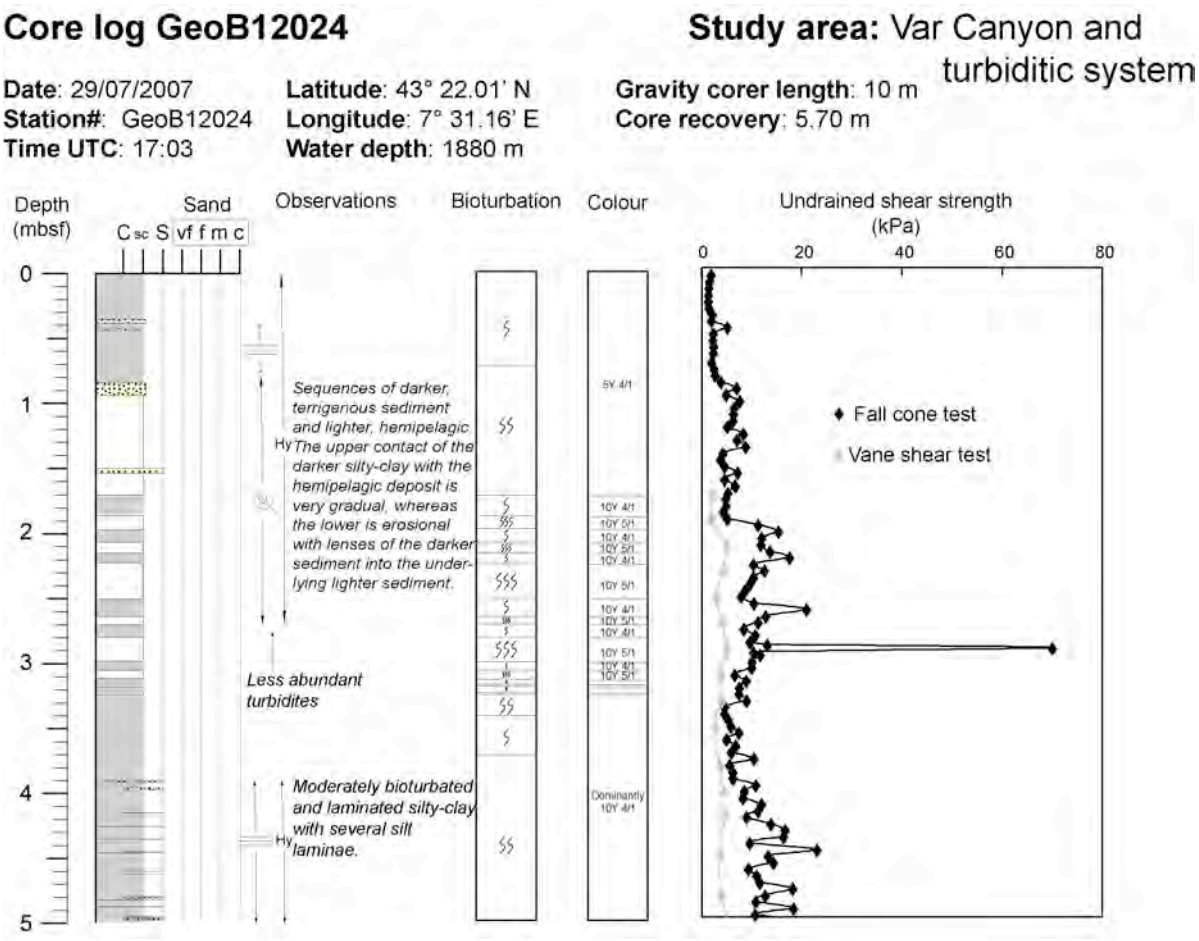

Var Canyon turbiditic system

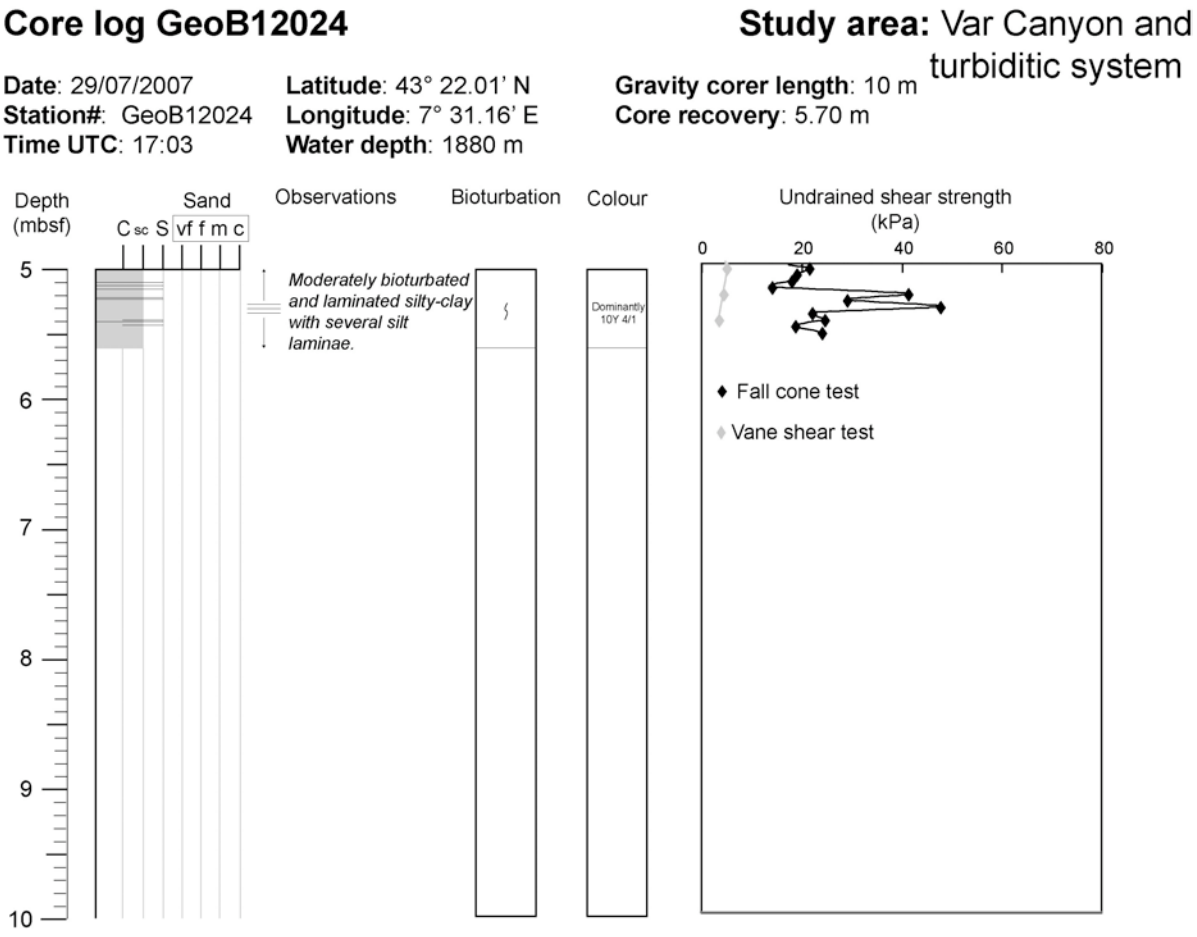

Var Canyon turbiditic system

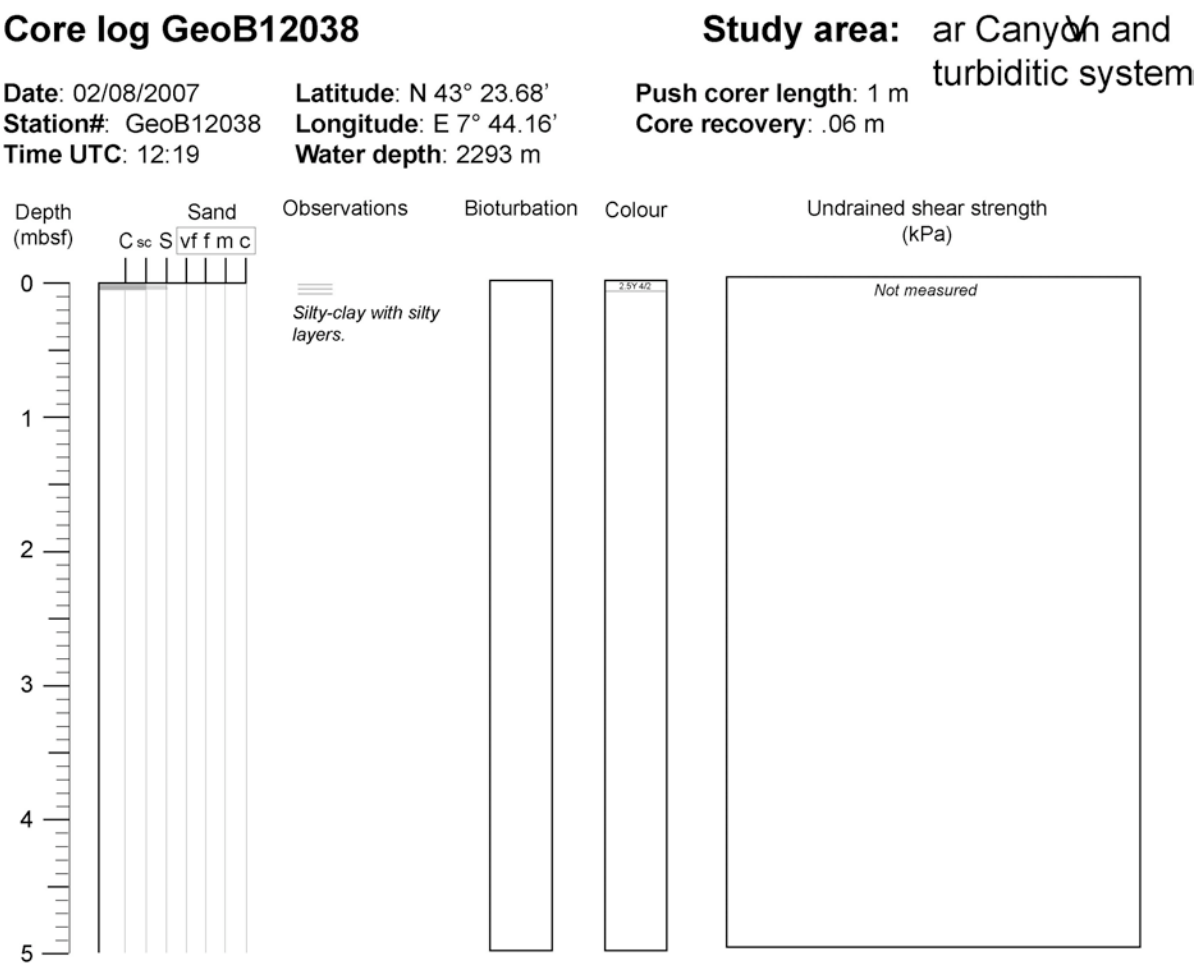

Var Canyon turbiditic system

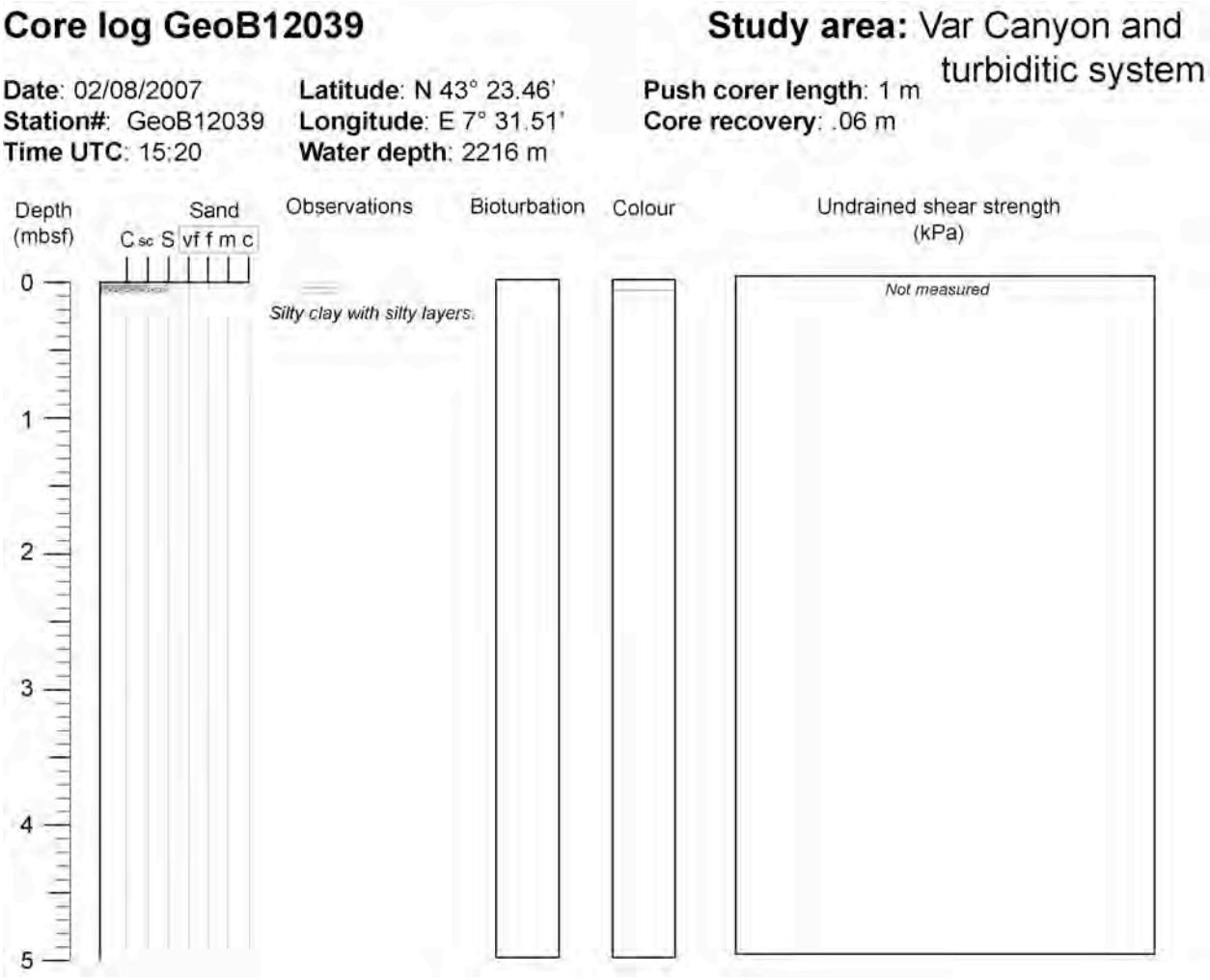

Var Canyon turbiditic system

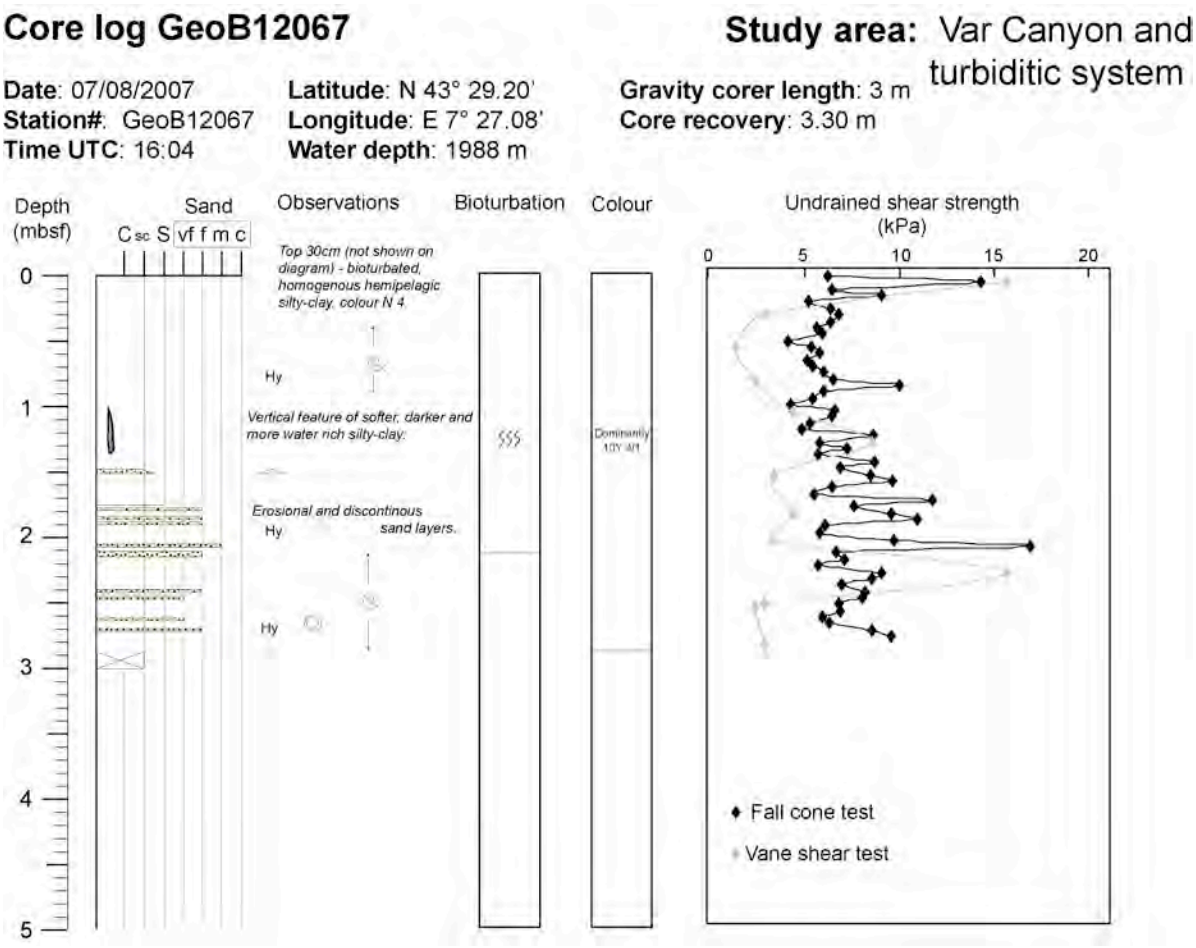

Var Canyon turbiditic system

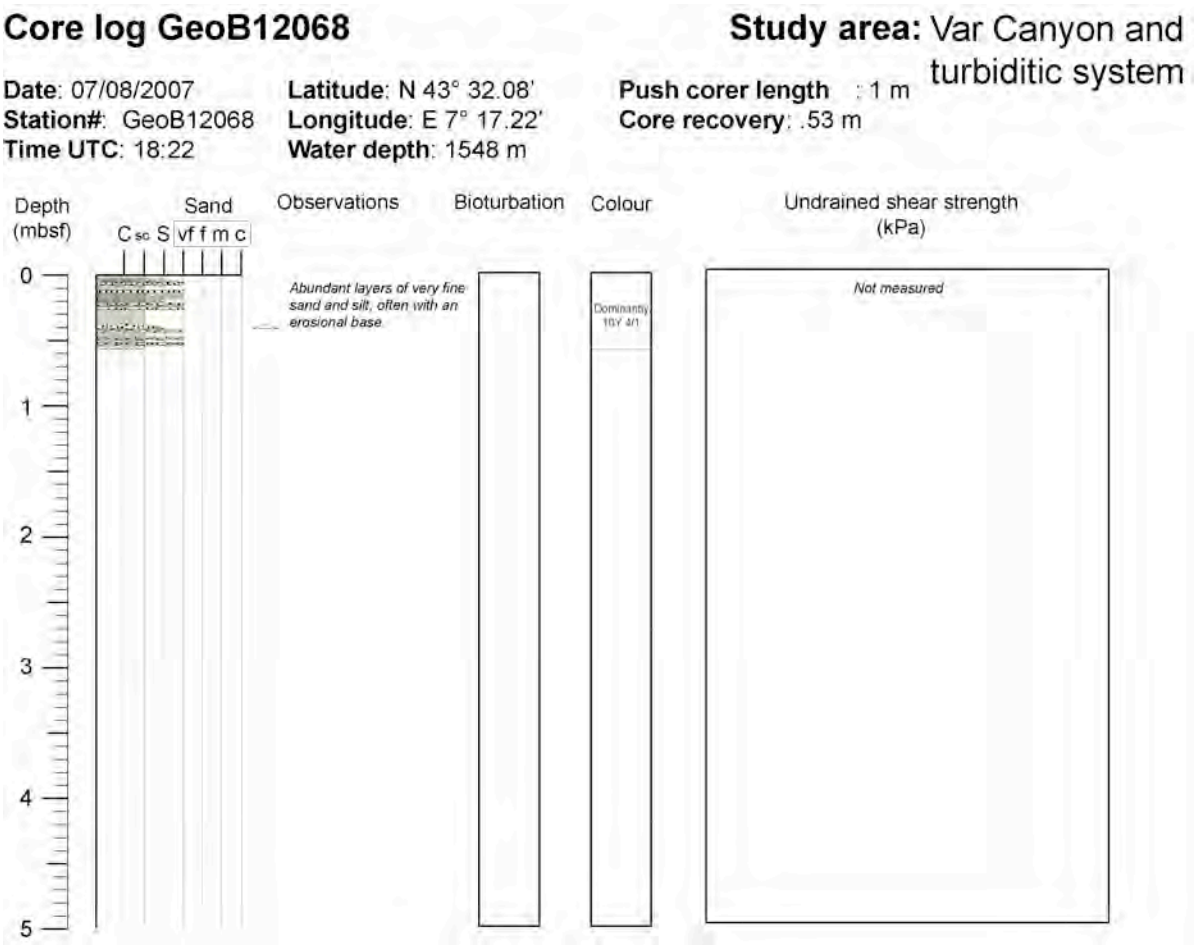

Var Canyon turbiditic system

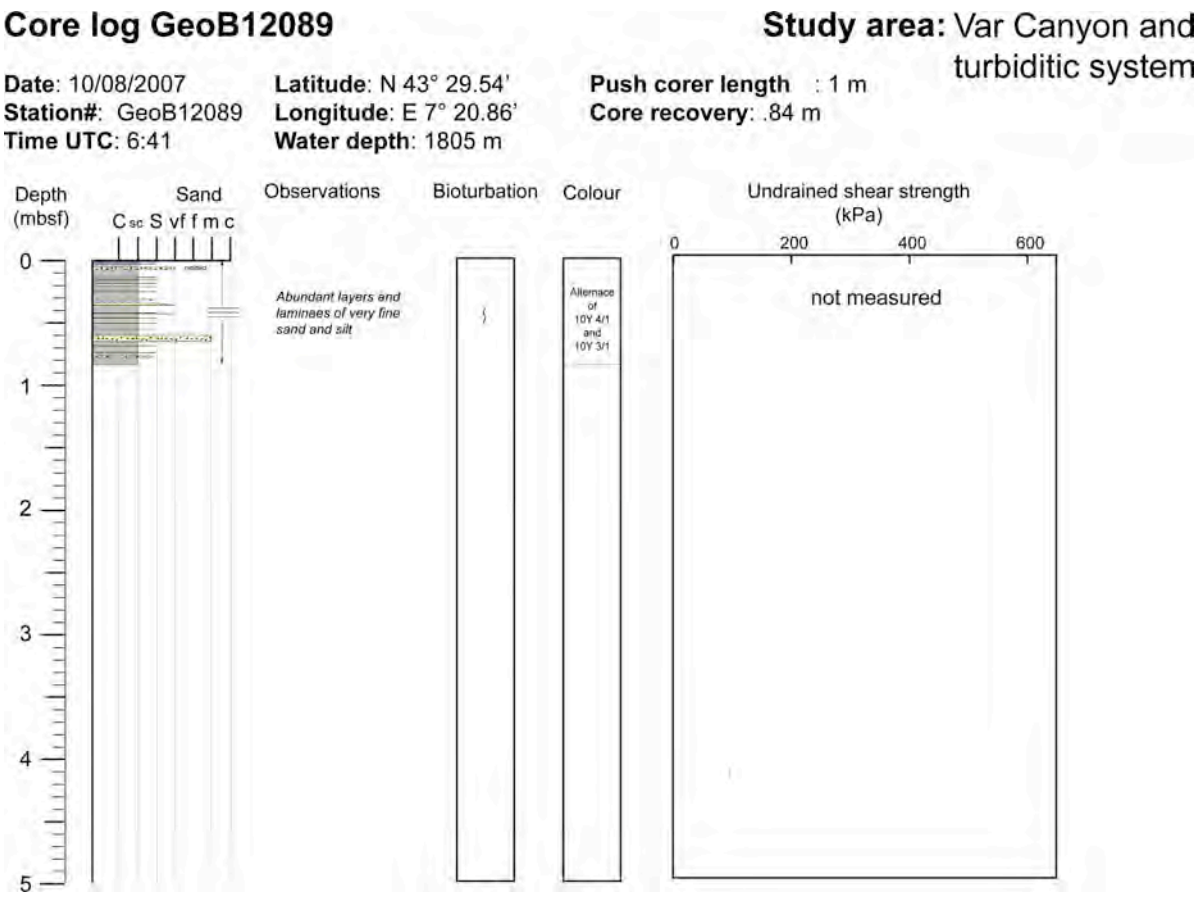

Var Canyon turbiditic system

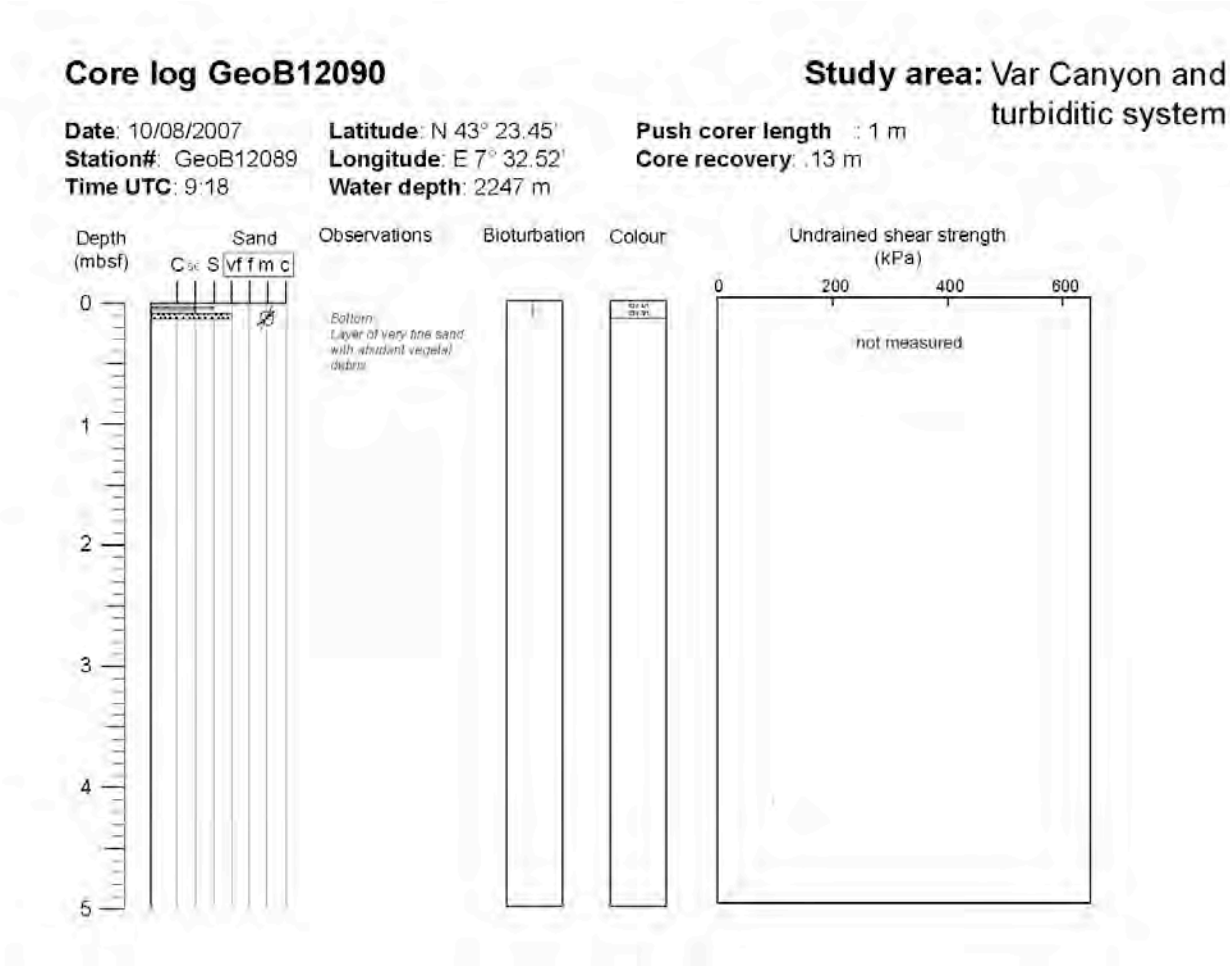

Appendix 9.4.: MSCL and physical properties data logs

(available in electronic version only)

Appendix 9.5.: Group photograph

From left to right:

A. Kopf, F. Girault, H. Hanff, M. Lange, T. Volen Krumova, W. Abraham, S. Stegmann, M.-A- Meier, S. Klar, B. Dennielou, N. Kaul, A. Förster, F. Strozyk, E. Alexandrakis, J. Blees, T. Haarmann, M. Hentscher.

Not on photograph:

K. Bogus, S. Krastel, Jan F. Metzen, V. Spiess.

Appendix 9.6.: Press coverage

SEITE 18 SONDERSEITE NR. 225 - MITTWOCH, 26. SEPTEMBER 2007

Hungriger Tsunami im Mittelmeer

Von Bord der „Meteor" aus untersuchten Bremer Wissenschaftler drei Wochen lang die Dynamik einer Hangrutschung im ligurischen Becken.

Von Winnie Abraham und Achim Kopf (Fotos)

Mit dem kleinen, ferngesteuerten Tauchroboter „Spy" wurde durch Videoaufnahmen am Meeresboden ein direkter Blick auf den Hang und dessen Kollaps gerichtet.

Von Bord der „Meteor" aus untersuchten Bremer Wissenschaftler drei Wochen lang die Dynamik einer Hangrutschung im ligurischen Becken. Im Oktober 1979 ereignete sich eine Rutschung am Kontinentalhang in der Bucht von Nizza. Durch den sich daraus entwickelnden vier Meter hohen Tsunami wurden Segelboote an den Strand geschleudert, Autos von überfluteten Uferstrassen geschwemmt, ein Teil des internationalen Flughafens zerstört und die aufgeschüttete Landzunge, auf der eine Hafenerweiterung geplant war, brach ab. Die rutschende Sedimentmasse verschwand im Meer, wo sie zwei Tiefseekabel in 2500 Meter Tiefe und 60 Meilen entfernt von der Küste zerbrach.

In Nizza plant man zurzeit erneut den Bau eines ins Meer ragenden Fährhafens. Aber wie sieht es inzwischen mit der Hangstabilität im ligurischen Becken aus, wie sicher ist der Untergrund, besteht das Risiko neuer Rutschungen?

Die Bauherren und Geldgeber werden sicherlich hohes Interesse an den Forschungsergebnissen Bremer Wissenschaftler haben, die im Juli/August drei Wochen lang in diesem Gebiet den Kontinentalhang unter die Lupe nahmen.

Kombination von mehreren Prozessen

Fahrtleiter beim Projekt LIMALAMO (Ligurian Margin Landslide Measurements & Observatory) ist der Geotechniker Professor Achim Kopf vom DFG-Forschungszentrum Ozeanränder an der Universität Bremen. Zusammen mit einem internationalen Team von Wissenschaftlern, Doktoranden und Studierenden will er mit der Forschungsreise die Wahrscheinlichkeit verschiedener Hypothesen überprüfen, die als Auslöser infrage kommen. „Wir haben die Spur der Rutschung verfolgt. Aus früheren Untersuchungen wissen wir, dass sich hier schon einige Erdbeben ereignet haben. Wir wollen herausfinden, ob die Rutschung vor Nizza durch Erdbebenaktivitäten hervorgerufen wurde, wie sie nachweislich durch tektonische Verschiebungen in den Alpen vorkommen, oder durch Süßwasseraustritte unter dem Meeresspiegel an diesem Hang, oder durch vorhandene Tonmineralpakete, die besonders leicht gleiten". Aber auch anthropogene Faktoren will der Wissenschaftler nicht ausschließen: „Natürlich kann der Kollaps vor 28 Jahren auch durch den Hafenbau ausgelöst worden sein. Unter Umständen ist es eine Kombination von mehreren Prozessen, d. h. das Zusammenwirken von natürlichen Abläufen oder in Wechselwirkung mit den damaligen Bauaktivitäten".

Eine Kollegin, Gabriela Dan vom französischen Meeresforschungsinstitut IFREMER in Brest, untersuchte in ihrer Dissertation die Folgen der Landgewinnung vor Nizza. Sie vertritt die These, dass das Hangsediment beim Hafenausbau ins Rutschen geraten ist, wo das Gewicht der errichteten Kaimauer den unterlagernden Sand zu stark belastete und durch Überdrücke im Porenwasser zwischen den Körnern zum Kollaps brachte.

Zur Untersuchung kamen vor Ort – vom Schiff aus, direkt über dem Hang – unterschiedlichste Methoden zum Einsatz. Dazu gehören Messungen durch Freifall – CPT (Cone Penetration Test) – Lanzen, mit denen Porenüberdrücke und die Festigkeit des Sediments zu bestimmen ist, zwei Parameter, aus denen sich maßgeblich das Rutschungsrisiko abgelesen lässt. Zur Identifizierung von Süßwasseraustritten als Rutschungsauslöser tragen Wärmestromlanzen bei, die den Temperaturgradienten messen und somit Durchstromraten des Wassers durch verschiedene Sedimentarten anzeigen. Ein weiterer Indikator ist der Salzgehalt des Wassers, der sich mit Leitfähigkeits-Sonden bestimmen lässt.

Nicht noch einmal

Auch die Datierung des Rutschungsmaterials ist notwendig, um Auskunft darüber zu geben, ob der Hang nach 1979 zur Ruhe gekommen ist, oder ob sich auch in jüngster Zeit immer wieder Sedimentmasse in Richtung Tiefe bewegt. Mit gezielten Schwerelotproben wurden Bohrkerne gesammelt und anhand ihrer Porenwasserchemie und Isotopenzusammensetzung kann in den nächsten Wochen im Labor in Bremen eine Datierung vorgenommen werden.

Ein weiteres Anliegen der Forschungsreise mit der „Meteor" war eine geophysikalische Voruntersuchung, durch die abgeklärt werden sollte, ob an diesem Hang Vorrichtungen für instrumentierte Bohrlöcher sowie ein Echtzeit-Monitoring verankert werden können. Diese Messmöglichkeiten, die im Rahmen des weltweiten Tiefseebohrungsprogramms „Integrated Ocean Drilling Program" installiert und mit einer Unterseestation verkabelt würden, könnten Datenmaterial bei Langzeitmessungen sammeln, und so eine Vorhersage von Rutschungen und weiteren Tsunamis in diesem Gebiet ermöglichen.

Es wird noch ein paar Monate dauern, bis die Daten der Messungen und Analysen der gesammelten Proben in Ergebnissen zusammengefasst werden können. Expeditionsleiter Achim Kopf ist sich nach Sichtung der ersten Daten sicher, dass natürliche Faktoren – ein starker Austritt von Süßwasser genau an dieser Stelle und anthropogene Faktoren – nämlich die Aufschüttung der Sandmassen für die Hafenerweiterung gemeinsame Auslöser der untermeerischen Rutschung waren.

„Ich würde an dieser Stelle vor Nizza kein zweites Mal versuchen, einen Hafen ins Meer zu bauen und an jedem anderen Platz an dieser Küste müsste auf jeden Fall der Hang und der Meeresboden genau untersucht werden, um auszuschließen, dass dort ein Süßwasserstrom austritt".

Der Tsunami in der Bucht von Nizza überflutete auch die Küstenstraßen der umliegenden Orte und wirbelte Autos herum. Ein Foto aus der Tageszeitung „Nice-Matin" vom 17. Oktober 1979

Studieren auf dem Forschungsschiff

Zur Gruppe, die auf der „Meteor" vor Nizza im Flach- und Tiefwasser Proben gezogen und Messungen vorgenommen hat, gehörten neben den Wissenschaftlern Studierende und Doktoranden.

Tim läuft zum dritten Mal mit einem Schraubenschlüssel übers Arbeitsdeck in Richtung Chemielabor. Morgen früh soll der erste Bohrkern gezogen werden und er wird zusammen mit Eleni, Michael und Jan die geochemischen Messungen durchführen: An kleinen Proben des Sediments und des Porenwassers, um den PH-Wert, den EH-Wert sowie Alkalität, Eisen- und Ammoniumgehalt zu bestimmen. Aber zurzeit funktioniert das Messsystem nicht einwandfrei, und so versuchen die drei Studierenden und Doktorand Michael eine Lösung für das Problem zu finden.

Mit Erfolg, am nächsten Tag – eingehüllt in dicke Jacken und Overalls – stehen sie im Kühlraum und können ihre Messdaten zusammentragen. Danach schleppen sie den Bohrkern zu der Sedimentologie-Gruppe. Hier haben die beiden Bachelorstudierenden Men-Andrin aus der Schweiz und Tsveta aus Bulgarien sowie die Doktorandin France von der ETH Zürich unter der Anleitung von Annika – Doktorandin an der Graduate School GLOMAR der Universität Bremen – alle Vorbereitungen zum Spalten des Kerns getroffen.

Diese Prozedur sieht erst einmal gar nicht wissenschaftlich aus. Um kleine Metallbänke, auf denen die Plastikröhre mit dem Sedimentkern ruhen wird, liegen Klebeband, schwarze Filzstifte, zwischen Holzgriffen gespannte Metalldrähte zum Teilen des Sedimentkerns, Lappen und Spachteln durcheinander. Alle Schritte müssen gelernt werden: Wie schlitzt man die Plastikhülle mit kleinen Sägen rechts und links auf? Wie beschriftet man die Kappen der Röhren, dass es eine Hälfte zum Archivieren gibt, die in den Kühlcontainer wandert und ins Bohrkernlager nach Bremen gebracht wird von der anderen Hälfte, die zur sofortigen Beschreibung und Beprobung zur Verfügung steht, unterschieden werden kann?

„Farbe dunkelgrau und Korngröße fein", fasst France ihre Sichtung des ersten kleinen Abschnitts des Probenmaterials zusammen. Es folgen Angaben zur Sedimentstruktur und eventuellem Fossilliengehalt. Men-Andrin und Tsveta machen die mechanischen Untersuchungen mit Scherflügelsonde und Fallkegelpenetrometer, und tragen die Werte in entsprechende Tabellen im Computer ein. Die Beteiligten lernen auf diese Weise das Gleitverhalten und die Festigkeit der einzelnen Sedimentlagen am untermeerischen Kontinentalhang zu bestimmen.

Jan, der im Masterstudiengang Marine Geosciences studiert, löst die Sensoren von den fünf Flügeln der Wärmestromlanze, die in 600 Metern Tiefe ins Sediment eingedrungen ist. Im geophysikalischen Labor werden aus den Metallkartuschen die gesammelten Daten in den Rechner übertragen. Jede Minute ist die Temperatur an allen fünf Sensoren gemessen worden. Auf dem Bildschirm baut sich eine Kurve auf. „Hier wird es plötzlich wärmer", kommentiert Jan die steigende Linie. „Das kann einen Austritt von Süßwasser am Hang bedeuten oder aber auch dass es sich um Sediment handelt, das vor nicht so langer Zeit weiter oben, in wärmerem Wasser gelagert hat und abgerutscht ist".

Einblicke ins Forschungsleben

„Daten sammeln: dafür müssen wir die Funktionsweise der Geräte verstehen und welches festgelegte Prozedere abläuft. Das Auswerten, mit dem Computer zu Ergebnissen kommen, ist dann der zweite Schritt und führt uns mit den anderen Gruppen und deren Ergebnissen zusammen", sagt Annika. Die Beteiligten merken schnell, dass sorgfältige Arbeit elementar wichtig ist, denn manchmal bauen die Versuche einer Gruppe auf den Aussagen der anderen Gruppe auf. Die Orte zum Beispiel, an denen am abgerutschten Hang in der Bucht von Nizza Messungen und Probenentnahmen vorgenommen werden, sind durch sogenannte Parasound-Messungen identifiziert worden.

Frank sitzt vor den Monitoren und befeuert den Meeresboden mit Schallwellen. Als Ergebnis liefern sie ein Profil des Meeresbodens und der oberen Sedimentschichten bis zu etwa 50 m darunter. „Ist das nicht eine tolle dreidimensionale Unterwasserkarte", freut sich Frank, der in einem Jahr seine Doktorarbeit beendet haben will. „Man kann an den Farben die jeweilige Wassertiefe erkennen, wie der Hang strukturiert ist, wo Canyons sind oder Abbruchkanten.

Was wir nicht wissen, warum der Hang an bestimmten Stellen Rutschungen aufweist, da sind dann die anderen Gruppen, die Sedimentologen und Geo-Chemiker und -Physiker mit ihren Analysen gefragt".

Forschendes Lernen unter Anleitung eines Wissenschaftlers. Statt im Hörsaal lernen die Studierenden im Labor auf dem Forschungsschiff „Meteor" an selbst vorbereiteten Bohrkernen alles über Sedimentologie.

Die Spannung steigt, wenn ein Gerät am Seil, das es in die Tiefe befördert, festgezurrt wird. Sitzen die Knoten richtig, und ist es der richtige Knoten, der sich im nassen Zustand auch wieder lösen lässt? Matthias, Hendrick und Steffen sind die Techniker, sie entscheiden, dass die Lanze lieber noch zusätzlich mit Kabelbindern abgesichert wird. Das sind teure Geräte, die dürfen nicht verloren gehen, außerdem können beim Verlust geplante Forschungsarbeiten nicht durchgeführt werden und es fehlen wichtige Ergebnisse.

Für die meisten der Gruppe ist es der erste Aufenthalt auf einem Forschungsschiff. Alle freuen sich, dass sie die Gelegenheit haben, Einblicke ins Forschungsleben zu bekommen.

„Es ist toll mitzuerleben, wie die Proben, die ich bisher nur in Bremen im Uni-Labor untersucht habe, gesammelt werden", sagt Eleni, die seit diesem Sommersemester im Bremer Bachelor-Studiengang Geowissenschaften studiert. Annika und Michael, beides Doktoranden wollen den anderen geowissenschaftlichen Bereichen hier über die Schulter gucken und verschieden Methoden kennen lernen. „Das geht hier ganz einfach, weil wir räumlich so nah zusammen arbeiten und jeder mitkriegt, welche Fragestellungen gerade in den jeweiligen Gruppen bearbeitet werden", findet auch France. So stehen dann auch alle auf dem Arbeitsdeck, wenn der Unterwasserroboter „Spy" oder die verschiedenen Messlanzen ins Wasser gebracht und Bohrkerne gezogen werden.

Sie diskutieren untereinander und mit den Wissenschaftlern in deutsch, englisch und französisch über die bisher gesammelten Ergebnisse, ihren Kampf mit den Geräten und der dazugehörigen Technik und erleben hautnah mit, wie wichtig es ist, dass die Messgeräte gut funktionieren, weil nur so gute Daten gesammelt werden können. Wie forschendes Lernen funktioniert kann man hier auf der „Meteor", einem der großen deutschen Forschungsschiffe, eindrucksvoll beobachten.

Weser Kurier, 26.09.2007

Publications of this series:

No. 1 **Wefer, G., E. Suess and cruise participants**
Bericht über die POLARSTERN-Fahrt ANT IV/2, Rio de Janeiro - Punta Arenas, 6.11. - 1.12.1985.
60 pages, Bremen, 1986.

No. 2 **Hoffmann, G.**
Holozänstratigraphie und Küstenlinienverlagerung an der andalusischen Mittelmeerküste.
173 pages, Bremen, 1988. (out of print)

No. 3 **Wefer, G. and cruise participants**
Bericht über die METEOR-Fahrt M 6/6, Libreville - Las Palmas, 18.2. - 23.3.1988.
97 pages, Bremen, 1988.

No. 4 **Wefer, G., G.F. Lutze, T.J. Müller, O. Pfannkuche, W. Schenke, G. Siedler, W. Zenk**
Kurzbericht über die METEOR-Expedition No. 6, Hamburg - Hamburg, 28.10.1987 - 19.5.1988.
29 pages, Bremen, 1988. (out of print)

No. 5 **Fischer, G.**
Stabile Kohlenstoff-Isotope in partikulärer organischer Substanz aus dem Südpolarmeer
(Atlantischer Sektor). 161 pages, Bremen, 1989.

No. 6 **Berger, W.H. and G. Wefer**
Partikelfluß und Kohlenstoffkreislauf im Ozean.
Bericht und Kurzfassungen über den Workshop vom 3.-4. Juli 1989 in Bremen.
57 pages, Bremen, 1989.

No. 7 **Wefer, G. and cruise participants**
Bericht über die METEOR - Fahrt M 9/4, Dakar - Santa Cruz, 19.2. - 16.3.1989.
103 pages, Bremen, 1989.

No. 8 **Kölling, M.**
Modellierung geochemischer Prozesse im Sickerwasser und Grundwasser.
135 pages, Bremen, 1990.

No. 9 **Heinze, P.-M.**
Das Auftriebsgeschehen vor Peru im Spätquartär. 204 pages, Bremen, 1990. (out of print)

No. 10 **Willems, H., G. Wefer, M. Rinski, B. Donner, H.-J. Bellmann, L. Eißmann, A. Müller, B.W. Flemming, H.-C. Höfle, J. Merkt, H. Streif, G. Hertweck, H. Kuntze, J. Schwaar, W. Schäfer, M.-G. Schulz, F. Grube, B. Menke**
Beiträge zur Geologie und Paläontologie Norddeutschlands: Exkursionsführer.
202 pages, Bremen, 1990.

No. 11 **Wefer, G. and cruise participants**
Bericht über die METEOR-Fahrt M 12/1, Kapstadt - Funchal, 13.3.1990 - 14.4.1990.
66 pages, Bremen, 1990.

No. 12 **Dahmke, A., H.D. Schulz, A. Kölling, F. Kracht, A. Lücke**
Schwermetallspuren und geochemische Gleichgewichte zwischen Porenlösung und Sediment
im Wesermündungsgebiet. BMFT-Projekt MFU 0562, Abschlußbericht. 121 pages, Bremen, 1991.

No. 13 **Rostek, F.**
Physikalische Strukturen von Tiefseesedimenten des Südatlantiks und ihre Erfassung in
Echolotregistrierungen. 209 pages, Bremen, 1991.

No. 14 **Baumann, M.**
Die Ablagerung von Tschernobyl-Radiocäsium in der Norwegischen See und in der Nordsee.
133 pages, Bremen, 1991. (out of print)

No. 15 **Kölling, A.**
Frühdiagenetische Prozesse und Stoff-Flüsse in marinen und ästuarinen Sedimenten.
140 pages, Bremen, 1991.

No. 16 **SFB 261 (ed.)**
1. Kolloquium des Sonderforschungsbereichs 261 der Universität Bremen (14.Juni 1991):
Der Südatlantik im Spätquartär: Rekonstruktion von Stoffhaushalt und Stromsystemen.
Kurzfassungen der Vorträge und Poster. 66 pages, Bremen, 1991.

No. 17 **Pätzold, J. and cruise participants**
Bericht und erste Ergebnisse über die METEOR-Fahrt M 15/2, Rio de Janeiro - Vitoria,
18.1. - 7.2.1991. 46 pages, Bremen, 1993.

No. 18 **Wefer, G. and cruise participants**
Bericht und erste Ergebnisse über die METEOR-Fahrt M 16/1, Pointe Noire - Recife,
27.3. - 25.4.1991. 120 pages, Bremen, 1991.

No. 19 **Schulz, H.D. and cruise participants**
Bericht und erste Ergebnisse über die METEOR-Fahrt M 16/2, Recife - Belem, 28.4. - 20.5.1991. 149 pages, Bremen, 1991.

No. 20 **Berner, H.**
Mechanismen der Sedimentbildung in der Fram-Straße, im Arktischen Ozean und in der Norwegischen See. 167 pages, Bremen, 1991.

No. 21 **Schneider, R.**
Spätquartäre Produktivitätsänderungen im östlichen Angola-Becken: Reaktion auf Variationen im Passat-Monsun-Windsystem und in der Advektion des Benguela-Küstenstroms. 198 pages, Bremen, 1991. (out of print)

No. 22 **Hebbeln, D.**
Spätquartäre Stratigraphie und Paläozeanographie in der Fram-Straße. 174 pages, Bremen, 1991.

No. 23 **Lücke, A.**
Umsetzungsprozesse organischer Substanz während der Frühdiagenese in ästuarinen Sedimenten. 137 pages, Bremen, 1991.

No. 24 **Wefer, G. and cruise participants**
Bericht und erste Ergebnisse der METEOR-Fahrt M 20/1, Bremen - Abidjan, 18.11.- 22.12.1991. 74 pages, Bremen, 1992.

No. 25 **Schulz, H.D. and cruise participants**
Bericht und erste Ergebnisse der METEOR-Fahrt M 20/2, Abidjan - Dakar, 27.12.1991 - 3.2.1992. 173 pages, Bremen, 1992.

No. 26 **Gingele, F.**
Zur klimaabhängigen Bildung biogener und terrigener Sedimente und ihrer Veränderung durch die Frühdiagenese im zentralen und östlichen Südatlantik. 202 pages, Bremen, 1992.

No. 27 **Bickert, T.**
Rekonstruktion der spätquartären Bodenwasserzirkulation im östlichen Südatlantik über stabile Isotope benthischer Foraminiferen. 205 pages, Bremen, 1992. (out of print)

No. 28 **Schmidt, H.**
Der Benguela-Strom im Bereich des Walfisch-Rückens im Spätquartär. 172 pages, Bremen, 1992.

No. 29 **Meinecke, G.**
Spätquartäre Oberflächenwassertemperaturen im östlichen äquatorialen Atlantik. 181 pages, Bremen, 1992.

No. 30 **Bathmann, U., U. Bleil, A. Dahmke, P. Müller, A. Nehrkorn, E.-M. Nöthig, M. Olesch, J. Pätzold, H.D. Schulz, V. Smetacek, V. Spieß, G. Wefer, H. Willems**
Bericht des Graduierten Kollegs. Stoff-Flüsse in marinen Geosystemen. Berichtszeitraum Oktober 1990 - Dezember 1992. 396 pages, Bremen, 1992.

No. 31 **Damm, E.**
Frühdiagenetische Verteilung von Schwermetallen in Schlicksedimenten der westlichen Ostsee. 115 pages, Bremen, 1992.

No. 32 **Antia, E.E.**
Sedimentology, Morphodynamics and Facies Association of a mesotidal Barrier Island Shoreface (Spiekeroog, Southern North Sea). 370 pages, Bremen, 1993.

No. 33 **Duinker, J. and G. Wefer (ed.)**
Bericht über den 1. JGOFS-Workshop. 1./2. Dezember 1992 in Bremen. 83 pages, Bremen, 1993.

No. 34 **Kasten, S.**
Die Verteilung von Schwermetallen in den Sedimenten eines stadtbremischen Hafenbeckens. 103 pages, Bremen, 1993.

No. 35 **Spieß, V.**
Digitale Sedimentographie. Neue Wege zu einer hochauflösenden Akustostratigraphie. 199 pages, Bremen, 1993.

No. 36 **Schinzel, U.**
Laborversuche zu frühdiagenetischen Reaktionen von Eisen (III) - Oxidhydraten in marinen Sedimenten.189 pages, Bremen, 1993.

No. 37 **Sieger, R.**
CoTAM - ein Modell zur Modellierung des Schwermetalltransports in Grundwasserleitern. 56 pages, Bremen, 1993. (out of print)

No. 38 **Willems, H. (ed.)**
Geoscientific Investigations in the Tethyan Himalayas. 183 pages, Bremen, 1993.

No. 39 **Hamer, K.**
Entwicklung von Laborversuchen als Grundlage für die Modellierung des Transportverhaltens von Arsenat, Blei, Cadmium und Kupfer in wassergesättigten Säulen. 147 pages, Bremen, 1993.

No. 40 **Sieger, R.**
Modellierung des Stofftransports in porösen Medien unter Ankopplung kinetisch gesteuerter Sorptions- und Redoxprozesse sowie thermischer Gleichgewichte. 158 pages, Bremen, 1993.

No. 41 **Thießen, W.**
Magnetische Eigenschaften von Sedimenten des östlichen Südatlantiks und ihre paläozeanographische Relevanz. 170 pages, Bremen, 1993.

No. 42 **Spieß, V. and cruise participants**
Report and preliminary results of METEOR-Cruise M 23/1, Kapstadt - Rio de Janeiro, 4.-25.2.1993. 139 pages, Bremen, 1994.

No. 43 **Bleil, U. and cruise participants**
Report and preliminary results of METEOR-Cruise M 23/2, Rio de Janeiro - Recife, 27.2.-19.3.1993 133 pages, Bremen, 1994.

No. 44 **Wefer, G. and cruise participants**
Report and preliminary results of METEOR-Cruise M 23/3, Recife - Las Palmas, 21.3. - 12.4.1993 71 pages, Bremen, 1994.

No. 45 **Giese, M. and G. Wefer (ed.)**
Bericht über den 2. JGOFS-Workshop. 18../19. November 1993 in Bremen. 93 pages, Bremen, 1994.

No. 46 **Balzer, W. and cruise participants**
Report and preliminary results of METEOR-Cruise M 22/1, Hamburg - Recife, 22.9. - 21.10.1992. 24 pages, Bremen, 1994.

No. 47 **Stax, R.**
Zyklische Sedimentation von organischem Kohlenstoff in der Japan See: Anzeiger für Änderungen von Paläoozeanographie und Paläoklima im Spätkänozoikum. 150 pages, Bremen, 1994.

No. 48 **Skowronek, F.**
Frühdiagenetische Stoff-Flüsse gelöster Schwermetalle an der Oberfläche von Sedimenten des Weser Ästuares. 107 pages, Bremen, 1994.

No. 49 **Dersch-Hansmann, M.**
Zur Klimaentwicklung in Ostasien während der letzten 5 Millionen Jahre: Terrigener Sedimenteintrag in die Japan See (ODP Ausfahrt 128). 149 pages, Bremen, 1994.

No. 50 **Zabel, M.**
Frühdiagenetische Stoff-Flüsse in Oberflächen-Sedimenten des äquatorialen und östlichen Südatlantik. 129 pages, Bremen, 1994.

No. 51 **Bleil, U. and cruise participants**
Report and preliminary results of SONNE-Cruise SO 86, Buenos Aires - Capetown, 22.4. - 31.5.93 116 pages, Bremen, 1994.

No. 52 **Symposium: The South Atlantic: Present and Past Circulation.**
Bremen, Germany, 15 - 19 August 1994. Abstracts. 167 pages, Bremen, 1994.

No. 53 **Kretzmann, U.B.**
^{57}Fe-Mössbauer-Spektroskopie an Sedimenten - Möglichkeiten und Grenzen. 183 pages, Bremen, 1994.

No. 54 **Bachmann, M.**
Die Karbonatrampe von Organyà im oberen Oberapt und unteren Unteralb (NE-Spanien, Prov. Lerida): Fazies, Zyklo- und Sequenzstratigraphie. 147 pages, Bremen, 1994. (out of print)

No. 55 **Kemle-von Mücke, S.**
Oberflächenwasserstruktur und -zirkulation des Südostatlantiks im Spätquartär. 151 pages, Bremen, 1994.

No. 56 **Petermann, H.**
Magnetotaktische Bakterien und ihre Magnetosome in Oberflächensedimenten des Südatlantiks. 134 pages, Bremen, 1994.

No. 57 **Mulitza, S.**
Spätquartäre Variationen der oberflächennahen Hydrographie im westlichen äquatorialen Atlantik. 97 pages, Bremen, 1994.

No. 58 **Segl, M. and cruise participants**
Report and preliminary results of METEOR-Cruise M 29/1, Buenos-Aires - Montevideo, 17.6. - 13.7.1994
94 pages, Bremen, 1994.

No. 59 **Bleil, U. and cruise participants**
Report and preliminary results of METEOR-Cruise M 29/2, Montevideo - Rio de Janiero 15.7. - 8.8.1994. 153 pages, Bremen, 1994.

No. 60 **Henrich, R. and cruise participants**
Report and preliminary results of METEOR-Cruise M 29/3, Rio de Janeiro - Las Palmas 11.8. - 5.9.1994. Bremen, 1994. (out of print)

No. 61 **Sagemann, J.**
Saisonale Variationen von Porenwasserprofilen, Nährstoff-Flüssen und Reaktionen in intertidalen Sedimenten des Weser-Ästuars. 110 pages, Bremen, 1994. (out of print)

No. 62 **Giese, M. and G. Wefer**
Bericht über den 3. JGOFS-Workshop. 5./6. Dezember 1994 in Bremen.
84 pages, Bremen, 1995.

No. 63 **Mann, U.**
Genese kretazischer Schwarzschiefer in Kolumbien: Globale vs. regionale/lokale Prozesse.
153 pages, Bremen, 1995. (out of print)

No. 64 **Willems, H., Wan X., Yin J., Dongdui L., Liu G., S. Dürr, K.-U. Gräfe**
The Mesozoic development of the N-Indian passive margin and of the Xigaze Forearc Basin in southern Tibet, China. – Excursion Guide to IGCP 362 Working-Group Meeting "Integrated Stratigraphy". 113 pages, Bremen, 1995. (out of print)

No. 65 **Hünken, U.**
Liefergebiets - Charakterisierung proterozoischer Goldseifen in Ghana anhand von Fluideinschluß - Untersuchungen. 270 pages, Bremen, 1995.

No. 66 **Nyandwi, N.**
The Nature of the Sediment Distribution Patterns in ther Spiekeroog Backbarrier Area, the East Frisian Islands. 162 pages, Bremen, 1995.

No. 67 **Isenbeck-Schröter, M.**
Transportverhalten von Schwermetallkationen und Oxoanionen in wassergesättigten Sanden. - Laborversuche in Säulen und ihre Modellierung -. 182 pages, Bremen, 1995.

No. 68 **Hebbeln, D. and cruise participants**
Report and preliminary results of SONNE-Cruise SO 102, Valparaiso - Valparaiso, 95.
134 pages, Bremen, 1995.

No. 69 **Willems, H. (Sprecher), U.Bathmann, U. Bleil, T. v. Dobeneck, K. Herterich, B.B. Jorgensen, E.-M. Nöthig, M. Olesch, J. Pätzold, H.D. Schulz, V. Smetacek, V. Speiß. G. Wefer**
Bericht des Graduierten-Kollegs Stoff-Flüsse in marine Geosystemen.
Berichtszeitraum Januar 1993 - Dezember 1995. 45 & 468 pages, Bremen, 1995.

No. 70 **Giese, M. and G. Wefer**
Bericht über den 4. JGOFS-Workshop. 20./21. November 1995 in Bremen. 60 pages, Bremen, 1996. (out of print)

No. 71 **Meggers, H.**
Pliozän-quartäre Karbonatsedimentation und Paläozeanographie des Nordatlantiks und des Europäischen Nordmeeres - Hinweise aus planktischen Foraminiferengemeinschaften.
143 pages, Bremen, 1996. (out of print)

No. 72 **Teske, A.**
Phylogenetische und ökologische Untersuchungen an Bakterien des oxidativen und reduktiven marinen Schwefelkreislaufs mittels ribosomaler RNA. 220 pages, Bremen, 1996. (out of print)

No. 73 **Andersen, N.**
Biogeochemische Charakterisierung von Sinkstoffen und Sedimenten aus ostatlantischen Produktions-Systemen mit Hilfe von Biomarkern. 215 pages, Bremen, 1996.

No. 74 **Treppke, U.**
Saisonalität im Diatomeen- und Silikoflagellatenfluß im östlichen tropischen und subtropischen Atlantik. 200 pages, Bremen, 1996.

No. 75 **Schüring, J.**
Die Verwendung von Steinkohlebergematerialien im Deponiebau im Hinblick auf die Pyritverwitterung und die Eignung als geochemische Barriere. 110 pages, Bremen, 1996.

No. 76 **Pätzold, J. and cruise participants**
Report and preliminary results of VICTOR HENSEN cruise JOPS II, Leg 6,
Fortaleza - Recife, 10.3. - 26.3. 1995 and Leg 8, Vítoria - Vítoria, 10.4. - 23.4.1995.
87 pages, Bremen, 1996.

No. 77 **Bleil, U. and cruise participants**
Report and preliminary results of METEOR-Cruise M 34/1, Cape Town - Walvis Bay, 3.-26.1.1996.
129 pages, Bremen, 1996.

No. 78 **Schulz, H.D. and cruise participants**
Report and preliminary results of METEOR-Cruise M 34/2, Walvis Bay - Walvis Bay, 29.1.-18.2.96
133 pages, Bremen, 1996.

No. 79 **Wefer, G. and cruise participants**
Report and preliminary results of METEOR-Cruise M 34/3, Walvis Bay - Recife, 21.2.-17.3.1996.
168 pages, Bremen, 1996.

No. 80 **Fischer, G. and cruise participants**
Report and preliminary results of METEOR-Cruise M 34/4, Recife - Bridgetown, 19.3.-15.4.1996.
105 pages, Bremen, 1996.

No. 81 **Kulbrok, F.**
Biostratigraphie, Fazies und Sequenzstratigraphie einer Karbonatrampe in den Schichten der
Oberkreide und des Alttertiärs Nordost-Ägyptens (Eastern Desert, N'Golf von Suez, Sinai).
153 pages, Bremen, 1996.

No. 82 **Kasten, S.**
Early Diagenetic Metal Enrichments in Marine Sediments as Documents of Nonsteady-State
Depositional Conditions. Bremen, 1996.

No. 83 **Holmes, M.E.**
Reconstruction of Surface Ocean Nitrate Utilization in the Southeast Atlantic Ocean Based
on Stable Nitrogen Isotopes. 113 pages, Bremen, 1996.

No. 84 **Rühlemann, C.**
Akkumulation von Carbonat und organischem Kohlenstoff im tropischen Atlantik:
Spätquartäre Produktivitäts-Variationen und ihre Steuerungsmechanismen. 139 pages, Bremen, 1996.

No. 85 **Ratmeyer, V.**
Untersuchungen zum Eintrag und Transport lithogener und organischer partikulärer Substanz
im östlichen subtropischen Nordatlantik. 154 pages, Bremen, 1996.

No. 86 **Cepek, M.**
Zeitliche und räumliche Variationen von Coccolithophoriden-Gemeinschaften im subtropischen
Ost-Atlantik: Untersuchungen an Plankton, Sinkstoffen und Sedimenten. 156 pages, Bremen, 1996.

No. 87 **Otto, S.**
Die Bedeutung von gelöstem organischen Kohlenstoff (DOC) für den Kohlenstoffffluß im Ozean.
150 pages, Bremen, 1996.

No. 88 **Hensen, C.**
Frühdiagenetische Prozesse und Quantifizierung benthischer Stoff-Flüsse in Oberflächensedimenten
des Südatlantiks. 132 pages, Bremen, 1996.

No. 89 **Giese, M. and G. Wefer**
Bericht über den 5. JGOFS-Workshop. 27./28. November 1996 in Bremen. 73 pages, Bremen, 1997.

No. 90 **Wefer, G. and cruise participants**
Report and preliminary results of METEOR-Cruise M 37/1, Lisbon - Las Palmas, 4.-23.12.1996.
79 pages, Bremen, 1997.

No. 91 **Isenbeck-Schröter, M., E. Bedbur, M. Kofod, B. König, T. Schramm & G. Mattheß**
Occurrence of Pesticide Residues in Water - Assessment of the Current Situation in Selected
EU Countries. 65 pages, Bremen 1997.

No. 92 **Kühn, M.**
Geochemische Folgereaktionen bei der hydrogeothermalen Energiegewinnung. 129 pages, Bremen 1997.

No. 93 **Determann, S. & K. Herterich**
JGOFS-A6 "Daten und Modelle": Sammlung JGOFS-relevanter Modelle in Deutschland.
26 pages, Bremen, 1997.

No. 94 **Fischer, G. and cruise participants**
Report and preliminary results of METEOR-Cruise M 38/1, Las Palmas - Recife, 25.1.-1.3.1997,
with Appendix: Core Descriptions from METEOR Cruise M 37/1. Bremen, 1997.

No. 95 **Bleil, U. and cruise participants**
Report and preliminary results of METEOR-Cruise M 38/2, Recife - Las Palmas, 4.3.-14.4.1997. 126 pages, Bremen, 1997.

No. 96 **Neuer, S. and cruise participants**
Report and preliminary results of VICTOR HENSEN-Cruise 96/1. Bremen, 1997.

No. 97 **Villinger, H. and cruise participants**
Fahrtbericht SO 111, 20.8. - 16.9.1996. 115 pages, Bremen, 1997.

No. 98 **Lüning, S.**
Late Cretaceous - Early Tertiary sequence stratigraphy, paleoecology and geodynamics of Eastern Sinai, Egypt. 218 pages, Bremen, 1997.

No. 99 **Haese, R.R.**
Beschreibung und Quantifizierung frühdiagenetischer Reaktionen des Eisens in Sedimenten des Südatlantiks. 118 pages, Bremen, 1997.

No. 100 **Lührte, R. von**
Verwertung von Bremer Baggergut als Material zur Oberflächenabdichtung von Deponien - Geochemisches Langzeitverhalten und Schwermetall-Mobilität (Cd, Cu, Ni, Pb, Zn). Bremen, 1997.

No. 101 **Ebert, M.**
Der Einfluß des Redoxmilieus auf die Mobilität von Chrom im durchströmten Aquifer. 135 pages, Bremen, 1997.

No. 102 **Krögel, F.**
Einfluß von Viskosität und Dichte des Seewassers auf Transport und Ablagerung von Wattsedimenten (Langeooger Rückseitenwatt, südliche Nordsee). 168 pages, Bremen, 1997.

No. 103 **Kerntopf, B.**
Dinoflagellate Distribution Patterns and Preservation in the Equatorial Atlantic and Offshore North-West Africa. 137 pages, Bremen, 1997.

No. 104 **Breitzke, M.**
Elastische Wellenausbreitung in marinen Sedimenten - Neue Entwicklungen der Ultraschall Sedimentphysik und Sedimentechographie. 298 pages, Bremen, 1997.

No. 105 **Marchant, M.**
Rezente und spätquartäre Sedimentation planktischer Foraminiferen im Peru-Chile Strom. 115 pages, Bremen, 1997.

No. 106 **Habicht, K.S.**
Sulfur isotope fractionation in marine sediments and bacterial cultures. 125 pages, Bremen, 1997.

No. 107 **Hamer, K., R.v. Lührte, G. Becker, T. Felis, S. Keffel, B. Strotmann, C. Waschkowitz, M. Kölling, M. Isenbeck-Schröter, H.D. Schulz**
Endbericht zum Forschungsvorhaben 060 des Landes Bremen: Baggergut der Hafengruppe Bremen-Stadt: Modelluntersuchungen zur Schwermetallmobilität und Möglichkeiten der Verwertung von Hafenschlick aus Bremischen Häfen. 98 pages, Bremen, 1997.

No. 108 **Greeff, O.W.**
Entwicklung und Erprobung eines benthischen Landersystemes zur *in situ*-Bestimmung von Sulfatreduktionsraten mariner Sedimente. 121 pages, Bremen, 1997.

No. 109 **Pätzold, M. und G. Wefer**
Bericht über den 6. JGOFS-Workshop am 4./5.12.1997 in Bremen. Im Anhang: Publikationen zum deutschen Beitrag zur Joint Global Ocean Flux Study (JGOFS), Stand 1/1998. 122 pages, Bremen, 1998.

No. 110 **Landenberger, H.**
CoTReM, ein Multi-Komponenten Transport- und Reaktions-Modell. 142 pages, Bremen, 1998.

No. 111 **Villinger, H. und Fahrtteilnehmer**
Fahrtbericht SO 124, 4.10. - 16.10.199. 90 pages, Bremen, 1997.

No. 112 **Gietl, R.**
Biostratigraphie und Sedimentationsmuster einer nordostägyptischen Karbonatrampe unter Berücksichtigung der Alveolinen-Faunen. 142 pages, Bremen, 1998.

No. 113 **Ziebis, W.**
The Impact of the Thalassinidean Shrimp *Callianassa truncata* on the Geochemistry of permeable, coastal Sediments. 158 pages, Bremen 1998.

No. 114 **Schulz, H.D. and cruise participants**
Report and preliminary results of METEOR-Cruise M 41/1, Málaga - Libreville, 13.2.-15.3.1998. Bremen, 1998.

No. 115 **Völker, D.J.**
Untersuchungen an strömungsbeeinflußten Sedimentationsmustern im Südozean. Interpretation sedimentechographischer Daten und numerische Modellierung. 152 pages, Bremen, 1998.

No. 116 **Schlünz, B.**
Riverine Organic Carbon Input into the Ocean in Relation to Late Quaternary Climate Change. 136 pages, Bremen, 1998.

No. 117 **Kuhnert, H.**
Aufzeichnug des Klimas vor Westaustralien in stabilen Isotopen in Korallenskeletten. 109 pages, Bremen, 1998.

No. 118 **Kirst, G.**
Rekonstruktion von Oberflächenwassertemperaturen im östlichen Südatlantik anhand von Alkenonen. 130 pages, Bremen, 1998.

No. 119 **Dürkoop, A.**
Der Brasil-Strom im Spätquartär: Rekonstruktion der oberflächennahen Hydrographie während der letzten 400 000 Jahre. 121 pages, Bremen, 1998.

No. 120 **Lamy, F.**
Spätquartäre Variationen des terrigenen Sedimenteintrags entlang des chilenischen Kontinentalhangs als Abbild von Klimavariabilität im Milankovi_- und Sub-Milankovi_-Zeitbereich. 141 pages, Bremen, 1998.

No. 121 **Neuer, S. and cruise participants**
Report and preliminary results of POSEIDON-Cruise Pos 237/2, Vigo – Las Palmas, 18.3.-31.3.1998. 39 pages, Bremen, 1998

No. 122 **Romero, O.E.**
Marine planktonic diatoms from the tropical and equatorial Atlantic: temporal flux patterns and the sediment record. 205 pages, Bremen, 1998.

No. 123 **Spiess, V. und Fahrtteilnehmer**
Report and preliminary results of RV SONNE Cruise 125, Cochin – Chittagong, 17.10.-17.11.1997. 128 pages, Bremen, 1998.

No. 124 **Arz, H.W.**
Dokumentation von kurzfristigen Klimaschwankungen des Spätquartärs in Sedimenten des westlichen äquatorialen Atlantiks. 96 pages, Bremen, 1998.

No. 125 **Wolff, T.**
Mixed layer characteristics in the equatorial Atlantic during the late Quaternary as deduced from planktonic foraminifera. 132 pages, Bremen, 1998.

No. 126 **Dittert, N.**
Late Quaternary Planktic Foraminifera Assemblages in the South Atlantic Ocean: Quantitative Determination and Preservational Aspects. 165 pages, Bremen, 1998.

No. 127 **Höll, C.**
Kalkige und organisch-wandige Dinoflagellaten-Zysten in Spätquartären Sedimenten des tropischen Atlantiks und ihre palökologische Auswertbarkeit. 121 pages, Bremen, 1998.

No. 128 **Hencke, J.**
Redoxreaktionen im Grundwasser: Etablierung und Verlagerung von Reaktionsfronten und ihre Bedeutung für die Spurenelement-Mobilität. 122 pages, Bremen 1998.

No. 129 **Pätzold, J. and cruise participants**
Report and preliminary results of METEOR-Cruise M 41/3, Vítoria, Brasil – Salvador de Bahia, Brasil, 18.4. - 15.5.1998. Bremen, 1999.

No. 130 **Fischer, G. and cruise participants**
Report and preliminary results of METEOR-Cruise M 41/4, Salvador de Bahia, Brasil – Las Palmas, Spain, 18.5. – 13.6.1998. Bremen, 1999.

No. 131 **Schlünz, B. und G. Wefer**
Bericht über den 7. JGOFS-Workshop am 3. und 4.12.1998 in Bremen. Im Anhang: Publikationen zum deutschen Beitrag zur Joint Global Ocean Flux Study (JGOFS), Stand 1/ 1999. 100 pages, Bremen, 1999.

No. 132 **Wefer, G. and cruise participants**
Report and preliminary results of METEOR-Cruise M 42/4, Las Palmas - Las Palmas - Viena do Castelo; 26.09.1998 - 26.10.1998. 104 pages, Bremen, 1999.

No. 133 **Felis, T.**
Climate and ocean variability reconstructed from stable isotope records of modern subtropical corals (Northern Red Sea). 111 pages, Bremen, 1999.

No. 134 **Draschba , S.**
North Atlantic climate variability recorded in reef corals from Bermuda. 108 pages, Bremen, 1999.

No. 135 **Schmieder, F.**
Magnetic Cyclostratigraphy of South Atlantic Sediments. 82 pages, Bremen, 1999.

No. 136 **Rieß, W.**
In situ measurements of respiration and mineralisation processes – Interaction between fauna and geochemical fluxes at active interfaces. 68 pages, Bremen, 1999.

No. 137 **Devey, C.W. and cruise participants**
Report and shipboard results from METEOR-cruise M 41/2, Libreville – Vitoria, 18.3. – 15.4.98. 59 pages, Bremen, 1999.

No. 138 **Wenzhöfer, F.**
Biogeochemical processes at the sediment water interface and quantification of metabolically driven calcite dissolution in deep sea sediments. 103 pages, Bremen, 1999.

No. 139 **Klump, J.**
Biogenic barite as a proxy of paleoproductivity variations in the Southern Peru-Chile Current. 107 pages, Bremen, 1999.

No. 140 **Huber, R.**
Carbonate sedimentation in the northern Northatlantic since the late pliocene. 103 pages, Bremen, 1999.

No. 141 **Schulz, H.**
Nitrate-storing sulfur bacteria in sediments of coastal upwelling. 94 pages, Bremen, 1999.

No. 142 **Mai, S.**
Die Sedimentverteilung im Wattenmeer: ein Simulationsmodell. 114 pages, Bremen, 1999.

No. 143 **Neuer, S. and cruise participants**
Report and preliminary results of Poseidon Cruise 248, Las Palmas - Las Palmas, 15.2.-26.2.1999. 45 pages, Bremen, 1999.

No. 144 **Weber, A.**
Schwefelkreislauf in marinen Sedimenten und Messung von in situ Sulfatreduktionsraten. 122 pages, Bremen, 1999.

No. 145 **Hadeler, A.**
Sorptionsreaktionen im Grundwasser: Unterschiedliche Aspekte bei der Modellierung des Transportverhaltens von Zink. 122 pages, 1999.

No. 146 **Dierßen, H.**
Zum Kreislauf ausgewählter Spurenmetalle im Südatlantik: Vertikaltransport und Wechselwirkung zwischen Partikeln und Lösung. 167 pages, Bremen, 1999.

No. 147 **Zühlsdorff, L.**
High resolution multi-frequency seismic surveys at the Eastern Juan de Fuca Ridge Flank and the Cascadia Margin – Evidence for thermally and tectonically driven fluid upflow in marine sediments. 118 pages, Bremen 1999.

No. 148 **Kinkel, H.**
Living and late Quaternary Coccolithophores in the equatorial Atlantic Ocean: response of distribution and productivity patterns to changing surface water circulation. 183 pages, Bremen, 2000.

No. 149 **Pätzold, J. and cruise participants**
Report and preliminary results of METEOR Cruise M 44/3, Aqaba (Jordan) - Safaga (Egypt) – Dubá (Saudi Arabia) – Suez (Egypt) - Haifa (Israel), 12.3.-26.3.-2.4.-4.4.1999. 135 pages, Bremen, 2000.

No. 150 **Schlünz, B. and G. Wefer**
Bericht über den 8. JGOFS-Workshop am 2. und 3.12.1999 in Bremen. Im Anhang: Publikationen zum deutschen Beitrag zur Joint Global Ocean Flux Study (JGOFS), Stand 1/ 2000. 95 pages, Bremen, 2000.

No. 151 **Schnack, K.**
Biostratigraphie und fazielle Entwicklung in der Oberkreide und im Alttertiär im Bereich der Kharga Schwelle, Westliche Wüste, SW-Ägypten. 142 pages, Bremen, 2000.

No. 152 **Karwath, B.**
Ecological studies on living and fossil calcareous dinoflagellates of the equatorial and tropical Atlantic Ocean. 175 pages, Bremen, 2000.

No. 153 **Moustafa, Y.**
Paleoclimatic reconstructions of the Northern Red Sea during the Holocene inferred from stable isotope records of modern and fossil corals and molluscs. 102 pages, Bremen, 2000.

No. 154 **Villinger, H. and cruise participants**
Report and preliminary results of SONNE-cruise 145-1 Balboa – Talcahuana, 21.12.1999 – 28.01.2000. 147 pages, Bremen, 2000.

No. 155 **Rusch, A.**
Dynamik der Feinfraktion im Oberflächenhorizont permeabler Schelfsedimente. 102 pages, Bremen, 2000.

No. 156 **Moos, C.**
Reconstruction of upwelling intensity and paleo-nutrient gradients in the northwest Arabian Sea derived from stable carbon and oxygen isotopes of planktic foraminifera. 103 pages, Bremen, 2000.

No. 157 **Xu, W.**
Mass physical sediment properties and trends in a Wadden Sea tidal basin. 127 pages, Bremen, 2000.

No. 158 **Meinecke, G. and cruise participants**
Report and preliminary results of METEOR Cruise M 45/1, Malaga (Spain) - Lissabon (Portugal), 19.05. - 08.06.1999. 39 pages, Bremen, 2000.

No. 159 **Vink, A.**
Reconstruction of recent and late Quaternary surface water masses of the western subtropical Atlantic Ocean based on calcareous and organic-walled dinoflagellate cysts. 160 pages, Bremen, 2000.

No. 160 **Willems, H. (Sprecher), U. Bleil, R. Henrich, K. Herterich, B.B. Jørgensen, H.-J. Kuß, M. Olesch, H.D. Schulz,V. Spieß, G. Wefer**
Abschlußbericht des Graduierten-Kollegs Stoff-Flüsse in marine Geosystemen.
Zusammenfassung und Berichtszeitraum Januar 1996 - Dezember 2000. 340 pages, Bremen, 2000.

No. 161 **Sprengel, C.**
Untersuchungen zur Sedimentation und Ökologie von Coccolithophoriden im Bereich der Kanarischen Inseln: Saisonale Flussmuster und Karbonatexport. 165 pages, Bremen, 2000.

No. 162 **Donner, B. and G. Wefer**
Bericht über den JGOFS-Workshop am 18.-21.9.2000 in Bremen: Biogeochemical Cycles: German Contributions to the International Joint Global Ocean Flux Study. 87 pages, Bremen, 2000.

No. 163 **Neuer, S. and cruise participants**
Report and preliminary results of Meteor Cruise M 45/5, Bremen – Las Palmas, October 1 – November 3, 1999. 93 pages, Bremen, 2000.

No. 164 **Devey, C. and cruise participants**
Report and preliminary results of Sonne Cruise SO 145/2, Talcahuano (Chile) - Arica (Chile), February 4 – February 29, 2000. 63 pages, Bremen, 2000.

No. 165 **Freudenthal, T.**
Reconstruction of productivity gradients in the Canary Islands region off Morocco by means of sinking particles and sediments. 147 pages, Bremen, 2000.

No. 166 **Adler, M.**
Modeling of one-dimensional transport in porous media with respect to simultaneous geochemical reactions in CoTReM. 147 pages, Bremen, 2000.

No. 167 **Santamarina Cuneo, P.**
Fluxes of suspended particulate matter through a tidal inlet of the East Frisian Wadden Sea (southern North Sea). 91 pages, Bremen, 2000.

No. 168 **Benthien, A.**
Effects of CO_2 and nutrient concentration on the stable carbon isotope composition of C37:2 alkenones in sediments of the South Atlantic Ocean. 104 pages, Bremen, 2001.

No. 169 **Lavik, G.**
Nitrogen isotopes of sinking matter and sediments in the South Atlantic. 140 pages, Bremen, 2001.

No. 170 **Budziak, D.**
Late Quaternary monsoonal climate and related variations in paleoproductivity and alkenone-derived sea-surface temperatures in the western Arabian Sea. 114 pages, Bremen, 2001.

No. 171 **Gerhardt, S.**
Late Quaternary water mass variability derived from the pteropod preservation state in sediments of the western South Atlantic Ocean and the Caribbean Sea. 109 pages, Bremen, 2001.

No. 172 **Bleil, U. and cruise participants**
Report and preliminary results of Meteor Cruise M 46/3, Montevideo (Uruguay) – Mar del Plata (Argentina), January 4 – February 7, 2000. Bremen, 2001.

No. 173 **Wefer, G. and cruise participants**
Report and preliminary results of Meteor Cruise M 46/4, Mar del Plata (Argentina) – Salvador da Bahia (Brazil), February 10 – March 13, 2000. With partial results of METEOR cruise M 46/2. 136 pages, Bremen, 2001.

No. 174 **Schulz, H.D. and cruise participants**
Report and preliminary results of Meteor Cruise M 46/2, Recife (Brazil) – Montevideo (Uruguay), December 2 – December 29, 1999. 107 pages, Bremen, 2001.

No. 175 **Schmidt, A.**
Magnetic mineral fluxes in the Quaternary South Atlantic: Implications for the paleoenvironment. 97 pages, Bremen, 2001.

No. 176 **Bruhns, P.**
Crystal chemical characterization of heavy metal incorporation in brick burning processes. 93 pages, Bremen, 2001.

No. 177 **Karius, V.**
Baggergut der Hafengruppe Bremen-Stadt in der Ziegelherstellung. 131 pages, Bremen, 2001.

No. 178 **Adegbie, A. T.**
Reconstruction of paleoenvironmental conditions in Equatorial Atlantic and the Gulf of Guinea Basins for the last 245,000 years. 113 pages, Bremen, 2001.

No. 179 **Spieß, V. and cruise participants**
Report and preliminary results of R/V Sonne Cruise SO 149, Victoria - Victoria, 16.8. - 16.9.2000. 100 pages, Bremen, 2001.

No. 180 **Kim, J.-H.**
Reconstruction of past sea-surface temperatures in the eastern South Atlantic and the eastern South Pacific across Termination I based on the Alkenone Method. 114 pages, Bremen, 2001.

No. 181 **von Lom-Keil, H.**
Sedimentary waves on the Namibian continental margin and in the Argentine Basin – Bottom flow reconstructions based on high resolution echosounder data. 126 pages, Bremen, 2001.

No. 182 **Hebbeln, D. and cruise participants**
PUCK: Report and preliminary results of R/V Sonne Cruise SO 156, Valparaiso (Chile) - Talcahuano (Chile), March 29 - May 14, 2001. 195 pages, Bremen, 2001.

No. 183 **Wendler, J.**
Reconstruction of astronomically-forced cyclic and abrupt paleoecological changes in the Upper Cretaceous Boreal Realm based on calcareous dinoflagellate cysts. 149 pages, Bremen, 2001.

No. 184 **Volbers, A.**
Planktic foraminifera as paleoceanographic indicators: production, preservation, and reconstruction of upwelling intensity. Implications from late Quaternary South Atlantic sediments. 122 pages, Bremen, 2001.

No. 185 **Bleil, U. and cruise participants**
Report and preliminary results of R/V METEOR Cruise M 49/3, Montevideo (Uruguay) - Salvador (Brasil), March 9 - April 1, 2001. 99 pages, Bremen, 2001.

No. 186 **Scheibner, C.**
Architecture of a carbonate platform-to-basin transition on a structural high (Campanian-early Eocene, Eastern Desert, Egypt) – classical and modelling approaches combined. 173 pages, Bremen, 2001.

No. 187 **Schneider, S.**
Quartäre Schwankungen in Strömungsintensität und Produktivität als Abbild der Wassermassen-Variabilität im äquatorialen Atlantik (ODP Sites 959 und 663): Ergebnisse aus Siltkorn-Analysen. 134 pages, Bremen, 2001.

No. 188 **Uliana, E.**
Late Quaternary biogenic opal sedimentation in diatom assemblages in Kongo Fan sediments. 96 pages, Bremen, 2002.

No. 189 **Esper, O.**
Reconstruction of Recent and Late Quaternary oceanographic conditions in the eastern South Atlantic Ocean based on calcareous- and organic-walled dinoflagellate cysts. 130 pages, Bremen, 2001.

No. 190 **Wendler, I.**
Production and preservation of calcareous dinoflagellate cysts in the modern Arabian Sea. 117 pages, Bremen, 2002.

No. 191 **Bauer, J.**
Late Cenomanian – Santonian carbonate platform evolution of Sinai (Egypt): stratigraphy, facies, and sequence architecture. 178 pages, Bremen, 2002.

No. 192 **Hildebrand-Habel, T.**
Die Entwicklung kalkiger Dinoflagellaten im Südatlantik seit der höheren Oberkreide. 152 pages, Bremen, 2002.

No. 193 **Hecht, H.**
Sauerstoff-Optopoden zur Quantifizierung von Pyritverwitterungsprozessen im Labor- und Langzeit-in-situ-Einsatz. Entwicklung - Anwendung – Modellierung. 130 pages, Bremen, 2002.

No. 194 **Fischer, G. and cruise participants**
Report and Preliminary Results of RV METEOR-Cruise M49/4, Salvador da Bahia – Halifax, 4.4.-5.5.2001. 84 pages, Bremen, 2002.

No. 195 **Gröger, M.**
Deep-water circulation in the western equatorial Atlantic: inferences from carbonate preservation studies and silt grain-size analysis. 95 pages, Bremen, 2002.

No. 196 **Meinecke,G. and cruise participants**
Report of RV POSEIDON Cruise POS 271, Las Palmas - Las Palmas, 19.3.-29.3.2001. 19 pages, Bremen, 2002.

No. 197 **Meggers, H. and cruise participants**
Report of RV POSEIDON Cruise POS 272, Las Palmas - Las Palmas, 1.4.-14.4.2001. 19 pages, Bremen, 2002.

No. 198 **Gräfe, K.-U.**
Stratigraphische Korrelation und Steuerungsfaktoren Sedimentärer Zyklen in ausgewählten Borealen und Tethyalen Becken des Cenoman/Turon (Oberkreide) Europas und Nordwestafrikas. 197 pages, Bremen, 2002.

No. 199 **Jahn, B.**
Mid to Late Pleistocene Variations of Marine Productivity in and Terrigenous Input to the Southeast Atlantic. 97 pages, Bremen, 2002.

No. 200 **Al-Rousan, S.**
Ocean and climate history recorded in stable isotopes of coral and foraminifers from the northern Gulf of Aqaba. 116 pages, Bremen, 2002.

No. 201 **Azouzi, B.**
Regionalisierung hydraulischer und hydrogeochemischer Daten mit geostatistischen Methoden. 108 pages, Bremen, 2002.

No. 202 **Spieß, V. and cruise participants**
Report and preliminary results of METEOR Cruise M 47/3, Libreville (Gabun) - Walvis Bay (Namibia), 01.06 - 03.07.2000. 70 pages, Bremen 2002.

No. 203 **Spieß, V. and cruise participants**
Report and preliminary results of METEOR Cruise M 49/2, Montevideo (Uruguay) - Montevideo, 13.02 - 07.03.2001. 84 pages, Bremen 2002.

No. 204 **Mollenhauer, G.**
Organic carbon accumulation in the South Atlantic Ocean: Sedimentary processes and glacial/interglacial Budgets. 139 pages, Bremen 2002.

No. 205 **Spieß, V. and cruise participants**
Report and preliminary results of METEOR Cruise M49/1, Cape Town (South Africa) - Montevideo (Uruguay), 04.01.2001 - 10.02.2001. 57 pages, Bremen, 2003.

No. 206 **Meier, K.J.S.**
Calcareous dinoflagellates from the Mediterranean Sea: taxonomy, ecology and palaeoenvironmental application. 126 pages, Bremen, 2003.

No. 207 **Rakic, S.**
Untersuchungen zur Polymorphie und Kristallchemie von Silikaten der Zusammensetzung $Me_2Si_2O_5$ (Me:Na, K). 139 pages, Bremen, 2003.

No. 208 **Pfeifer, K.**
Auswirkungen frühdiagenetischer Prozesse auf Calcit- und Barytgehalte in marinen Oberflächen-sedimenten. 110 pages, Bremen, 2003.

No. 209 **Heuer, V.**
Spurenelemente in Sedimenten des Südatlantik. Primärer Eintrag und frühdiagenetische Überprägung. 136 pages, Bremen, 2003.

No. 210 **Streng, M.**
Phylogenetic Aspects and Taxonomy of Calcareous Dinoflagellates. 157 pages, Bremen 2003.

No. 211 **Boeckel, B.**
Present and past coccolith assemblages in the South Atlantic: implications for species ecology, carbonate contribution and palaeoceanographic applicability. 157 pages, Bremen, 2003.

No. 212 **Precht, E.**
Advective interfacial exchange in permeable sediments driven by surface gravity waves and its ecological consequences. 131 pages, Bremen, 2003.

No. 213 **Frenz, M.**
Grain-size composition of Quaternary South Atlantic sediments and its paleoceanographic significance. 123 pages, Bremen, 2003.

No. 214 **Meggers, H. and cruise participants**
Report and preliminary results of METEOR Cruise M 53/1, Limassol - Las Palmas – Mindelo, 30.03.2002 - 03.05.2002. 81 pages, Bremen, 2003.

No. 215 **Schulz, H.D. and cruise participants**
Report and preliminary results of METEOR Cruise M 58/1, Dakar – Las Palmas, 15.04..2003 – 12.05.2003. Bremen, 2003.

No. 216 **Schneider, R. and cruise participants**
Report and preliminary results of METEOR Cruise M 57/1, Cape Town – Walvis Bay, 20.01. – 08.02.2003. 123 pages, Bremen, 2003.

No. 217 **Kallmeyer, J.**
Sulfate reduction in the deep Biosphere. 157 pages, Bremen, 2003.

No. 218 **Røy, H.**
Dynamic Structure and Function of the Diffusive Boundary Layer at the Seafloor. 149 pages, Bremen, 2003.

No. 219 **Pätzold, J., C. Hübscher and cruise participants**
Report and preliminary results of METEOR Cruise M 52/2&3, Istanbul – Limassol – Limassol, 04.02. – 27.03.2002. Bremen, 2003.

No. 220 **Zabel, M. and cruise participants**
Report and preliminary results of METEOR Cruise M 57/2, Walvis Bay – Walvis Bay, 11.02. – 12.03.2003. 136 pages, Bremen 2003.

No. 221 **Salem, M.**
Geophysical investigations of submarine prolongations of alluvial fans on the western side of the Gulf of Aqaba-Red Sea. 100 pages, Bremen, 2003.

No. 222 **Tilch, E.**
Oszillation von Wattflächen und deren fossiles Erhaltungspotential (Spiekerooger Rückseitenwatt, südliche Nordsee). 137 pages, Bremen, 2003.

No. 223 **Frisch, U. and F. Kockel**
Der Bremen-Knoten im Strukturnetz Nordwest-Deutschlands. Stratigraphie, Paläogeographie, Strukturgeologie. 379 pages, Bremen, 2004.

No. 224 **Kolonic, S.**
Mechanisms and biogeochemical implications of Cenomanian/Turonian black shale formation in North Africa: An integrated geochemical, millennial-scale study from the Tarfaya-LaAyoune Basin in SW Morocco. 174 pages, Bremen, 2004. Report online available only.

No. 225 **Panteleit, B.**
Geochemische Prozesse in der Salz- Süßwasser Übergangszone. 106 pages, Bremen, 2004.

No. 226 **Seiter, K.**
Regionalisierung und Quantifizierung benthischer Mineralisationsprozesse. 135 pages, Bremen, 2004.

No. 227 **Bleil, U. and cruise participants**
Report and preliminary results of METEOR Cruise M 58/2, Las Palmas – Las Palmas (Canary Islands, Spain), 15.05. – 08.06.2003. 123 pages, Bremen, 2004.

No. 228 **Kopf, A. and cruise participants**
Report and preliminary results of SONNE Cruise SO175, Miami - Bremerhaven, 12.11 - 30.12.2003. 218 pages, Bremen, 2004.

No. 229 **Fabian, M.**
Near Surface Tilt and Pore Pressure Changes Induced by Pumping in Multi-Layered Poroelastic Half-Spaces. 121 pages, Bremen, 2004.

No. 230 **Segl, M. , and cruise participants**
Report and preliminary results of POSEIDON cruise 304 Galway – Lisbon, 5. – 22. Oct. 2004. 27 pages, Bremen 2004

No. 231 **Meinecke, G. and cruise participants**
Report and preliminary results of POSEIDON Cruise 296, Las Palmas – Las Palmas, 04.04 – 14.04.2003. 42 pages, Bremen 2005.

No. 232 **Meinecke, G. and cruise participants**
Report and preliminary results of POSEIDON Cruise 310, Las Palmas – Las Palmas, 12.04 – 26.04.2004. 49 pages, Bremen 2005.

No. 233 **Meinecke, G. and cruise participants**
Report and preliminary results of METEOR Cruise 58/3, Las Palmas - Ponta Delgada, 11.06 - 24.06.2003. 50 pages, Bremen 2005.

No. 234 **Feseker, T.**
Numerical Studies on Groundwater Flow in Coastal Aquifers. 219 pages. Bremen 2004.

No. 235 **Sahling, H. and cruise participants**
Report and preliminary results of R/V POSEIDON Cruise P317/4, Istanbul-Istanbul , 16 October - 4 November 2004. 92 pages, Bremen 2004.

No. 236 **Meinecke, G. und Fahrtteilnehmer**
Report and preliminary results of POSEIDON Cruise 305, Las Palmas (Spain) - Lisbon (Portugal), October 28th – November 6th, 2004. 43 pages, Bremen 2005.

No. 237 **Ruhland, G. and cruise participants**
Report and preliminary results of POSEIDON Cruise 319, Las Palmas (Spain) - Las Palmas (Spain), December 6th – December 17th, 2004. 50 pages, Bremen 2005.

No. 238 **Chang, T.S.**
Dynamics of fine-grained sediments and stratigraphic evolution of a back-barrier tidal basin of the German Wadden Sea (southern North Sea). 102 pages, Bremen 2005.

No. 239 **Lager, T.**
Predicting the source strength of recycling materials within the scope of a seepage water prognosis by means of standardized laboratory methods. 141 pages, Bremen 2005.

No. 240 **Meinecke, G.**
DOLAN - Operationelle Datenübertragung im Ozean und Laterales Akustisches Netzwerk in der Tiefsee. Abschlußbericht. 42 pages, Bremen 2005.

No. 241 **Guasti, E.**
Early Paleogene environmental turnover in the southern Tethys as recorded by foraminiferal and organic-walled dinoflagellate cysts assemblages. 203 pages, Bremen 2005.

No. 242 **Riedinger, N.**
Preservation and diagenetic overprint of geochemical and geophysical signals in ocean margin sediments related to depositional dynamics. 91 pages, Bremen 2005.

No. 243 **Ruhland, G. and cruise participants**
Report and preliminary results of POSEIDON cruise 320, Las Palmas (Spain) - Las Palmas (Spain), March 08th - March 18th, 2005. 57 pages, Bremen 2005.

No. 244 **Inthorn, M.**
Lateral particle transport in nepheloid layers – a key factor for organic matter distribution and quality in the Benguela high-productivity area. 127 pages, Bremen, 2006.

No. 245 **Aspetsberger, F.**
Benthic carbon turnover in continental slope and deep sea sediments: importance of organic matter quality at different time scales. 136 pages, Bremen, 2006.

No. 246 **Hebbeln, D. and cruise participants**
Report and preliminary results of RV SONNE Cruise SO-184, PABESIA, Durban (South Africa) – Cilacap (Indonesia) – Darwin (Australia), July 08th - September 13th, 2005. 142 pages, Bremen 2006.

No. 247 **Ratmeyer, V. and cruise participants**
Report and preliminary results of RV METEOR Cruise M61/3. Development of Carbonate Mounds on the Celtic Continental Margin, Northeast Atlantic. Cork (Ireland) – Ponta Delgada (Portugal), 04.06. – 21.06.2004. 64 pages, Bremen 2006.

No. 248 **Wien, K.**
Element Stratigraphy and Age Models for Pelagites and Gravity Mass Flow Deposits based on Shipboard XRF Analysis. 100 pages, Bremen 2006.

No. 249 **Krastel, S. and cruise participants**
Report and preliminary results of RV METEOR Cruise M65/2, Dakar - Las Palmas, 04.07. – 26.07.2005. 185 pages, Bremen 2006.

No. 250 **Heil, G.M.N.**
Abrupt Climate Shifts in the Western Tropical to Subtropical Atlantic Region during the Last Glacial. 121 pages, Bremen 2006.

No. 251 **Ruhland, G. and cruise participants**
Report and preliminary results of POSEIDON Cruise 330, Las Palmas – Las Palmas, November 21th – December 03rd, 2005. 48 pages, Bremen 2006.

No. 252 **Mulitza , S. and cruise participants**
Report and preliminary results of METEOR Cruise M65/1, Dakar – Dakar, 11.06.- 1.07.2005. 149 pages, Bremen 2006.

No. 253 **Kopf, A. and cruise participants**
Report and preliminary results of POSEIDON Cruise P336, Heraklion - Heraklion, 28.04. – 17.05.2006. 127 pages, Bremen, 2006.

No. 254 **Wefer, G. and cruise participants**
Report and preliminary results of R/V METEOR Cruise M65/3, Las Palmas - Las Palmas (Spain), July 31st - August 10th, 2005. 24 pages, Bremen 2006.

No. 255 **Hanebuth, T.J.J. and cruise participants**
Report and first results of the POSEIDON Cruise P342 GALIOMAR, Vigo – Lisboa (Portugal), August 19th – September 06th, 2006. Distribution Pattern, Residence Times and Export of Sediments on the Pleistocene/Holocene Galician Shelf (NW Iberian Peninsula). 203 pages, Bremen, 2007.

No. 256 **Ahke, A.**
Composition of molecular organic matter pools, pigments and proteins, in Benguela upwelling and Arctic Sediments. 192 pages, Bremen 2007.

No. 257 **Becker, V.**
Seeper - Ein Modell für die Praxis der Sickerwasserprognose. 170 pages, Bremen 2007.

No. 258 **Ruhland, G. and cruise participants**
Report and preliminary results of Poseidon cruise 333, Las Palmas (Spain) – Las Palmas (Spain), March 1st – March 10th, 2006. 32 pages, Bremen 2007.

No. 259 **Fischer, G., G. Ruhland and cruise participants**
Report and preliminary results of Poseidon cruise 344, leg 1 and leg 2, Las Palmas (Spain) – Las Palmas (Spain), Oct. 20th –Nov 2nd & Nov. 4th – Nov 13th, 2006. 46 pages, Bremen 2007.

No. 260 **Westphal, H. and cruise participants**
Report and preliminary results of Poseidon cruise 346, MACUMA. Las Palmas (Spain) – Las Palmas (Spain), 28.12.2006 – 15.1.2007. 49 pages, Bremen 2007.

No. 261 **Bohrmann, G., T. Pape, and cruise participants**
Report and preliminary results of R/V METEOR Cruise M72/3, Istanbul – Trabzon – Istanbul, March 17th – April 23rd, 2007. Marine gas hydrates of the Eastern Black Sea. 130 pages, Bremen 2007.

No. 262 **Bohrmann, G., and cruise participants**
Report and preliminary results of R/V METEOR Cruise M70/3, Iraklion – Iraklion, 21 November – 8 December 2006. Cold Seeps of the Anaximander Mountains / Eastern Mediterranean. 75 pages, Bremen 2008.

No. 263 **Bohrmann, G., Spiess, V., and cruise participants**
Report and preliminary results of R/V Meteor Cruise M67/2a and 2b, Balboa -- Tampico -- Bridgetown, 15 March -- 24 April, 2006. Fluid seepage in the Gulf of Mexico. Bremen 2008.

No. 264 **Kopf, A., and cruise participants**
Report and preliminary results of Meteor Cruise M73/1: LIMA-LAMO (Ligurian Margin Landslide Measurements & Observatory), Cadiz, 22.07.2007 – Genoa, 11.08.2007. 170 pages, Bremen 2008.